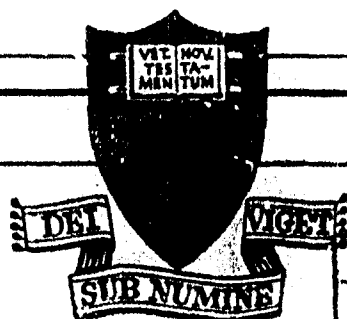
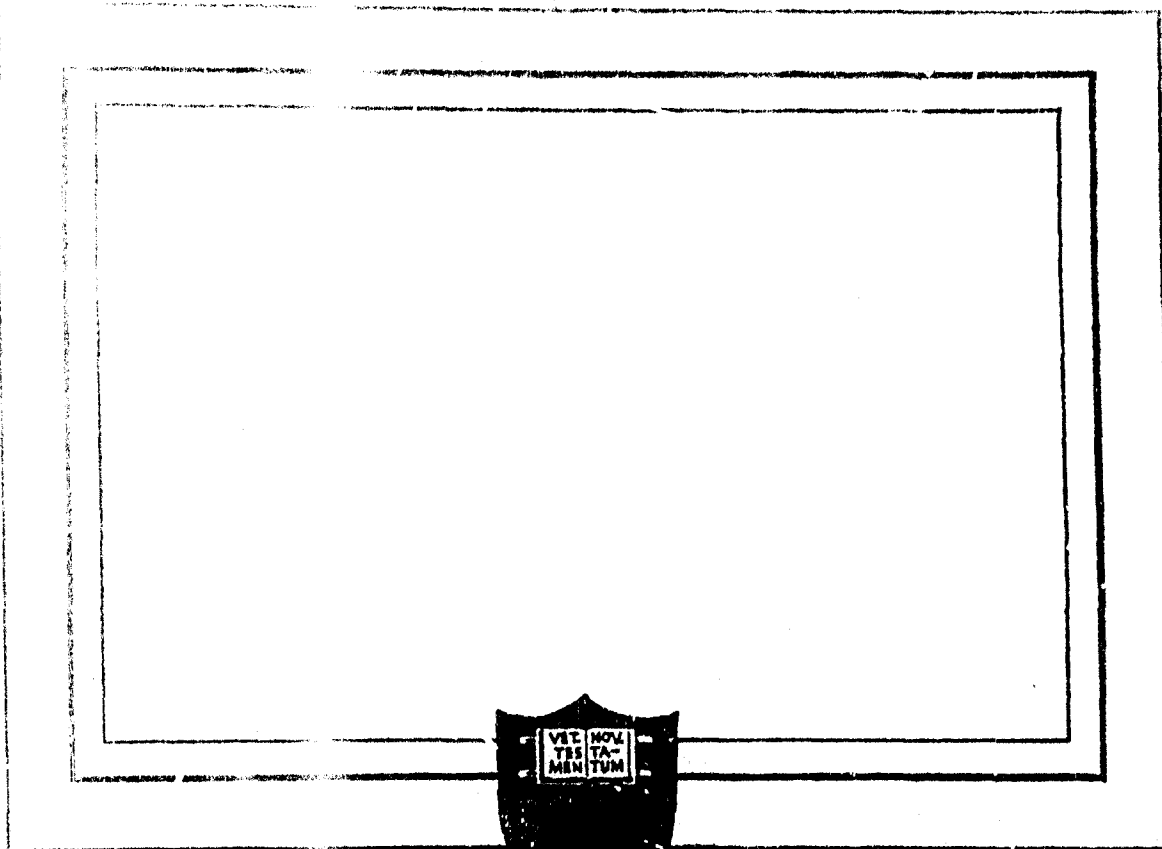
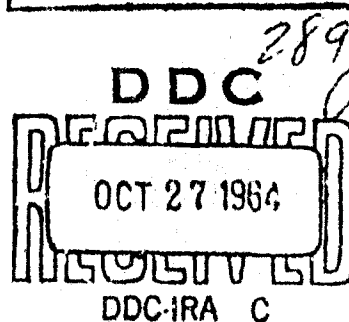


AD 607334



COPY	1	OF	3	cat
HARD COPY			\$.	6.00
MICROFICHE			\$.	1.50



PRINCETON UNIVERSITY

DEPARTMENT OF  
AEROSPACE AND MECHANICAL SCIENCES

ARCHIVE COPY

AIR FORCE OFFICE OF SCIENTIFIC RESEARCH

/ Contract AF 49(638) - 1268

THE GAS PHASE DECOMPOSITION

of

HYDRAZINE PROPELLANTS

by

Igor J. Eberstein

/Technical Report 708

Department of Aerospace and Mechanical Sciences

Approved by:

Irvin Glassman

Irvin Glassman  
Professor of  
Aeronautical Engineering

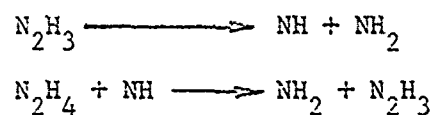
Reproduction, translation, publication, use and disposal in whole or in part by or for the United States Government is permitted.

Guggenheim Laboratories for the Aerospace Propulsion Sciences  
Department of Aerospace and Mechanical Sciences  
Princeton University  
Princeton, New Jersey

1964

is fastest, hydrazine decomposition is slowest, and the monomethylhydrazine decomposition rate is intermediate.

Reaction mechanisms for the thermal gas phase decomposition of hydrazine, and its methyl derivatives, were postulated and studied numerically. The postulated mechanism for hydrazine decomposition differs from those suggested by other investigators in that it includes a set of branching reactions:



Rate constants computed from the mechanism agree closely with rates measured experimentally, and the computed stoichiometry agrees with that observed experimentally.

A study of hydrazine-water mixtures showed their rates to be slower than those of the anhydrous material by approximately a factor of 10, and independent of the amount of water added. Slightly wet hydrazine behaved kinetically like the hydrazine-water mixtures. Thus it seems that water inhibits the gaseous decomposition of hydrazine by very effectively suppressing some reaction step. It is suggested that the  $\text{N}_2\text{H}_3$  radical may be formed in a vibrationally excited state, from which it can either branch to give  $\text{NH} + \text{NH}_2$ , or be deactivated to a relatively stable form by collision with other molecules. Then, water may inhibit branching by greatly promoting the vibrational relaxation of  $\text{N}_2\text{H}_3^*$ .

### ABSTRACT

Reaction rate data on gas phase hydrazine decomposition and an understanding of the decomposition mechanism are of general scientific interest. Furthermore, such understanding can contribute toward a solution of the problems associated with the use of hydrazine compounds as rocket propellants. These considerations led to a study of the kinetics of hydrazine and two of its methyl derivatives.

→ The decomposition of hydrazine, hydrazine-water mixtures, UDMH, and monomethylhydrazine ~~were~~<sup>were</sup> studied in the Princeton adiabatic flow reactor. This reactor consists of a cylindrical quartz section and a conical nozzle. The walls of the reactor are heated electrically to prevent heat loss to the ambient air. Hot nitrogen carrier gas flows through the reactor and is rapidly mixed with small quantities of gas phase reactant, which is injected perpendicularly to the main stream at the throat of the nozzle. The mixing is followed by chemical reaction which can stretch over a length of approximately 30 inches. Progress of reaction is followed by measuring the longitudinal variation of temperature with a silica coated Platinum - Pt/Rh thermocouple. The temperature regime of the study was approximately 800 - 1000 deg. K. A water cooled probe was used to take samples near the end of the reaction zone.

The overall reaction order of all three monopropellants was found to be very close to unity, and the following first order rate constants were obtained for decomposition in a 3 inch duct:

Substance	Pre-exponential factor, sec <sup>-1</sup>	Activation Energy kcal/mole
N <sub>2</sub> H <sub>4</sub>	10 <sup>10.33</sup>	36.2
UDMH	10 <sup>8.84</sup>	26.7
MMH	10 <sup>13.4</sup>	47.0

→ A comparison of the reaction rates of the three monopropellants showed<sup>d</sup> that, in the temperature regime of this study, UDMH decomposition

R-11

### ABSTRACT

Reaction rate data on gas phase hydrazine decomposition and an understanding of the decomposition mechanism are of general scientific interest. Furthermore, such understanding can contribute toward a solution of the problems associated with the use of hydrazine compounds as rocket propellants. These considerations led to a study of the kinetics of hydrazine and two of its methyl derivatives.

The decomposition of hydrazine, hydrazine-water mixtures, UDMH, and monomethylhydrazine were studied in the Princeton adiabatic flow reactor. This reactor consists of a cylindrical quartz section and a conical nozzle. The walls of the reactor are heated electrically to prevent heat loss to the ambient air. Hot nitrogen carrier gas flows through the reactor and is rapidly mixed with small quantities of gas phase reactant, which is injected perpendicularly to the main stream at the throat of the nozzle. The mixing is followed by chemical reaction which can stretch over a length of approximately 30 inches. Progress of reaction is followed by measuring the longitudinal variation of temperature with a silica coated Platinum - Pt/Rh thermocouple. The temperature regime of the study was approximately 800 - 1000 deg. K. A water cooled probe was used to take samples near the end of the reaction zone.

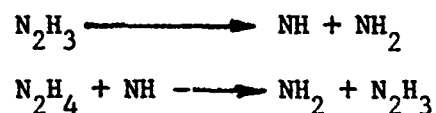
The overall reaction order of all three monopropellants was found to be very close to unity, and the following first order rate constants were obtained for decomposition in a 3 inch duct:

Substance	Pre-exponential factor, $\text{sec}^{-1}$	Activation Energy kcal/mole
$\text{N}_2\text{H}_4$	$10^{10.33}$	36.2
UDMH	$10^{8.84}$	26.7
MMH	$10^{13.4}$	47.0

A comparison of the reaction rates of the three monopropellants shows that, in the temperature regime of this study, UDMH decomposition

is fastest, hydrazine decomposition is slowest, and the monomethylhydrazine decomposition rate is intermediate.

Reaction mechanisms for the thermal gas phase decomposition of hydrazine, and its methyl derivatives, were postulated and studied numerically. The postulated mechanism for hydrazine decomposition differs from those suggested by other investigators in that it includes a set of branching reactions:



Rate constants computed from the mechanism agree closely with rates measured experimentally, and the computed stoichiometry agrees with that observed experimentally.

A study of hydrazine-water mixtures showed their rates to be slower than those of the anhydrous material by approximately a factor of 10, and independent of the amount of water added. Slightly wet hydrazine behaved kinetically like the hydrazine-water mixtures. Thus it seems that water inhibits the gaseous decomposition of hydrazine by very effectively suppressing some reaction step. It is suggested that the  $\text{N}_2\text{H}_3$  radical may be formed in a vibrationally excited state, from which it can either branch to give  $\text{NH} + \text{NH}_2$ , or be deactivated to a relatively stable form by collision with other molecules. Then, water may inhibit branching by greatly promoting the vibrational relaxation of  $\text{N}_2\text{H}_3^*$ .

### ACKNOWLEDGMENTS

The author wishes to thank Professor Irvin Glassman for guidance and encouragement provided throughout the course of this study.

The author also wishes to thank Mr. Maurice Webb who helped with the solution of many of the engineering problems encountered in the course of this investigation. Furthermore, the assistance of Messrs. F. Smith, A. Bozowski, and J. Sivo in actually carrying out the experimental and technical phase of this study is gratefully acknowledged. Thanks are also extended to Mr. R. Sawyer who measured the radial velocity profiles in the flow reactor, did most of the monomethylhydrazine work, and generally assisted in carrying out the experimental research effort.

The assistance of the FMC Corporation, who analysed the liquid samples, and of the Princeton University Chemistry Department who permitted use of their infrared equipment for the analysis of the gas samples, is gratefully acknowledged.

The financial support and encouragement of the United States Air Force Office of Scientific Research, Propulsion Sciences Division under Grant No. AF 62-90 was essential in carrying out this investigation. Also, this work made use of computer facilities supported by National Science Foundation Grant NSF-GP 579.

Members of the Forrestal Research Center Computing Group, and especially Mr. Lanny Hoffman, are thanked for the assistance provided in carrying out the computational part of the study.

Thanks are extended to the Drafting Staff, especially Mr. T. Poli, and Mrs. K. Walter who produced the figures in their final form. Messrs. K. Donaldson and D. Neiler are thanked for their photographic work. Also, special gratitude is extended to Miss Anne Dennis, who spent many an hour typing this thesis.

Finally, sincere thanks are extended to all those who in any way assisted in the many faceted work of this investigation.

TABLE OF CONTENTS

	<u>PAGE</u>
TITLE PAGE	i
ABSTRACT	ii
ACKNOWLEDGEMENTS	iv
TABLE OF CONTENTS	v
LIST OF FIGURES	vii
INTRODUCTION	1
 CHAPTER I	
THEORETICAL CONSIDERATIONS	5
A. Electronic and Molecular Structure	6
B. The Arrhenius Expression for Elementary Reactions	9
C. Elementary Reactions in Chain Processes	12
D. The Steady State Approximation	18
 CHAPTER II	
A BRIEF REVIEW OF EXPERIMENTAL METHODS USED FOR THE STUDY OF CHEMICAL KINETICS	23
A. Flash Photolysis	24
B. Ignition Limits Experiments	25
C. The Laminar Flame	27
D. Shock Tube Studies	33
E. Isothermal Bombs	34
F. Isothermal Flow Reactors	40
G. Surface Reactions	43
H. The Princeton Adiabatic Flow Reactor	48
 CHAPTER III	
THE EFFECT OF TURBULENCE ON CHEMICAL KINETICS MEASUREMENTS IN THE ADIABATIC FLOW REACTOR	51
 CHAPTER IV	
EXPERIMENTAL APPARATUS AND PROCEDURE	59
A. Start of Reaction, Mixing, and Turbulence Effects	59
B. Flow Reactor and Carrier Gas System	62
C. Temperature Measurement	63
D. Gaseous Fuel Injection	65
E. Vaporization of Propellants	66
F. Product Gas Sampling	67

	<u>PAGE</u>
CHAPTER V. ANALYSIS OF EXPERIMENTAL DATA	69
A. Derivation of Data Reduction Formulas	69
B. Determination of Reaction Order	75
C. Reproducibility and Plots of Experimental Data	78
D. Integration Analysis of Data	79
E. Chemical Analysis of Reaction Products	80
CHAPTER VI DISCUSSION OF EXPERIMENTAL RESULTS	81
A. Hydrazine Decomposition	81
B. Decomposition of Hydrazine - Water Mixtures	85
C. The Decomposition of UDMH	86
D. Decomposition of Monomethylhydrazine	89
E. Comparison of $N_2H_4$ , UDMH, MMH	90
CHAPTER VII DECOMPOSITION MECHANISMS	92
A. Hydrazine	94
B. UDMH	107
C. Monomethylhydrazine	112
D. Comparison of Decomposition Mechanisms of Hydrazine, Monomethylhydrazine, and Unsymmetrical Dimethylhydrazine	114
CONCLUSIONS	115
REFERENCES	119
FIGURES	126
APPENDICES	
A. Data Reduction	
B. Calibrations	
C. Error Analysis	
D. Computations	

LIST OF FIGURES

1. Normal Oscillations of the  $N_2H_4$  Molecule.
2. Jost Shock Tube Studies of  $N_2H_4$  Decomposition.
3. Temperature Distribution in a Reacting Solid at Various Time Intervals.
4. Reactor Temperature Profiles.
5. Longitudinal Temperature Traces.
6. Effect of Carrier Gas Velocity on Decomposition Rate.
7. Drawing of Chemical Kinetic Flow Reactor.
8. Photo of Flow Reactor Assembly.
9. Quartz Reactor Tube.
10. Schematic of Carrier Gas Flow System.
11. Schematic of Temperature Control Servo System.
12. Photo of Temperature Control Servo System.
13. Photo of Main Control Panel.
14. Photo of Main Control Panel.
15. Thermocouple Electric Schematic.
16. Temperature Measuring and Recording Instruments.
17. Temperature Probe Drive Assembly.
18. Photo of Probe Coating Apparatus.
19. Photo of Injector Assembly.
20. Schematic of Fuel Vapor and Diluent Nitrogen System.
21. Schematic of Reactant Feed System.
22. Photo of Evaporator.
23. Evaporator Assembly.
24. Drawing of Sampling Probe.
25. Photo of Sampling Probe Components.
26. Photo of Infrared Absorption Cell.
27. Radial Temperature Profile in Reactor.
28. Radial Velocity Profile in Reactor.
29. Standard Deviation of Activation Energy versus Assumed Reaction Order for the Hydrazine Data.
30. St. Dev. of Eact vs. n for UDMH.
31. St. Dev. of Eact vs. n for Monomethylhydrazine.
32. Reproducibility of Hydrazine Data.
33. Reproducibility of UDMH Data.
34. Reproducibility of Monomethylhydrazine Data.

35. Arrhenius Plot of 3-inch Duct Anhydrous Hydrazine Data.
36. Decomposition of  $\text{N}_2\text{H}_4/\text{H}_2\text{O}$  Mixtures in 3-inch Duct.
37. Decomposition of  $\text{N}_2\text{H}_4/\text{H}_2\text{O}$  Mixtures in 4-inch Duct.
38. Decomposition of Wet Hydrazine in 3-inch Duct.
39. Decomposition of Wet Hydrazine in 4-inch Duct.
40. Decomposition of UDMH in 2-inch Duct.
41. Decomposition of UDMH in 3-inch Duct.
42. Decomposition of UDMH in 4-inch Duct.
43. Decomposition of Monomethylhydrazine in 3-inch Duct.
44. Decomposition of Monomethylhydrazine in 4-inch Duct.
45. Integration Analysis of Hydrazine Data.
46. Integration Analysis of UDMH Data.
47. Integration Analysis of Monomethylhydrazine Data.
48. Infra-red Spectrum of Standard Ammonia Sample.
49. Infra-red Spectrum of Gaseous Decomposition Products of UDMH.
50. Infra-red Spectrum of Gaseous Decomposition Products of Monomethylhydrazine.
51. Infra-red Spectrum of Condensate in Acetone Solution.
52. Comparison of Reaction Rates of  $\text{N}_2\text{H}_4$ , UDMH, MMH.
53. Data Obtained in Adiabatic Flow Reactor Compared with Jost Shock Tube Data.
54. Logarithmic Plot of Free Radical Concentration vs. Time for Hydrazine Decomposition.
55. Free Radical Concentration vs. % reacted for Hydrazine Decomposition.
56. Rate Constant vs. % reacted for Hydrazine Decomposition.
57. Free Radical Concentration after 10% Reaction vs. Temperature.
58. First Hydrazine Decomposition Mechanism Compared with Experimental Data.
59. Dependence of Overall Decomposition Rate on Hydrazine Concentration.
60. Dependence of Hydrazine Decomposition Rate on Third Body Concentration.
61. Effect on Overall Rate of the Variation of Initiation and Branching Rate Constants.
62. UDMH Decomposition Calculations.

## INTRODUCTION

Hydrazine has many qualities which make it attractive as a rocket propellant. Being non-carbonaceous, it can be used with flourine oxidizers to give a hypergolic, high energy propellant combination. Furthermore, hydrazine is a storable fuel, and is hypergolic with such storable oxidizers as nitrogen tetroxide.

The potential of hydrazine as a rocket propellant was recognized at a relatively early date. Thus hydrazine hydrate, in combination with alcohol and water, was used to power German rocket aircraft at the time of the Second World War (1). Hydrazine is mentioned as an attractive rocket propellant in Russian space literature (2), and is used extensively in American guided missile -, and space programs.

Hydrazine is not only an attractive rocket fuel. It is also a high energy, clean burning monopropellant. Thus, it can be used to drive turbines for propellant pumps, and for auxiliary power. Since hydrazine is a storable monopropellant, it can also be profitably used in midcourse correction units. This was done in the Mariner Venus Spacecraft in 1962 (3). Furthermore, it has been proposed that hydrazine be used to pressurize fuel tanks, and thus do away with pumps (4).

But, together with all its very attractive properties, hydrazine also has a very serious drawback. It has a tendency to undergo explosive decomposition. This tendency severely undermines the practical usefulness of hydrazine as a rocket propellant.

The methyl derivatives of hydrazine exhibit a greater stability than the unsubstituted specie, and like hydrazine, they are storable. However, their catalytic decomposition and ignitability are slower than those of hydrazine, making them less useful for auxiliary power units, and as hypergolic propellants. Also, the carbonaceous nature of the methyl substituted hydrazines makes them less useful with flourine oxidizers.

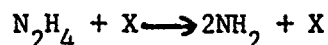
In the methyl substituted hydrazines, some of the desirable properties of the unsubstituted specie are sacrificed in favor of greater stability for use in rocket systems. Thus, UDMH was used in the Jupiter-C missile which launched the Explorer I satellite (5), and hydrazine-UDMH mixtures have been studied for use in Titan II (6).

It was felt that a fundamental understanding of hydrazine decomposition could contribute toward a solution of the problems associated with its use as a rocket propellant. Furthermore, rate data on gas phase hydrazine decomposition and an understanding of the decomposition mechanism are of general scientific interest. These considerations led to a study of the kinetics of hydrazine and some of its methyl derivatives. This investigation forms the center of gravity of the work described herein.

A number of studies of hydrazine decomposition have been conducted by other investigators.

Thus, hydrazine decomposition has been a favorite reaction in laminar flame studies (7, 8, 9, 10, 11). Generally, the dependence of flame speed on temperature is used to deduce an activation energy for the reaction. Furthermore, flames may be studied spectroscopically, as was done by Hall and Wolfhard (12) who observed bands due to  $\text{NH}_2$  and  $\text{NH}$  radicals in hydrazine decomposition flames.

Szwarc (13) used a flow reactor to study the reaction



in the presence of toluene, which acts as a scavenger for  $\text{NH}_2$  radicals, thus suppressing the chain decomposition of hydrazine.

Ramsay (14) studied the flash photolysis of hydrazine vapor. Like Wolfhard, he observed  $\text{NH}_2$  and  $\text{NH}$  radicals in absorption. Ramsay also found that if an excess of helium (100 mm) were added to the hydrazine (8 mm), the hydrazine would not decompose except at a considerably higher flash intensity.

Jost (15) studied hydrazine decomposition in a shock tube, and obtained half-lives of hydrazine as a function of temperature. A rate constant - temperature plot may be obtained from these data, which were taken in the temperature range 1100 deg. K. to 1540 deg. K.

In the low temperature regime, hydrazine decomposition in isothermal bombs was studied by Thomas (16) and Lucien (17).

Though the above studies have yielded considerable data on hydrazine decomposition, only the shock tube work of Jost, which was carried out at approximately the same time as the Princeton study, gives quantitative information on overall rate constants in the homogeneous gas phase as a function of temperature.

As regards UDMH, Cordes (18) studied its decomposition in

an isothermal flow reactor in helium carrier gas, obtaining overall rate constants as functions of temperature.

The author is not aware of any kinetics studies on the decomposition of monomethylhydrazine, nor of any experimental study to compare the kinetic behavior of hydrazine and its derivatives. Such a study was carried out in the Princeton adiabatic flow reactor in order to gain a better understanding of the similarities and differences between hydrazine and its methyl-substituted derivatives.

As will be evident from the subsequent discussion, the adiabatic flow reactor can be made to yield quantitative information on overall rate constants as a function of temperature. Furthermore, the turbulent, adiabatic flow reactor does not suffer from the mixing and temperature non-uniformity problems encountered in isothermal bombs and in isothermal flow reactors (19, 20). Finally, the adiabatic flow reactor provides data in a reaction rate regime which is generally too slow for ordinary shock tubes, and too fast for isothermal bombs, or even isothermal flow reactors.

A special section is devoted to the discussion of different experimental techniques for obtaining kinetics data. The specific merits and limitations of the adiabatic flow reactor will be discussed in that section.

The purpose of the experimental study was to obtain quantitative information on reaction rate constants as a function of temperature for the homogeneous gas phase decomposition of hydrazine and its methyl derivatives.

The data obtained in this study were used to reach a better understanding of the chemical kinetic mechanisms by which the decompositions proceed, and to compare the kinetic behavior of hydrazine and its methyl derivatives.

Despite all the work done on hydrazine decomposition, the overall mechanism by which this decomposition proceeds is still not understood. For the case of the hydrazine derivatives the situation is even worse.

Though some decomposition mechanisms have been proposed by the various investigators, none of these has been shown to quantitatively predict both the absolute value of the rate constant and overall activation energy, and none of the proposed mechanisms has been shown to be

valid over a wide temperature range. One reason for this difficulty is the great complexity of the free radical mechanisms which govern the decomposition of hydrazine and its derivatives. Generally, it is not possible to reduce the set of differential equations deducible from the mechanism to an analytical expression which may be compared with experimental observations. Rather, it becomes necessary to make further assumptions regarding the behavior of free radicals in order to simplify the algebra to a point where a solution can be obtained (21). Because high speed electronic computers have become available, it is now possible to solve the set of differential equations deducible from the reaction mechanism without making any further assumptions. It is thus possible to obtain exactly the rate constants predicted by the mechanism. The rate constant-temperature plots obtained from the mechanism may then be compared directly with those obtained by experiment. This approach also makes it possible to study the validity of the steady state assumption for the particular mechanism. Unlike simple Arrhenius expressions, which generally are only valid in a narrow temperature range, a complete mechanism can be used with much greater confidence to predict rates over a wide temperature range.

Reaction mechanisms for the decomposition of hydrazine, UDMH, and monomethyl hydrazine were investigated by numerically solving the differential equations determined by the mechanisms. A discussion of suggested mechanisms and results of computations is presented.

In general, the following approach was used: Reaction rates were measured in the flow reactor over a temperature range of some 200 deg. C, and chemical samples were taken at the end of the reaction zone with a water cooled probe. Spectroscopic and other data available in the literature were used to initially establish a mechanism. The differential equations given by the mechanism were then integrated numerically, and the rate constants and stoichiometry predicted by the mechanism were compared with those obtained experimentally. The temperature range of the study was approximately 800 to 1000 deg. K. It is interesting to note that the computations yield concentration-time curves for reactants, intermediates, and products. If these could be measured experimentally, then such data, in conjunction with information presented in this thesis, could conceivably

result in a mechanism which is quantitative and unique.

The material in this thesis is organized into seven main sections. First, a theoretical background is presented. This involves a discussion of molecular structure, and a brief review of the fundamentals of chemical kinetics with particular reference to the validity of the steady state assumption. Second, a discussion of experimental approaches to the study of chemical kinetics and previous work on hydrazine is presented. Laminar flames, shock tubes, isothermal flow reactors and isothermal bombs, flash photolysis, and explosion limit studies are discussed in particular as they pertain to the study of hydrazine and its methyl derivatives. Third, a description of apparatus and of experiments performed in this study is presented. The principle and operation of the adiabatic flow reactor are discussed, and a treatment of the effect which turbulence has on the chemical kinetics measurements is presented. The results of the measurements are then presented and discussed considering such factors as the most appropriate overall order for the reaction. After this discussion, reaction mechanisms for hydrazine and its derivatives are postulated. This section is followed by a discussion of the results of computations performed on the postulated mechanisms. It should be noted that though the experimental data have been reduced using a simple Arrhenius expression, this correlation has been looked upon as empirical. An understanding of the mechanism of decomposition was sought by comparing the computed behavior of various mechanisms with results of the series of experiments performed in this study and the results of other investigations.

As a concluding remark, it should be noted that hydrazine vapor is very explosive and extremely difficult to handle experimentally. Consequently, quite formidable engineering difficulties had to be overcome. The resulting complexity of the experimental apparatus and the severe setbacks in the experimental effort caused by several hydrazine explosions made it quite impossible to attain the high degree of reliability, thoroughness and sophistication of experimental effort which would have been possible if the substance studied had been more reliable and less hazardous and capricious than hydrazine.

## CHAPTER I

### THEORETICAL CONSIDERATIONS

A brief theoretical background is presented. The discussion is organized as follows. First, the electronic and molecular structures of hydrazine, unsymmetrical dimethylhydrazine, and monomethylhydrazine are considered. This consideration is followed by a discussion of the meaning of the Arrhenius expression for elementary reactions. A discussion of elementary reactions in chain processes is then presented, and is followed by a consideration of the validity of the steady state hypothesis for homogeneous gas phase reactions.

#### A. Electronic and Molecular Structure

In a quantum mechanical study of hydrazine, Penny and Sutherland (22) found that the  $(2_s)^2$  shell of the nitrogen atom shows a distinct tendency to break up under the influence of neighboring atoms. Consequently, one has to deal not with a pure configuration  $(2_s)^2 (2_p)^3$  but with a mixture of  $(2_s)^2 (2_p)^3$  and  $(2_s) (2_p)^4$ . Now, if one of the  $2_s$  electrons is removed, there remains the configuration  $(2_s) (2_p)^3$ , identical to that of the tetravalent carbon atom. The four valencies of the carbon atom are disposed tetrahedrally, and their great bonding power arises from the hybridization of the  $2_s$  and  $2_p$  wave functions (23). If the  $2_s$  electron which was removed from the N atom is now restored, not into the  $2_s$  orbit, but into one of the already singly occupied tetrahedral orbits, then an " " atom is obtained with powerful valence bonds along three of the tetrahedral directions, and a pair of electrons of opposite spins occupying the fourth (22). Penny and Sutherland (22) consider a hydrazine constructed from such nitrogen atoms to be the most stable one possible.

The following average bond strengths appear to be applicable to the hydrazine molecule (24):

N - N	60 kcal/mole
N - H	88 kcal/mole

Herzberg (25) gives the following ground state bond distances:

N - H	$r_0 = 1.014 \times 10^{-8} \text{ cm}$
N - N	$r_0 = 1.5 \times 10^{-8} \text{ cm}$

All bond angles are approximately  $108 \pm 10$  degrees (26).

From spectroscopic observations, Fresenius and Karweil (27) conclude that of three molecular structures possible for hydrazine, i.e. the tub form, the seat form, and the totally unsymmetrical form, the one existing at ordinary temperatures is the totally unsymmetrical form. At ordinary temperatures there is no rotation about the N - N bond, but only twisting. Fresenius and Karweil (27) assign to hydrazine a potential barrier for rotation of 6 to 10 kcal, in agreement with the value found by Penny and Sutherland (22) who calculated 0.33 electron volts for the higher barrier. These authors also calculated a smaller barrier of 0.2 ev. The acceptance of this second barrier leads to acceptance of two forms of  $N_2H_4$  which result by rotation of one of the  $NH_2$  groups about the N - N bond.

Modes and frequencies of oscillation for hydrazine as found by Fresenius and Karweil are shown in Figure 1.

An interesting possibility to consider is the migration of H atoms. Thus Audrieth and Ogg (26) state that it is conceivable that hydrazine may exist in a tautomeric amine-imide form  $H_3N \longrightarrow NH$  and that proton migration may have occurred to give a molecule with such a structure. There is some chemical evidence to indicate that such an amine-imide structure is possible for certain hydrazine derivatives. Thus phenylhydrazine undergoes thermal decomposition involving migration of the NH radical from the ortho to the para position, with the formation of p-phenylene-diamine (26).

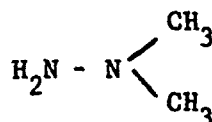
It will be seen later that the migration of hydrogen atoms can result in some interesting reactions.

Now, let us proceed to a discussion of the two methyl derivatives of hydrazine, which are of interest in this study.

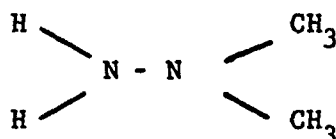
From electron diffraction studies, Beamer (28) determined the following angles and bond distances in unsymmetrical dimethylhydrazine:

C - N	$1.47 \pm 0.03 \text{ \AA}$
N - N	$1.45 \pm 0.03 \text{ \AA}$
N - H	$1.04 \text{ \AA}$ (assumed)
C - H	$1.09 \text{ \AA}$ (assumed)
C - N - C	$110^\circ \pm 4^\circ$
C - N - N	$110^\circ \pm 4^\circ$

An interesting feature of the UDMH molecule is that the masses of  $\text{NH}_2$  and  $\text{CH}_3$  are very much alike, i.e. the ratio of the molecular weights of the two groups is 16:15. If this ratio is compared with 1:15 between hydrogen and  $\text{CH}_3$ , it appears more correct to consider UDMH as a substituted ammonia, rather than as a substituted hydrazine. Thus, UDMH should be written as



rather than as



From the electronic structure considerations for the nitrogen atom, it was found that the N atom has four electron clouds which are qualitatively similar. Of these only three are being used for bond formation. Thus, there appears to be a possibility for resonance, which, together with the short observed N - N bond distance makes it quite likely that the N - N bond is stronger than 60 kcal. Diebeler, Franklin and Reese (29) made electron impact studies of hydrazine, and the methyl substituted hydrazines. From these, they computed the N - N bond in UDMH to be 72 kcal/mole, which tends to confirm the above considerations.

One would expect the bond strengths in monomethylhydrazine to be intermediate between those of hydrazine and UDMH. This expectation is confirmed by Diebeler et al. (29) who give 67 kcal/mole as the strength of the N - N bond in monomethylhydrazine. However, the mechanical and steric structures of monomethylhydrazine should not be treated as simple averages between those of hydrazine and UDMH.

Diebeler et al. (29) find that in monomethylamine the N - C bond is 80 kcal/mole, in dimethylamine 87 kcal, and in trimethylamine 94 kcal. The electron cloud contribution which can be provided by an  $\text{NH}_2$  group is likely to be weaker than that provided by a  $\text{CH}_3$  group. Consequently, one would expect the N - C bond in UDMH to be slightly

weaker than the corresponding bond in trimethylamine, and the N - C bond in monomethylhydrazine to be slightly weaker than the corresponding bond in dimethylamine. The N - C bond strengths for UDMH and monomethylhydrazine were thus estimated to be 90 kcal/mole and 83 kcal/mole respectively.

In summary, the following values of bond strengths appear to be applicable to the methyl derivatives of hydrazine.

UDMH

N - N	72 kcal/mole
N - C	90 kcal/mole
N - H	88 kcal/mole
C - H	98 kcal/mole

Monomethylhydrazine

N - N	67 kcal/mole
N - C	83 kcal/mole
N - H	88 kcal/mole
C - H	98 kcal/mole

It is seen from the above that for all the hydrazines the N - N bond is the weakest.

B. The Arrhenius Expression for Elementary Reactions

The rate constant for elementary reactions may usually be written as

$$k = A \exp [-E/RT]$$

where A is the "preexponential factor" and E is the "activation energy." The meaning of these terms will now be examined.

If a molecule AB has an energy  $E^*$  above the ground state value for the molecule, there is a finite probability that at some time this energy will be concentrated in an A - B vibrational or rotational mode. If  $E^*$  exceeds the A - B bond strength, then such concentration of energy can lead to rupture of the A - B bond, resulting in the reaction



The value of  $E^*$  which is necessary in order that the above process take place is the activation energy E. For a simple molecule, the probability that  $E^*$  exceeds E is  $\exp (-E/RT)$ .

For a diatomic molecule the probability that the vibrational

energy exceeds  $E$  is  $\exp(-E/RT)$  if the vibrational levels are continuous, which is almost true of the very high vibrational levels. If, in addition, the effects of rotation may be neglected, then this pre-exponential factor is the same as vibration frequency, and the rate of decomposition is the product of the vibration frequency and the probability that the vibrational energy exceeds the activation energy.

For a bimolecular reaction



the preexponential factor may be interpreted as the product of collision frequency and a steric factor.  $E^*$  is then the translational kinetic energy released as a result of the collision. In this simplified model, the contributions of initial rotational and vibrational energy of the AB molecule are ignored.

It should be pointed out that in the above models, the chemical processes were assumed to be sufficiently slow so that a Boltzmann energy distribution was always maintained.

Hinshelwood (30) considered the contribution of vibrational and rotational energy to  $E^*$ , and found the probability that  $E^*$  exceeds  $E$  to be given by the expression

$$\frac{(E/RT)^{m-1}}{(m-1)!} \exp(-E/RT)$$

where  $m = n/2 =$  number of degrees of freedom of the molecule and  $n$  is the number of 'square terms' in which the energy of the molecule is distributed. In deriving the above expression, it is assumed that there is free energy transfer between modes. However, the probability that all the 'mechanical' energy of a molecule is available to a particular mode, is less than unity. Thus, the rate constant is properly written as

$$k = \nu PB \exp(-E/RT)$$

where

$$B = \frac{(E/RT)^{m-1}}{(m-1)!}$$

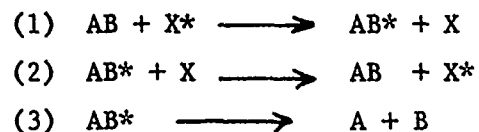
and  $P$  is the probability that the energy contained in the molecule is available in the time  $\tau = 1/\nu$ . For a complex molecule, the number  $B$  is quite large. However,  $P$  is likely to be quite small, so that  $BP$  can have a large range of values.

A more thorough discussion of different models of molecular decomposition is given by Benson (31).

In a gas, the Boltzmann distribution of energies is maintained by collisional energy transfer. Consequently, it appears more correct to write the decomposition reaction



as the result of three reactions, i.e.



Reactions 1 and 2 serve to maintain the Boltzmann energy distribution for the AB molecule, whereas reaction 3 results in the depletion of active AB molecules from this distribution.

It is now possible to speak of 'high pressure' and 'low pressure' limits of quasi-unimolecular processes. Benson (32) distinguishes these as follows:

In the high pressure limit deactivation of active molecules is much more rapid than decomposition, and an equilibrium amount of active species may be assumed to exist. In the low pressure limit, the opposite is true, i.e. the rate of decomposition of active molecules is far more rapid than the rate of deactivation. There is no equilibrium amount of active specie, and practically every activation results in reaction.

At the high pressure limit, the effectiveness with which the third body X transfers energy in a collision is of little consequence. However, at the low pressure limit, the effectiveness of the third body X is of great importance. Also, third body effectiveness is important for determining the pressures at which a reaction behaves in a 'high pressure' or 'low pressure' manner.

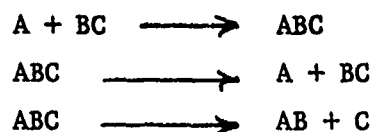
The rapidity of the depletion reaction, 3, also plays an important role in determining whether a particular reaction behaves in the 'high pressure' or 'low pressure' manner. Thus, a very rapid decomposition reaction could result in 'low pressure' behavior even at relatively high pressures.

Considerations similar to the ones discussed above hold for overall bimolecular reactions.

Thus, the reaction



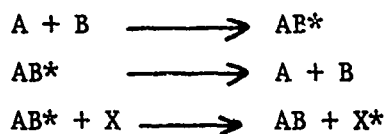
may be written as the sum of the reactions



and the reaction



may be written as the sum of the reactions

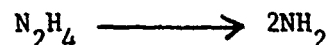


In the following section the elementary reactions of chain processes, i.e. initiation, termination, propagation, and branching will be discussed in the light of the above considerations.

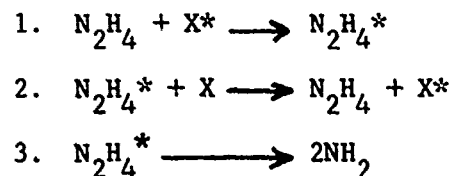
### C. Elementary Reactions in Chain Processes

Chain reactions consist of 4 fundamental types of steps, namely initiation, propagation, branching, and termination. These reactions will now be discussed, with particular reference to the decomposition of hydrazine and its derivatives.

First, consider the initiation reaction for hydrazine decomposition, i.e.



This reaction may be considered to consist of three elementary steps, namely:



At the low pressure limit  $R_3 \gg R_2$ , whereas at the high pressure limit,  $R_2 \gg R_3$  and the rate of decomposition of  $N_2H_4$  is independent of the third body concentration.

First, consider conditions at the high pressure limit.

The rate of decomposition of  $N_2H_4$  may then be written

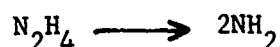
$$\frac{d}{dt}[N_2H_4] = -\frac{d}{dt}[N_2H_4^*] = [N_2H_4^*]$$

where  $k$  is the rate constant of decomposition of the activated complex. It seems that an upper limit on  $k$  would correspond to the vibration frequency of the bond to be broken. For hydrazine, the wave number of the N - N stretching bond is  $850 \text{ cm}^{-1}$  (27). Thus

$$k_{\text{max}} = 2.0 \times 10^{13} \text{ sec}^{-1}. \text{ Then, one may write}$$

$$-\frac{d}{dt}[N_2H_4] = 2.0 \times 10^{13} \times BP \exp\left(\frac{-E}{RT}\right) \times [N_2H_4]$$

Szwarc (13) decomposed hydrazine in a toluene carrier gas in a silica flow reactor. Toluene acted as a scavenger for  $NH_2$  radicals. Consequently, he was able to investigate the reaction



which he concluded to be a homogeneous, unimolecular gas reaction having a rate constant

$$k = 4 \times 10^{12} \exp\left(\frac{-60,000}{RT}\right) \text{ sec}^{-1}$$

Writing

$$k = PB \exp(-E/RT)$$

where  $B$  is the factor accounting for energy available in other modes of the molecule, and  $P$  is the probability that this energy is available in the time  $\tau = 1/\nu$ , it is found that  $BP \sim 0.2$ .

However, Gilbert (20) found that, contrary to assumption, the flow in Szwarc's reactor was not isothermal, but that there must have been a strong temperature effect due to heat transfer in the entrance region of the reactor. Gilbert (20) analytically corrected for the heat transfer effect, and re-interpreted Szwarc's data as favoring a second order formation for  $NH_2$  radicals, rather than a first order formation. Gilbert found a rate constant

$$k = 10^{19} \exp\left(\frac{-60,000}{RT}\right) \text{ cc/mole-sec}$$

which he assumed to be the low pressure value in a quasi-unimolecular rate process.

The question now arises whether the results of Szwarc's measure-

ments, as interpreted by Gilbert, can be applied at the conditions experienced in the Princeton adiabatic flow reactor. In Szwarc's experiment the following values are representative.

Toluene pressure	=	7.6 mm Hg
Hydrazine pressure	=	0.76 mm Hg
Temperature	=	1000°K

In the adiabatic flow reactor:

Nitrogen pressure	750 mm Hg
Hydrazine pressure	10 mm Hg
Temperature	1000°K

A clue to the pressure at which transition from 'low pressure' to 'high pressure' behavior occurs may be found in the results of laminar flame studies.

Thus Gilbert (33) found in the literature that below one atmosphere the laminar flame speed was independent of pressure, while at higher pressures it is inversely proportional to the square root of pressure, indicating an overall first order reaction at higher pressures.

Hydrazine decomposition in the flow reactor was found to be first order with respect to hydrazine. However, the carrier gas concentration was not varied, so there is no way to tell whether the reaction is truly at its high pressure limits or whether it behaves in the low pressure manner, with  $X = N_2 =$  carrier gas.

If the relative third body effectiveness of hydrazine and nitrogen for the initiation reaction is evaluated in the light of relaxation experiments, one would tend to conclude that hydrazine is much more effective than nitrogen, and that hydrazine decomposition should proceed as if the nitrogen were absent. However, laminar flame experiments (34) show that hydrazine decomposition at hydrazine pressures corresponding to its partial pressure in the flow reactor is second order. Thus, it must be concluded that the effectiveness of nitrogen as a third body cannot be ignored. This conclusion is further supported by evidence presented by Bradley (35) who concluded that molecules which are extremely effective third bodies for vibrational relaxation prove to be ineffective in the activation required to promote unimolecular decomposition. Bradley (35) also finds that the

magnitudes of the efficiencies differ in the two cases, the spread being much less with unimolecular reaction processes. Thus it is found (36, 37) that in promoting a typical reaction such as the dissociation of nitrous oxide the efficiency relative to that of the parent molecule ranges from 1.5 in the case of  $H_2O$  to 0.2 for Ar, whereas the efficiency ranges from 1.0 for  $N_2O$  to 100 for  $H_2O$  in the case of simple vibrational energy transfer in the same molecule. From this one can deduce the very important conclusion that trace impurities, which can be very important in relaxation experiments, are likely to be unimportant in determining chemical reaction rate.

Since the effectiveness of nitrogen as a third body is not known, it is not possible to decide whether hydrazine initiation in the flow reactor behaves in a true 'high pressure' manner or whether 'low pressure' behavior with nitrogen as third body is a more correct description of the process. If the nitrogen efficiency is as high as unity, then 'high pressure' behavior would be expected. If, however, such efficiency is as low as 0.2 or 0.1 then 'low pressure' behavior, with nitrogen as the third body would be expected. In the latter case there would be a slight effect of hydrazine concentration on the rate. (It will be seen later that hydrazine decomposition flames were second order at pressures as high as 10 cm Hg. A third body efficiency of nitrogen of 0.1 would make its "effective" pressure 7.6 cm Hg, thus placing the reaction in the 'low pressure' regime. At 1%  $N_2H_4$ , hydrazine pressure is still only 1 cm Hg, thus the slight effect of hydrazine concentration.)

In the light of the information presented by Bradley (35) 'low pressure' behavior with nitrogen as the 'third body' seems to be the most likely process occurring in the flow reactor.

Similar considerations hold for the decomposition of UDMH and monomethylhydrazine.

Termination reactions are reactions of the type



A general, second order termination reaction may be written



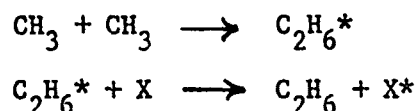
Again, one may visualize a high pressure and a low pressure limit. In

the high pressure regime, deactivation by collision is so rapid that reaction 3 becomes unimportant, whereas in the low pressure limit deactivation by collision is no longer a rapid process, and reaction 2 becomes unimportant. It should also be noted that heteropolar molecules can undergo deactivation by radiation, i.e.



However, such deactivation is likely to be important only at low pressures, since radiation transition times are generally long compared with time between collisions, even at moderate pressures.

It appears that transition from 'low pressure' to 'high pressure' behavior for recombination reactions occurs at much lower pressures than for initiation, or dissociation reactions. Thus, Kistiakowsky and Roberts (38) have measured the high pressure rate constant for the reaction



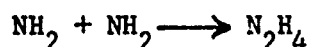
and found its value to be

$$k = 3.7 \times 10^{13} \text{ cc/mole-sec}$$

at 440°K. They found this rate to decrease with pressure below 10 mm. Compare this finding with the results of Gray and Lee (34) who found hydrazine decomposition to be second order at pressures as high as 10 cm.

However, it is not difficult to find an explanation for this difference. A deactivation collision merely requires a molecule, which has a very high probability of being close to the ground state, to be able to receive from AB\* enough energy to deactivate AB\* to AB. In the case of dissociation, the third body, X, must not only be able to transmit its energy to the reacting molecule, but it must also have the necessary energy in the first place. Since most molecules are generally close to the ground state, the requirements for an activating collision are consequently much more severe than for a deactivating collision. Indeed, it seems likely that whereas deactivation of an excited molecule can take place in a few collisions, many collisions are necessary to provide a molecule with its dissociation energy.

Because of the similarity between CH<sub>3</sub> recombination and the reaction



it is reasonable to assume that the rate constant for this reaction will also be approximately  $10^{13}$  cc/mole-sec.

Propagation reactions are reactions of the type

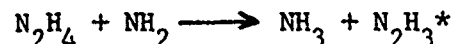


where A and B are free radicals, AA is a reactant molecule, and AB is a product molecule. Again, the reaction proceeds in steps.



This sequence may be visualized as follows: reaction 1 can occur if AA and B possess sufficient kinetic energy between them to overcome the coulombic repulsion. According to Eyring (39) such energy is about 8 kcal/mole. Once AAB is formed, the energy of the bond AB is released to the 'activated complex'. If reaction 2 is exothermic, then the activation energy of the overall reaction could be just 8 kcal/mole. If, on the other hand, reaction 2 is endothermic, then the activation energy of the overall reaction should be that required to overcome the coulombic repulsion plus the difference between the bond energies AA and AB (39). However, this model must be used with great caution, as it has been demonstrated (40) that such thermodynamic considerations alone cannot always account for the magnitude of activation energies.

It may be worth remarking that the product molecules can be formed in states which are vibrationally or electronically excited. Thus it is possible to have a reaction

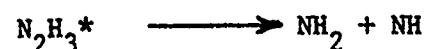


where the  $N_2H_3^*$  radical is formed in an excited state.

Branching reactions are reactions in which a radical can react, in a single step, to form two or more radicals, thereby continuing the chain, and starting a new one (41). This can occur by simple, unimolecular decomposition of a radical, like



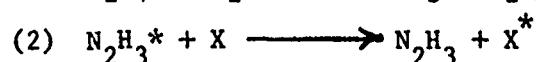
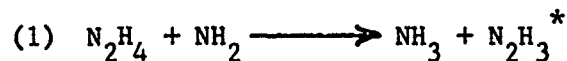
or in a bimolecular decomposition, like



or the branching reaction may result from the interaction of a free radical and a reactant molecule, like



Another possibility was suggested by Ramsay (14) for hydrazine decomposition, namely:



It is seen that in this case even an inert third body can play a role in determining the rate of the branching reaction.

In the above discussion, a brief review of the elementary reactions of chain processes was presented, and is to serve as background for postulating reaction mechanisms. For a thorough discussion of chain reactions reference is made to Semenov (42), and to the works cited above.

#### D. The Steady State Approximation

In analyzing chain mechanisms in the past, it has been customary to resort to the stationary state hypothesis, which states (43) that after a brief initial period, the concentration of activated molecules reaches a state where the concentration of active species is independent of time, except in so far as the concentrations of reactant and product molecules depend on time. The validity of this hypothesis will now be examined. Three regimes will be considered.

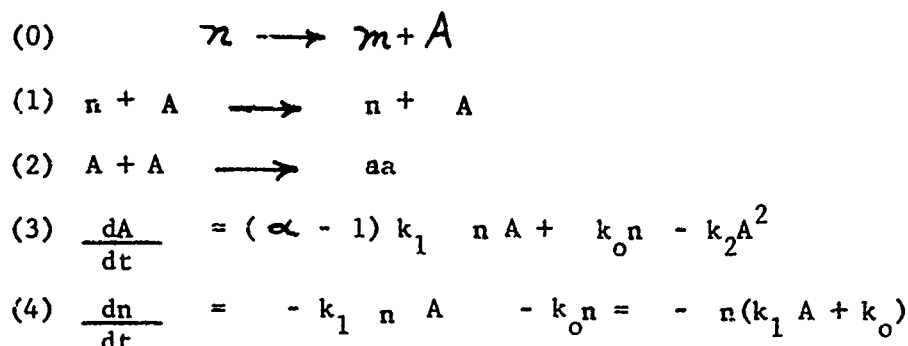
- A. Moderate temperature with a large amount of branching.
- B. Very high temperatures.
- C. Low to moderate temperature with either no branching at all, or a small amount of branching.

Reference is made to the Christiansen-Kramers expression for reaction rate (43)

$$-\frac{dn}{dt} = \frac{k_1}{(k_4/k_3)} \frac{n^2}{n + (1 - \alpha)}$$

where  $\alpha$  is the number of active particles produced when an active particle collides with an ordinary molecule. Chain branching reactions correspond to  $\alpha > 1$ . If  $\left(\frac{k_4}{k_3}\right)n \sim 1$  the denominator can ap-

proach zero, or even become negative. The former case implies a very rapid reaction whereas the latter merely means that the steady state hypothesis is invalid. However, it was assumed in the derivation of the Christiansen-Kramers expression (43) that deactivation of active particles proceeds through collisions with reactant molecules. Generally, recombination reactions involve two, rather than one active particle. Thus one may write



It is clear that as reaction proceeds, the value of  $n$  decreases monotonically, and shortly after  $A$  reaches its peak concentration i.e. when  $\frac{dA}{dt} = 0$ , the first two right hand terms in

Equation 3 will decrease below the value of the third term, and  $\frac{dA}{dt}$  will become negative.

Now, consider the case when the temperature is moderate, but there is a large amount of branching. Since initiation reactions generally have a very high activation energy, it is likely that  $k_0$  will be small. The rate equations may then be written as follows:

$$\begin{aligned}
 \frac{dA}{dt} &= (\alpha - 1) k_1 n A - k_2 A^2 \\
 \frac{dn}{dt} &= -k_1 n A
 \end{aligned}$$

The first of these equations may be re-written as

$$k_2 A^2 - (\alpha - 1) k_1 n A + \frac{dA}{dt} = 0$$

The steady state hypothesis requires that it be permissible to approximate the above as

$$\begin{aligned}
 k_2 A^2 &= (\alpha - 1) k_1 n A \\
 A &= (\alpha - 1) k_1 / k_2 \quad n
 \end{aligned}$$

But if  $k_1$  and  $\alpha$  are very large, then

$$\frac{dA}{dt} \approx (\alpha - 1) k_1 n A$$

in the initial phase of reaction. Since,  $k_1$  is large,  $dn/dt$  is also large, and by the time  $dA/dt$  approaches zero, a significant amount of reactant has already been consumed. Also, the concentration of A is now so high that  $-dn/dt$  is very large, and in the second phase of the reaction

$$\frac{dA}{dt} \approx -k_2 A^2$$

Since  $n$  has decreased very rapidly.

Thus it is seen that in the case of a rapid branching reaction the steady state hypothesis may not be applied, even though the reaction rate always remains finite. Semenov (44) has given the term "degenerate branching" to the case discussed.

At high temperatures without branching the situation is very similar, only there the initiation reaction plays the dominant role.

By a process of elimination it is seen that the steady state hypothesis can only apply to cases where the amount of branching is small, and where the initiation reaction is slow compared with the propagation reactions. In such a case the concentration level of free radicals will be low, and will be reached before a significant amount of reactant has been used up.

For such a case

$$\frac{dA}{dt} = k_1 (\alpha - 1) A - k_2 A^2 + k_0 n$$

$$\frac{dn}{dt} = -n(k_0 + k_1 A) \approx -n k_1 A$$

If an expression for  $A$  can be obtained, it is then possible to obtain an explicit expression for the reaction rate. Solution of the first equation for  $A$  yields

$$A^2 = \left( \frac{k_1 (\alpha - 1) + k_0}{k_2} \right) n - \frac{1}{k_2} \frac{dA}{dt}$$

$$A = \left[ \left( \frac{k_1 (\alpha - 1) + k_0}{k_2} \right) n - \frac{1}{k_2} \frac{dA}{dt} \right]^{1/2}$$

In essence, the steady state approximation assumes the second term in

the expression on the previous page to be small compared with the first. This requirement is far less stringent than the requirement than  $dA/dt = 0$ . If it is satisfied, then

$$A = \left[ n \frac{k_1 (\alpha - 1) + k_0}{k_2} \right]^{1/2}$$

and

$$\frac{dn}{dt} = -k_1 n^{3/2} \left[ \frac{k_1 (\alpha - 1) + k_0}{k_2} \right]^{1/2}$$

Several limiting cases may now be considered. If there is no branching, then

$$\frac{dn}{dt} = -n^{3/2} k_1 \sqrt{\frac{k_0}{k_2}}$$

If, on the other hand, the initiation reaction is unimportant, and the main free radical supply is by branching, then the expression for the rate becomes

$$\frac{dn}{dt} = \frac{3}{2} n^{1/2} k_1 \left[ \frac{k_1 (\alpha - 1)}{k_2} \right]^{1/2}$$

Note that the reaction rate never becomes infinite because, in the cases treated, the branching is first order, whereas the termination is second order. This type of "degenerate" branching was the kind encountered in the mechanisms postulated for the decomposition of hydrazine and its derivatives.

In summary, the steady state hypothesis can only be applied when the "steady state" concentrations of free radicals are sufficiently low that they can be produced without a significant consumption of reactant, and when almost all the reactant is consumed by propagation reactions. It might be remarked that the implication of the steady state hypothesis is not that the free radical concentrations stay constant, but merely that the concentration of active species depends on time only insofar as the concentration of reactant molecules depends on time. Thus, the steady state approximation merely requires that

$$\frac{dA}{dt} \ll k_1 n A$$

which is not as stringent as

$$\frac{dA}{dt} = 0$$

Computations on free radical mechanisms show that the inequality can be satisfied for some reactions, whereas the equality to zero is never true for more than an instant.

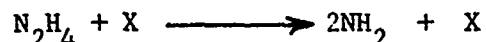
Another difficulty with applying the steady state hypothesis is that many mechanisms of practical interest are so complex that an explicit solution for the reaction rate cannot be obtained without introducing many questionable assumptions.

## CHAPTER II

### EXPERIMENTAL METHODS USED FOR THE STUDY OF CHEMICAL KINETICS

Two fundamentally different approaches to the study of chemical kinetics are known. On one hand there is the study of individual free radical, or elementary reactions by such techniques as electron beam or free molecule beam experiments. On the other hand, there is the study of overall reactions under different experimental conditions. The overall rate data obtained may then be used for gaining understanding of the reaction mechanism.

It might be noted that under suitable conditions, this second approach can be used to study elementary reactions. Thus Szwarc (13) used a flow reactor to study the reaction



In the research conducted by the author, overall reaction rates were studied, and the rate data thus obtained were used for gaining understanding of reaction mechanisms. On one hand, empirical expressions for overall behavior of the reactions studied can be of practical value. On the other, understanding of the overall mechanisms of reaction was of considerable interest.

Partly because of the above considerations, the following discussion will be restricted to some of the better known overall approaches to the study of chemical kinetics. These will be discussed in terms of experiments performed on hydrazine, UDMH or monomethylhydrazine.

It is possible to classify kinetics experiments into many different categories, depending on the particular properties which are of primary interest.

Thus one may speak about experiments for studying fast reactions as compared with those used to study slow reactions. Or experiments may be grouped into one class if they all maintain a particular physical property constant. One may speak of isothermal or adiabatic reactions, and of constant volume or constant pressure processes. Or experiments may be classified into the ones which involve steep gradients of temperature and concentration, and the ones where such gradients are shallow.

Of course, kinetics experiments must also be classified ac-

according to whether the reaction takes place in the gas, liquid, or solid phase, or at an interface. However, gas phase reactions are of primary interest in this study, and reactions in other media will only be discussed insofar as they throw light on gas phase reactions, or if consideration of such reactions is necessary to understand a reaction which is believed to take place in the gas phase.

In the following discussion no particular attempt to classify the different experiments into a few large groupings has been made. However, their similarities will become apparent from the discussion. Flash photolysis and ignition limits experiments are discussed. This is followed by a discussion of shock wave experiments and laminar flame studies. Then isothermal bombs and isothermal flow reactors are discussed. Finally, a brief treatment of surface reactions is presented. The inclusion of surface reactions is due to the important role that container walls may play in studies of gas phase reactions. The Princeton adiabatic flow reactor is discussed in a separate section.

#### A. Flash Photolysis

Two types of photolysis are possible. The substance of interest may be exposed to radiation in a narrow frequency range, designed to break a specific bond, or the species under consideration may be subjected to white light continuum radiation. The latter method is used in flash photolysis. In flash photolysis, low pressure gas in a transparent container is exposed to radiation from an electric discharge having a duration of the order of a millisecond. Subsidiary flashes may then be put through the photolysis tube timed at various short intervals. The absorption spectrum of these subsidiary flashes may then be analysed for bands characteristic of free radicals.

One difficulty with the method is that quite high temperatures may be reached, and the phenomena occurring are often difficult to interpret (45). Another difficulty encountered if flash photolysis results are to be used for the interpretation of thermal reactions, is the presence and reaction of electronically excited species (46).

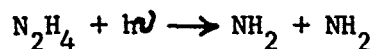
It is of course possible to combine the flash photolysis approach described above with chemical analysis of reaction products, or with some other measure of the reaction rate, such as might be obtained from the pressure rise in the container.

The latter approach was followed by Ramsey (14). Ramsey (14)

introduced anhydrous hydrazine at 8 mm pressure into his absorption tube. The hydrazine vapor was then subjected to flash photolysis.  $\text{NH}_2$  bonds in the region 4500-7500  $\text{\AA}$ , and NH bonds near 3600  $\text{\AA}$  were observed, and the pressure in the system after photolysis was approximately doubled. An infrared spectrum of the products in the region 2-15 microns indicated that 80% of the hydrazine had decomposed. The ammonia and hydrazine were condensed with liquid air, and the residual gas was shown by mass spectrometer analysis to consist of hydrogen and nitrogen in the ratio  $\text{H}_2/\text{N}_2 = 1.5$ .

Ramsey (14) further found that if an excess of helium (100 mm) were added to the hydrazine (8 mm), and the mixture was subjected to photolysis, no  $\text{NH}_2$  and NH spectra were observed, and no appreciable decomposition of hydrazine took place.

Ramsey postulates the following reactions



and suggests that the decrease in the overall reaction and the reduction in the intensity of the NH and  $\text{NH}_2$  absorption spectra by addition of small amounts of helium may be due to stabilization of the  $\text{N}_2\text{H}_3$  radical by collision.

It is interesting to note that Gunning (47) found the  $\text{N}_2\text{H}_3$  radical to be quite stable at room temperature. This observation suggests the possibility that the  $\text{N}_2\text{H}_3$  radical is formed in a vibrationally excited state, from which it may either decompose or become deactivated by collision.

In the later discussion, it will be seen that results obtained in the Princeton adiabatic flow reactor do not contradict Ramsey's hypothesis.

#### B. Ignition Limits Experiments

According to the theory of thermal explosion, an explosion occurs when the amount of heat developed by chemical reaction exceeds the heat which can be transferred out through the walls of the vessel. Frank-Kamenetski (48) developed the heat balance equations for the case of pure conduction. He found that explosion occurs if a non-dimensional parameter  $\delta$  exceeds a certain maximum value, where

$$\delta = \frac{Q}{\lambda} \cdot \frac{E}{RT_0} \cdot r^2 Z C^m e^{-E/RT_0}$$

The maximum value for  $\delta$  is calculated theoretically by Frank-Kamenetski (48) and is found to be 2.0 for a cylindrical vessel and 3.32 for a spherical vessel.

Gray and Spencer (49) used the Frank-Kamenetski theory to interpret the results of their ignition experiments. Gray and Spencer determined the critical pressure limits of spontaneous ignition by measuring the total pressure of reaction mixture necessary for ignition on admission to a hot vessel at a given temperature.

The theory was developed for heat conduction from the gas to a cold wall, whereas heat is transferred from a hot wall to the cool gas in the Gray and Spencer experiments. In this case it would seem that ignition occurs if heat generation in the gas layer next to the wall exceeds the rate at which heat can be conducted into the interior cool gas. However, this process is very similar to what is assumed in the Frank-Kamenetski theory. Also, the fundamental physical parameters, except the radius, are the same. Thus it is not surprising that the Frank-Kamenetski theory does correlate the results of ignition limits experiments of the kind conducted by Gray and Spencer. The value of

$\delta$ , however, must not be expected to be that calculated theoretically.

Obviously, ignition limits experiments only have meaning for gas phase reactions insofar as catalytic initiation of the wall surface is unimportant.

The Frank-Kamenetski expression may be re-written as

$$\frac{C^m}{T^2} = \left( \frac{\delta \lambda R}{Q r^2 Z E} \right) \exp(E/RT)$$

But  $C = n/V$ , and for an ideal gas

$$PV = nRT \text{ and } C_i = \frac{P_i}{RT}$$

It follows that for a first order reaction, one may write

$$\ln \left( \frac{P_1}{T^3} \right) = \frac{E}{RT} + \ln \left( \frac{\delta \lambda R^2}{Q r^2 Z E} \right)$$

If the second term on the right had is assumed to be approximately con-

stant, then an activation energy may be obtained by plotting

$\ln (P_1/T^3)$  versus  $1/T$ . For UDMH decomposition, Gray and Spencer found the activation energy to be  $28 \pm 1$  kcal/mole.

### C. The Laminar Flame

The laminar flame is a steep gradient device, it is isobaric, and may be used to study reactions generally classed as being rapid.

The laminar flame has been studied extensively. It can be used for kinetics purposes in two ways, namely it may be observed spectroscopically to yield information on the free radicals taking part in the reaction, and it can be made to yield an "activation energy" of the chemical reaction.

Spectroscopic studies of laminar flames will be discussed first. Hall and Wolfhard (12) studied hydrazine decomposition flames at subatmospheric pressures. Spectroscopic work by these authors indicates strong emission of "ammonia alpha bands" attributed to  $\text{NH}_2$  radicals, and weaker emission at 3360 angstroms attributed to  $\text{NH}$  radicals. The pure decomposition flames are yellow-brown in color and of low luminosity; there is an after glow of the same color but with lower intensity.

It is seen that both  $\text{NH}_2$  and  $\text{NH}$  radicals play a role in hydrazine decomposition, and that the  $\text{NH}_2$  radicals are the more abundant ones.

Further usefulness of the laminar flame for kinetics purposes stems from the fact that the flame speed, and its variation with flame temperature, may be used to deduce an activation energy.

The flame speed is affected by the chemical heat release of the reaction, the heat capacity of the mixture, the conduction and diffusion of heat, diffusion of active species, and possibly the back diffusion of products. Thus the processes which determine the laminar flame speed are many and complex.

If both the reaction mechanism and the transport properties are known with reasonable certainty, this information may be used to predict temperature and concentration profiles, and ultimately the laminar flame speed. Information obtained in the Princeton study of hydrazine may be useful for a detailed numerical analysis of hydrazine flames.

The other two approaches to analysis of laminar flames, which will be briefly discussed in what follows, are the simple thermal

theory and Van Tiggelen's active particle diffusion theory. Use of these theories to interpret hydrazine flame speed data will also be discussed.

In the simple thermal theory of flame propagation the following assumptions are made: (1) the flame is one-dimensional, (2) it is steady with respect to time, (3) velocity gradients may be neglected, hence viscosity terms in the momentum equation may be ignored, (5) the effect of gravitational and other similar fields may be ignored, (6) the loss of energy by radiation is negligible, (7) the hot boundary for the flame reaction zone is assumed to be the condition of thermodynamic equilibrium at the adiabatic flame temperature, (8) the reaction rate is described by

$$w = A \exp \left[ \frac{-E}{RT} \right]$$

(9) diffusion is important only as it affects the energy balance, (10) specific heat and thermal conductivity are constant throughout the reaction zone, (11) the thermal diffusivity is equal to the molecular diffusivity, (12) the total number of molecules is constant.

If it is further assumed that the flame can be split into a preheat zone in which no chemical reaction occurs, and a reaction zone in which the net energy loss due to mass transfer may be neglected in comparison with the chemical reaction and heat conduction terms, the following expression for the flame speed may be derived:

$$u = \frac{k}{\rho C_p} \frac{1}{T_m - T_o} \sqrt{\int_{T_i}^{T_m} \frac{2\rho Q\alpha}{k} dT}$$

where  $k$  is thermal conductivity

$C_p$  is heat capacity

$\rho$  is density

$$\rho\alpha = w = A \exp \left[ \frac{-E}{RT} \right]$$

$Q$  = heat release due to reaction

$T_i$  = inflection point temperature

$T_m$  = mean flame temperature

$T_o$  = initial temperature

$T_f$  = final temperature

Setting  $T_m = T_f$   
 $T_i = T_o$

the following expression is obtained

$$u = \frac{k}{\rho_o C_p} \frac{1}{T_f - T_o} \sqrt{\int_{T_o}^{T_f} \frac{2\rho_o \alpha}{k} dT}$$

The above development is derived in detail in Emmons (50).

Adams and Stocks (8) use an integrated version of the above expression, i.e.

$$S^2 = \left[ \frac{2\lambda}{\rho_o L} \cdot \frac{(RT_f^2)^2}{E (T_f^2 - T_o^2)} \right] B \exp \left[ \frac{-E}{RT} \right]$$

where  $\lambda$  is thermal conductivity

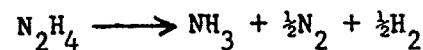
$L$  is the heat of reaction

$\rho_o$  is the initial density of the vapor.

If the assumption is made that the determining process in flame propagation is heat transfer, then it is permissible to deduce an overall activation energy for the chemical reaction from flame speed measurements. If, however, diffusion of active species is the dominant process, the situation is far more complex, and one can no longer expect an activation energy deduced from laminar flame studies to be applicable to the chemical reaction under other experimental conditions.

Let us proceed to consider some hydrazine flame experiments which were analyzed on the basis of the simple thermal theory.

Murray and Hall (7) measured flame speeds in hydrazine, and in hydrazine-water mixtures. They also analyzed the reaction products, and found that these pointed to a reaction

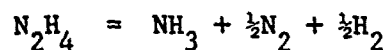


Adams and Stocks (8) measured the rate of burning of hydrazine-water mixtures in capillary tubes in a nitrogen atmosphere, and prepared an Arrhenius plot of the data of Murray and Hall (7) and Adams and Stocks. The slope of their curve gives the apparent activation energy of the reaction which decreases with decreasing temperature from 45 kcal/mole at 1950°K to some 30 kcal/mole at 1400°K.

Gray, Lee, Leach and Taylor (9) used two experimental methods

for the study of hydrazine decomposition. In one case, gaseous hydrazine was introduced into a squat glass cylinder 20 cm diam., 20 cm depth, which contained two tungsten electrodes at the center. As the flame travels to the walls, the pressure rises, and both the burned and unburned gases are compressed. As a result, the movement of the flame depends on both the burning rate and the gas flow. However, during the initial phase of the combustion, the increase in pressure is small, and the linear speed of the flame,  $S_L$ , is very close to the speed relative to the burned gas,  $S_D$ . Even when the radius of the flame sphere is 0.3 times the radius of the vessel, the pressure has risen only 3% and  $S = .98 S_D$ . The pressure range which can be studied in a glass vessel extends from very low values up to about 10 cm Hg.

The second method used by Gray and Lee (9) involved the burning of liquid hydrazine in narrow tubes, in a pressure range between 10 cm Hg and 76 cm Hg. The products from the decomposition flame of liquid hydrazine were unaffected by changes in pressure, and corresponded closely to the equation:



However, Gray and Lee (9) did find a small decrease in flame speed at pressures below 5 cm Hg. This they attribute to their method of measurement.

In the thermal theory at laminar flame propagation the flame speed varies with pressure as

$$S \sim P^{\left(\frac{n-2}{2}\right)}$$

where  $n$  is the overall order of the chemical reaction. Thus the pressure independence of flame speed observed by Gray and Lee indicates a second order reaction for hydrazine decomposition.

Using Semenov's flame theory, Gray and Lee (9) found an activation energy of 36 kcal/mole.

Gilbert (33) found in the literature that below one atmosphere, the normal flame speed was independent of pressure while at higher pressures it is inversely proportional to the square root of pressure, indicating an overall first order reaction at higher pressures.

The other approach to a chemical interpretation of laminar flame data is by way of VanTiggelen's active particle diffusion theory.

VanTiggelen (51) states that the flame propagates because

active particles diffuse upstream where they engage in propagation, branching, and termination reactions. Apparently, the initiation reactions take place in the very hot downstream part of the flame.

The equation of Smoluchowsky gives the total number of collisions  $Z_t$  when a particle diffuses over a given linear distance  $d$ :  $Z_t = 3 d^2 / 4 \lambda^2$

Then, VanTiggelen (51) goes on to say that in order to compensate all losses, each chain carrier has to diffuse over a distance  $d$ , such that branching occurs once. Then

$$Z_t (v - \beta) = 1 = 3 \pi d^2 (v - \beta) / 4 \lambda^2$$

For a normal flame front, the flame speed  $V$  is equal to  $d/t$ , thus

$$V = c \sqrt{(\pi/3)(v - \beta)}$$

where

$$c = \sqrt{8RT/\pi M}$$

and

$$V_0 = VT/T_0$$

it follows that

$$V_0 = 2T_0 \sqrt{(2R/3MT)(v - \beta)}$$

where  $M$  is the mean molecular weight of chain carriers.

According to VanTiggelen (51), this relation is the basic expression of burning velocity. Next, VanTiggelen goes on to neglect beta, and to write  $v$  in terms of an Arrhenius expression. Then:

$$V_0 = 2T_0 \sqrt{2R/3MT} \sqrt{[A]^a [B]^b e^{-E/RT} \rho^{(a+b)}}$$

where  $A$  and  $B$  are reacting species.

One may question VanTiggelen's assumption that chain branching species are the only ones whose diffusion is important. Surely, it is possible for laminar flames to propagate in mixtures which react in a straight (non-branching) manner. Thus it seems that the interpretation of 'activation energy' measured in laminar flames still is not quite clear.

VanTiggelen and De Jaegere (11) measured flame speeds in premixed laminar flames of hydrazine and inert, and also in hydrazine, inert, and oxidizer. In keeping with VanTiggelen's theory, they found

that their results on hydrazine flames could be correlated by the expression

$$u = \frac{K}{\sqrt{T}} \sqrt{f(\%) \exp\left(\frac{-E}{RT}\right)}$$

where  $T$  is the proper mean flame temperature, and  $f(\%)$  is the initial mole fraction of hydrazine.

VanTiggelen and De Jaegere (11) found an apparent activation energy of 28 kcal/mole. They also found that this activation energy did not change whether they had to do with a decomposition flame or a combustion flame, and that in the case of the combustion flames it was independent of the nature of the oxidant.

In summary, the following information about hydrazine decomposition has been obtained from laminar flame speed measurements.

From spectroscopic observation of flames, one may conclude that the radicals  $\text{NH}_2$  and  $\text{NH}$  are present.

The stoichiometry of hydrazine decomposition follows the path.



The adiabatic flame temperature in this case is  $1660^\circ\text{C}$  (7).

The following activation energies for hydrazine decomposition have been deduced from flame speed measurements: On the basis of the data of Murray and Hall (7) and Adams and Stocks (8), Adams and Stocks found a curve which decreased with decreasing temperature from 45 kcal/mole at  $1950^\circ\text{K}$  to 30 kcal/mole at  $1400^\circ\text{K}$ . Gray, Lee, Leach, and Taylor (9) report an activation energy of 36 kcal/mole, and VanTiggelen and De Jaegere (11) report 28 kcal/mole.

The last authors used VanTiggelen flame theory, and interpret their activation energy as pertaining to a branching reaction important in hydrazine decomposition.

The other flame experiments were interpreted on the basis of thermal theory, thus giving an "overall" activation energy of the reaction.

However, it should be noted that the relations between activation energy and flame speed given by the two theories are both of the form.

$$u = Kf(T, C) \sqrt{\exp\left(\frac{-E}{RT}\right)}$$

where  $f$  is a relatively weak function of temperature and concentration. Thus the difference of the thermal theory approach and the diffusion theory approach does not really lie in how activation energy is related to flame speed, but rather in how the activation energy deduced from flame speed measurements should be related to the mechanism of the chemical reaction.

Since the interpretation of flame speed measurements is uncertain because of the importance of diffusion in flames, a way to resolve the difficulty would be to study the chemical reaction under conditions where diffusion is not important. This is one of the thoughts which lead to the construction of the Princeton adiabatic flow reactor in which heat transfer to the unreacted gas and back diffusion of active species are rendered negligible.

#### D. Shock Tube Studies

Shock tubes have been used extensively for the study of chemical kinetics. One reason for their usefulness in kinetics studies is that changes in physical properties through the shock are so rapid that chemical reactions can be safely assumed not to take place until after the shock front. Thus Hornig (53) describes the shock front as acting as "a 'switch' by which the temperature, pressure, density, and flow velocity can be changed instantaneously." Of course, the thickness of shock waves is finite, and it would be worthwhile to inquire into typical values of shock front thickness, and number of collisions in the shock wave. Greene and Hornig (53) studied the shape and thickness of shock fronts in argon, hydrogen, nitrogen, and oxygen. They found that the number of collisions through the shock front is generally less than 30, and that the shock wave thickness is generally less than 0.002 mm. The Mach number range of the investigation was approximately 1.1 to 2.1. The pressure was approximately an atmosphere.

Thus, the number of collisions through the shock wave is very small compared with the pre-exponential factors in most chemical reactions.

For the case of no chemical reaction, the overall process in a shock wave may be thought of as occurring in two stages, i.e. (a) an initial compression in the shock front during which no internal degrees of freedom are excited, and (b) a subsequent relaxation during which the density changes from that characteristic of the unrelaxed state to that of the completely equilibrated state (53).

For a gas at atmospheric pressure and 300°K, Hornig (52) finds that the initial compression occurs in about 10 collisions or about  $10^{-9}$  seconds. He also finds that at least at low temperatures, rotational equilibration takes place in about 10 collisions, except in hydrogen where it takes about 350 collisions. Thus the initial compression and rotational relaxation takes place in times measured in millimicroseconds. Chemical reaction rates which are of interest in propulsion have transient response times measured in microseconds, and overall reaction times measured in milliseconds. Thus it is perfectly justifiable to consider the initial compression and the rotational relaxation to be instantaneous. However, vibrational relaxation may not be dispensed with so easily. Kantrowitz (54) measured vibrational relaxation in  $\text{CO}_2$  at temperatures close to 100°F and at pressures close to atmospheric. He found relaxation times to be in the order of 3 microseconds, and requiring somewhat above 30,000 collisions. There is thus the possibility that initially the chemical reaction is taking place in a gas whose internal degrees of freedom are not fully relaxed.

Jost (15) studied hydrazine decomposition in a shock tube. He spectroscopically measured the decay of hydrazine concentration behind the shock front. Jost (15) presents an Arrhenius plot of the half-lives of the reaction. From this he deduces an activation energy of 43 kcal/mole. Jost's plot of half life vs.  $1/T$  is reproduced in Figure 2.

One of the limitations of the shock tube is that it can only be used to study relatively rapid reactions. This is because the time during which the stagnant region behind the reflected shock is undisturbed is relatively short. At higher temperatures the useful time is also short because for long times heat losses become important, and conditions in the stagnant region are no longer uniform, making it difficult to interpret the results.

#### E. Isothermal Bombs

Whereas shock tubes are most useful for studying rapid reactions, isothermal bombs are best adapted to the study of slow reactions.

Isothermal bomb experiments are among the oldest techniques employed in the study of chemical kinetics. The reactants are placed in a bomb which is immersed in a constant temperature bath, and the

progress of reaction is measured either by the rate of change of pressure at constant volume, or by the rate of change of volume at constant pressure. As will be evident shortly, the rate of heat release due to chemical reaction must be quite small in an isothermal bomb. The temperature equations for the bomb are shown below. Heat release due to chemical reaction:

$$\left(\frac{\partial T}{\partial t}\right)_{\text{CHEM}} = \left(\frac{\Delta H}{\rho C_p}\right) [C]^n B e^{-E/RT} \quad (1)$$

Heat loss by conduction:

$$\left(\frac{\partial T}{\partial t}\right)_{\text{COND.}} = \left(\frac{k}{\rho C_p}\right) \nabla^2 T \quad (2)$$

Overall equation:

$$\left(\frac{\partial T}{\partial t}\right) = \left(\frac{\Delta H}{\rho C_p}\right) [C]^n B e^{-E/RT} + \left(\frac{k}{\rho C_p}\right) \nabla^2 T \quad (3)$$

Steady state equation:

$$\nabla^2 T + \left(\frac{\Delta H}{k}\right) [C]^n B e^{-E/RT} = 0 \quad (4)$$

where

- T is the temperature in degrees
- t is time
- $\Delta H$  is the enthalpy of reaction, in calories per gm.-mole-degree
- $C_p$  is the heat capacity at constant pressure in calories per gm.-mole-degree
- $\rho$  is the density in moles per liter
- [C] is the concentration in gm.-mole per liter
- $e^{E/RT}$  the temperature coefficient of the chemical reaction
- $[C]^n B e^{E/RT}$  is the chemical reaction rate as represented by a simple Arrhenius type expression
- k is the effective thermal conductivity of the substance in the bomb

If the uniform temperature assumption is to be valid, it is necessary that  $\nabla^2 T \sim 0$  in the bomb. It then follows from Equation (4) that the following must hold:

$$\left(\frac{\Delta H}{k}\right) [C]^n B e^{-E/RT} \sim 0 \quad (5)$$

For reactions which are of interest in propulsion  $\Delta H$  is large. It follows that optimum conditions for an isothermal bomb experiment involve minimum concentration of reactant, maximum conductivity of the reacting mixture, and usually low temperature. Ideally, a mixture composed of a small amount of reactant in an inert of high conductivity, such as helium, should be studied at a low temperature. Of course, it may be quite possible to achieve  $\nabla^2 T \sim 0$  by merely making one or two of the terms in Equation (5) small.

A different way of achieving an almost constant temperature is to use a bomb of very small diameter, in which case even a moderately large temperature gradient will only give a small overall temperature variation.

The differential equation of heat conduction in an infinitely long cylinder with heat generation by first order chemical reaction was solved by Nichols and Presson (55). Some of the results of these authors are reproduced in the following. Figure 3 shows the temperature distribution as a function of the radius at various time intervals during the reaction. A 2" diameter solid was studied.

Though Presson's calculations were made for a cylindrical solid, his results are perfectly valid for a gas in a long cylinder, provided heat transfer is by conduction.

Of course it may be argued that in the gas phase, or liquid phase "isothermal" bomb, heat transfer is not only by conduction, but by convection as well, and that consequently the temperature profiles in the bomb will be different, and smoother, than those calculated by Presson. However, the purpose of this discussion is not to present an exhaustive study of isothermal bombs, but merely to review their principle and general problems. So, this condition will not be treated.

Thomas (16) measured the decomposition reaction rate of hydrazine by measuring the rise of pressure in a constant volume bomb, into which small quantities of liquid hydrazine had initially been

introduced. The whole bomb was immersed in a constant temperature bath.

One of the difficulties with this apparatus was that the time required to reach temperature equilibrium in the bomb was of the same order of magnitude as the reaction time. But if uniform temperature conditions are to be maintained, it is necessary that the process of temperature equalization by conduction-convection be much more rapid than any temperature rise produced by chemical reaction. Since this condition was not satisfied in Thomas's experiment, the temperature in his bomb was probably not uniform.

Thomas (16) introduced some liquid hydrazine into his bomb which was then closed and placed in a constant temperature bath. Then the pressure in the bomb was measured as a function of time. Thomas varied the amount of liquid charged to his bomb from 8 ml. to 28 ml. (The total bomb volume was 36 ml.) For all cases he measured the rate of pressure rise at 500 psi, and found that there was no deviation in this rate due to changes in volume of the initial liquid charge. This shows that the decomposition does not proceed in the liquid phase, for if it did, the rate of pressure rise would be a function of the liquid volume. But let us note that when the amount of liquid introduced into the cylindrical bomb is varied the area of the liquid-vapor interface remains constant so that a reaction whose rate is controlled by a vaporization step would also behave in the manner observed by Thomas.

Now, let us proceed to consider an isothermal constant pressure experiment on hydrazine decomposition. Such an experiment was performed by Lucien (17).

Lucien (17) studied the isothermal, constant pressure decomposition of hydrazine and of hydrazine-ammonia mixtures. His apparatus consisted of a J tube immersed in a constant temperature bath. The bottom of the J was filled with mercury. The upper part of the short leg was the reaction chamber and in the long leg a constant nitrogen pressure was maintained above the mercury column.

Lucien used J tubes of very small diameters (his I.D.'s were 3.00, 5.00, 5.56 and 7.00 mm.) Also, he allowed longer time for thermal equilibrium to be established than did Thomas. Generally,

his reaction times were in tens of minutes for a vessel of larger diameter. Consequently, the uniform temperature assumption in Lucien's (17) experiment is likely to be much better than in the constant volume bomb experiment performed by Thomas.

In the Lucien (17) experiment, liquid reactant was introduced above the mercury in the short leg of the J. As reaction proceeded, a vapor space was formed above the liquid. The progress of reaction was then measured by observing the change in height of the mercury column. According to Lucien, the initial gas space is formed by the vaporization of hydrazine and ammonia. Lucien (17) found that, after an initial changing part, the total reaction rate remained constant with time. With the progress of time, the vapor space above the liquid increased. Lucien assumed that the partial pressure of hydrazine in the gas phase was equal to its vapor pressure. At constant temperature and constant partial pressure of reactant the rate of change of volume per unit volume should be constant. Consequently, the total observed rate should increase as the volume of the gas space increased. Since such an increase was not observed, it is reasonable to conclude that the rate determining step of the reaction does not take place in the gas phase.

But Lucien went further to say that the reaction must take place in the liquid phase. Let us note that this conclusion is contradicted by the experiment of Thomas (16) who found that the reaction could not take place in the liquid phase. Also, another experimental observation by Lucien (17) serves to contradict his conclusion about liquid phase reaction. Lucien found that the rate of decomposition was inversely related to pressure, and increased very rapidly as the difference between the confining pressure, and the vapor pressure of hydrazine decreased.

If we have a reaction like:

$$\text{N}_2\text{H}_4 (\text{liq.}) \rightleftharpoons \text{NH}_3 (\text{gas}) + \text{H}_2 (\text{g}) + \text{N}_2 (\text{g}) + \text{heat}$$

only the backward reaction will be pressure dependent. However, at the temperatures and pressures of the experiment, the free energy change of decomposition of hydrazine is quite large, and therefore, the equilibrium of the above reaction is strongly to the right.

We must conclude that under the conditions in Lucien's

experiment, the net rate of hydrazine decomposition will be almost equal to the forward rate of the above reaction. But, at least for moderate pressure differences, liquid phase reactions do not depend on pressure. Thus, the pressure dependence observed certainly cannot be due to a liquid phase reaction.

Suppose that the reaction takes place in the vapor phase, but that the slowest step is evaporation. The evaporation rate will (as found) depend inversely on the difference between the confining pressure and the vapor pressure of hydrazine.

Note that Lucien's vaporization takes place at a temperature above the normal boiling temperature of hydrazine. Under these conditions it is not unlikely that one gets a reaction of the kind:



The activation energy for such a reaction would be

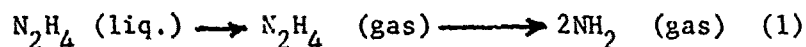
$$E_{\text{total}} = H_{\text{evap.}} + E_{\text{bond rupture}}$$

As shown by Penner (58) vaporization may be treated as a rate process. The heat of vaporization of hydrazine is 9.6 kcal/mole. Szwarc (13) reports that the energy of the N-N bond in hydrazine is 60 kcal/mole.  $E_{\text{total}}$  would then be 69.6 kcal/mole which is remarkably close to a value of 72 kcal/mole found by Lucien (17).

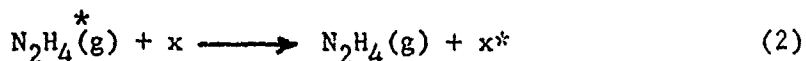
Another feature about the proposed reaction step is that it would exhibit the kind of pressure dependence observed by Lucien.

Consider the vaporization process in the following manner.

If there is vaporization into a vacuum, then



If, on the other hand, there is a gas above the liquid, one may also get the reaction



$\text{X}^* \rightarrow \text{dissipation X}$

Reaction (1) would lead to decomposition, whereas reaction (2) would lead to ordinary vaporization of hydrazine.

An increase in the liquid temperature would lead to an increase in both reactions (1) and (2), whereas an increase in confining

pressure would lead only to an increase of the fraction of vaporization proceeding by reaction (2) and thus decrease the production of free radicals. On the other hand, a decrease in confining pressure would decrease the fraction of reaction proceeding by mechanism (2). Thus, a decrease in the confining pressure would increase the rate of production of free radicals, and thus the rate of hydrazine decomposition.

It follows from the above that the less the confining pressure and the greater the vapor pressure, the more rapid the reaction. This is exactly the behavior observed by Lucien (17).

#### F. Isothermal Flow Reactors

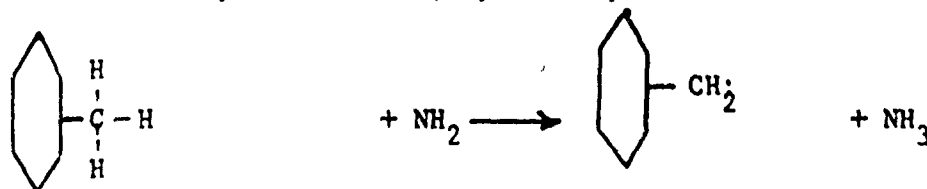
The isothermal flow reactor is similar to the isothermal bomb, in that in both an attempt is made to maintain constant temperature throughout the fluid in the reactor.

The laminar isothermal reactor has the same problem with respect to radial temperature uniformity as does the isothermal bomb. Furthermore, Batten (19) found that over a range of experimental conditions in a conventional laboratory flow reactor, the bulk of the gas streams through the tubular reactor without diffusing laterally to any appreciable extent. This condition results in a decidedly shorter reaction time for reactant passing along the center of the tube, than for material flowing near the periphery. Batten (19) goes on to say that an effect of this kind can vitiate completely calculations of contact time based on an assumption of plug flow.

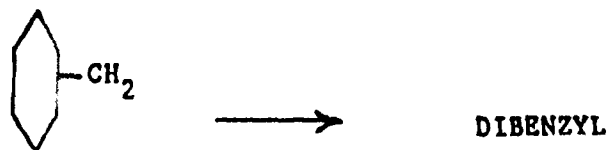
Despite such difficulties, a discussion of kinetics studies using such flow reactors appears worthwhile.

Szwarc (13) decomposed hydrazine in a toluene carrier gas in a silica flow reactor which he assumed to be isothermal.

The purpose of the toluene carrier gas was to remove  $\text{NH}_2$  radicals as soon as they were formed, by the rapid reaction



followed by



The products leaving the flow reactor were analyzed.

Knowledge of the composition of reactants and products, and of the time spent in the reactor, made it possible to calculate the rate of the reaction.



A value for the activation energy of the reaction was deduced from a series of experiments run at different reactor temperatures.

Szwarc concluded that the above reaction is a homogeneous, unimolecular gas reaction, the rate constant being

$$k = 4 * 10^{12} \exp \left[ \frac{-60,000}{RT} \right] \text{ sec}^{-1}$$

In Szwarc's experiment, some hydrazine did decompose to yield ammonia, nitrogen and hydrogen. Szwarc (13) found that packing of the reaction vessel, which increased the surface area about  $2\frac{1}{2}$  times caused a roughly proportional increase in the hydrazine decomposition reaction. From this he concluded that in his reactor, the overall reaction is essentially a surface reaction.

Szwarc found that toluene is an effective scavenger for  $\text{NH}_2$  radicals. Therefore, the amount of hydrazine decomposed into  $\text{NH}_2$  radicals must be directly related to the amount of dibenzyl formed. Since the amount of dibenzyl formed was independent of the surface area, Szwarc concluded that N-N bond rupture is a homogeneous, gas phase reaction.

Gilbert (20) considered Szwarc's reactor to be composed of an entrance region or volume of no reaction, followed by a practically isothermal reacting region. Gilbert proceeded to analyze the behavior of first and second order reactions in such a non-isothermal reactor. From his analysis, Gilbert concluded that Szwarc's data favor a second order formation of  $\text{NH}_2$  radicals, rather than a first order formation. For a second order reaction, i.e.



Gilbert (20) calculated the rate constant to be approximately.

$$k = 10^{19} \exp \left[ \frac{-60,000}{RT} \right] \text{ cc/mole-sec.}$$

Cordes (18) used what was essentially an isothermal flow reactor to study the rate of decomposition of UDMH. Cordes passed helium

gas, free of oxygen, through a saturator containing the 1,1 dimethylhydrazine. The saturator was immersed in a constant temperature bath to ensure a constant rate of evaporation. The saturated stream was mixed with a stream of pure helium, so that the concentration entering the reactor could be varied. The reactor was a standard pyrex flow reactor of the isothermal type. The temperature of the reactor was controlled manually with a pair of heater coils. Cordes measured the temperature profile along the reactor, and found it to vary by about 5 degrees K. The residence time in the reactor was found by dividing the internal volume of the reactor by the flow rate. The negative logarithm of the fraction of unreacted material was then divided by the residence time to give an empirical first order rate constant.

The products leaving the reactor were analyzed. A mass spectral analysis showed the presence of methane, ethane and propane in the ratios 1/0.14/0.002. An infra-red study showed the presence of ammonia and dimethylamine. Methylene methylamine was also found. However, the main products were methane and nitrogen with smaller amounts of hydrogen. Cordes found the ratio of nitrogen to methane to be  $0.59 \pm 0.07$ . Raleigh (57) mentioned that, based on chromatographic analysis, Aerojet had found the following decomposition products (mole per mole of UDMH):

H <sub>2</sub>	0.38
N <sub>2</sub>	0.67
CH <sub>4</sub>	1.40
C <sub>2</sub> H <sub>6</sub>	0.09
HCN	0.43
NH <sub>3</sub>	0.23

$$N_2 / CH_4 = 0.48$$

$$C_2H_6 / CH_4 = 0.064$$

What is especially interesting about the Aerojet work is that they found large quantities of HCN. Cordes (18) had concluded that HCN was not among the decomposition products, since a chemical test for cyanide had given a negative result.

Cordes (18) calculated the following first order rate constant

$$k = 10^{\beta} \exp \left[ \frac{-E}{RT} \right] \text{ sec}^{-1}$$

$$\beta = 7.83 \pm 0.21$$

$$E = 28.68 \pm 0.68 \text{ kcal/mole}^{\circ}\text{K}$$

The limits of error are one standard deviation.

Cordes packed his reactor with pyrex rods. The packed reactor had a surface/volume ratio of  $5.37 \text{ cm}^{-1}$  as compared to  $1.43 \text{ cm}^{-1}$  for the unpacked reactor. The data for the packed reactor gave the following results:

$$\beta = 7.45 \pm 2.6$$

$$E = 28.4 \pm 8.1 \text{ kcal/mole}$$

where the errors listed are the combined contributions of the standard deviations at the individual temperatures.

Cordes concluded that UDMH decomposition takes place in the gas phase.

It has been found that the two main objections to the classic isothermal flow reactors is a non-uniform radial temperature and improper mixing at the entrance section. An improvement in uniformity could be achieved if the mixing and heat transfer properties of the fluid in the reactor could be improved. One way to do this is by going to a highly turbulent stream. Furthermore, conditions at the entrance can be markedly improved if the abrupt entrance section of the classic "pyrex reactor" is replaced by a gently diverging conical section. Furthermore, the heat transfer problem could be eliminated altogether if the reactor were made adiabatic rather than isothermal. These ideas were followed in the development of the Princeton adiabatic flow reactor.

#### G. Surface Reactions

Generally surface reactions have a much lower activation energy than do homogeneous reactions. As a consequence of this, reaction is often more rapid at the surface than in the gas phase. The high speed of many surface reactions is probably due to adsorption at the surface, which is a low activation energy process, followed by a shift of the electron cloud of the reacting molecule which weakens the bonds between its atoms, thus facilitating dissociation of the reactant molecule, or attack by another molecule.

Of course, not all surfaces are equally active, and it is worthwhile to look at a few of the factors which play a role in the

activity of surfaces as catalysts.

In the following, two types of surfaces will be considered, namely metals and silica. Metals will be treated first.

Eberstein and Glassman (58) correlated the empirical observations made on metal catalysis of hydrazine decomposition by Wolfe (59), and suggested a mechanism by which metal surfaces may enhance hydrazine decomposition. Part of this development will be reproduced in what follows.

Recall the electronic and molecular structure of hydrazine discussed earlier. It was found that each of the two nitrogen atoms in hydrazine has four electron clouds which are qualitatively similar. Of these, only three form regular bonds. The electron pair not taken up in regular bond formation may form association bonds. Such association bonds may be either with the hydrogen atoms of other hydrazine molecules, or with atoms of a different substance, such as a metal. Association of hydrazine molecules with each other to form double molecules has been reported by Fresenius and Karweil (27).

With the above discussion in mind, look at some elements whose catalytic activity toward hydrazine is known from experimental evidence.

Wolfe (59) gives the following metals as those enhancing the decomposition of hydrazine: Copper, chromium, manganese, nickel, iron. Metals which do not enhance decomposition are: Cadmium, zinc, magnesium, aluminum.

A look at the electronic structures of these substances shows that the non-catalysts either have completely empty d-subshells, or completely filled ones, whereas the catalysts have incompletely filled d-subshells. A comparison of the last two subshells of both catalysts and non-catalysts is shown below

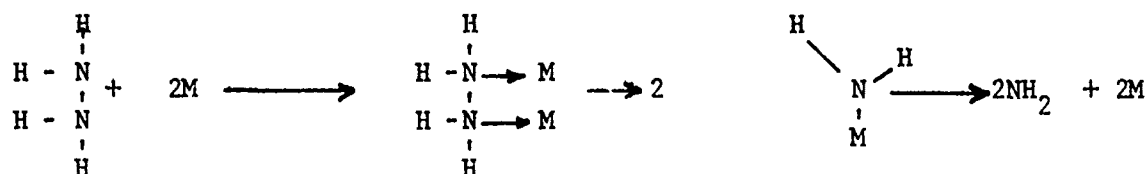
Last Two Subshells

	<u>Non Catalysts</u>			<u>Catalysts</u>	
Zn	$(3_d)^{10}$	$(4_s)^2$	Cr	$(3_d)^5$	$(4_s)^1$
Cd	$(4_d)^{10}$	$(5_s)^2$	Mn	$(3_d)^5$	$(4_s)^2$
Mg	$(2_p)^6$	$(3_s)^2$	Fe	$(3_d)^6$	$(4_s)^2$
Al	$(3_s)^2$	$(3_p)^1$	Ni	$(3_d)^6$	$(4_s)^2$
			Pt	$(5_d)^9$	$(6_s)^1$
			Cu*	$(3_d)^9$	$(4_s)^2$

It is known that d-orbitals, if they are not completely occupied by unshared electron pairs, play an important part in bond formation (60), and it is generally believed that with metals the electronic configuration, in particular of the d-band, is an index of catalytic activity (61). In this theory it is believed that in the "adsorption" of the gas on the metal surface, electrons are donated by the gas to the d-band of the metal, thus filling up the fractional deficiencies or holes in the d-band (62).

In hydrazine decomposition, adsorption is followed by further surface reactions which probably involve the formation and interaction of free radicals.

The following initiation reaction is proposed:



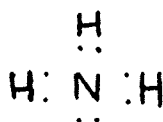
Because the N-N bond is weakened in the adsorption process, the activation energy for such a reaction would be much lower than the 60 kcal/mole measured by Szwarc (13) for the homogeneous gas phase initiation.

For inhibition of surface adsorption and reaction on metals the effectiveness of atoms or molecules as catalyst poisons will depend on their size, and the strength of bonding to the catalyst, and will therefore depend on geometric and electronic considerations (62). Molecules containing elements from the periodic table headed by sulphur and phosphorus were found to act as catalyst poisons, if the potentially poisonous substance had free electron pairs, e.g.

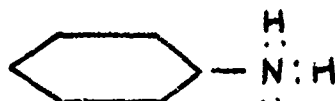


(62).

Following the above line of reasoning, a probable poison for heterogeneous hydrazine decomposition would be ammonia:



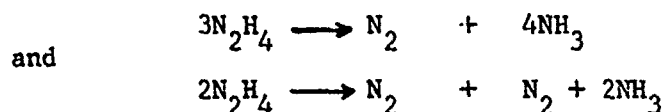
Another probable poison is aniline



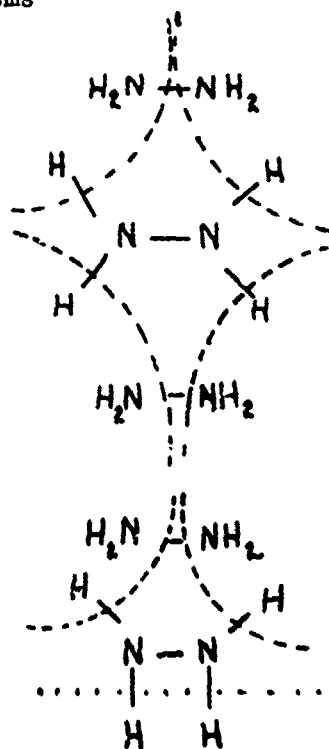
The large size of the aniline molecule can make this substance especially effective, since relatively few aniline molecules could thus deactivate a large area of catalyst surface.

In his work with hydrazine, Szwarc (13) concluded that heterogeneous hydrazine decomposition on a silica surface does not involve free radicals. Szwarc reached this important conclusion from the following observation. Though an increase in surface area of silica did increase the overall rate of decomposition of hydrazine, the rate of formation of dibenzyl was unaffected. Insofar as practically all  $\text{NH}_2$ , and presumably other, radicals react with the toluene carrier to produce dibenzyl, the above observation implies that no free radicals are produced on the silica surface.

For heterogeneous decomposition of hydrazine on a silica surface, Szwarc (13) proposes the reactions



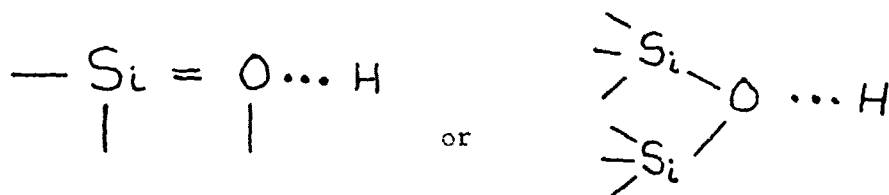
and surface mechanisms



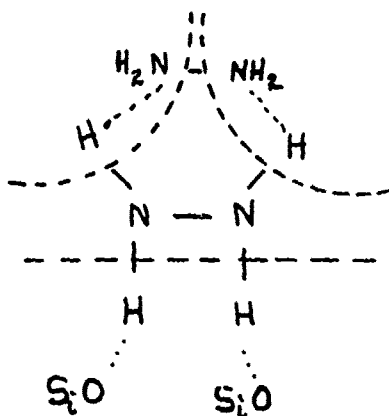
Kant and McMahon (63) studied the thermal decomposition of hydrazine in a pyrex reaction vessel at total pressures of 10mm - 12mm of mercury and at temperatures between 270C and 330C. Half-times of decomposition were 4 to 12 minutes. Under the above conditions, surface decomposition of hydrazine is likely to predominate over gas-phase decomposition. The authors concluded that a free radical mechanism was inconsistent with their experimental results. This supports Szwarc's (13) assertion that the decomposition of hydrazine on a silica surface does not proceed by a free radical mechanism.

In view of the above, it must be assumed that  $\text{NH}_2 - \text{H}$  and  $\text{H} - \text{H}$  bonds are formed no later than the breakage of the  $\text{N} - \text{H}$  and  $\text{N} - \text{N}$  bonds shown in Szwarc's mechanism. It is, however, not likely that some bonds break, and others form at the same instant. It is much probable that weak association bonds between hydrazine molecules form first, and that the formation of association bonds is followed by rupture of the bonds of the hydrazine molecule. If the above argument is accepted, then the absence of free radicals in hydrazine decomposition on a silica surface points to the conclusion that the first step in the heterogeneous decomposition on silica involves the association of hydrazine molecules on the surface.

Green et al (64) suggest that silica could chemisorb hydrogen atoms by means of a loose bond which might be a three-electron one:



It may well be that hydrazine molecules associate with atoms of the silica surface and with each other in a way like that shown below



In cases where surface reactions are undesirable, it may be possible to inhibit them, by treating the surface with a substance that associates more readily with the surface than do the reactants.

Thus Baldwin et al, (65), (66), have studied reactions of hydrogen-oxygen, and of hydrogen peroxide in boric acid coated vessels. Though the boric acid does not completely inactivate the surface, Baldwin et al do claim a significant inhibition effect of boric acid on the surface reaction. These findings are in agreement with data of Green et al (64) who in their studies of hydrogen atom recombination on silica found that washing the surface with acid lowers its activity.

Boric acid cannot be used with hydrazine, since the two would probably react with each other. However, it is conceivable that substances like hydrogen of ammonia might inhibit the surface without appreciably affecting the gas phase reaction.

Since it is likely that hydrazine decomposition on silica involves association of hydrazine molecules on the surface, this reaction may be inhibited by compounds tending to prevent such association. It is conceivable that some hydrocarbons may serve this purpose by hydrogen bonding with the N atoms in hydrazine. In connection with this, it should be noted that the energy of the C-H...N hydrogen bond is 3.28 kcal/mole as compared with only 1.3 kcal/mole for the N-H...N hydrogen bond (67). Some inhibitors, such as butane, hexane, and heptane (68) may work by the above mechanism. However, it is also possible that hydrocarbons inhibit gas phase decomposition.

#### H. The Princeton Adiabatic Flow Reactor

It was seen that rate data for hydrazine are available in the fast rate regime of shock tubes and laminar flames, and in the slow rate regime of isothermal bombs. It would be desirable to obtain rate data in an intermediate regime, since knowledge of rate data over as great a temperature span as possible is needed to really draw conclusions about reaction mechanisms. The Princeton adiabatic flow reactor can be used to obtain rate data in the intermediate rate regime. Also, this reactor is such that there is essentially no back diffusion of heat or active species. Thus, results obtained in the adiabatic flow reactor can be compared with laminar flame results to determine whether a flame of a particular substance is best described by the thermal or active particle theory of flame propagation.

Since no radial heat transfer is desired, radial variations in temperature may be eliminated. If the reactor is operated in the regime of turbulent flow, then radial velocity profiles will also be quite flat. Finally, the entrance section can be made to consist of a gently diverging nozzle, thus eliminating the non-uniform flow problems which were found to plague isothermal reactors.

It may be argued that turbulent flow introduces problems of its own. However, it will be shown that turbulence does not significantly affect the chemical kinetics measurements in the reactor.

The adiabatic flow reactor is operated as follows:

A cool stream of reactant is introduced into and mixed rapidly with a heated inert gas. By properly adjusting the velocity of the carrier gas, reaction may be made to commence downstream of the injection point, and go to completion in the length of the reactor. Only small quantities of reactant are introduced compared with the mass flow of carrier gas. Consequently, the change in total concentration of reactant is small, and the increase in temperature due to the exothermic reaction is also small. Since the zone in which reaction takes place can be made quite long, gradients in temperature and concentration are very slight. Consequently, heat transfer to the unreacted gas, and back-diffusion of active species are negligible.

The rate data are obtained by measuring longitudinal temperature profiles. Such profiles are shown in Figures 4 and 5.

Ideally, each element of fluid is adiabatic and microscopically homogeneous. Thus, the temperature rise is proportional to the amount of reactant consumed, i.e.

$$T - T_i = \frac{Q}{C_p} (X - X_i)$$

where  $X$  is mole fraction of reactant.

Similarly

$$T_f - T = \frac{Q}{C_p} (X - X_f)$$

but the reaction goes to completion, and  $X_f = 0$ . Thus

$$X = \frac{C_p}{Q} (T_f - T)$$

and

$$\frac{dx}{dt} = \frac{C_p}{Q} \frac{dT}{dt}$$

For a first order reaction

$$-\frac{1}{X} \frac{dx}{dt} = \frac{1}{T_F - T} \frac{dT}{dt}$$

Taking account of the relationship between the mole fraction and the concentration, Crocco, Glassman and Smith (69) developed the following expression for a first order reaction

$$k = -\frac{1}{C} \frac{dC}{dt} = (T_f/T) \frac{1}{T_F - T} \frac{dT}{dt}$$

The discussion pertaining to the Princeton adiabatic flow reactor consists of three parts. First, the effect of turbulence on the chemical rate measurements is considered. Then a description of the experimental apparatus and procedure is presented. This presentation is followed by a discussion of how the experimental data were analysed.

CHAPTER III.

THE EFFECT OF TURBULENCE ON CHEMICAL KINETICS MEASUREMENTS IN THE  
ADIABATIC FLOW REACTOR

Ways in which turbulence can affect measurements in the flow reactor fall into three categories:

- (1) Enhancement of longitudinal heat and mass transfer to a point where the "adiabatic element" assumption no longer holds.
- (2) Temperature fluctuations of such high frequency that the steady-state kinetics assumption does not apply.
- (3) The rate at the mean value of the fluctuating temperature, which is measured, might be significantly different from the mean of the fluctuating rate.

To study the importance of longitudinal heat transfer, a one-dimensional differential element of the flow reactor is treated as one in which heat diffusion, convective and reactive terms are in evidence in much the same way as the thermal theory of flame propagation was treated by Zeldovich-Frank-Kamenetski-Semenov except that the thermal conductivity is replaced by an eddy conductivity. The resulting expression which is obtained is

$$\frac{dQ}{dx} = \dot{m} C_p \frac{dT}{dx} + A \frac{d^2T}{dx^2}$$

where

Q is the rate of energy release per unit time

$\dot{m}$  is the mass flow rate

A is the crosssectional area of the reactor tube

x is the axial direction of flow

$\epsilon$  is the turbulent eddy conductivity

For  $\epsilon \rightarrow 0$  there is no heat transfer, and the element is in an adiabatic state. Then, the temperature gradient is an adiabatic temperature gradient, and one may write

$$\frac{dQ}{dx} = \dot{m} C_p \left( \frac{dT}{dx} \right)_{ad}$$

The overall equation then becomes

$$\left( \frac{dT}{dx} \right)_{ad} = \frac{dT}{dx} + \frac{\epsilon A}{\dot{m} C_p} \frac{d^2 T}{dx^2}$$

or

$$\left( \frac{dT}{dx} \right)_{ad} = \frac{dT}{dx} (1 + \beta)$$

where

$$\beta = \frac{\epsilon A \frac{d^2 T}{dx^2}}{\dot{m} C_p \frac{dT}{dx}}$$

An estimate of the eddy conductivity in the three inch flow reactor was made from the expression

$$\frac{\epsilon}{k} = Nu = 0.023 Re^{0.8} Pr^{1/3}$$

For an actual experimental run, the following values were calculated:

$$\begin{aligned} Nu &= 86.5 \\ \epsilon &= 0.0133 \text{ cal/cm sec deg C} \\ \frac{\dot{m} C_p}{\epsilon A} &= 14.6 \text{ cm}^{-1} \\ \frac{dT}{dx} &= 2.1 \text{ deg C/cm} \\ \frac{d^2 T}{dx^2} &= 0.15 \text{ deg C/cm/cm} \\ \beta &= 0.5\% \end{aligned}$$

An experiment with a very steep axial temperature gradient was chosen in order to obtain a conservative estimate of  $\beta$ . Thus it is seen that the Princeton adiabatic flow reactor is not troubled with longitudinal heat transfer problems.

Since temperature and concentration gradients in the reactor are proportional to each other, an argument similar to that made for the importance of longitudinal heat transfer may be used to show that longitudinal mass transfer is not important.

The interaction between chemical relaxation and turbulent fluctuations is more difficult to determine. It has been treated by Predvolitev (70) and Corrsin (71).

Predvolitev (70) assumes that the rate of the chemical process is a single valued and explicit function of the components of the fluctuating velocity of the turbulent stream. He concludes by stating that the problem of evaluating a measurable rate of a chemical reaction under turbulent conditions resolves itself into determining the correlation coefficient of the turbulent stream and the  $\frac{\partial c}{\partial t}$ , where  $\frac{\partial c}{\partial t}$  is the reaction rate corresponding to given values of the  $u$  and  $v$  components of the fluctuating velocity of the stream. It seems that Predvolitev merely suggests an avenue of approach to the study of the interaction of turbulence and chemical reaction rate without really offering a solution to the problem.

Corrsin (71) describes the nature of turbulence, and especially isotropic turbulent mixing as "the problem of predicting the statistical properties of an isotropic scalar fluctuation field which is randomly convected (= "stirred") by isotropic turbulence while simultaneously being smeared out by molecular diffusion."

According to Hinze (72) turbulent motion "can be assumed to consist of the superposition of eddies of various sizes and vorticities with distinguishable upper and lower limits. The upper size limit of the eddies is determined mainly by the size of the apparatus, whereas the lower limit is determined by viscosity effects and decreases with increasing velocity of the average flow, other conditions remaining the same. Within these smallest eddies the flow is no longer turbulent, but viscous, and molecular effects are dominant." Batchelor (73) states that the energy of turbulent motion dies away effectively to zero long before length scales comparable with the mean free path are reached. It seems reasonable to assume that the only ways in which the chemical kinetics within these smallest eddies can be affected are by turbulent pressure fluctuations in the fluid and by molecular diffusion of species into or out of the tiny eddy. If the "mean free path" of the eddy is sufficiently small so that the eddy does not travel into regimes whose concentration and temperature are drastically different, then the eddy will not encounter steep gradients, and the rate of change of conditions in the eddy due to diffusion effects will be slow. For flow in a circular pipe, an eddy "mean free path" is likely to be less than the pipe diameter, and for Reynold's numbers in

the experiment (i.e., Re 10,000)

$$l \approx 0.2 D \quad (74)$$

for  $D = 3''$ ,  $l \approx 0.6''$

The reaction in the reactor is spread over approximately 30." Thus an eddy encounters approximately a 2% change in concentration, and approximately a two degree difference in temperature. It seems safe to say that gradients are sufficiently shallow so that diffusion will not cause any rapid fluctuations of temperature or concentration within an eddy. As regards pressure fluctuations, and temperature fluctuations due to compressibility, Wight (75) has shown that these do not significantly affect the chemical kinetics.

Laurence (76) studied intensity, scale, and spectra of turbulence in the mixing region of a free subsonic jet. At a Reynold's number as high as 300,000, Laurence (76) found a sharp drop in spectral density of the turbulence as the frequency increased above 1000 cps. This results in a characteristic time of approximately 1 millisecc. If one assumes that the characteristic frequency of oscillation is inversely proportional to the viscous damping, i.e., directly proportional to Reynold's number, a characteristic time of 30 millisecc is obtained for  $Re = 10,000$ .

Taking

$$\bar{u} \approx 0.03 \quad (74)$$

$$l \approx 0.2 D$$

a characteristic time of 20 milliseccs is obtained. At  $1000^\circ K$ , the time required to reach a kinetic steady state is somewhat less than 0.1 millisecc. The time required for the free radical system to adjust to a temperature change of a few degrees is likely to be less.

Thus it seems safe to assume that steady state kinetics do prevail in the flow reactor.

The temperature probe measures an average temperature of the turbulent eddies which flow past it. Now, is the reaction rate deduced from this average temperature the same as the average rate? The fluctuating temperature which the probe sees may be represented as follows:

$$\frac{T(t)}{\bar{T}} = 1 + a_n f(t)$$

where

$$-1 \leq f(t) \leq 1$$

$$\bar{T} = \frac{1}{\tau} \int_0^{\tau} T(t) dt$$

By definition, the mean temperature is a constant independent of time. Thus one may write

$$\frac{1}{\tau} \int_0^{\tau} \frac{T(t)}{\bar{T}} dt = 1$$

It follows that:

$$\int_0^{\tau} f(t) dt = 0$$

The overall rate constant  $k$  may be written in terms of an Arrhenius expression

$$k(T) = A \exp \left[ \frac{-E}{RT} \right]$$

$$k(\bar{T}) = A \exp \left[ \frac{-E}{R\bar{T}} \right]$$

$$\frac{k(T)}{k(\bar{T})} = \exp \left[ \frac{E}{R\bar{T}} \left( 1 - \frac{\bar{T}}{T} \right) \right]$$

$$-\frac{\bar{T}}{T} = \frac{1 + a_n f(t) - 1}{1 + a_n f(t)} = \frac{a_n f(t)}{1 + a_n f(t)}$$

for small  $a_n$

$$\frac{a_n f(t)}{1 + a_n f(t)} \approx a_n f(t)$$

For small  $a_n$

$$\frac{k(T)}{k(\bar{T})} = \frac{1}{\tau} \int_0^{\tau} \frac{k(T)T}{k(\bar{T})} dt = \frac{1}{\tau} \int_0^{\tau} \exp \left[ \frac{E a_n f(t)}{R\bar{T}} \right] dt$$

$$e^x = 1 + x + \frac{1}{2} x^2 + \frac{1}{6} x^3 + \dots$$

$$\int_0^{\tau} f(t) dt = 0$$

and

$$f^2(t) \leq 1$$

$$\text{Thus } \frac{1}{\tau} \int_0^{\tau} a_n^2 f^2(t) dt \leq a_n^2$$

$$\delta = \frac{k(T) - k(\bar{T})}{k(\bar{T})} \leq \frac{1}{2} \left( \frac{E a_n}{RT} \right)^2$$

if higher order terms are neglected.

For the case where  $f(t) = \sin t$

$$\frac{1}{\tau} \int_0^{\tau} \sin^2 t dt = \frac{1}{2}$$

and

$$\delta = \frac{1}{4} \left( \frac{E a_n}{RT} \right)^2$$

Now, assume the temperature fluctuation to be 10% of the total temperature spread.

Typical operating values are

$$\text{spread} = 100 \text{ deg K}$$

$$\bar{T} = 800 \text{ deg K}$$

$$K(\bar{T}) = 100 \text{ sec}^{-1}$$

$$E = 30 \text{ kcal/mole}$$

Under these conditions

$$\frac{E}{RT} = 18.9; \quad n = \frac{1}{80}$$

$$\frac{nE}{RT} = \frac{18.9}{80} = 2.36 \times 10^{-1}$$

$$\frac{n^2 E^2}{RT} = 5.56 \times 10^{-2}$$

$$\delta = 2.78 \times 10^{-2} = 2.8\%$$

for  $X = 0.236$

$$e^X = 1.266$$

$$1 + X + \frac{X^2}{2} = 1.259$$

If all the integrals

$$\frac{1}{\tau} \int_0^{\tau} f^n(t) dt = 1$$

which results in the maximum possible deviation,

$$\delta_{\max} = 2.78\% \left( \frac{1.266}{1.259} \right) = 2.8\%$$

It follows that under normal operating conditions of the

flow reactor, differences between mean rate and rate at mean temperature are small and may be neglected.

It might be noted that if  $\Delta T$  is only 2 deg as was estimated from an approximate "eddy mean free path," then  $\delta$  becomes as little as 0.2%.

For a first order reaction, there is no effect if the concentration is oscillated. For an  $n^{\text{th}}$  order reaction, the following analysis applies

$$R = C^n$$

where  $R$  is the rate divided by the Arrhenius expression.

Taking

$$C = \bar{C} (1 + b_n g(c))$$

where

$$-1 \leq g \leq 1$$

and

$$\int_0^{\tau} g(C) dt = 0$$

$$\frac{\overline{R(C)}}{R(\bar{C})} = \frac{1}{\tau} \int_0^{\tau} \left( \frac{C}{\bar{C}} \right)^n dt$$

for  $n = 2$  this becomes

$$y = \frac{\overline{R(C)}}{R(\bar{C})} - R(\bar{C}) \leq b_n^2$$

if  $b_n$  is as large as 10%,  $y$  is still only 1% and for the expected  $b_n$  of 2%,  $y = 0.04\%$  and thus the effect of concentration oscillations is also negligible.

If density variations are neglected for the moment, a heat balance for a fluid element shows the following

$$c_o - c = \frac{Q}{C_p} (T - T_o)$$

where

- $c$  is concentration
- $T$  is temperature
- $Q$  is chemical heat release

$C_p$  is heat capacity of the carrier gas

Differentiating the above expression yields:

$$-\frac{dC}{dt} = \frac{Q}{C_p} \frac{dT}{dt}$$

Since the reaction goes to completion,  $C_F = 0$  and

$$C = \frac{Q}{C_p} (T_f - T)$$

$$-\frac{1}{C} \frac{dC}{dt} = \frac{1}{T_f - T} \frac{dT}{dt}$$

for a first order reaction.

In the preceding it was shown that there is no significant smearing out of the temperature profile by longitudinal heat transfer. This means that the quantity deduced from the experimental data really is

$$-\frac{1}{C} \frac{dC}{dt}$$

It was further shown that steady state kinetics apply. Thus it seems reasonable that the overall reaction can be approximated by an Arrhenius expression

$$-\frac{1}{C} \frac{dC}{dt} = k(T) = A \exp \left[ \frac{-E}{RT} \right]$$

for a first order reaction.

Finally, it was shown that the rate at the mean temperature seen by the thermocouple is the same as the mean rate in the turbulent field seen by the probe. Thus the measured temperature is appropriate for use in the Arrhenius expression.

It may be concluded that the turbulence level in the reactor is such that the chemical kinetics measurements are not affecting by the existing turbulence.

In what follows, a description of the experimental apparatus will be presented.

## CHAPTER IV

### EXPERIMENTAL APPARATUS AND PROCEDURE

The flow reactor used in the experiments is a modified version of that used by Crocco, Glassman, and Smith (69) for the study of ethylene oxide decomposition, and by Swigart (77) in his study of the hydrogen-oxygen reaction.

A hot carrier gas flows through a quartz duct whose walls are heated electrically to the carrier gas temperature to prevent heat loss to the ambient air. The reactor consists of a cylindrical section, the inside diameter of which may be varied in one inch steps between 1 inch and 4 inches, and a conical section. The wide part of the cone is joined with the main cylindrical section, whereas the narrow part is joined with another conical section to form a nozzle. At the throat of this nozzle, small quantities of gas phase reactant are injected perpendicularly to the main stream. Since the gas velocities in the nozzle are quite high, rapid mixing results. The mixing is followed by chemical reaction. When a steady state has been reached in the reactor, the longitudinal temperature profile is measured.

The discussion of the apparatus will be presented in five sections. First, time at which reaction starts, mixing, and turbulence effects will be treated. Then, the flow reactor and its carrier gas supply will be discussed in detail. The temperature measurement technique will be presented. This will be followed by a discussion of the gaseous fuel injection assembly and the fuel vaporization system.

#### A. Start of Reaction, Mixing, and Turbulence Effects

This problem may be considered to have three aspects, namely, decomposition in the fuel supply line, decomposition in the injectors, and a reaction which is so rapid that it progresses significantly before mixing with the carrier gas is complete. All of these aspects have been investigated.

The problem of decomposition in the fuel supply line was investigated for hydrazine-water mixtures containing up to 80% hydrazine by weight. This study was conducted as follows: The fuel vapor supply line was disconnected from the injection manifold, and instead was connected to a water cooled pyrex condensing coil. The fuel vaporization system was then operated in a manner identical to that employed in the kinetics experiments. The condensate was analysed for hydrazine using the direct iodine method (78). The behavior of hydrazine-water mixtures of various strengths was studied. These mixtures ranged from 50% hydrazine to 80% hydrazine. In all cases, analysis of the condensate showed hydrazine content to be within 1% of that in the initial liquid. It should be mentioned that, apart from the safety hazard, the above type experiments are not likely to be very fruitful for studying anhydrous hydrazine behavior. Since all the decomposition products of hydrazine are gaseous, the concentration of hydrazine in the condensate would be independent of the amount of hydrazine decomposed.

In a previous study, stainless steel injectors and a stainless steel flow reactor had been employed. Under these conditions, hydrazine reacted in the fuel injectors. This condition was obvious from the following observations: The binder in the glass wool packing around the injectors smoked, indicating that the injectors got very hot, and no temperature profiles characteristic of reaction could be obtained in the flow reactor, and indicated that the hydrazine was consumed before it could react in the flow reactor.

In the present all-quartz system neither of these difficulties was encountered. Therefore, the amount of decomposition in the fuel injectors must have been negligibly small. If there was some decomposition in the injectors, then the reactor temperature traces should be sensitive to the amount of diluent nitrogen mixed with the hydrazine vapor prior to injection. However, no effect was observed when the amount of diluent gas was varied.

From the above considerations it may be concluded that there is no decomposition of reactant prior to injection into the hot carrier gas.

A consideration of the processes taking place in the mixing region shows the following ones to be important: local relaxation of temperature between carrier gas and reactant, mixing downstream of the injection point to produce uniform radial distributions of temperature and concentration, and initial buildup of free radicals to "steady state" concentrations.

The slowest step in local temperature relaxation is vibrational relaxation of the reactant molecule. However, this is likely to occur within a few microseconds. From cold gas injection traces, the mixing distance was estimated to be approximately 3 inches, which corresponds to about 0.5 milliseconds under normal operating conditions. However, computations on reaction mechanisms showed that the time necessary to reach a chemical steady state is in the order of 0.1 milliseconds.

Thus the mixing region is a region of non-uniform chemical reaction. Furthermore, the steady state free radical concentration follows an Arrhenius type dependence on temperature. As a result, the reaction rate immediately following the mixing region will be higher than that which would have been attained if mixing had been instantaneous.

However, the very rapidity of free radical reactions which made it impossible for mixing to be completed before the commencement of chemical reaction, becomes very valuable once mixing has been achieved. Since the chemical system very rapidly adjusts to a given temperature and reactant concentration, the reaction rate in the radially uniform region downstream of the mixing zone will be a function only of temperature and concentration, and not of previous history.

The general turbulence level in the reactor, and the effectiveness of the mixing process are related to the carrier gas flow rate. If the mixing process is very critical, or if turbulence effects have an important influence on chemical reaction rates, then varying the carrier gas flow rate should have an effect on the rate constants obtained. The results of these experiments are shown in Figure 6. No effect of velocity variation on rate constant is apparent. From analysis of the effect that turbulence is likely to have on chemical reaction rate, given earlier, it

was indeed concluded that under conditions encountered in the flow reactor the effect of turbulent fluctuation should be very small. This experimental observation also agrees with the conclusion that the detailed nature of the mixing process does not affect chemical reaction rates measured downstream of the mixing region.

#### B. Flow Reactor and Carrier Gas System

A drawing of the chemical kinetic flow reactor is shown in Figure 7, and a photograph of the apparatus is shown in Figure 8. Figure 9 shows the quartz reactor removed from the assembly.

As was already stated, the reactor consists of a cylindrical section, the inside diameter of which may be varied in one inch steps between 1 inch and 4 inches, and a conical section. The wide part of the cone is joined with the main cylindrical section, whereas the narrow part is joined with another conical section to form a nozzle. The divergent section of the cone has a half-angle of 15 degrees, this being the steepest angle for which there is no separation of the flow.

The quartz reactor is surrounded by a metal sleeve which is heated electrically to a mean reactor temperature so as to prevent heat losses to the ambient air.

Ceramic beds are used to heat the carrier gas. Before the experiment is performed, these beds are heated by oil burners, bringing the ceramic packing to 1000°C or more. During the heating process, the exhaust gases bypass the reactor. Since packed beds are treated extensively in engineering literature no further discussion of them will be given here. Note that a drawing of the packed beds used is shown in Figure 7.

During the experiment, carrier gas is passed through the two beds in series. Upon leaving the second bed it is mixed with cold carrier gas so that the temperature level may be properly adjusted. The temperature of the carrier gas is maintained constant by a servo system which varies the ratio of hot-to-cold gas. The total carrier gas flow is metered by a

critical flow orifice, and the hot and cold gas valves are located downstream of this orifice, so that varying the ratio of cold to hot gas does not change the total flow rate of carrier. Figure 10 shows a schematic of the carrier flow system. Figure 11 shows a schematic of the temperature control servo system, which is shown in a photograph in Figure 12.

The nitrogen, which was used as a carrier gas was obtained from a 2000 psi bank of compressed nitrogen which in turn was filled from a liquid nitrogen storage tank.

Photographs of the control panels for the apparatus are shown in Figures 13 and 14.

#### C. Temperature Measurement

Longitudinal temperature profiles in the duct were measured with a silica coated Pt/Pt - 13% Rh thermocouple. The output from the thermocouple was fed to a circuit of the type shown in Figure 15. The change in temperature during a run was small compared to the mean temperature of the run. Thus, maximum accuracy can be obtained if a full scale deflection of the measuring instrument is made to correspond to the change of temperature during a run. This was done by placing a bucking potentiometer in the thermocouple circuit. As a result, a signal corresponding to a differential temperature was fed to the Leeds and Northrup variable range, variable zero Speedomax recording potentiometer shown in Figure 16.

Prior to a set of experimental runs, a series of runs without reactant was made to determine the carrier gas temperature at which heat exchange with the reactor walls is minimized. The experimental runs were then conducted at temperatures close to this minimum heat transfer temperature. After a series of runs, traces without reactant were again made. It was observed that initially there is a slight temperature profile of smaller extent, but same shape as that observed during reaction. From this observation it was concluded that the tube wall tends to assume the temperature of the gas.

The temperature probe drive assembly is shown in Figure 17. The probe is held by a trolley which rides on the T-bar. This trolley is pulled by a cable wound around a drum, as shown in the figure. The microswitch which rides on the cam is connected to a marker pen on the speedomax. This provides a record of the motion of the probe on the same paper on which the temperature trace is taken. The second microswitch shown stops the drive motor when the probe is in the fully in position. A similar switch is provided for the fully out position. The probe travels a total distance of 38.1 inches in 62.5 seconds.

The thermocouple is made of 0.0015 inch Platinum and Pt/13% Rh wires. Since platinum surfaces are highly catalytic to the rate of chemical reactions, the thermocouple probe was coated with silica. The tip of the probe was placed in a propane-air flame into which small quantities of hexamethyldisiloxane had been introduced. Part of the propane stream was bubbled through the silicone at room temperature, and then recombined with the main flow, which was then passed through a Meker burner. A thin, glassy coating of silica was obtained in a few minutes. A photograph of the probe coating apparatus and a temperature probe is shown in Figure 18. A skilled technician can learn to make these probes in a few days.

Two problems now arise. Does the experimenter know when the silica coating breaks off or cracks, and does the coating significantly slow down the response of the thermocouple. Hydrazine decomposition on platinum is so rapid, and involves so much heat that exposed platinum wire is quickly melted, breaking the thermocouple. When the thermocouple is broken, the recording pen simply goes off scale. Thus it is easy to detect the breakage or flaking off of the silica coating.

Swigart (77) made a check on the response time of the thermocouple. Passing air through the bed and injecting cold nitrogen through the injector a traverse was made through the mixing section. Then, the probe was stopped at approximately  $\frac{1}{2}$  inch intervals through the mixing section and steady state temperatures recorded. This was repeated with a coated thermocouple. Swigart (77) found that all four resulting

traces were identical within experimental error.

#### D. Gaseous Fuel Injection

Vapor phase reactant is injected perpendicular to the carrier gas stream through four quartz tubes. The injector assembly is shown in Figure 19. Cold nitrogen can also be injected through these injectors. A schematic of the fuel vapor and diluent nitrogen system is shown in Figure 20. Both the flow rate of diluent nitrogen, and of fuel are metered by non-critical orifices. Pipe taps are employed. The pressure differences across the orifices were measured using mercury manometers.

It was found convenient to control the fuel flow indirectly. The metering orifice was connected to the source of fuel vapor through a pneumatic on-off valve. The pressure at the source was maintained constant. In this case it is clear that the amount of fuel flow may be regulated by regulating the pressure downstream of the orifice. This pressure depends upon the amount of diluent nitrogen flow, and may be varied by varying the flow rate of the diluent nitrogen. It is true that such an arrangement does result in a loss of flexibility, i.e. the fuel flow rate cannot be varied independently of the diluent nitrogen flow rate. However, previous experiments have shown that the amount of diluent used has no measurable effect on the reaction rates of the substances studied.

It is also possible to deduce reactant flow rates from the mass flow rate of carrier gas, and the ratio of reactant flow to carrier flow. This ratio, in turn, may be obtained from a thermodynamic calculation based on the heat of reaction of propellant, the heat capacity of the carrier gas, and the temperature rise of the gas in the flow reactor.

Because of the hazardous nature of the substances studied, the experiments were carried out remotely. Also, it was necessary to use all Teflon lines for the vapor, since even materials which are classed as 'compatible' with hydrazine corroded and then became catalytic to hydrazine decomposition. 304 stainless steel is an example of such

behavior. When a 304 stainless steel vapor line, in which a hydrazine explosion had occurred, was examined, the color of the inside surface was green and dark gray, indicating compounds of nickel and chromium, both of which are catalysts for hydrazine decomposition.

The substances which have been investigated, namely hydrazine, UDMH, and monomethyl-hydrazine are liquids at room temperature and pressure. Thus some means must be employed to prevent condensation in the vapor lines. This was accomplished by placing an annular line around the vapor line, and flowing hot oil through the jacket.

Because of the hazardous nature of the hydrazine family monopropellants, great care was taken to purge the vapor lines with nitrogen before, and after, a series of experiments.

#### E. Vaporization of Propellants

Since the substances studied are liquids at room temperature, whereas vapor is desired, it is necessary to provide a means for vaporizing the propellants. All three monopropellants are hazardous to handle. As is well known, hydrazine vapor is especially explosive. Thus, a rather elaborate system for converting the liquids into gases was needed. A schematic of this system is shown on Figure 21. Approximately 100 psi of nitrogen is applied to the propellant in the liquid tank. This pressure forces the liquid propellant through 3 spray nozzles which impinge on the walls of an evaporator which, in turn, is immersed in a hot oil bath. A picture of the evaporator is shown in Figure 22. The evaporator is coated with Teflon on the inside, and all vapor lines are made of Teflon because of the extreme sensitivity of hydrazine vapor to catalysis by metal surfaces. A photo of the evaporator assembly is shown in Figure 23. Note the protective shield around the evaporator assembly. This shield was necessary to protect the remaining apparatus, and possibly personnel, from damage caused by evaporator explosions.

The pressure in the evaporator is controlled by a back pressure regulator placed in parallel with the main fuel vapor supply line. A

neoprene diaphragm fits over a vapor line from the evaporator. This diaphragm is pressed over the vapor port by nitrogen pressure which can be regulated to any desired value. If the gas in the evaporator exceeds the regulator pressure, the excess gas is vented until the pressure again returns to the desired value. This control is quite good and, except at high fuel flow rates to the reactor when there is no excess fuel vapor available, it is possible to maintain constant pressure in the evaporator. The neoprene diaphragms must be replaced at regular intervals since they are attacked and made spongy by t. hydrazine vapor.

The evaporator is also provided with a burst disc and with pneumatic valves which can be used to vent it at any time. The vent gas goes into a water aspirator.

The vaporization system is purged with nitrogen before, and after, a series of runs.

The heat transfer fluid used was Pydraul F-9, manufactured by Monsanto Chemical Company. This is a silicone-base, fire-resistant oil with good heat transfer and vapor pressure characteristics. The oil is heated in a separate vessel with electric heaters, and two gear-pumps are used to circulate the heated oil past the evaporator. This oil is also circulated through a jacket placed around the propellant vapor lines, so as to prevent condensation of the vapor.

#### F. Product Gas Sampling

Chemical samples were taken near the exit of the flow reactor using a water-cooled probe. A drawing of the probe is shown on Figure 24, and a photo of the sampling probe is shown in Figure 25. Samples were drawn into 1 liter and 2 liter glass sampling bulbs which had previously been flushed with argon and evacuated. The time required to fill a 2 liter sampling bulb is approximately 2 minutes. It should be noted that at the point in the reactor where the sample is taken, all rapid reactions have already occurred. Thus quenching is not as critical as it would be if a sample were taken, say in the middle of the reaction zone. The time required to cool the sample gas from 500°C (773°K) to 200°C was

estimated to be 1.4 milliseconds. Time of reaction in the flow reactor was 30-60 milliseconds. Thus, the quenching capability of the sampling probe is considered to be adequate.

Analysis for hydrogen, methane, and higher hydrocarbons was performed on a Beckman GC-1 Gas Chromatograph using primarily a Linde Molecular Sieve column. Because of the small concentrations present, it was not convenient to use chromatography to analyse for ammonia. Rather, the more sensitive technique of infra-red absorption was used in this case. A 10 cm single pass absorption cell was used. A photo of the cell is shown in Figure 26. The infrared analysis was carried out using a Perkin Elmer model 21 spectrophotometer.

## Chapter V

### ANALYSIS OF EXPERIMENTAL DATA

A formula for deducing rate constants from the temperature traces obtained from the flow reactor was first developed by Crocco, Glassman, and Smith (1) who obtained the following for a first order overall reaction:

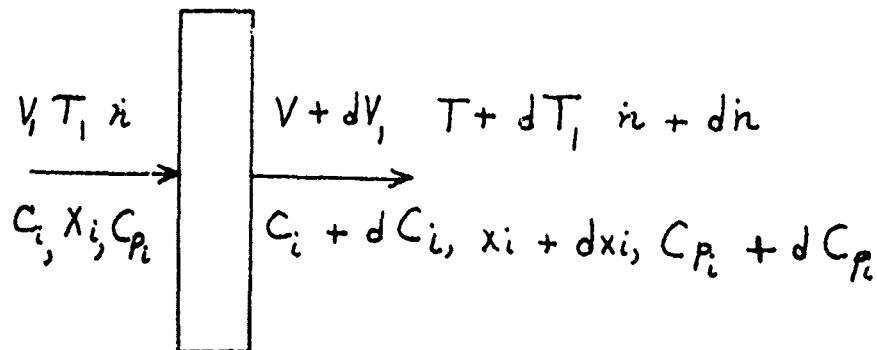
$$k = (T_f/T) \frac{1}{T_f - T} \frac{dT}{dt}$$

In this section the above formula will be derived and extended to overall reaction orders other than unity.

This derivation will be followed by a discussion of methods for determining the appropriate order of reaction. Then, a discussion of the reproducibility of data will be presented, together with consideration of the principal sources of error. Plots of experimental data will then be shown, and a method for integrating out the "error noise" will be discussed.

#### A. Derivation of Data Reduction Formulas

Consider a crosssectional element of the flow reactor, as shown below



where

V is velocity of the gas stream  
 $C_i$  is concentration of the  $i^{\text{th}}$  specie  
 $X_i$  is the mole fraction of the  $i^{\text{th}}$  specie  
 $T$  is the temperature  
 $\dot{n}$  = total mole flow rate  
 $C_{pi}$  = heat capacity of  $i^{\text{th}}$  specie  
 $H_i$  = chemical enthalpy of  $i^{\text{th}}$  specie  
 $h_i$  = specific enthalpy of  $i^{\text{th}}$  specie

In this analysis it is assumed that heat transfer with the reactor walls is negligibly small. This assumption is not completely valid, and failure to satisfy it accounts for much of the scatter of data.

In what follows, the flow in the reactor is assumed to be truly one-dimensional, and the pressure in the reactor is assumed to be constant throughout the region of interest.

The validity of assuming one-dimensionality was checked experimentally by measuring radial profiles of temperature and velocity. Such profiles are shown in Figures 27 and 28, and are seen to be quite flat, confirming the validity of the one-dimensionality assumption.

The validity of the constant pressure assumption may be checked by treating the reaction in the duct as Raleigh heating. It is found that  $\Delta P/P$  is approximately 0.03% through the reaction zone, and the pressure may safely be assumed to be constant.

It is further assumed that there is no longitudinal transport of mass or heat. As was shown in the section on turbulence, the error introduced by this assumption is less than 1%.

Within the validity of the assumptions made above, a crosssectional element of fluid is isobaric, adiabatic, and radially homogeneous. An energy balance for such an element of fluid is shown below.

$$\dot{n} \sum_i x_i h_i = (\dot{n} + d\dot{n}) \sum_i (h_i + dh_i) (x_i + dx_i)$$

$$\dot{n} \sum_i x_i h_i = (\dot{n} + d\dot{n}) \sum_i (h_i x_i + h_i dx_i + x_i dh_i)$$

The mole fraction of reactant rarely exceeds 2%. Thus,  $\frac{\Delta n}{n} \approx 2\%$  and, as a first approximation, it is possible to neglect  $dn$ . The above equation then becomes

$$\sum_i (h_i dx_i + x_i dh_i) = 0$$

It is now possible to split  $h_i$  into two terms, i.e.  $h_i = H_i + C_{pi}(T - T_0)$  where  $H_i$  contains the chemical enthalpy of the  $i^{\text{th}}$  specie.  $H_i$  is characteristic of the particular specie only, and is not a function of  $T$  or  $x$ . Thus,  $dH_i = 0$  for conditions in the reactor, and:

$$dh_i = C_{pi} dT + (T - T_0) dC_{pi}$$

$$\sum_i x_i dh_i = \bar{C}_p dT + (T - T_0) d\bar{C}_p$$

where  $\bar{C}_p$  is the mean heat capacity of the gas in the reactor.

Now, consider three species: reactant, product, and carrier, having subscripts  $r$ ,  $p$ ,  $c$  respectively. Then

$$\sum_i H_i dx_i = (H_r - m H_p) dx_r$$

Since carrier is neither generated nor consumed  $dx_c = 0$ . Also,  $dx_p = -m dx_r$  where  $m$  is the stoichiometric index.

Thus

$$\sum_i H_i dx_i = (H_r - m H_p) dx_r$$

Similarly

$$\begin{aligned} \sum_i C_{pi} (T - T_0) dx_i &= (T - T_0) (C_{pr} - m C_{pp}) dx_r \\ &= (T - T_0) \Delta_r C_p dx_r \end{aligned}$$

It is seen that the quantity

$$\sum_i h_i dx_i$$

is simply the heat released by decomposition of reactant at temperature  $T$ . Thus, the above term may be re-written as  $-Q dx_r$

The energy balance equation may now be written as follows:

$$-Q dx_r = \bar{C}_p dT + (T - T_0) d\bar{C}_p$$

$$\left( \frac{-Q}{\bar{C}_p T_0} \right) dx_r = \frac{dT}{T_0} + \frac{(T - T_0)}{T_0} \frac{d\bar{C}_p}{\bar{C}_p}$$

The temperature change occurring in the reactor is generally less than 100 deg K. For nitrogen at 900 deg. K,  $\Delta C_p / C_p$  for a 100 degree temperature change is approximately 2%. The concentrations of reactants and products are so small that the effect of variations in their heat capacity is second order, and is likely to be less than the effect of variations in the specific heat of the carrier gas.

Taking  $T_0$  to be 1000 deg. K and  $\Delta T = 100$  deg. K

$$\frac{\Delta T}{T_0} = 0.1 \quad \frac{\Delta T}{T_0} \cdot \frac{\Delta \bar{C}_p}{\bar{C}_p} = 0.002$$

It is seen that the error introduced by assuming constant heat capacity is about 2%, which is no worse than errors introduced by previous assumptions.

Now, a simple expression for the change of reactant mole fraction as a function of temperature is obtained, i.e.

$$-dx = \left( \frac{C_p T_0}{Q} \right) \frac{dT}{T_0}$$

The concentration,  $C$  is the product of mole fraction and molar density, i.e.

$$C = x \rho_N$$

For an ideal gas at constant pressure

$$\rho_N = \frac{n}{V} = \frac{P}{RT}$$

and

$$\frac{d\rho_N}{\rho_N} = - \frac{dT}{T}$$

Now, 
$$\frac{dC}{C} = \frac{dx}{x} + \frac{d\rho_N}{\rho_N}$$

$$\frac{dC}{C} = \frac{dx}{x} - \frac{dT}{T}$$

$$\frac{dC}{C^m} = \left( \frac{1}{\rho_N} \right)^{m-1} \left( \frac{dx}{x} - \frac{dT}{T} \right)$$

It was shown that

$$dx = - \left( \frac{C_p T_0}{Q} \right) \frac{dT}{T_0}$$

It follows that

$$- \int_{x}^{x_f} dx = \left( \frac{C_p T_0}{Q} \right) \int_T^{T_f} \frac{dT}{T_0} = \left( \frac{C_p T_0}{Q} \right) \left( \frac{T_f - T}{T_0} \right)$$

Since the reaction goes to completion,  $X_f = 0$ , and one may write

$$X = \left( \frac{C_p T_0}{Q} \right) \frac{T_f - T}{T_0}$$

$$\frac{dX}{X} = \frac{-dT}{T_f - T}$$

In the above it was assumed that  $\frac{C_p T_0}{Q}$  is constant. This assumption is valid to within 2% or so.

It follows from the above derivations that

$$\frac{dX}{X} - \frac{dT}{T} = - \frac{T_f}{T} \frac{dT}{T_f - T}$$

For an ideal gas

$$\rho = \rho_0 \left( \frac{T_0}{T} \right)$$

Let

$$S = \frac{1}{\rho_0} \frac{Q}{C_p T_0} \quad \text{then} \quad \frac{1}{\rho X} = \frac{T}{T_0} S \frac{T_0}{T_f - T} - \frac{ST}{T_f - T}$$

Substituting these results into the equation for  $dc/c^m$ , the following is obtained:

$$\frac{-dc}{c^m} = \left( \frac{ST}{T_f - T} \right)^{m-1} \frac{T_f}{T} \frac{dT}{T_f - T}$$

The velocity  $V$  is related to the reference velocity  $V_0$  as follows

$$V = V_0 \left( \frac{T}{T_0} \right)$$

Also

$$\frac{dT}{dt} = V \frac{dT}{dl}$$

where  $l$  is distance along the axis of the reactor.

Substituting these expressions into the rate constant formula, the following is obtained

$$k_m = \frac{-1}{c^m} \frac{dc}{dt} = \left( \frac{ST}{T_f - T} \right)^{m-1} V_0 \frac{T_f}{T_0} \frac{1}{T_f - T} \frac{dT}{dl}$$

$$k_m = \frac{T_f}{T_0} V_0 S^{m-1} \left( \frac{T}{T_f - T} \right)^m \frac{1}{T} \frac{dT}{dl}$$

This expression was used to deduce rate constants from the experimental data.

#### B. Determination of Reaction Order

The  $n^{\text{th}}$  order rate constant,  $k_n$  was derived to be

$$k_n = \frac{T_f}{T_0} V S^{n-1} \left( \frac{T}{T_f - T} \right)^n \frac{dT}{dl}$$

The quantity in the first parenthesis does not vary much during a run, and may be approximated as constant for the following discussion. Then, one may write:

$$k_n \approx B \left( \frac{T}{T_f - T} \right)^n \frac{dT}{dl}$$

It is clear from this formula that as  $T$  approaches  $T_f$

any errors in the temperature measurement are magnified. Thus, it was found practical to discard the part of the temperature trace where  $T_f - T$  was less than 10 deg. K.

The data may be reduced assuming different orders of reaction. If the standard deviations of activation energy, or preexponential factor, for a least square line through the  $n^{\text{th}}$  order kinetics data are then plotted against the assumed order, the resulting curve has a minimum. This minimum corresponds to the overall order of reaction which gives the best correlation of experimental data. However, this type of analysis can be somewhat misleading. Reference to the formula for the rate constant shows that the quantity

$$\frac{T}{T_f - T}$$

is raised to the  $n^{\text{th}}$  power, where  $n$  is the order of reaction. The result of this operation is that the importance of errors in temperature are magnified for higher orders and suppressed for lower ones. Thus, one would expect the "true" overall order of the reaction to be somewhat greater than that indicated by the above method.

There is also a second means of determining the order of reaction. It is possible to write:

$$\begin{aligned} \text{Rate} / C^n &= k_n = A \exp(-E/RT) \\ \text{Rate} / C^{n+m} &= k_m = (A/C^m) \exp(-E/RT) \\ k_m &= k_n / C^m \end{aligned}$$

where  $n$  is the "true" order of reaction, and  $(n + m)$  is the assumed order. A plot of  $\ln(k_n)$  versus  $1/T$  will give a straight line. However, a plot of  $\ln(k_m)$  versus  $1/T$  will give a curve, as will be evident from the

following analysis.

If logarithms are taken of both sides of the above expression, the following results:

$$\ln k_m = \ln A - m \ln C - \frac{E}{RT}$$

However, C is proportional to  $(T_f - T)/T$  and it is permissible to write  $C = (T_f - T)/BT$  where B is approximately constant. It is then permissible to re-write the above expression as follows:

$$\ln k_m = \ln A + m \ln B - m \ln \left( \frac{T_f - T}{T} \right) - \frac{E}{RT}$$

Taking derivatives of both sides:

$$\frac{dk_m}{k_m} = \frac{m T_f dT}{T(T_f - T)} - \frac{E}{R} d\left(\frac{1}{T}\right)$$

and

$$\frac{d(\ln k_m)}{d(1/T)} = -m \frac{T T_f}{T_f - T} - \frac{E}{R}$$

If m is positive, i.e. if the assumed order is higher than the true order, then the absolute value of the slope will increase as T approaches  $T_f$ , i.e. as the temperature during the run increases. If, on the other hand, m is negative, i.e. the assumed order is lower than the true order, then the absolute value of the slope will decrease as the temperature during a run increases. For  $m=0$  a straight line results.

From the expression for the rate constant, i.e.

$$k \approx B \left( \frac{T}{T_f - T} \right)^n \frac{dT}{dl}$$

it may be seen that errors in temperature, and particularly in  $T_f$ , will contribute curvature to an Arrhenius plot of the data. If the measured

value of  $T_F$  is lower than the true adiabatic value, then the measured rate constants at higher temperature will appear to be too high, giving an upward curvature to the Arrhenius plot. Similarly, a downward curvature results if the measured value of  $T_F$  is too high.

Insofar as errors in temperature, and particularly in  $T_F$ , are random, curvature due to such errors should be randomly positive or negative, and should thus average out if the assumed order corresponds to the true order. If, however, the assumed order differs from the true order, then the curvature should be predominantly in one direction.

If both the standard deviation-assumed order plot, and the curvature method described above indicate the same value for the order of reaction, then indeed, a reasonable amount of faith may be placed in such a value.

Plots of the standard deviation of the activation energy versus assumed order for hydrazine, UDMH and monomethylhydrazine are shown in Figures 29, 30, and 31. For hydrazine the minimum is at  $n = 0.9$ , for UDMH it is at  $n = 0.75$ , and for monomethylhydrazine the standard deviation is least for  $n = 1$ .

However, curvature analyses of individual runs showed the best order for all three substances to be very close to unity.

The best order predicted by the two analyses is probably different because the least square approach is likely to indicate a reaction order which is too low. However, the very low value of  $n$  indicated for UDMH should make one consider the possibility that the overall reaction order might be less than unity.

### C. Reproducibility and Plots of Experimental Data

Reproducibility of data was reasonable, considering the accuracy generally obtainable with chemical kinetics data. However, two principal sources of error may be distinguished, namely heat transfer to the reactor walls, and fluctuations of fuel flow rate during a run.

An indication of the reproducibility of hydrazine data is given in Figure 31. The two runs shown were taken on different days and picked randomly from the data without any attempt to show the best possible reproducibility. Actually, plots of all data show the reproducibility of runs to often be much better than is shown in Figure 32. The "hump" in the data for run 752 is probably due to a fuel surge. Reproducibility plots for UDMH and monomethylhydrazine are shown in Figures 33 and 34. In all cases, the lines drawn are the least square lines determined by all the data.

From all runs it was concluded that the error in experimental points is approximately  $\pm 50\%$ .

Arrhenius plots for the three substances studied are shown in Figures 35 for hydrazine, 36, 37, 38, 39 for  $N_2H_4/H_2O$  mixtures, 40, 41, 42 for UDMH, and 43, 44 for monomethylhydrazine.

The different type points show data taken on different days.

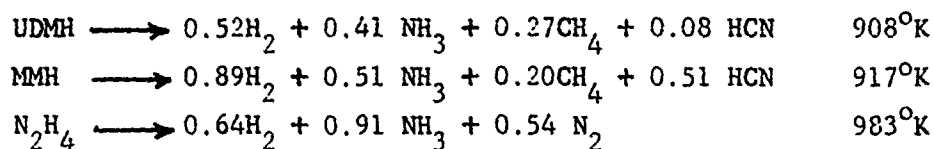
#### D. Integration Analysis of Data

If the scatter in the kinetics data obtained from the flow reactor is due to random errors, then it should be possible to integrate out the "signal" from the "noise." The following technique was employed. The temperature regime in which data had been obtained was divided into  $N$  equal intervals of  $1/T$ . In each of these intervals an average value of  $\ln k$  and an average value of  $1/T$  was obtained from the experimental points. These average values were then used as the coordinates of a new point. If an infinite number of experimental points were available, the intervals could be made infinitesimally small, and a resulting curve could be completely determined. However, only a little over 200 points were available.  $N$  was chosen to be 20-30 giving approximately 7-10 "raw data" points for each "reduced" point. The results of this operation on data for hydrazine, UDMH and monomethylhydrazine taken in the 3 inch duct are shown in Figures 45, 46, and 47. The lines drawn are least square lines determined from the original data points.

### E. Chemical Analysis of Reaction Products

Chemical samples were taken near the exit of the reactor using the water cooled probe discussed earlier. The samples were collected in pyrex vessels which were stored at room temperature, and later analyzed for hydrogen and methane using a Beckman GC-1 gas chromatograph. A molecular sieve column was used, and the chromatograph had been calibrated with standard samples of hydrogen and methane. The samples were also analyzed by infrared absorption. A 10 cm single pass absorption cell with NaCl windows was used in conjunction with a Perkin-Elmer model 21 spectrophotometer. Infra-red traces of the gas samples are shown in Figures 48, 49, 50. The infra-red spectrum of the hydrazine decomposition products is identical with that of the standard ammonia sample, so only the ammonia sample trace is shown. The traces for the decomposition products of UDMH and monomethylhydrazine show methane and HCN in addition to ammonia. It appears that UDMH yields more methane and less HCN than does monomethylhydrazine.

The approximate stoichiometry for the decomposition of hydrazine and its methyl derivatives was found to be:



For the case of hydrazine decomposition, nitrogen was computed by difference.

For the decomposition of both UDMH and monomethylhydrazine a brown tarry deposit was formed on the water cooled probe. An infra-red spectrum of this tarry deposit in acetone solution is shown in Figure 51. Cordes (18) found a similar deposit when he decomposed UDMH in a flow reactor. Cordes (18) concluded that this tarry deposit was a polymer of methylene methyl amine. The spectrum in Figure 51 does not contradict this conclusion.

## CHAPTER VI

### DISCUSSION OF EXPERIMENTAL RESULTS

Once the order of reaction has been determined, the empirical correlation of data may be presented in terms of an Arrhenius expression. The next problem is to determine the range of applicability of the expressions obtained. It has two aspects. Firstly, one should know under what conditions it is permissible to approximate a complex reaction mechanism by the relatively simple Arrhenius expression. This problem is discussed in the section on mechanisms. Secondly, it is important to know what impurities the reactants contain, and what effect such impurities have on the measured reaction rate. Because of the large quantities of reagents used in the experiments, it was not possible to purify the reagents to a state of very high purity. However, chemical analyses of the reagents used are presented. The applicability of results obtained in this study to reactants of very high purity may then be tested by small laboratory scale kinetics experiments performed using both reactants of the type used in this study, and reactants of very high purity.

#### A. Hydrazine Decomposition

Figure 53 shows a comparison between data obtained in the flow reactor and results of shock tube studies by Jost (15). Though the excellent agreement is undoubtedly fortuitous, it nonetheless shows that good agreement can be obtained between chemical kinetics data taken by different investigators, using different types of apparatus. It also shows the usefulness of the adiabatic flow reactor for studying reaction rates which are too slow for ordinary shock tubes and too fast for isothermal bombs, or even isothermal flow reactors.

The activation energy for hydrazine decomposition obtained in the flow reactor study agrees well with that deduced from laminar flame studies by Gray and Lee (9) who obtained 36 kcal/mole, but does not agree

with the value of 28 kcal/mole obtained from flame studies by Van Tiggelen and DeJaegere (11). However, the latter value is due to a different interpretation of the flame data, i.e. Van Tiggelen and DeJaegere used a mean flame temperature in their Arrhenius plot, whereas Gray and Lee used the final temperature (78).

From the chemical kinetics standpoint, the flow reactor may be described as a "semi-dilute" system. For vibrational relaxation, and most free radical reactions, collisions with the nitrogen carrier gas are so ineffective that they may be ignored. Initiation reactions are the one important exception. It has been found that, for initiation reactions, the spread of third body effectiveness is relatively small, as contrasted to such spread for a process like vibrational relaxation (35).

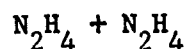
Thus it may be expected that, for conditions in the flow reactor, the initiation reaction for hydrazine decomposition would behave in a "pseudo low pressure manner" with nitrogen being the primary activating body, since its concentration is much higher than that of hydrazine. If one assumes a third body effectiveness of 0.2 for the nitrogen carrier gas, then for a 1% hydrazine-nitrogen mixture the "effective pressure" for the initiation reaction would be 160 mm Hg.

Gilbert (33) found that below one atmosphere the laminar flame speed was independent of pressure, while at higher pressures it is inversely proportional to the square root of pressure, indicating an overall first order reaction at higher pressures. This may be interpreted as follows. At lower pressures, initiation reactions are proportional to the number of collisions, and the initiation rate is given by the expression

$$\frac{d}{dt} [\text{NH}_2]_{\text{initiation}} = 2k [\text{N}_2\text{H}_4] [\text{N}_2\text{H}_4]$$

At higher pressures, however, collisions are sufficiently frequent to maintain an equilibrium amount of excited  $\text{N}_2\text{H}_4^*$ , and the rate of the initiation reaction is determined by the unimolecular rate of decomposition of the  $\text{N}_2\text{H}_4^*$ , hence the first order behavior at higher pressures.

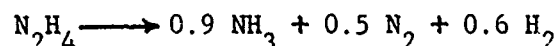
However, the adiabatic flow reactor studies would seem to fall in the low pressure regime, 160 mm Hg, and indeed they do. Only in this case the initiation reaction collisions are not



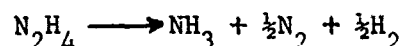
but rather  $\text{N}_2 + \text{N}_2\text{H}_4$ . Thus the initiation reaction should indeed be first order with respect to hydrazine, as was indicated by the experiments.

The above analysis also suggests that the initiation reaction should be first order with respect to nitrogen.

Gas samples were taken near the exit of the flow reactor using the water cooled probe discussed previously. These samples were analyzed for hydrogen by gas chromatography, and for ammonia by infrared absorption. The stoichiometry was found to be approximately



It is interesting to compare the above with stoichiometry observed in flame studies. Murray and Hall (7) measured flame speeds in hydrazine and in hydrazine-water mixtures. They also analyzed the reaction products and found that these pointed to a reaction



which is very similar to the stoichiometry found in this study.

It is interesting to compare the above results with the stoichiometry given by equilibrium calculations. Sawyer (79) calculated the equilibrium stoichiometry both for the decomposition of pure hydrazine, and for the decomposition of dilute hydrazine nitrogen mixtures of the kind studied in the flow reactor. For both cases he found that, above 800 deg. K the products are hydrogen and nitrogen with only small amounts of ammonia.

The difference between the equilibrium--and observed stoichiometry is to be explained as follows: Fairly large quantities of ammonia are formed in the rapid decomposition of hydrazine. The stoichiometry observed in this case is determined by the nature of the reaction mechanism, rather than by equilibrium considerations.

The composition of products formed in the rapid reaction subsequently adjusts to an equilibrium composition. For hydrazine decomposition, such adjustment is likely to be very slow. The truth of this statement may be seen from the following considerations.

Firstly the conversion reaction between ammonia and hydrogen plus nitrogen



is known to be generally slow in either direction. It is certainly slow compared with the rate of hydrazine decomposition.

Secondly, the time required to cool a sample of product gas is only a tenth of the reaction time allowed for hydrazine decomposition, so that only a short time is allowed for a slow reaction.

Thirdly, the samples are stored at room temperature and atmospheric pressure in pyrex vessels. Under these conditions conversion of ammonia to hydrogen and nitrogen is almost certain to be absent.

Thus it may be concluded that the stoichiometry measured in the flow reactor experiments does indeed correspond to that determined by the reaction mechanism.

Application of the stoichiometry information presented above to the study of reaction mechanisms will be presented in the section on reaction mechanisms.

Since purity of the reactants used is an important factor for judging areas in which the kinetics results are applicable, a study of reactant purity was made. An analysis of the reagent, conducted by the AMC Corporation (57), showed the following:

Ammonia:	8.3%
Water:	0.5%
Aniline:	0.3%
Hydrazine:	90.9% (by difference)

An experiment for investigating the effect that small amounts of impurities have on the reaction rate has already been suggested.

### B. Decomposition of Hydrazine-Water Mixtures

The effect of adding large amounts of water to the hydrazine was studied. It was found that the rate of decomposition of hydrazine-water mixtures was slower than that of the anhydrous material by approximately a factor of 10, and was independent of the amount of water added. Mixtures studied were 75%  $N_2H_4$ /25%  $H_2O$  and 50%  $N_2H_4$ /50%  $H_2O$ . Since the hydrate is 69.5%  $N_2H_4$ /31.5%  $H_2O$ , the mixtures studied lie on either side of the hydrate.

Arrhenius plots of rate data for hydrazine-water mixtures are shown in Figures 36 and 37.

It was also found that slightly wet hydrazine behaved kinetically like the hydrazine-water mixtures. Rate data for such hydrazine is shown in Figures 38 and 39. It is seen that wet hydrazine, and hydrazine water mixtures decompose at a rate which appears to be independent of the surface-to-volume ratio of the reactor.

An analysis of the "wet" hydrazine (57) showed the following composition:

	Sample I	Sample II
Ammonia	1.1%	7.5%
Water	0.9%	0.8%
Aniline	0.4%	0.7%
Hydrazine	97.6%	91.0%

(There did not appear to be any difference in the kinetic behavior of Samples I and II)

Apparently, water inhibits the gas phase decomposition of hydrazine by what seems like a very efficient suppression of some reaction step. It is interesting to speculate how such inhibition may take place.

It has been suggested by Ramsay (14) that  $N_2H_3$  radicals may be stabilized by collision.

Furthermore, it is known that chemical reaction products and

free radicals may be formed in vibrationally excited states.

Now, consider the possibility that the  $N_2H_3$  radical is formed in a vibrationally excited state, from which it can either branch to give  $NH + NH_2$ , i.e.



or be deactivated to a relatively stable form of  $N_2H_3$ , i.e.



The inhibitive effect of water now becomes apparent, namely to vibrationally relax the  $N_2H_3$  radical, and thus prevent it from branching into  $NH + NH_2$ . In this connection it should be noted that water is generally excellent for promoting vibrational relaxation. Third body efficiencies of 100 times greater than those of other substances have been reported for water (35). Also, some of the vibration frequencies of the water molecule are very close to some vibration frequencies of the  $N_2H_4$  molecule and thus the  $N_2H_3$  molecule. Consequently, a possibility for resonance transfer of vibrational energy between the two molecules exists.

A brief discussion of experimental observations for the thermal decomposition of hydrazine was presented. A detailed discussion of the decomposition mechanism will be presented in the section on reaction mechanisms.

### C. The Decomposition of Unsymmetrical Dimethyl Hydrazine

Unsymmetrical Dimethyl hydrazine was decomposed in the adiabatic flow reactor. The carrier gas was nitrogen, and the duct material was quartz. Decomposition studies were conducted in a 2 inch duct, a 3 inch duct, and a 4 inch duct. Within the accuracy of the experimental data the variation of surface to volume ratio had no effect on the observed rate. It thus seems reasonable to conclude that UDMH decomposition is not affected by the reactor walls, and is a truly

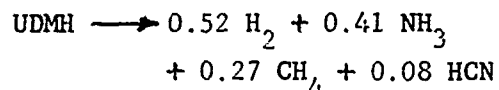
homogeneous gas phase reaction. This conclusion is in agreement with that reached by Cordes (18) in a similar study.

The overall reaction order was found to be approximately unity, again in agreement with Cordes (18).

Cordes (18) found an activation energy of 28 kcal/mole for UDMH decomposition in a isothermal flow reactor. Furthermore, Spencer and Gray (49), who studied UDMH ignition, also report an activation energy of 28 kcal/mole.

The activation energy found by the above investigators agrees with that found in the Princeton kinetics studies. However, the rates obtained by Cordes (18) are significantly lower than those obtained in this study. It is conceivable that fluid dynamic effects of the type discussed by Ballen (19) may account for the low rates observed by Cordes.

The stoichiometry of UDMH decomposition found in this study was approximately



It is interesting to compare this with the stoichiometry found by Cordes (18), that reported by Aerojet (57), and that calculated for equilibrium conditions by Sawyer (79).

Cordes (18) reports nitrogen and methane to be the primary decomposition products, with smaller quantities of higher hydrocarbons. Cordes reports that a mass spectral analysis of a decomposition sample showed the presence of methane, ethane and propane in the ratios 1/0.14/0.02. The infra-red spectra taken in the Princeton study do indicate small amounts of ethane, in addition to appreciable quantities of methane (see Fig. 49). Cordes also found relatively small quantities of hydrogen, the  $\text{H}_2/\text{CH}_4$  ratio being approximately 0.1. The ratio  $\text{N}_2/\text{CH}_4$  was 0.6. Cordes did not find HCN, but did observe the formation of a viscous liquid which had an infrared spectrum identical with the trimer of methylene methylamine.



The above consideration would explain why so little methane and HCN was observed in the Princeton study, as compared with the stoichiometry reported by Raleigh.

A much more detailed chemical analysis over a wide temperature range would be required before the observed stoichiometry could really be used to determine a reaction mechanism.

A chemical analysis of the UDMH used in this study (57) showed the following composition

Ammonia:	0.2%
Dimethylamine:	0.2%
Methylene dimethyl hydrazine:	0.2%
Water:	0.1%

It is seen that only very small amounts of impurities are present.

The reaction mechanism of UDMH decomposition will be discussed in a later section.

#### D. Decomposition of Monomethylhydrazine

Monomethylhydrazine was decomposed in a 3 inch duct and in a 4 inch duct, using nitrogen carrier gas.

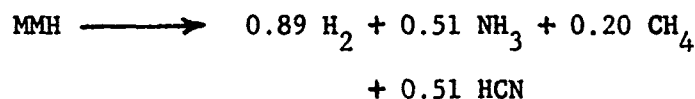
The decomposition was found to be first order with respect to monomethylhydrazine, the overall rate constant being

$$k = 10^{13.4} \exp -47,000 / RT$$

for decomposition in the 3 inch duct.

The reaction rates observed when monomethylhydrazine was decomposed in the 4 inch duct were slightly lower than those observed with the 3 inch duct. This observation may be interpreted as indicating a surface effect. However, more 4 inch duct decomposition data should be obtained before much faith is placed in the above deduction.

For monomethylhydrazine, the following gaseous decomposition products were observed



Note that more hydrogen and considerably more HCN is formed than for the case of UDMH decomposition.

An analysis of the monomethylhydrazine used showed the following (57)

Ammonia plus

Methylamine :	0.5%
UDMH :	0.1%
$\text{N}_2\text{H}_4$ :	0.1%
Water :	2%
Unidentified :	0.5%

#### E. Comparison of $\text{N}_2\text{H}_4$ , UDMH, MMH

Arrhenius plots for reaction rates of hydrazine, UDMH and monomethylhydrazine are shown in Figure 52.

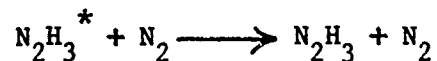
It is somewhat surprising that the reaction rate of hydrazine, which is known for its poor chemical stability, is the slowest. One interpretation of this observation is that the particular reactions which promote the explosive decomposition of hydrazine vapor cannot take place under conditions such as those found in the flow reactor.

Conditions in the flow reactor are such that surface effects must be slight, because of the large volume/surface ratio and the use of quartz as a wall material. Furthermore, the hydrazine vapor is mixed with large quantities of the nitrogen carrier gas.

At first glance it seems like nitrogen may take part in the reaction



and thus curtail branching. This possibility cannot be ruled out entirely. However, the third body effectiveness of  $N_2$  in the above reaction is likely to be very small, in which case the importance of the reaction



is likely to be slight.

Thus it is not unlikely that the rate of homogeneous gas phase decomposition of hydrazine is indeed relatively slow, and that hydrazine explosions are surface initiated. This conclusion is confirmed by the strong effect which most surface materials have on the decomposition of hydrazine vapor.

A detailed discussion of the decomposition mechanisms of hydrazine and its two methyl derivatives will be presented in the section on reaction mechanisms.

## CHAPTER VII

### DECOMPOSITION MECHANISMS

The reaction mechanisms of related species, such as those of hydrazine and its methyl derivatives, may be discussed together as a group, analyzed quantitatively, and finally compared again.

An alternate approach is to discuss reaction mechanisms for the individual substances, analyze the mechanisms, and then make comparisons. This latter method has the advantage that no a priori similarities are assumed.

In the subsequent discussion, the second approach is followed. Reaction mechanisms for the individual species are suggested and analyzed. Then a comparison of decomposition mechanisms of hydrazine, UDMH and monomethyl hydrazine is presented.

But before proceeding to a discussion of specific mechanisms it seems that a consideration of different means for analyzing reaction mechanisms would be worthwhile.

Perhaps the oldest and best known way of analyzing complex reaction mechanisms makes use of the steady state approximation. This approach has two drawbacks. Firstly, it tells nothing about the transient behavior of the system, and secondly the equations describing a complex reaction mechanism often cannot be solved even after the steady state approximation is made.

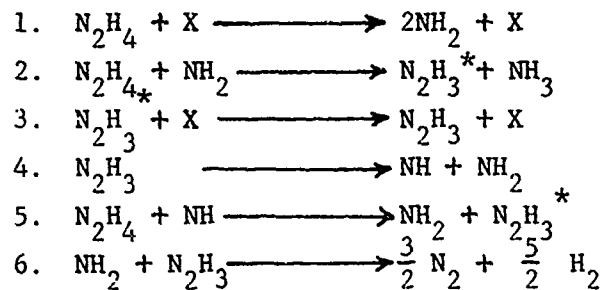
A more sophisticated approach has been suggested by Wei and Prater (80) who developed a method for analyzing reaction systems of molecular species which have the characteristic that the coupling between each pair of species is by first order reactions only. Wei and Prater essentially consider a series of coupled, linear, first order differential equations.

Unfortunately, the equations describing the reaction mechanisms considered for the decomposition of hydrazine and its methyl derivatives

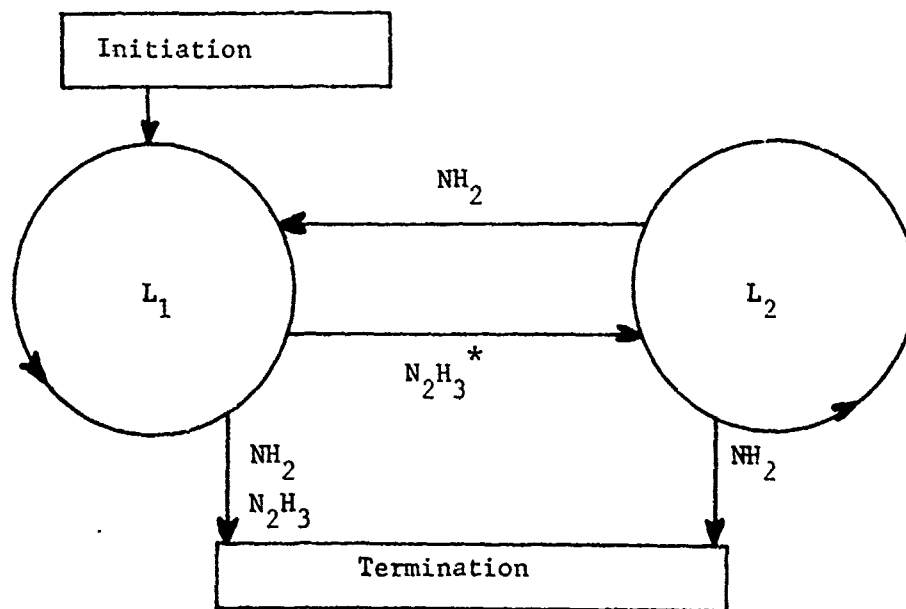
are non-linear, so that it is not possible to use an unmodified Wei-Prater type of analysis.

It might, however, be possible to consider a complex reaction mechanism in terms of loops and links.

Consider the following simplified reaction scheme for hydrazine decomposition



It is now possible to consider reactions 2 and 3 as a loop, L1, and reactions 4 and 5 as a loop, L2. The reaction mechanism may then be visualized in the following geometrical scheme.



Then, the "speed" of a loop will depend upon the amount of free radicals available to that particular loop, and thus on the rates at which the loop gains and loses free radicals.

It is conceivable that a method of mathematical analysis based on the above model could be developed for the treatment of complex reaction mechanisms.

However, the approach followed in this study was the "brute force" one of numerical computation. On one hand, the primary interest was in understanding the behavior of the suggested reaction mechanisms as rapidly and completely as possible, on the other, computing equipment was readily available.

In what follows, reaction mechanisms for the decomposition of hydrazine and its derivatives are suggested, and numerically analyzed. The results of the analysis are then discussed and used as a basis for conclusions about the reaction mechanisms.

The numerical methods employed are discussed in the appendices.

#### A. Hydrazine

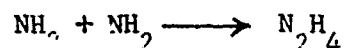
From the previous discussion, it seems reasonable to assume that the initiation reaction for the thermal decomposition of hydrazine is



the rate constant being

$$k = 10^{19} \exp \left( \frac{-60,000}{RT} \right) \text{ cc/mole-sec}$$

Similarly, the reverse reaction

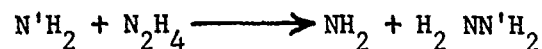


must be considered. By analogy with methyl radical recombination (38), the rate constant for this reaction may be expected to be

$$k = 10^{13} \text{ cc/mole-sec}$$

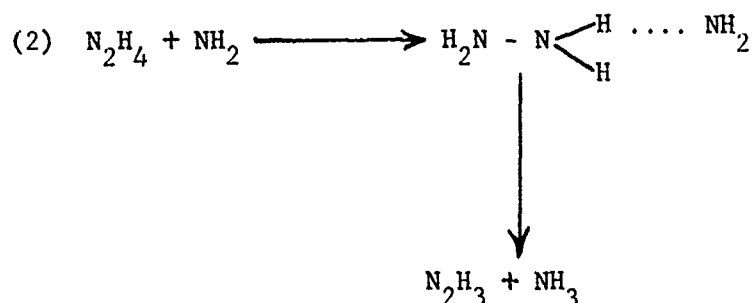
The question of likely propagation reactions now arises.

It seems reasonable that the  $\text{NH}_2$  radicals formed by the initiation reactions should attack hydrazine molecules. The simple exchange reaction



will be ignored, as it does not contribute to the decomposition.

If, however, the  $\text{NH}_2$  attacks a hydrogen atom in hydrazine, the following reaction is likely

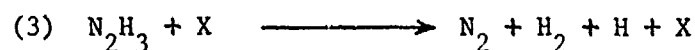


The rate constant for this reaction was taken to be

$$k_2 = 10^{13} \exp \frac{-7,000}{RT}$$

in agreement with the value chosen for it by Gilbert (21)

Both Gilbert (21) and Adams and Stocks (8) suggest the reactions



The rate constant for the reaction 3 was taken to be

$$k_3 = 10^{13} \exp \frac{-20,000}{RT} \quad \text{cc/mole-sec}$$

The constant for reaction 4 was measured by Birse and Melville (81) and found to be

$$k_4 = 10^{13} \exp \frac{-7,000}{RT} \quad \text{cc/mole-sec}$$

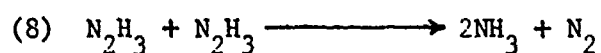
Though neither Gilbert (21) nor Adams and Stocks (8) include any branching reactions in their mechanisms, such a reaction was included in the mechanisms studied here. The reasons for this are as follows:

1. If  $N_2H_3$  can decompose in the complex manner of reaction 3, it should also be able to decompose by simple rupture of the N - N bond.

2. The NH radical has been observed in flames (12).

3. Without branching, the overall activation energy of the reaction computed from the mechanism was found to be too high. (An activation energy of 36 kcal/mole was observed experimentally)

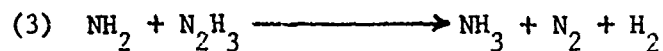
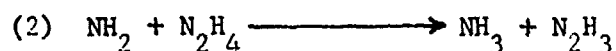
At first glance, the third reason seems in error, since  $NH_2$  formation is first order with respect to hydrazine, whereas all the termination reactions are second order. These are, in agreement with those suggested by Gilbert (21), as follows:



Also, the reverse of the initiation reaction, i.e.



Now, consider the simplified mechanism



$$\frac{d}{dt} [N_2H_3] = k_2 [NH_2] [N_2H_4] - k_3 [NH_2] [N_2H_3]$$

at steady state:

$$[N_2H_3] = \frac{k_2}{k_3} [N_2H_4]$$

$$\begin{aligned} \frac{d}{dt} [NH_2] &= 2k_1 [N_2H_4] [X] - k_2 [N_2H_4] [NH_2] \\ &\quad - k_3 [NH_2] [N_2H_3] \end{aligned}$$

at steady state:

$$2k_1 [N_2H_4] [X] = [NH_2] \left\{ k_2 [N_2H_4] + k_3 [N_2H_3] \right\}$$

substituting for  $[N_2H_3]$

$$2k_1 [N_2H_4] [X] = [NH_2] [N_2H_4] \left\{ k_2 + k_2 \right\}$$

$$\frac{k_1}{k_2} [X] = [NH_2]$$

If the overall rate is directly proportional to  $NH_2$  concentration, as is reasonable to assume, the overall activation energy of the reaction without branching should be 53 kcal/mole. For the case of negligible branching, numerical solution of the complete mechanism at 900°K and 1000°K gives an activation energy of 57.5 kcal/mole.

The rate constants for the termination reactions were taken to be as follows

$$k_7 = 10^{12.5} \text{ cc/mole-sec}$$

$$k_8 = 10^{12.3} \text{ cc/mole-sec}$$

$$k_9 = 10^{15} \text{ cc/mole-sec}$$

$$k_{10} = 10^{13} \text{ cc/mole-sec}$$

Certainly the values of  $k_7$ ,  $k_8$ , and  $k_{10}$  are such as one would normally expect. The value of  $k_9$ , however, does appear to be somewhat high.

The following branching reaction seems to be reasonable:



It is most probable that the NH thus formed will react with hydrazine, which is the most abundant specie. Thus, the following reaction is postulated:



The result is a very powerful set of branch reactions.

Since decomposition of  $N_2H_3$  by reaction 5 appears to be easier than by reaction 3, the activation energy was taken as being slightly less, i.e. 18 kcal/mole.

One would expect atomic hydrogen to be more active than NH. If this is indeed the case, then the activation energy for reaction 6 should be higher than for reaction 4. It was taken as 10 kcal/mole.

It is realized that NH is a very active radical, and that the above assumption may be invalid. But, since all NH is consumed by reaction 6, the value of  $k_6$  does not affect either the stoichiometry of the overall reaction, or the overall rate.

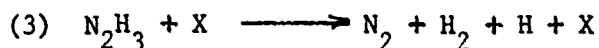
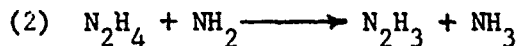
In summary, the mechanism is as follows:

#### Initiation



$$k_1 = 10^{19} \exp \frac{-60,000}{RT}$$

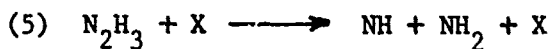
#### Propagation



$$k_2 = k_4 = 10^{13} \exp \frac{-7,000}{RT} \quad \text{cc/mole-sec}$$

$$k_3 = 10^{13} \exp \frac{-20,000}{RT} \quad \text{cc/mole-sec}$$

#### Branching

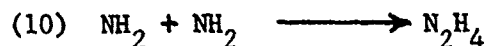


$$k_5 = 10^{12.8} \exp \frac{-18,000}{RT} \quad \text{cc/mole-sec}$$

$$k_6 = 10^{14} \exp \frac{-10,000}{RT} \quad \text{cc/mole-sec}$$

#### Termination





$$k_7 = 10^{12.5} \text{ cc/mole-sec}; k_8 = 10^{12.3}; k_9 = 10^{15}; k_{10} = 10^{13}$$

The above mechanism was solved numerically on a 7090 electronic computer. The differential equations describing the above mechanism and details of the program may be found in appendix C.

Since reaction rates are functions of the independent variables concentration and temperature, it was felt that the mechanism should be studied at different temperatures, keeping concentration constant, and at different concentrations, keeping temperature constant. It is realized that the case is somewhat hypothetical, since the quantity which is kept constant in physical systems usually is either volume or pressure, rather than concentration. However, concentration is the more fundamental quantity, and was therefore used.

The usefulness of such computation is three-fold. Firstly, it shows up the transient characteristics of the reaction. Secondly, a detailed study of a reasonable mechanism can bring out expected modes of behavior for the reaction. Such predictions can suggest critical experiments to verify or disprove the validity of the postulated reaction mechanism. Once a reasonable amount of faith can be placed in the proposed mechanism, then it may be used to predict behavior of the reaction over a much wider range of temperature and concentration than can be measured experimentally.

The approach followed was to analyze the behavior of several reasonable reaction mechanisms in an attempt to, on one hand, make predictions concerning the behavior of hydrazine in regimes other than that covered by the experimental study, and on the other hand, show up problem areas in the comparison of experiment and theory.

The mixture chosen for initial study was one containing

10% reactant, and 90% third body. The concentration was taken to be that of an ideal gas at standard conditions, i.e. 1 atmosphere pressure and 273 degrees Kelvin. This was kept the same as cases at different temperatures were considered. In a physical system this would require the pressure to be different at different temperatures.

The results of the computation for isothermal conditions at 1000°K are shown in Figures 58, 59, and 60. A free radical steady state is reached after some 80 micro-seconds, or after approximately 1.5% of the reactant has been consumed. After the reaction is about 80% complete, the rate constant begins to drop sharply.

Some chemical kinetics experiments are performed under such conditions that only a very small percentage of the reactant is consumed. Reference to Figures 59 and 60 shows that rates measured for cases where the extent of reaction is very small can be significantly below the "fully developed" rates.

Reference to Figure 55 shows that assuming constant free radical concentration may be good for some radicals and very poor for others. Reference to Figure 55 also indicates that the steady state assumption is not permissible at the beginning of the reaction, and as the reaction goes to completion.

An examination of Figures 55 and 56 shows up essentially four regimes. First, there is the initial build up of free radicals, and of the rate constant. The build up is followed by a short plateau region, which is the region in which the steady state assumption is valid. This "steady state" rate constant was used to determine the calculated curve in Figure 58. The plateau region is followed by a region in which the first order rate constant decreases linearly. In this region, an empirical rate constant of order greater than unity would be deduced experimentally. The final region shows a sharp non-linear decrease of the rate constant and of the free radical concentrations.

It is seen from the above that the reaction order which would be observed empirically, if the mechanism is correct, does not necessarily

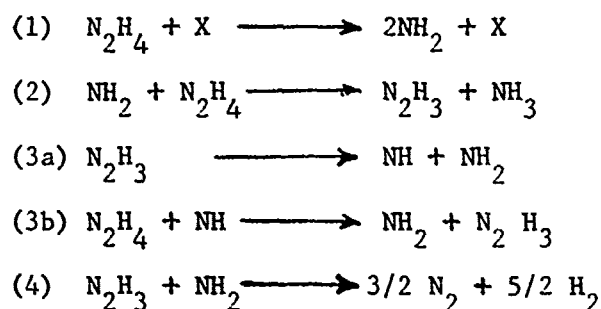
correspond to the "steady state" reaction order.

There exist two ways in which an empirical reaction order may be deduced. One of these ways is to measure the rate after a certain fraction of reactant is consumed for a series of experiments in which the initial reactant concentration is varied. The other way is to let the reaction go to completion, and use the function of rate and concentration thus obtained to determine an optimum reaction order.

For a reaction obeying steady state kinetics the two procedures would give identical results. If, on the other hand, steady state kinetics are not followed, then the two procedures can conceivably give different results.

At this time it might be worthwhile to consider what meaning can be attached to the "overall reaction order" for a reaction obeying steady state kinetics.

Consider the following simplified reaction mechanism for hydrazine decomposition.



This mechanism may be further simplified by combining reactions 3A and 3B into a single reaction



A steady state analysis of the above mechanism gives the following expression for the overall reaction rate:

$$-\frac{d}{dt} [\text{N}_2\text{H}_4] = k_A [\text{N}_2\text{H}_4] [\text{X}] + k_B [\text{N}_2\text{H}_4] [\text{N}_2\text{H}_3]$$

$$\text{where } k_A = 2k_1 ; k_B = k_2 k_3 / k_4$$

If  $k_A$  and  $k_B$  are of the same order of magnitude, then the reaction will be second order at high hydrazine concentrations, and first order with respect to hydrazine at low concentrations unless X is  $N_2H_4$ . A reaction which is second order down to very low concentrations would indicate that either  $k_B \gg k_A$  or that X is  $N_2H_4$ . On the other hand, a reaction which is first order up to very high concentrations, shows that X is not  $N_2H_4$ , and that  $k_A \gg k_B$ .

If this simplified mechanism were used to interpret the experimentally observed reaction order of unity, one would conclude that the third body is not hydrazine, and that most of the free radicals are supplied by the initiation reaction, rather than by the postulated branching reactions.

At higher hydrazine concentrations the reaction is approximately first order with respect to hydrazine, whereas the overall order exceeds unity at low hydrazine concentrations.

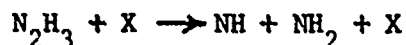
If the initial build-up phase is ignored, it is found that the overall first order rate constant is a function only of temperature and concentration, and is independent of initial reactant concentration. Thus it does not matter whether the rate constant is determined by varying initial reactant concentration and measuring the rate after a certain fraction of reaction is completed, or whether rate as a function of concentration is determined by measuring a series of rates at different concentrations as a reaction is allowed to go to completion. The first order overall rate constant is plotted against hydrazine concentration in Figure 59.

The overall rate was found to be first order with respect to third body concentration as may be seen from Figure 60.

It is conceivable that the branching reaction is a result of the simple unimolecular decomposition

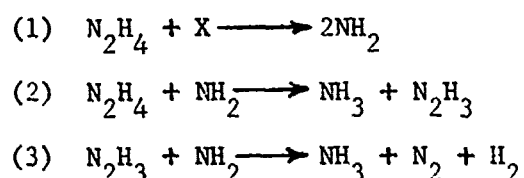


rather than



The only effect of eliminating the third body from the decomposition of the  $\text{N}_2\text{H}_3$  radical would be to change the effect of third body concentration on the overall rate. It may be seen from Figure 60 that the overall reaction rate is still first order with respect to third body concentration, but that the proportionality constant is now much less. Such behavior would, indeed, be expected.

The overall rate was found to be more sensitive to variations in the branching rate constants than to variations in the initiation rate constants, as may be seen in Figure 61, without branching, the overall reaction rate was found to be too low, and the activation energy too high. (For negligible branching, numerical solution of the complete mechanism at  $900^\circ\text{K}$  and  $1000^\circ\text{K}$  gives an activation energy of  $57.5 \text{ kcal/mole}$ ). By considering the simplified mechanism



it was shown that, in the absence of branching, one would expect a high activation energy.

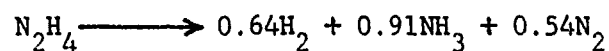
One may plot the logarithm of the computed rate constant against  $1/T$ , and compare the resulting curve with those obtained experimentally.

This is done in Figure 58. Agreement between the calculated rate constants and experimental values obtained in this study and in a shock tube study conducted by Jost (15) is seen to be good. The calculated values do fall significantly below those obtained in an isothermal bomb experiment conducted by Thomas (16). However, reference to Thomas's experiment suggests that his reaction was wall-catalyzed. Such an interpretation accounts for the high rate constants and low activation energy found by Thomas.

The stoichiometry of the reaction, as computed from the mechanism, is shown in the table below. The decomposition products shown are for one mole of hydrazine.

Temperature	Ammonia	Nitrogen	Hydrogen
1600 deg. K	0.915	0.545	0.59
1400	0.905	0.545	0.646
1200	0.87	0.56	0.68
1100	0.87	0.56	0.68
1000	0.895	0.545	0.655

The measured stoichiometry, at 983°K, was

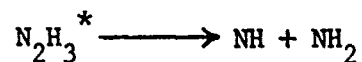


The agreement between the calculated and measured stoichiometry is seen to be remarkably good. Also, the insensitivity of the calculated stoichiometry to variations in temperature indicates that there is little uncertainty introduced into the measured stoichiometry by the fact that the reactor is adiabatic rather than isothermal.

Thus it is seen that the postulated mechanism is in good agreement with both the measured stoichiometry and the measured reaction rate data.

However, this mechanism does not explain the effect that water has on hydrazine decomposition. The observation that small quantities of water can considerably depress the gas phase decomposition rate and that adding relatively large quantities of water has no additional effect on the rate indicates that the water very effectively suppresses some essential reaction step.

It has been suggested by Ramsay (14) that the  $\text{N}_2\text{H}_3$  radical is formed in an excited state,  $\text{N}_2\text{H}_3^*$  which may either branch to give  $\text{NH} + \text{NH}_2$ , i.e.

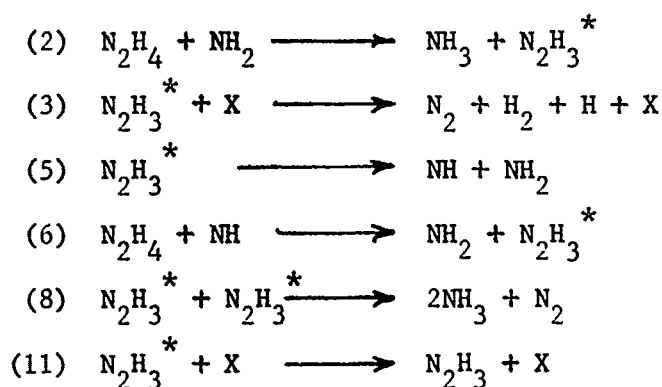


or be deactivated to a relatively stable form of  $N_2H_3$ , i.e.



This deactivated  $N_2H_3$  can no longer branch into  $NH + NH_2$ , but can partake in termination reactions. As was discussed previously, water would be excellent for promoting the relaxation of  $N_2H_3$ .

On the basis of the above considerations, a modified mechanism for hydrazine decomposition was suggested. The following modifications were introduced:



The predicted overall rate of the mechanism can be made to agree with that observed experimentally if  $k_{11}$  is set equal to  $10^{6.5}$  cc/mole-sec. This corresponds to a third body effectiveness for relaxation of approximately  $10^{-7.5}$ , or rather that ratio of branching/deactivation probabilities is

$$b/d = \frac{10^{8.4} \exp \frac{-18,000}{RT}}{10^{6.5} [X]}$$

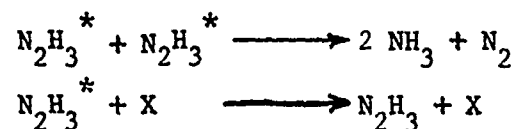
or

$$\frac{b}{d} = \frac{10^{1.9} \exp \frac{-18,000}{RT} \text{ mole/cc}}{[X]}$$

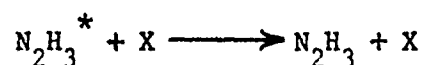
It is believed that the above mechanism for hydrazine

decomposition may explain why the hydrazine decomposition rate is relatively low under conditions in the flow reactor, in spite of the great tendency of pure hydrazine vapor to explode.

The  $N_2H_3^*$  may leave the reaction mechanism by two termination reactions, i.e.



At high temperatures the concentration of  $N_2H_3^*$  is so high that the second order termination reaction dominates. At low temperatures, however, the first order termination reaction is the most important, and the reaction rate can be seriously affected by varying the effectiveness of the reaction



Thus the rate at 800 degrees Kelvin can be made to increase more than a hundred-fold by letting the rate constant of the above reaction go to zero.

This modified mechanism is being further investigated.

Two mechanisms for the decomposition of hydrazine have been investigated. Good agreement with experimental observations has been shown. This is a significant advance over previous investigations where only a vague compatibility of suggested mechanisms with experimental data has been indicated.

There are two areas in which further research on hydrazine decomposition would be useful. One of these is the study of hydrazine decomposition rates at temperatures below 800 degrees Kelvin with, and without additives. A truly major contribution to understanding the reaction mechanism could be made by studying the transient build up, and disappearance of free radicals, and the effect of additives on this behavior.

Mechanisms for the decomposition of the two methyl-derivatives

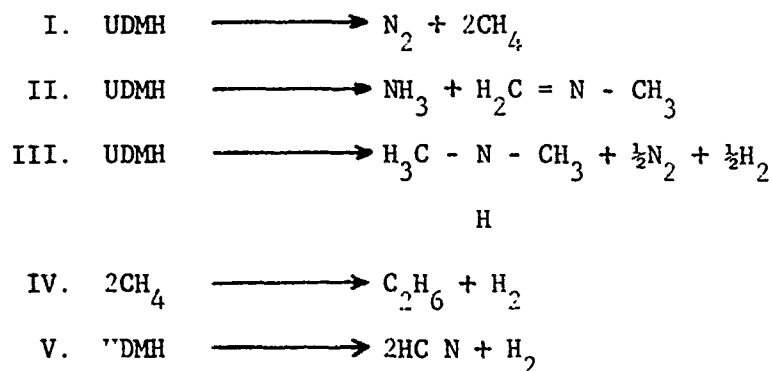
of hydrazine are far more complex, and cannot really be established with much reliability from the available data. However, such mechanisms have been postulated, and will be briefly discussed in what follows.

### B. Unsymmetrical Dimethylhydrazine

Unfortunately a mechanism for UDMH decomposition must be more complex than those proposed for hydrazine.

It appears that the best approach is to study one or several simplified mechanisms.

The decomposition of unsymmetrical dimethylhydrazine may be imagined to proceed in a manner described by the following overall reactions:

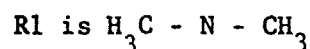


In what follows, a simplified reaction mechanism for the decomposition of unsymmetrical dimethylhydrazine is suggested.

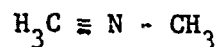
The following initiation reaction is proposed:



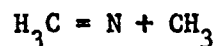
$$k_1 = 10^{22} \exp \frac{-72,000}{\text{RT}} \text{ cc/mole-sec}$$



The nitrogen of R1 is deficient in electrons. However, it may attract some carbon electrons to form a double, and eventually triple bond with the carbon. The result is the unstable compound



The singly bound  $\text{CH}_3$  group can break off easily enough to give

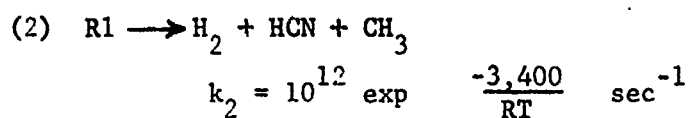


The  $\text{H}_3\text{CN}$  can break up into  $\text{H}_2 + \text{HCN}$ .

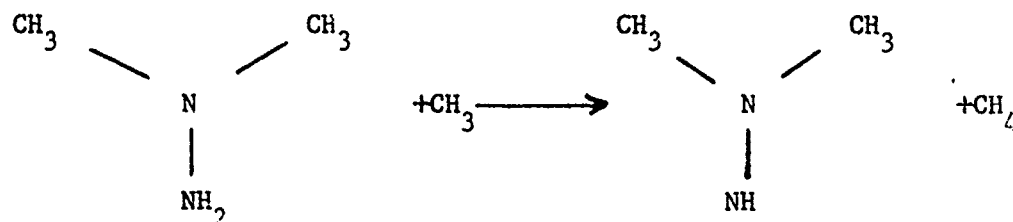
The overall reaction is



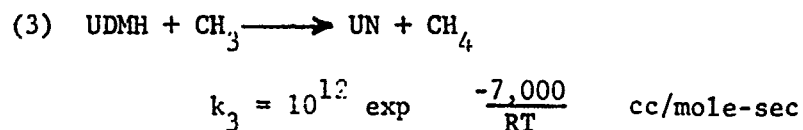
The reaction is endothermic by approximately 3.4 kcal/mole. If this value is used for the activation energy, one may write:



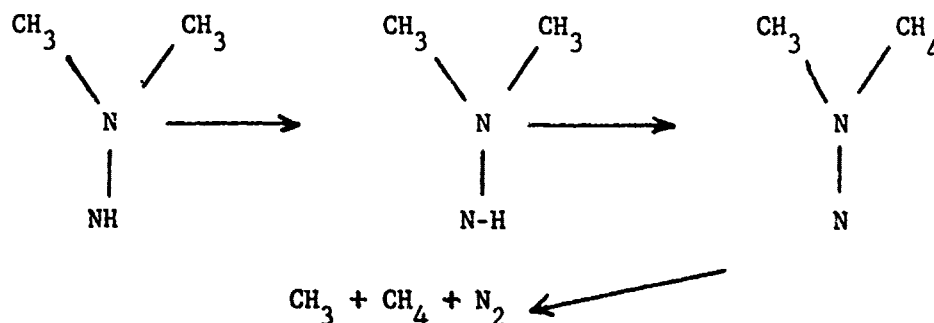
Methyl radicals may react with UDMH as follows:



or



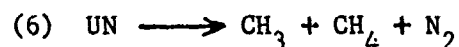
where UN is the radical  $\text{HNN}(\text{CH}_3)_2$ . This radical may rearrange as follows:



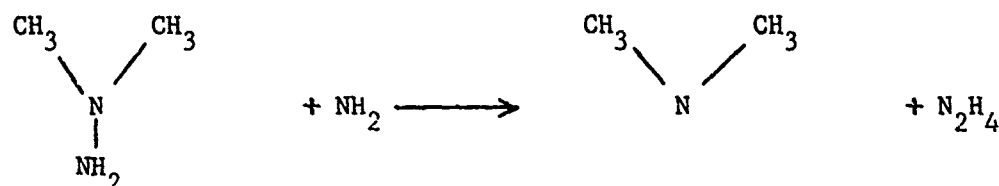
The rate constant for this reaction was taken to be the same as that for reaction (2), i.e.

$$k_6 = 10^{12} \exp \frac{-3,400}{RT} \text{ sec}^{-1}$$

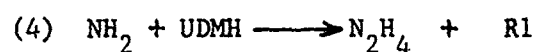
where



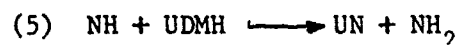
$\text{NH}_2$  radicals may react with UDMH as follows



or



Similarly

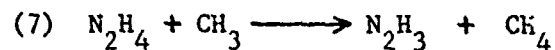


Reasonable rate constants are:

$$k_4 = 10^{11} \exp \frac{-7,000}{RT}$$

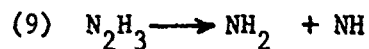
$$k_5 = 10^{14} \exp \frac{-7,000}{RT} \text{ cc/mole-sec}$$

The hydrazine thus formed would behave like an intermediate rather than like a product. Hydrazine may react with methyl and amin radicals in the reactions



$$\text{where } k_7 = k_8 = 10^{14} \exp \frac{-7,000}{RT} \text{ cc/mole-sec}$$

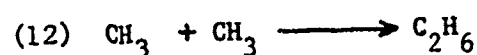
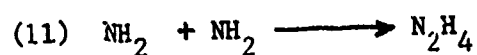
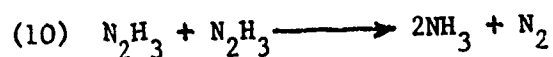
It may be assumed that the  $\text{N}_2\text{H}_3$  radical thus formed is unstable and decomposes in the branching reaction



$$k_9 = 10^{11} \exp \frac{-18,000}{RT} \text{ sec}^{-1}$$

where Eq is taken as that found to be appropriate in the hydrazine decomposition reaction.

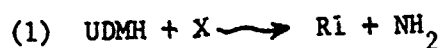
Finally, the following termination steps are proposed:



$$k_{10} = k_{11} = k_{12} = 10^{12} \text{ cc/mole-sec}$$

In summary, the following reaction mechanism is obtained:

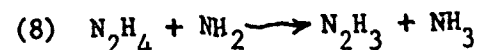
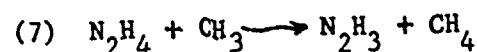
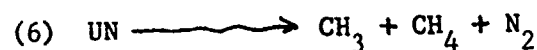
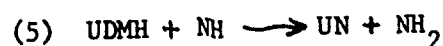
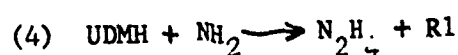
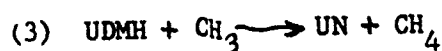
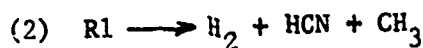
#### Initiation



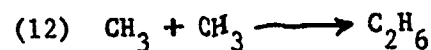
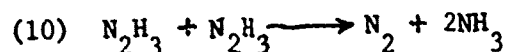
#### Branching



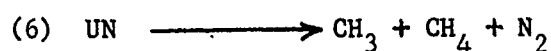
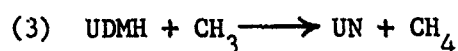
#### Propagation



#### Termination

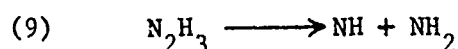
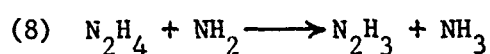
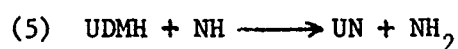
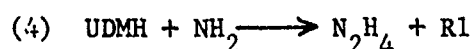


It may be noted that reactions 3 and 6 form a loop which converts UDMH to methane and nitrogen, i.e.

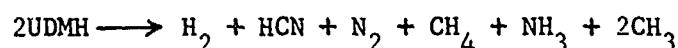


giving the stoichiometry UDMH  $\text{N}_2 + 2\text{CH}_4$

Reactions 4, 5, 8, 9 serve to convert UDMH to ammonia, R1, and UN, i.e.



R1 decomposes by reaction (2) to give hydrogen, HCN, and methyl radicals which may be used in the 3-6 loop. Similarly UN is used in the 3-6 loop. The 4, 5, 8, 9 loop may be used to give the stoichiometry

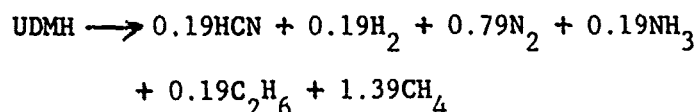


It may be seen from this that the branching reaction not only boosts the above loop, but also supplies  $\text{CH}_3$  radicals to the 3-6 loop.

On the other hand, reaction 7 converts  $\text{CH}_3$  radicals into  $\text{N}_2\text{H}_3$  which supply the 4, 5, 8, 9 loop.

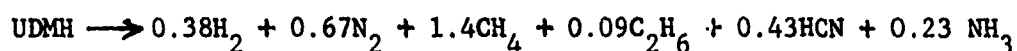
The complete reaction mechanism was solved numerically. The first order rate constant, as a function of temperature, was made to agree with that observed experimentally. However, the  $k$  vs. % reacted relationship is seen to be a complex function of temperature. The value of  $k$  taken for comparison with experimentally observed values was that where the slope of the  $k$  vs. % reacted curve was zero. (See Figure 62). If the  $k$  vs. % reacted relationship is as complex as that shown in Fig. 62, then a simple first order reduction would, indeed, show considerable scatter.

The stoichiometry computed at 900 deg. K is



the nitrogen, methane, and ammonia produced agree well with the Aerojet

stoichiometry reported by Raleigh, i.e.,



whereas the amount of hydrogen and HCN computed from the mechanism are significantly less.

The stoichiometry observed in the adiabatic flow reactor at 908 deg. K is



showing much more hydrogen and ammonia than was computed, and reported by Raleigh.

The concentrations of methane and HCN are suspect because of possible polymerization of these two substances in the cool region near the sampling probe.

In general, the postulated mechanism for UDMH decomposition agrees reasonably well with experimental observations.

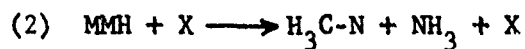
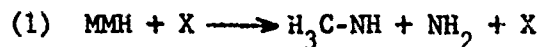
However, detailed observation of reaction rate as a function of concentration and temperature over a wide range of both variables is required before it will be possible to place any great faith in the suggested mechanism.

In the reaction mechanism postulated for UDMH decomposition hydrazine is an intermediate. Thus addition of hydrazine to UDMH should speed up the UDMH decomposition rate, if the suggested mechanism is correct.

### C. Monomethylhydrazine

A mechanism for the homogeneous, gas phase decomposition of monomethylhydrazine was developed in collaboration with Sawyer (82). This mechanism is as follows:

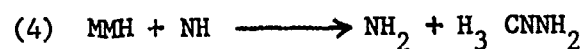
#### Initiation



$$k_1 = 10^{22} \exp (67,000/RT) \text{ cc/mole-sec}$$

$$k_2 = 5 \times 10^{21} \exp (67,000/RT) \text{ cc/mole-sec}$$

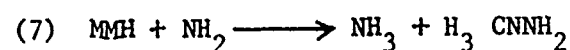
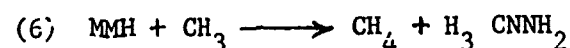
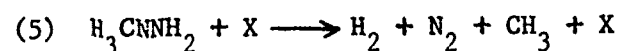
### Branching



$$k_3 = 10^{14} \exp (-18,000/RT) \text{ cc/mole-sec}$$

$$k_4 = 10^{13} \exp (-7,000/RT) \text{ cc/mole-sec}$$

### Propagation

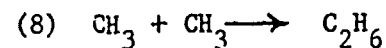


$$k_5 = 10^{14} \exp (-18,000/RT)$$

$$k_6 = 10^{13} \exp (-7,000/RT)$$

$$k_7 = 10^{13} \exp (-7,000/RT)$$

### Termination

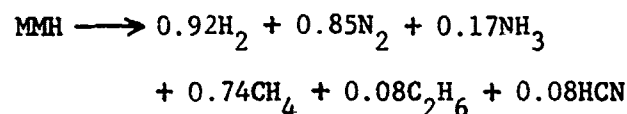


$$k_8 = 10^{13} \text{ cc/mole-sec}$$

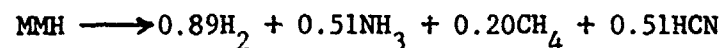
$$k_9 = 10^{14} \exp (-10,000/RT) \text{ sec}^{-1}$$

Sawyer (82) studied this mechanism numerically, and found its rate behavior to agree with that observed experimentally.

The following stoichiometry was computed at 900°K



Observations of stoichiometry in the adiabatic flow reactor showed at 917°:

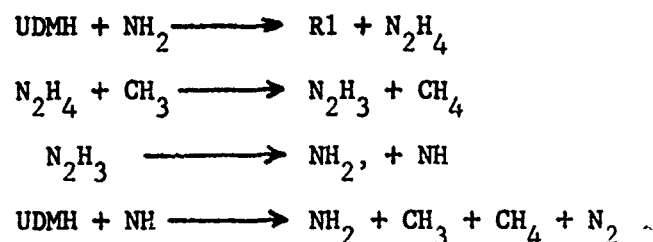


The hydrogen calculated agrees with that observed, whereas the experiment shows much more ammonia and HCN than computed. The experimental methane, and HCN, values are likely to be much too low because of polymerization.

D. Comparison of Decomposition Mechanisms of Hydrazine, Monomethylhydrazine and Unsymmetrical Dimethylhydrazine

A comparison of the suggested reaction mechanisms shows that UDMH and monomethylhydrazine have not only the  $\text{NH}_2$  and  $\text{NH}$  free radicals, but also the very effective  $\text{CH}_3$  radicals. This may explain why the overall gas phase rates of the methyl derivatives of hydrazine are faster than those of the parent substance.

The next question to be answered is why UDMH decomposition has a faster rate and lower activation energy than monomethylhydrazine decomposition. The postulated mechanisms show a quite effective branching chain for UDMH decomposition, i.e.



whereas the branching reaction for monomethyl-hydrazine decomposition, i.e.



is not part of a true branching chain, since  $\text{H}_3\text{CNH}$  is only formed in the initiation reaction



### CONCLUSIONS

The adiabatic flow reactor yields overall rate constants as functions of temperature and concentration in a reaction rate regime too fast for isothermal bombs and even isothermal flow reactors, and too slow for ordinary shock tubes.

Furthermore, the difficulties encountered in obtaining a kinetic interpretation of laminar flame-, isothermal bomb-, and isothermal flow reactor studies are avoided, since longitudinal diffusion of heat and active species in the adiabatic flow reactor is unimportant, radial variations in temperature may be eliminated, and radial velocity profiles are quite flat.

The one-dimensional flow pattern in the reactor is achieved by operating it in the regime of turbulent flow. Consequently, the effect of turbulence on the kinetics measurements had to be investigated. A method was developed by which an estimate may be made of this effect, and it was found that, for conditions encountered in the flow reactor, the effect of turbulence on chemical kinetics is small enough to be neglected.

An error analysis of the flow reactor showed the most serious experimental error to be due to violation of the adiabaticity assumption near the end of the reaction zone. This difficulty may be overcome by heating the reactor duct in such a manner that heat transfer is minimized. The present single electrical winding should be replaced by several, individually controlled coils. The current in these coils may then be adjusted in such a manner that the wall temperature and the gas temperature are within a few degrees of each other. If this is done, then it should be possible to reduce experimental error to less than 5%.

The activation energy for hydrazine decomposition obtained in the flow reactor study agrees with that deduced from laminar flame studies by Gray and Lee (9). Diffusion in the adiabatic flow reactor is unimportant, and the activation energy refers to the overall reaction. Thus, agreement of activation energy and stoichiometry obtained in the adiabatic flow reactor with the results of flame observations suggests that hydrazine decomposition flames should be interpreted on the basis of the thermal theory of flame propagation.

A comparison of the first order rates of the three monopropellants shows that, in the temperature regime of this study, i.e. 800 - 1000 deg. K. UDMH decomposition is fastest, hydrazine decomposition is slowest, and the monomethylhydrazine decomposition rate is intermediate. It is somewhat surprising that the reaction rate of hydrazine, which is known for its poor stability, should be the slowest. It is not unlikely, however, that the rate of homogeneous gas phase hydrazine decomposition is indeed relatively slow, and that hydrazine explosions are surface initiated. Such a conclusion is confirmed by the strong effect which most surface materials have on the decomposition of hydrazine vapor.

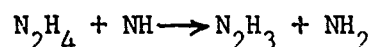
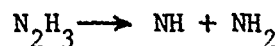
It was found that the activation energy of decomposition is highest for monomethylhydrazine, lowest for UDMH, and intermediate for hydrazine. The reaction mechanisms which have been postulated for the thermal gas phase decomposition of hydrazine and its methyl derivatives provide an explanation for the observed experimental trends.

Results of electron impact studies by Dibeler (29) show that the N-N bond is strengthened by the addition of methyl groups. Now, the initiation reactions for the decomposition of hydrazine and its methyl derivatives involve rupture of the N-N bond. Thus, initiation is easiest for hydrazine, most difficult for UDMH, and intermediate for MMH, suggesting the following relation of activation energies: UDMH MMH  $N_2H_4$ . But, the methyl substitution has an additional effect, namely to provide a source of methyl radicals which facilitate and enhance the chain effects. This consideration suggests the following relation of reaction rates:  $UDMH > MMH > N_2H_4$ , which is, indeed, observed. It is further suggested that the low overall activation energy of UDMH decomposition is due to a branching reaction, which however does not occur in monomethylhydrazine decomposition.

The decomposition of hydrazine, UDMH, and monomethylhydrazine were studied in the adiabatic flow reactor, and an explanation for the observed behavior has been presented. Further light can be shed on the problem by spectroscopic studies to experimentally identify the radicals taking part in the decomposition of the substituted hydrazines, and by

measurement of overall reaction rates in the presence of additives. Such additives as mercury- or lead alkyls to supply methyl radicals, and acetylene to scavenge radicals should be especially interesting. Below 1000 deg. K polymerization is the most important reaction of acetylene (45). It follows, that in the temperature range of this study, acetylene would be an excellent radical scavenger.

The mechanism for hydrazine decomposition suggested in this study differs from those postulated by previous investigators, in that it includes a set of branching reactions

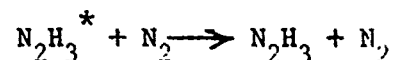


Without branching, the overall activation energy computed from the mechanism was too high, and the overall rate too low.

The logarithm of the computed 'steady state' rate constant was plotted against  $1/T$ . The resulting curve was found to agree with experimental data obtained in this study and in shock tube studies by Jost (15). Also, the stoichiometry calculated from the mechanism agreed with that measured experimentally. This is a significant advance over previous investigations where only a vague compatibility of suggested mechanisms with experimental results had been indicated.

It was found that the rate of decomposition of hydrazine-water mixtures was slower than that of the 'anhydrous' material by approximately a factor of 10, and was independent of the amount of water added. Thus it seems that water inhibits the gaseous decomposition of hydrazine by very effectively suppressing some reaction step. To explain this effect, it is suggested that the  $\text{N}_2\text{H}_3$  radical is formed in an excited state,  $\text{N}_2\text{H}_3^*$  which can either branch to give  $\text{NH} + \text{NH}_2$ , or be deactivated by collision to a relatively stable form. Then, small amounts of water can relax  $\text{N}_2\text{H}_3^*$  and thus suppress branching.

Unless the third body effectiveness of nitrogen is very low, the reaction



could make the overall rate of decomposition of hydrazine relatively low under conditions in the flow reactor, and yet quite rapid in pure hydrazine vapor.

Computations on the postulated reaction mechanisms showed that, if the initial build-up phase is ignored, then the overall first order rate constant is a function only of temperature and concentration, and is independent of initial reactant concentration. This means that free radical concentrations, and the overall rate, are independent of the previous history of the reaction. Thus, it is legitimate to write

$$-dC/dt = k (T) f (C,T)$$

However,  $f(C,T)$  is not a simple power function of concentration, and may only be approximated as such over quite narrow ranges of concentration and temperature. This conclusion is not surprising, and may indeed be deduced from the steady state treatment of a simplified mechanism. However, it shows a theoretical reason why data which are analysed according to an overall Arrhenius expression of the type

$$-dC/dt = k (T)C^n$$

must necessarily scatter.

Insofar as  $f(C,T)$  is characteristic of a particular mechanism, an accurate determination of  $f(C,T)$  would provide the maximum information which can be obtained from overall reaction rate measurements. Such a determination should be possible with an improved version of the adiabatic flow reactor.

There are two areas in which further research on hydrazine decomposition would be useful. One is the study of hydrazine decomposition rates at temperatures below 800 deg. K with, and without additives. The other is a study of the transient free radical buildup. A major contribution to understanding the reaction mechanism, and to the general field of chemical kinetics, could be made by studying the transient build-up, and disappearance of free radicals, and the effects of additives on this behavior.

REFERENCES

1. Herrick, J. W. (ed) and Burgess, E. (ed), "Rocket Encyclopedia Illustrated," Los Angeles 1959 Aero Publishers. p. 211.
2. Shternfeld, Ari, "Soviet Space Science" 2ed. New York, 1959, Basic Books. p. 89.
3. Smith, W. W., Development of a Trajectory-Correction Propulsion System for Spacecraft. Technical Report 32-205. Jet Propulsion Laboratory 1961. Pasadena, Calif.
4. Lee, D. H. and Evans, D. D., The Development of a Heated-Hybrid Generated Gas Pressurization System for Propellant Tanks. Technical Report 32-375. Jet Propulsion Laboratory, 1963, Pasadena, California.
5. Strunk, W. G., Preparation and Properties of Unsymmetrical Dimethylhydrazine. Chemical Engineering Progress, Vol. 54, No. 7, July 1958. p. 45.
6. Liberto, R. R., An Industrial Survey of Titan II Propellants. Report 8111-950001 Bell Aerosystems Company, September 1960.
7. Murray, R. C. and Hall, A. R., Flame Speeds in Hydrazine Vapor and in Mixtures of Hydrazine and Ammonia with Oxygen. Transactions of the Faraday Society, 47:743-751, 1951.
8. Adams, G. K. and Stocks, G. W., The Combustion of Hydrazine. Fourth (International) Symposium on Combustion, Baltimore, 1953, Williams and Wilkins, p. 239.
9. Gray, P., Lee, J. C., Leach, H. A., Taylor, D. C., The Propagation and Stability of the Decomposition Flame of Hydrazine. Sixth (International) Symposium on Combustion. New York, 1956 Reinhold, p. 255.
10. Gilbert, M. and Altman, D., Mechanism and Flame Speed for Hydrazine Decomposition. Prog. Rep. 20-278, Jet Propulsion Laboratory, 1955. Pasadena, California.
11. DeJaegere, S. et Van Tiggelen, A., Propagation de la Flamme dans les Melanges D'Hydrazine. Revue de l'Institut Francais du Petrole of Annales des Combustibles Liquides. Vol. XIII, No. 4, April 1958.

12. Hall, A. R. and Wolfhard, H. G., Hydrazine Decomposition Flames at Subatmospheric Pressures. Trans., Faraday Soc. Vol. 52, 1956. pp. 1520-1525.
13. Szwarc, M. The Dissociation Energy of the N-N Bond in Hydrazine. Proc. Royal Soc. A-198 (1949) p. 267.
14. Ramsay, D. A., The Absorption Spectra of Free NH and NH<sub>2</sub> Radicals Produced in the Flash Photolysis of Hydrazine. J. Phys. Chem. Vol. 57, p. 415 (1953).
15. Jost, W., Investigation of Gaseous Detonations and Shock Wave Experiments with Hydrazine. Aeronautical Research Laboratories Report ARL 62-330, April 1962.
16. Thomas, D. D., The Thermal Decomposition of Hydrazine. Prog. Rep. 9-14 Jet Propulsion Laboratory, 1947, Pasadena, Calif.
17. Lucien, H., The Thermal Decomposition of Hydrazine. J. Chem. Eng. Data, Vol. 6. No. 4. Oct. 1961, pp. 584-586.
18. Cordes, H. F. The Thermal Decomposition of 1, 1 Dimethylhydrazine. J. Phys. Chem. Vol. 65, pp. 1473-1477, Sept 1961.
19. Batten, J. J., A Possible Error in the Measurement of Rate Constants of Gaseous Reactions by Flow Techniques. Australian Journal of Applied Science, Vol. 12, No. 1 (March 1961) p. 11.
20. Gilbert, M., An Approximate Treatment of Hydrazine Decomposition in a Laminar, non-Isothermal Flow. Jet Propulsion Laboratory Progress Report 20-336. Pasadena, Calif., July 1957.
21. Gilbert, M., The Hydrazine Flame. Jet Propulsion Laboratory Progress Report 20-318. Pasadena, Calif. March 1957.
22. Penney, W. and Sutherland, G. The Theory of the Structure of Hydrogen Peroxide and Hydrazine. J. Chem. Phys. 2, 492 (1934).
23. Van Vleck, J. On the Theory of the Structure of CH<sub>4</sub> and Related Molecules: Part II. J. Chem. Phys. Vol. 1 (1933)<sup>4</sup> p. 219.
24. Based on Paulings original table, but including modifications to allow for recent changes in the preferred values of some of the thermodynamic functions. See W. F. Aftermath, A. E. Thesis, California Institute of Technology, Pasadena, 1953.

25. Herzberg, G. "Spectra of Diatomic Molecules." Van Nostrand, Princeton, New Jersey. 1957, 2nd ed, p. 195.
26. Audrieth, L. F. and Ogg, B. "The Chemistry of Hydrazine." Wiley, New York. 1951. pp. 65, 186.
27. Fresenius, W. and Karweil, J. The Normal Oscillations and the Configuration of Hydrazine. Z. Physikal Chem. ABT. B. Bd. 44, Heft 1, pp. 5-12.
28. Beamer, W. The Molecular Structure of Two Dimethylhydrazines by Electron Diffraction. J. Am. Chem. Soc. Vol. 70, p. 2979. (Sept. 1948).
29. Dibeler, V. H., Franklin, J. L., Pease, R. M. Electron Impact Studies of Hydrazine and the Methyl-Substituted Hydrazines. Am. Chem. Soc. Jour. Vol. 81, pt. 1 (1958) p. 68.
30. Hinshelwood, C. N., "The Kinetics of Chemical Change." Oxford, 1955, The University Press. p. 79.
31. Benson, S. W. "The Foundations of Chemical Kinetics." New York, 1960, McGraw-Hill, pp. 211-318.
32. Benson, loc. cit. pp. 228-238.
33. Gilbert, M. Combustion and Flame, 2, 137, 149 (1958) Cited by Boudart, M. Chemical Kinetics and Combustion. Presented at the VIII International Symposium on Combustion, Sept. 1960.
34. Gray, P., Lee, J. C., Leach, H. A., Taylor, D. C., The Propagation and Stability of the Decomposition Flame of Hydrazine. Sixth (International) Symposium on Combustion, New York, 1956, Reinhold, p. 255.
35. Bradley, J. N. "Shock Waves in Chemistry and Physics." New York 1962, Wiley, pp. 197-198.
36. Knudsen, V. O. and Fricke, E. J. Acoust. Soc. Amer. 12, 255 (1940). Cited by Bradley (35).
37. Eucken, A., and Numann, E. F. Physik. Chem. B36, 163 (1937). Cited by Bradley (35).
38. Kistiakowsky, G. B. and Roberts, E. K. J. Chem. Phys., 21, 1637 (1953). Cited by Davidson, N. and Sowden, R. G. "Annual Review of Physical Chemistry." Vol. 6, pp. 303-326, edited by Rollefson, G. K., and Powell, R. E. Stanford, California, 1955, Annual Reviews Inc.

39. Glasstone, S., Laidler, K. J. and Eyring, H. "The Theory of Rate Processes" New York, 1951, McGraw-Hill, P. 257.
40. Pritchard, H. O., Pyke, J. B. and Trotman-Dickinson, A. F., J. Am. Chem. Soc. 77, 285 (1955) cited by Porter, G. "Annual Review of Physical Chemistry" Vol. 7, pp. 207-230, edited by Eyring, H., Christensen, C. J. and Johnson, H. S. Stanford, Calif. 1956, Annual Reviews.
41. Livingston, R. Evaluation and Interpretation of Rate Data in "Technique of Organic Chemistry." Vol. VIII, Part I. New York, 1961, Interscience, p. 168.
42. Semenov, N. "Chemical Kinetics and Chain Reactions" Oxford, 1935, The Clarendon Press, pp. 1-87.
43. Moelwyn-Hughes, E. A. "Physical Chemistry" Cambridge, 1951, The University Press. pp. 545-546.
44. Semenov, loc. cit. pp. 73-84.
45. Steacie, E. W. R. "Atomic and Free Radical Reactions." New York, 1954, Reinhold, pp. 31-32, 172.
46. Wettermark, G. High Intensity Photolysis Studies of Acetone and Some Aliphatic Aldehydes. Arkiv for Kemi, B 18, N 1. Stockholm, 1961.
47. Gunning, H. E. Comment to Ramsay, op. cit. (14).
48. Frank-Kamenetsky, D. A. Calculation of Thermal Explosion Limits Acta Phys.-Chim U.R.S.S. 1939, 10, 365.
49. Gray, P. and Spencer, M. Combustion of Unsymmetrical Dimethyl Hydrazine: Spontaneous Ignition in Decomposition and Oxidation. Combustion and Flame, Vol. 6. (Dec. '62) pp. 337-345.
50. Emmons, H. W. Flow Discontinuities Associated with Combustion. Princeton Series on High Speed Aerodynamics and Jet Propulsion. Vol. III. Fundamentals of Gas Dynamics. p. 584.
51. Van Tiggelen, A. and Deckers, J. Chain Branching and Flame Propagation. Sixth (International) Symposium on Combustion. New York, 1956, Reinhold, p. 61.

52. Horning, D. F. The Production of Unstable Species in Shock Waves. Wright Air Development Center Technical Report 57-217. "Unstable Chemical Species: Free Radicals, Ions, and Excited Molecules" May 1957.
53. Greene, E. F. and Horning, D. F. The Shape and Thickness of Shock Fronts in Argon, Hydrogen, Nitrogen and Oxygen. J. Chem. Phys. Vol. 21, p. 617.
54. Kantrowitz, A. Heat Capacity Lag in Gas Dynamics. J. Chem. Phys. Vol. 14, p. 161.
55. Presson, A. G. Solution of a Heat Transfer Problem with the Electronic Differential Analyzer. Section Report No. 9-65. Jet Propulsion Laboratory, California Institute of Technology. Pasadena, California March 16, 1953.
56. Penner, S. S. Melting and Evaporation as Rate Processes. Memo No. 9-10. Jet Propulsion Laboratory, California Institute of Technology. Pasadena, California, January 6, 1948.
57. Raleigh, C. W. FMC Corporation, Personal Communication.
58. Eberstein, I. J. and Glassman, I. Consideration of Hydrazine Decomposition. Progress in Astronautics and Rocketry Vol. 2. "Liquid Rockets and Propellants" New York, 1960, Academic Press. pp. 351-366.
59. Wolfe, W. Engineering Report 126, Part E - Corrosion and Stability. Olin Mathieson Company, 1953.
60. Pauling, Linus. Nature of the Chemical Bond. 2nd. ed. Cornell University Press, Ithaca, New York, 1948.
61. Dowden, Machenzie, Trapnell. Hydrogen-Deuterium Exchange on the Oxides of Transition Metals. Vol. IX (1957) in series on Advances in Catalysis. Academic Press.
62. Baker and Jenkins. The Electronic Factors in Catalysis. Vol. VII (1955) Advances in Catalysis.
63. Kant, A. and McMahon, W. J. Thermal Decomposition of Hydrazine Technical Report No. Wal TR 804/20 Watertown Arsenal Laboratories October 1959.

64. Green, M., Jennings, K. R.; Linnett, J. W., Shoefield, D. Recombination of Atoms at Surfaces. Part 7 -- Hydrogen Atoms at Silica and other Similar Surfaces. Trans. Faraday Soc. Vol. 55. December 1959.
65. Baldwin, R. B. and Brattan, D. The Decomposition of Hydrogen Peroxide in the Presence of Inert Gases and Hydrogen. Abstract of Papers at the Eighth Symposium (International) on Combustion, Pasadena, Calif. August 28 - September 2, 1960.
66. Baldwin, R. and Mayor, L. The Slow Reaction and Second Limit of the Hydrogen--Oxygen Reaction in Boric Acid Coated Vessels. Seventh Symposium (International) on Combustion, London, Butterworths, 1958.
67. Pauling, Linus. "Nature of the Chemical Bond" 2nd. ed. Ithaca, New York, 1948. Cornell University Press.
68. Bull, Soc. Chim. France. June 1959, pp. 962-1018 (Cited by L. H. Diamond, Food Machinery and Chemical Corp. Princeton, New Jersey, Feb. 10, 1960).
69. Crocco, L., Glassman, I., and Smith, I. E. Kinetics and Mechanism of Ethylene Oxide Decomposition at High Temperatures. J. Chem. Phys. Vol. 31, No. 2, (August 1959) pp. 506-510.
70. Predvolitov, A. S. The Rates of Chemical Reactions in Turbulent Streams. Inzhenero-Fizicheski Zhurnal, 11, 3 (1960).
71. Corrsin, S. Statistical Behavior of a Reacting Mixture in Isotropic Turbulence. The Physics of Fluids. Vol. 1, No. 1 (Jan-Feb) 1958.
72. Hinze, J. O. "Turbulence, An Introduction to Its Mechanism and Theory." New York, 1959, McGraw-Hill, pp. 3-7.
73. Batchelor, G. K. "The Theory of Homogeneous Turbulence." Cambridge, 1953, The University Press.
74. Lewis, B. and von Elbe, G. "Combustion, Flames and Explosions of Gases" New York, 1951, Academic Press. p. 488.
75. Wight, H. M. Study of Influence of Sound Waves on Chemical Reaction Rates. Aero. Report U-858. AFOSR-TR- 60-60.
76. Laurence, J. C. Intensity, Scale, and Spectra of Turbulence in Mixing Region of Free Subsonic Jet. NACA Report 1292.

77. Swigart, Rudolph J. A Study of the Kinetics of the Hydrogen-Oxygen Reaction in a New Flow Reactor. Aeronautical Engineering Laboratory Report No. 432. Princeton University, August 1958. Princeton, New Jersey.
78. DeJaegere, S. Personal Communication. Sept. 6, 1963. University of California, Los Angeles.
79. Sawyer, R. F. Equilibrium Compositions of Hydrazine, Monomethylhydrazine, and UDMH/Nitrogen Mixtures. Gugg. Lab. Report, Forrestal Research Center. June 1963.
80. Wei, J. and Prater, C. D. The Structure and Analysis of Complex Reaction Systems. "Advances in Catalysis" Vol. 13, New York, 1962. Academic Press. pp. 203-392.
81. Birse, E. A. B. and Melville, H. W. "The Reaction of Atomic Hydrogen with Hydrazine," The Proceedings of the Royal Society A-175: 164-186, Cambridge University Press, London, 1940.
82. Sawyer, R. F. Personal Communication. Princeton University. December 1, 1963.

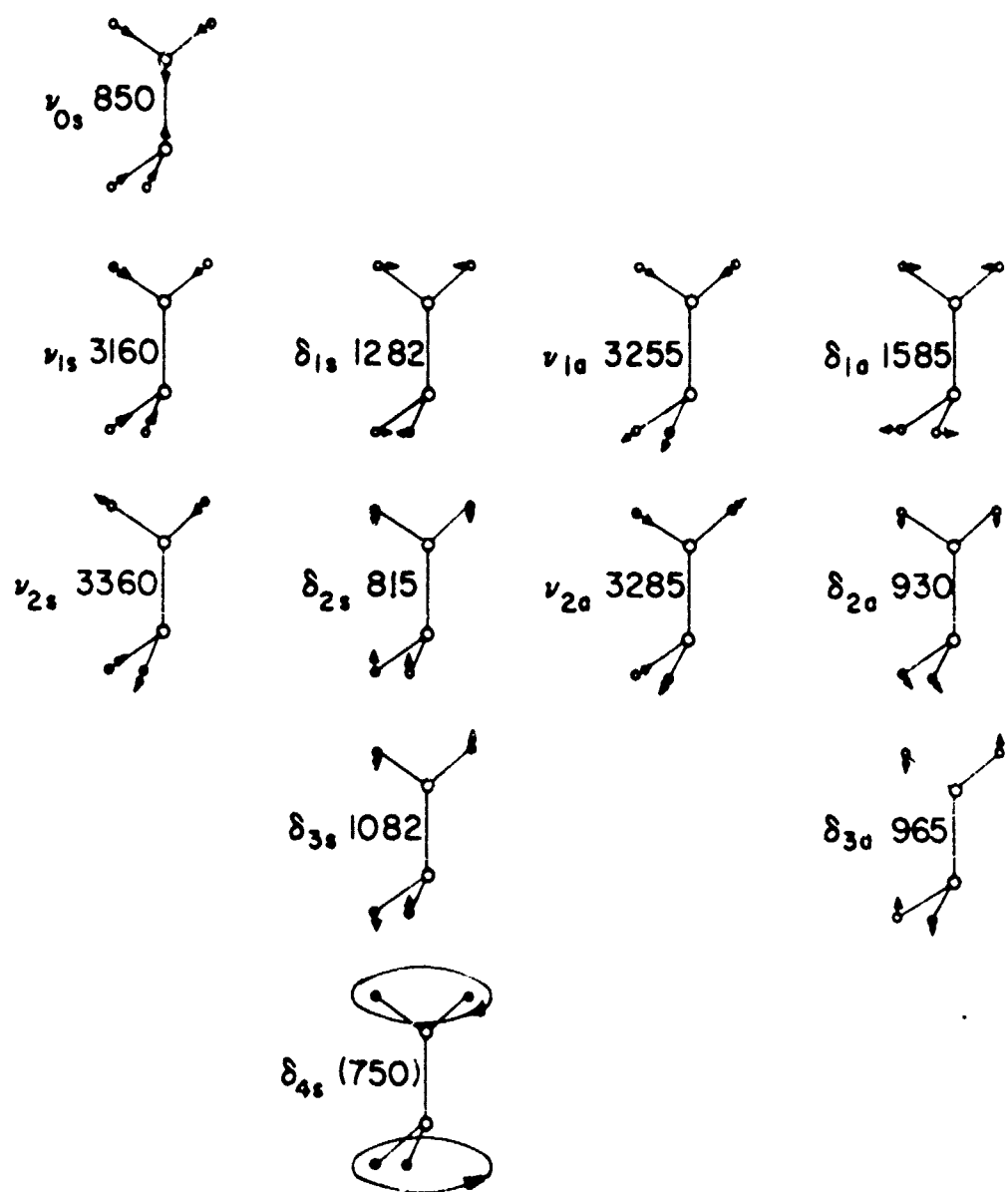


FIG. 1 NORMAL OSCILLATIONS OF THE  $N_2H_4$  MOLECULE

FIGURE 1

JOST'S HYDRAZINE DECOMPOSITION RESULTS  
ARRHENIUS PLOT OF HALF-LIVES

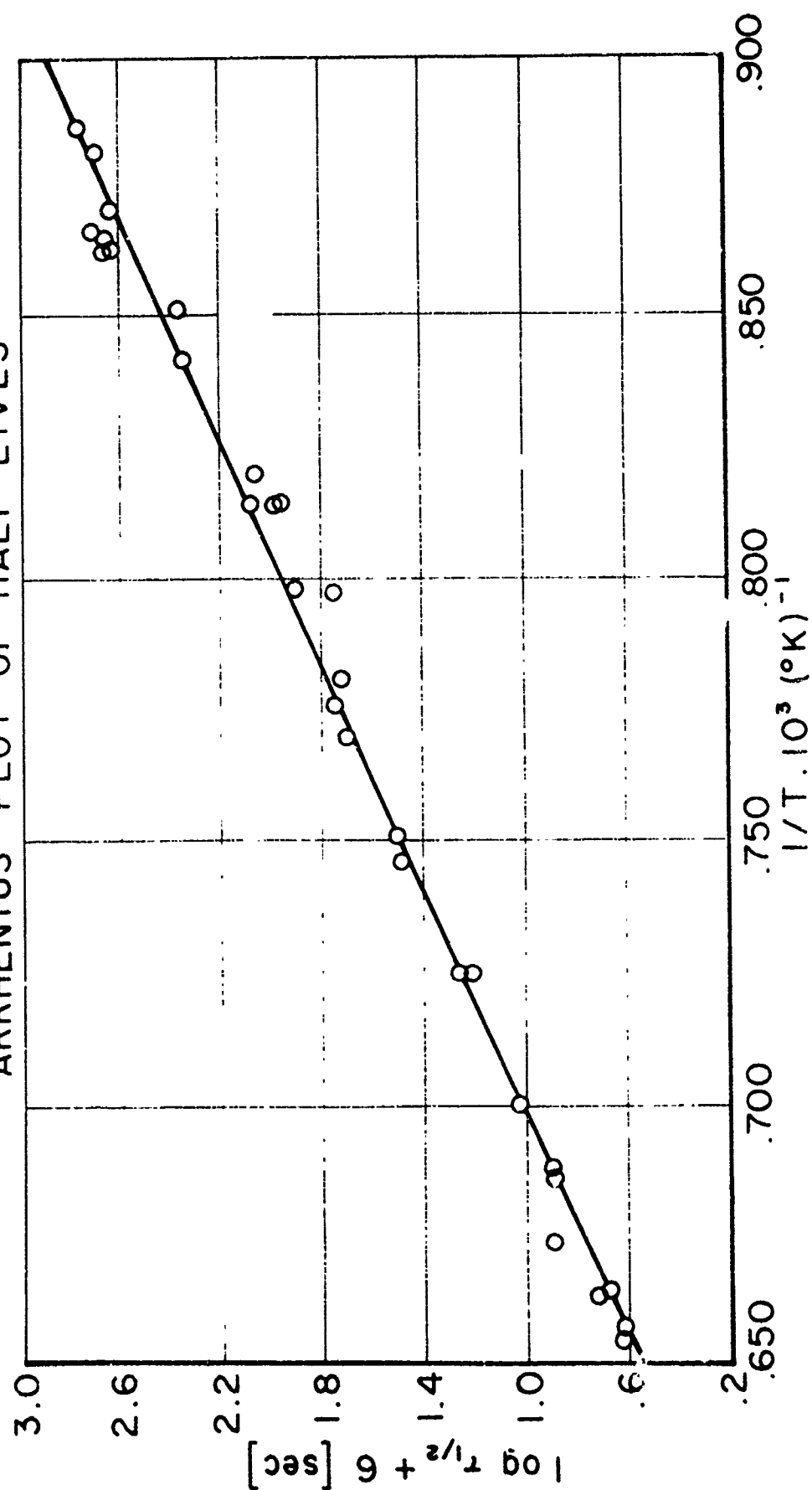


FIGURE 2

# TEMPERATURE DISTRIBUTION IN A REACTING SOLID AT VARIOUS TIME INTERVALS (PRESSON)

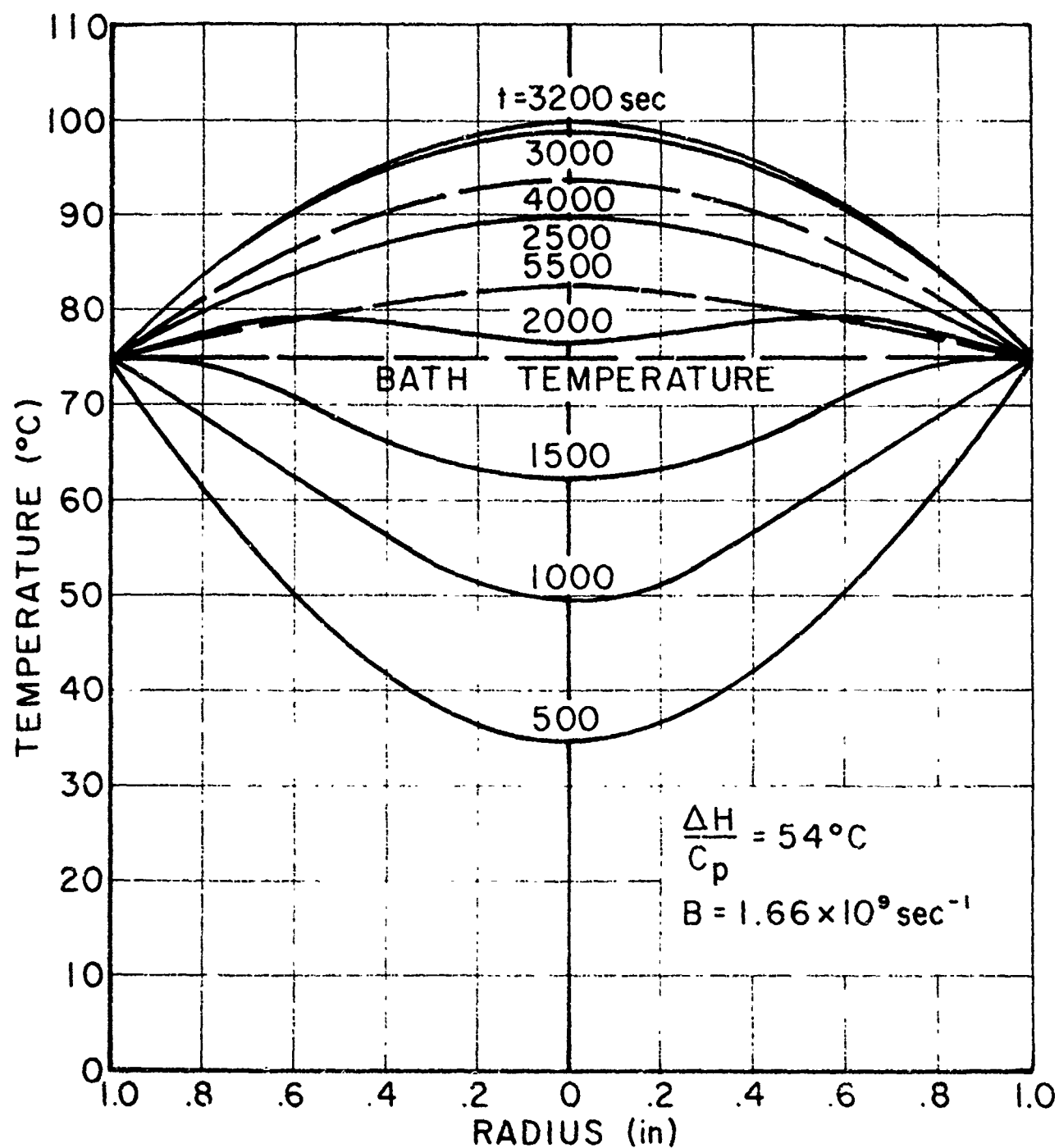
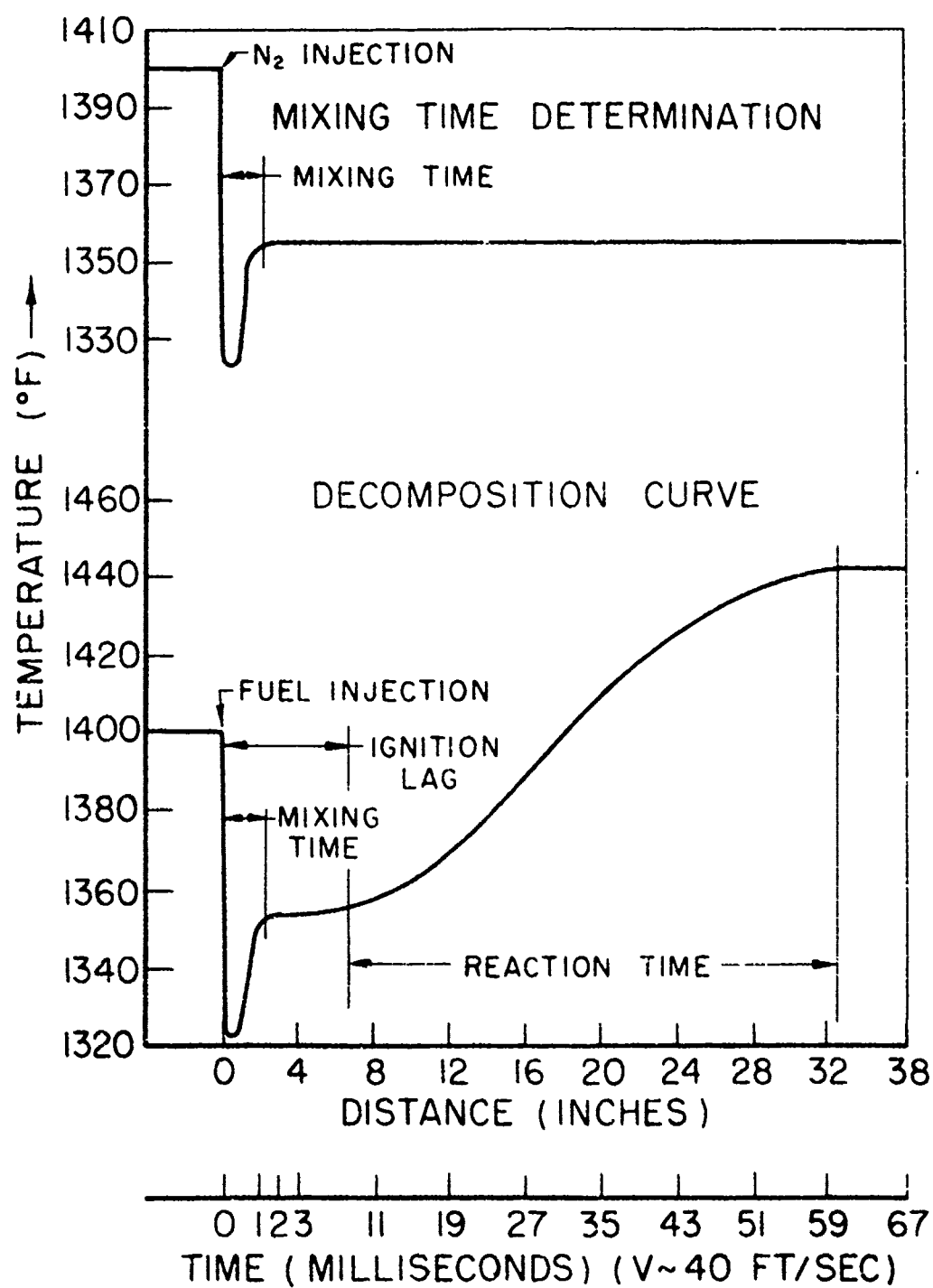


FIGURE 3

JPR 1962

HOT INERT  
CARRIER GASES



REACTOR TEMPERATURE PROFILES

FIGURE 4

# LONGITUDINAL TEMPERATURE TRACES

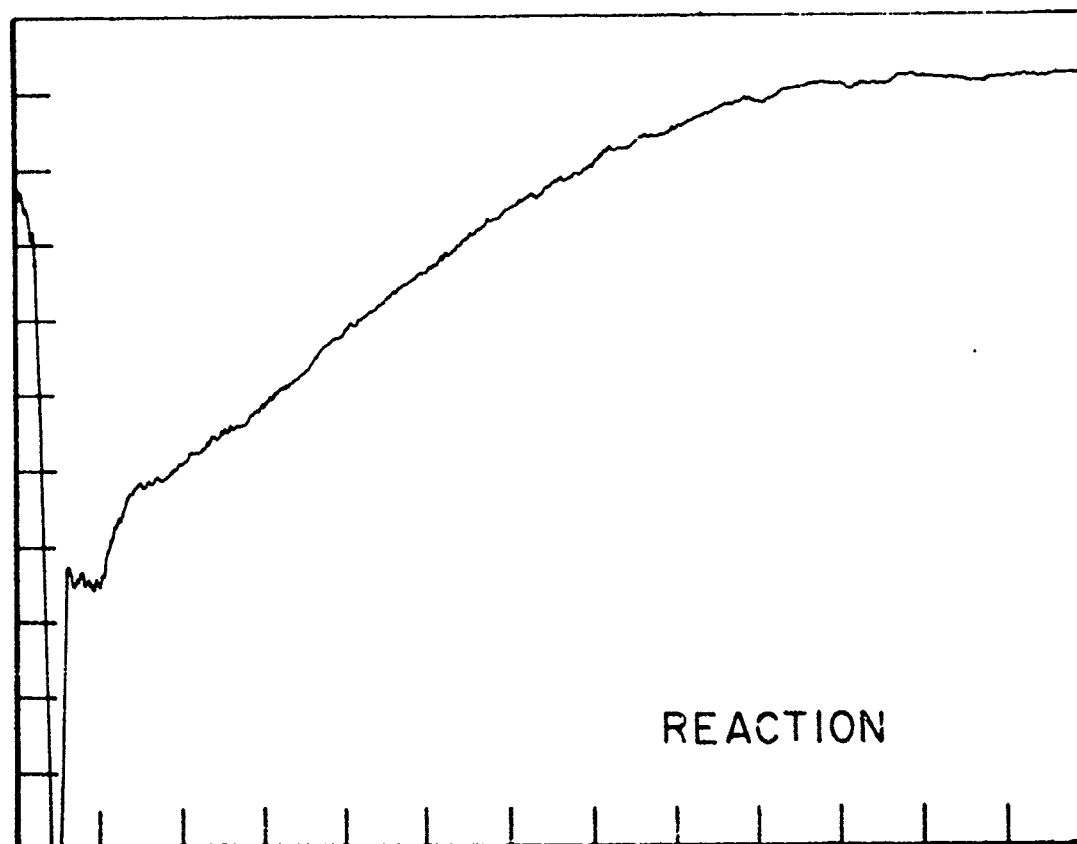
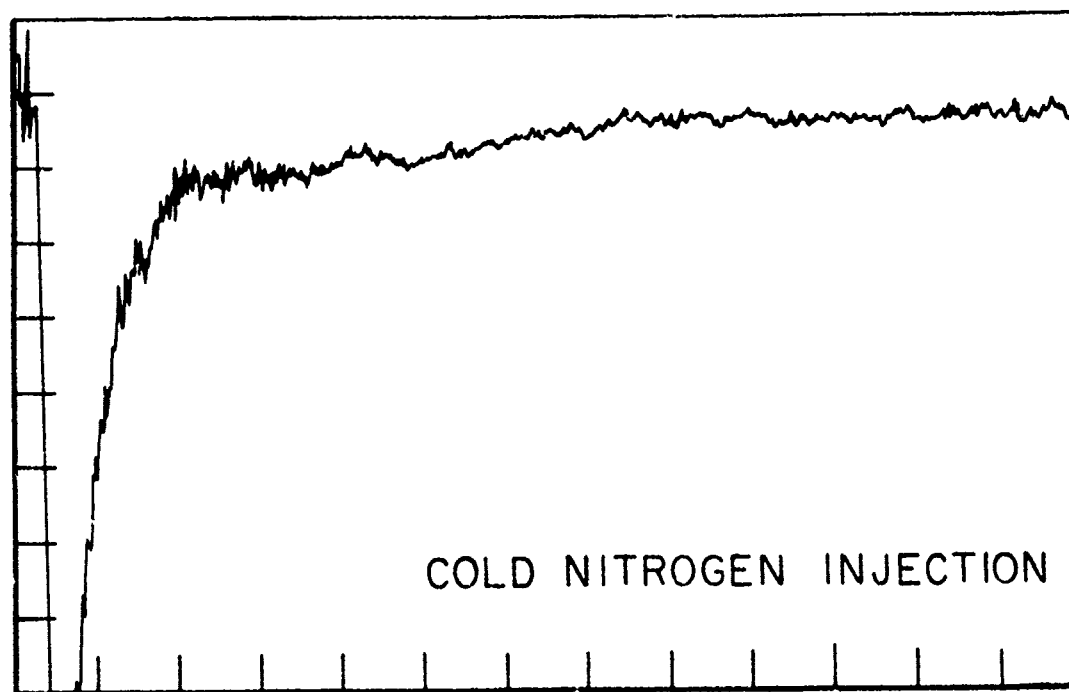


FIGURE 5

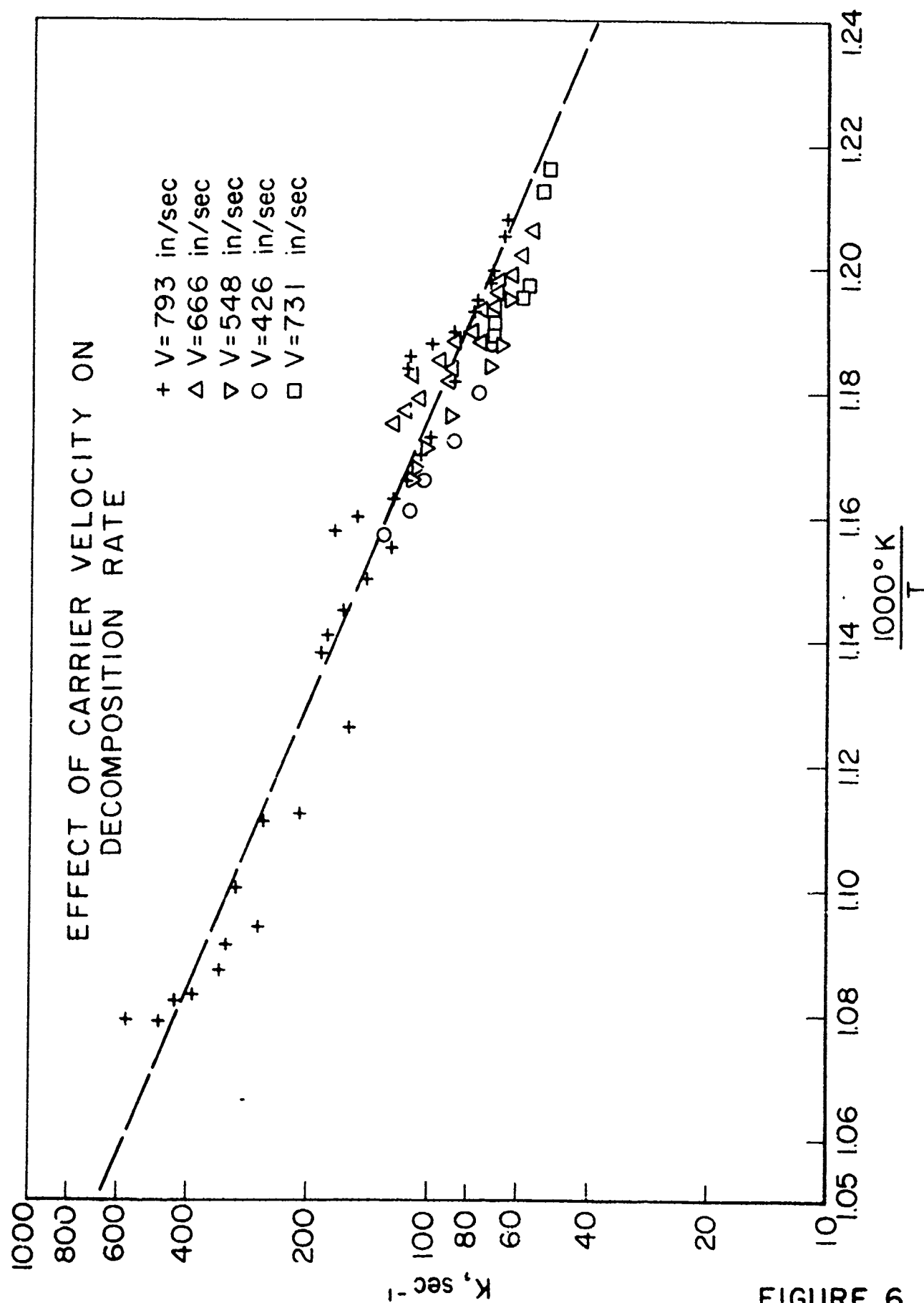
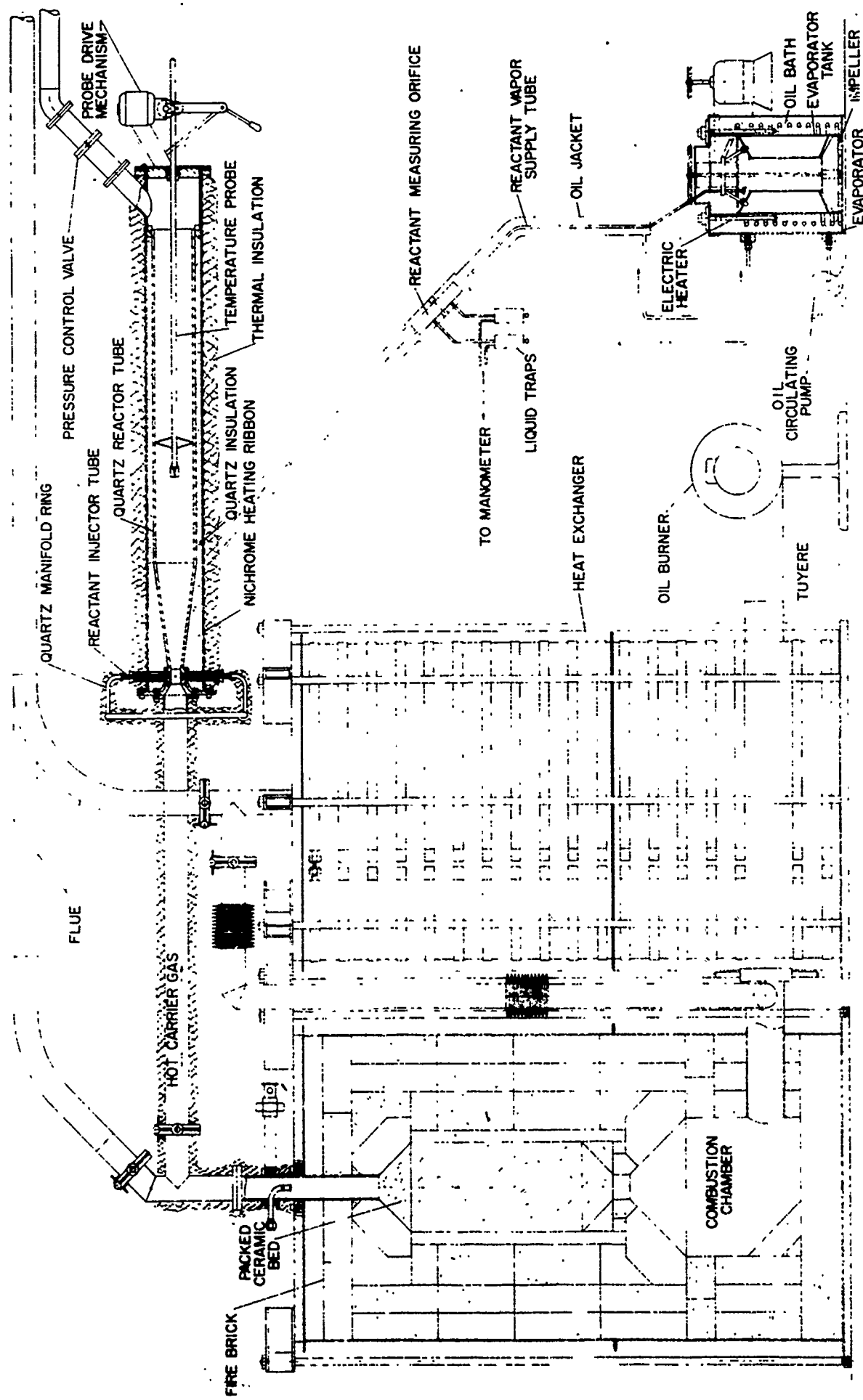


FIGURE 6



# CHEMICAL KINETIC FLOW REACTOR

**FIGURE 7**



OVERALL VIEW OF FLOW REACTOR ASSEMBLY



QUARTZ REACTOR TUBE

FIGURE 9

# SCHEMATIC OF CARRIER GAS FLOW SYSTEM

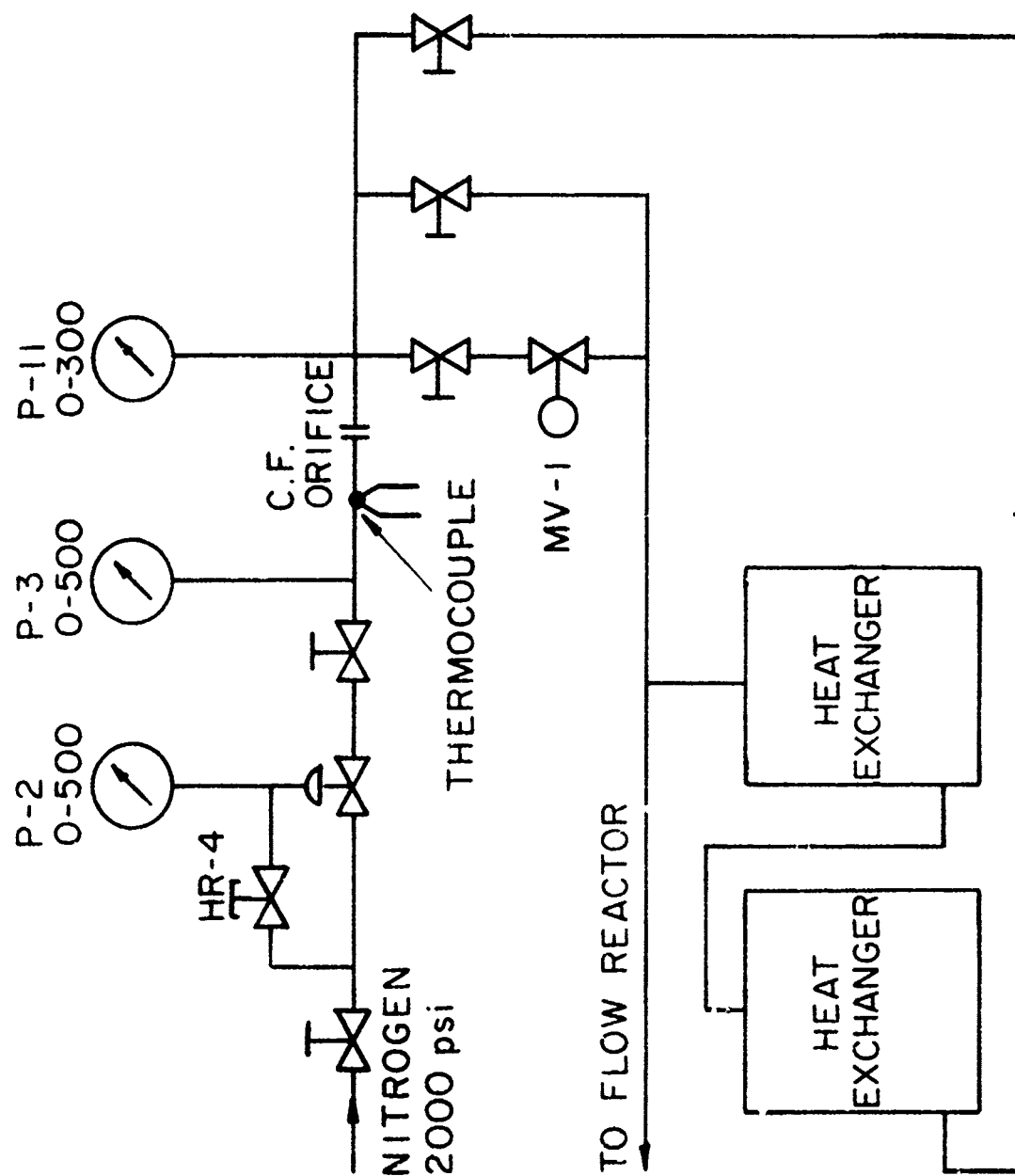


FIGURE 10

# SCHEMATIC OF TEMPERATURE SERVO CONTROL SYSTEM

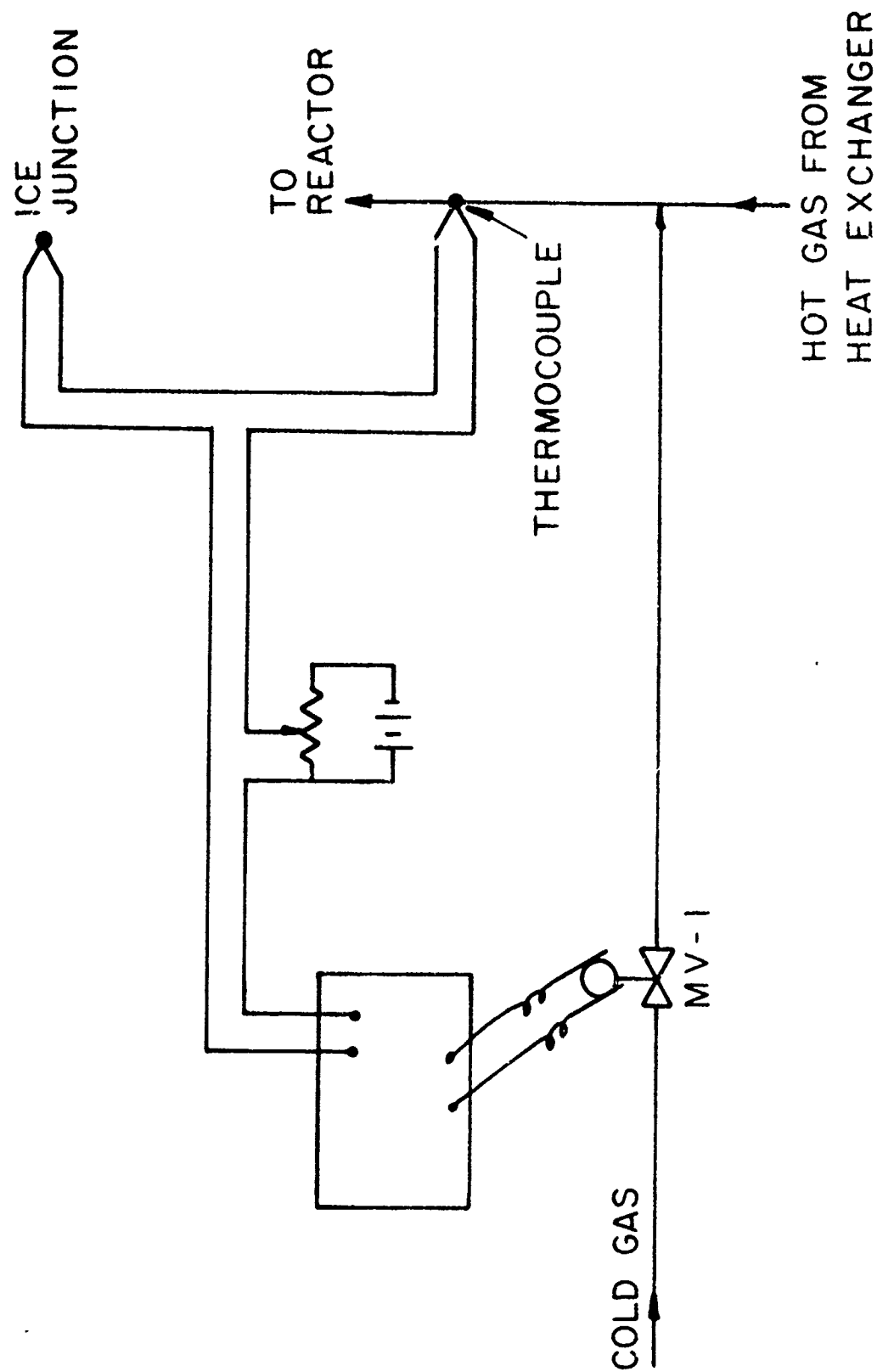


FIGURE 11

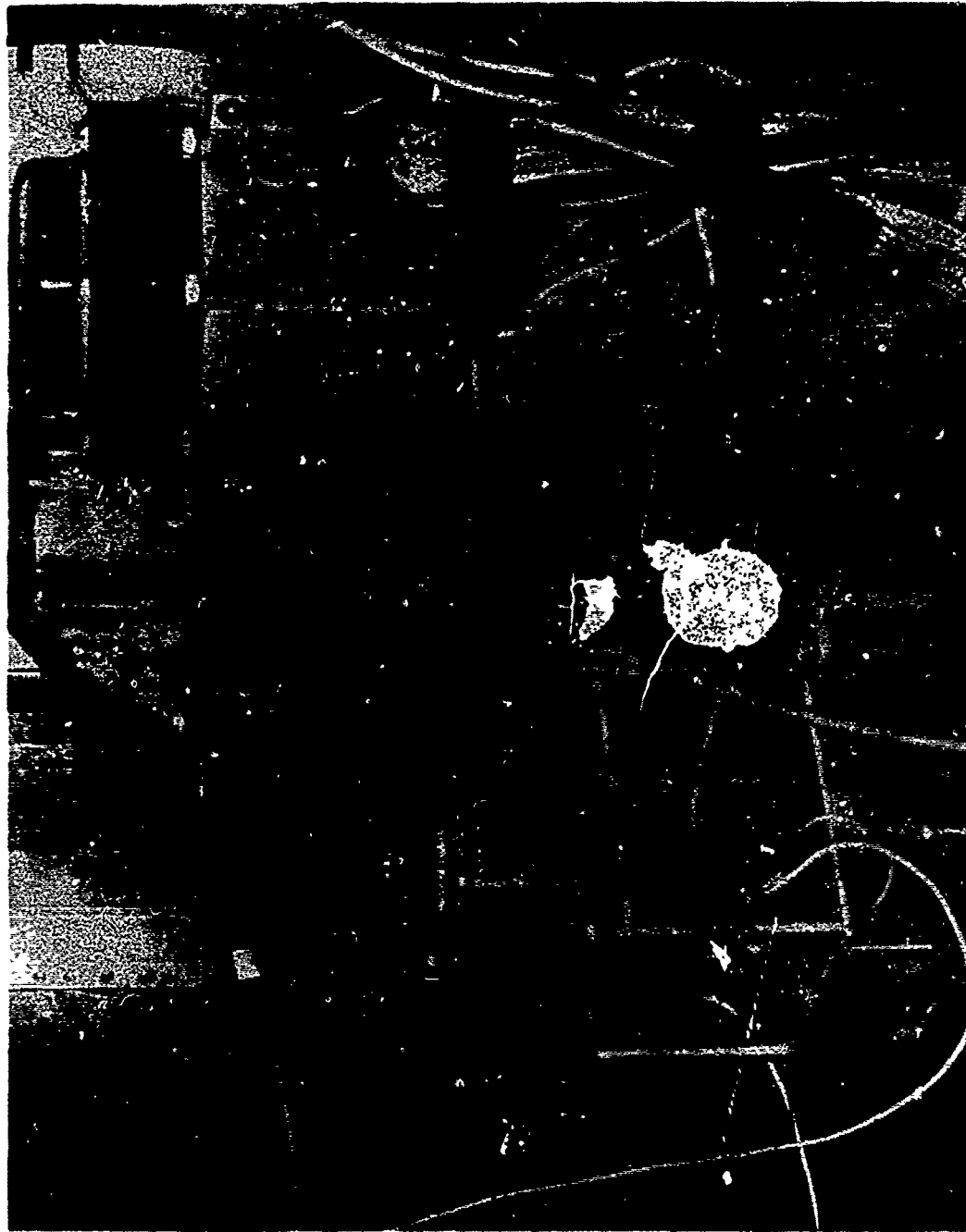
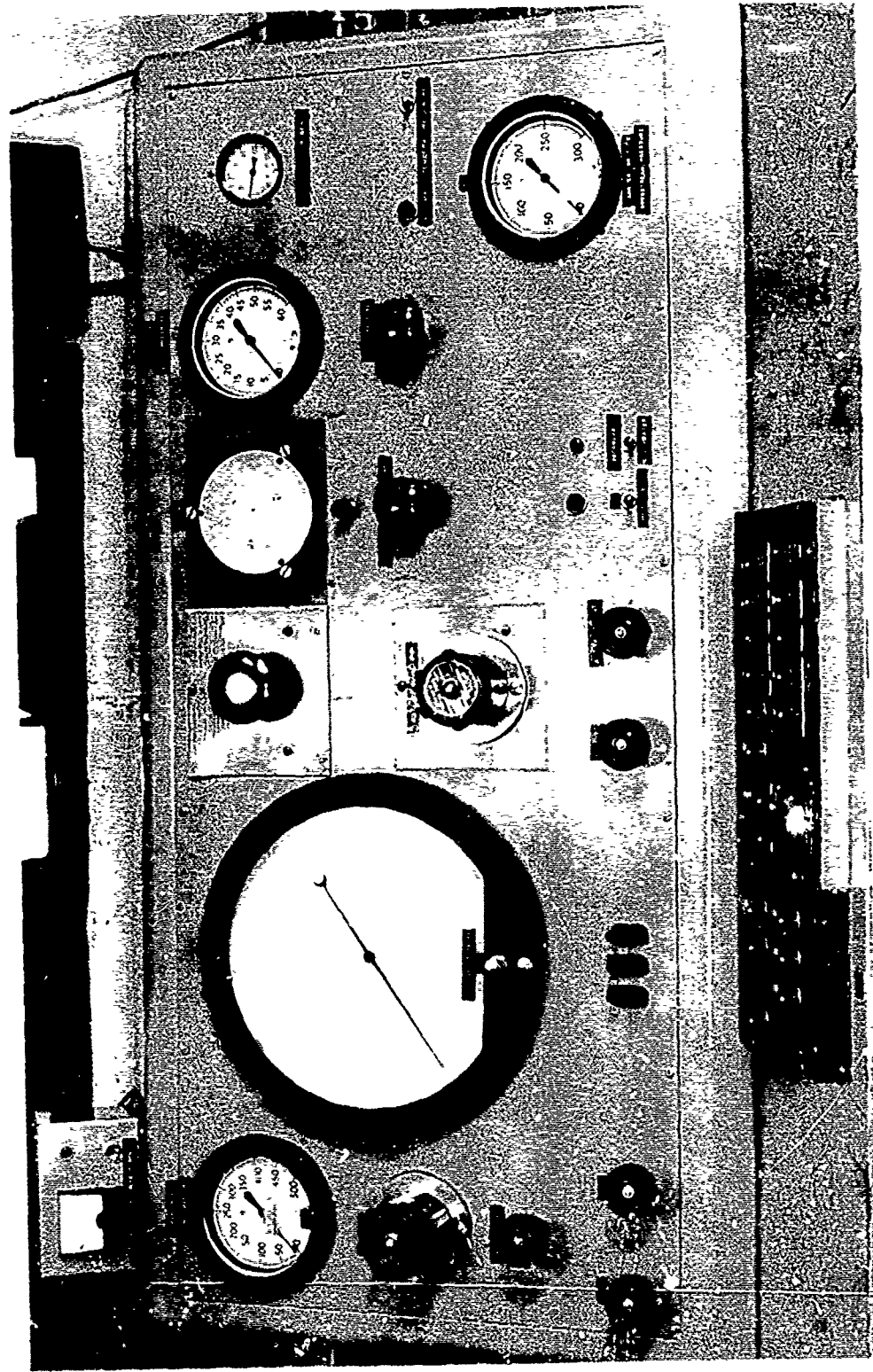


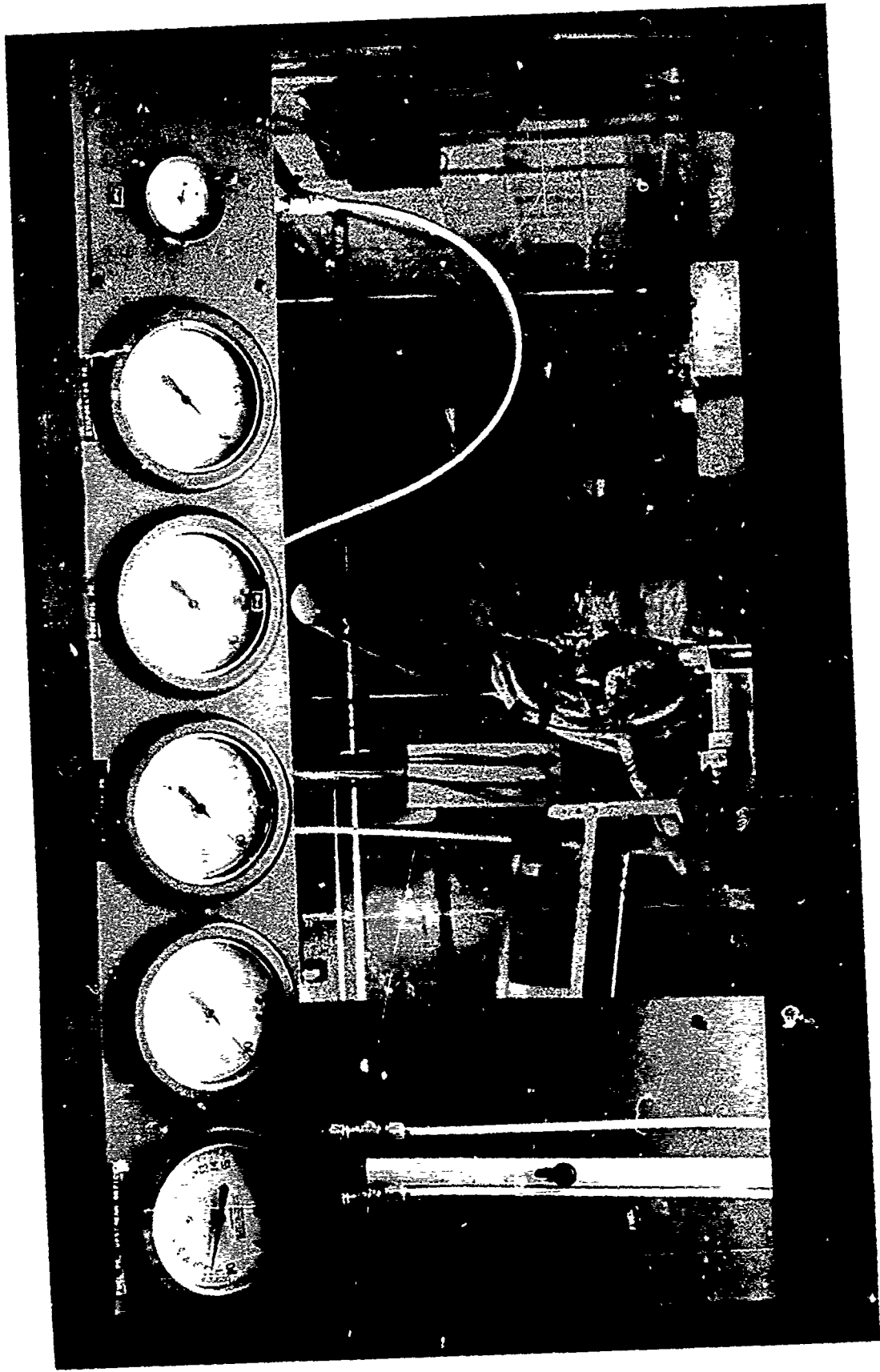
PHOTO OF TEMPERATURE CONTROL SERVO SYSTEM

FIGURE 12



MAIN CONTROL PANEL

FIGURE 13



MAIN CONTROL PANEL

FIGURE 14

# THERMOCOUPLE ELECTRIC SCHEMATIC

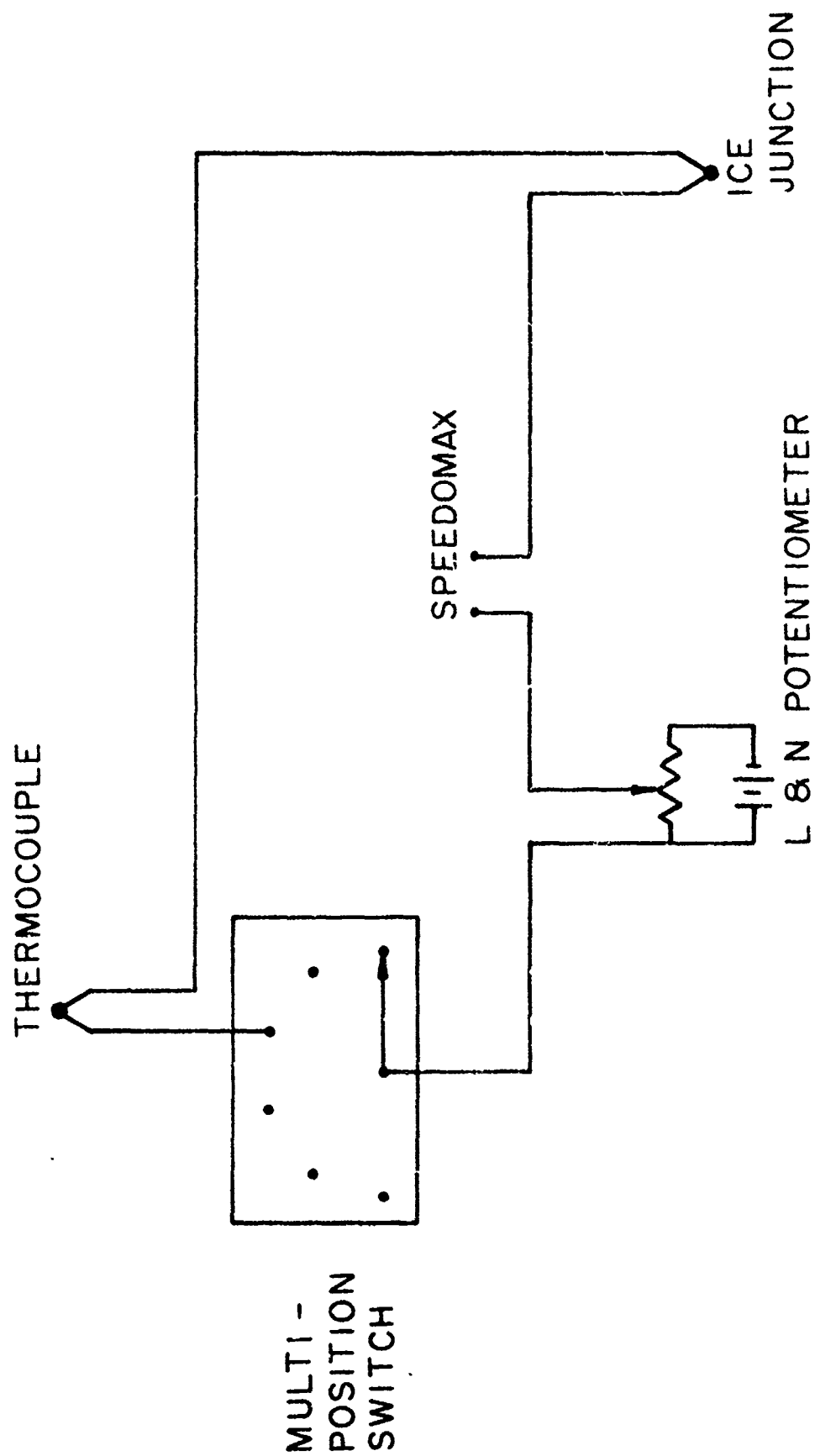
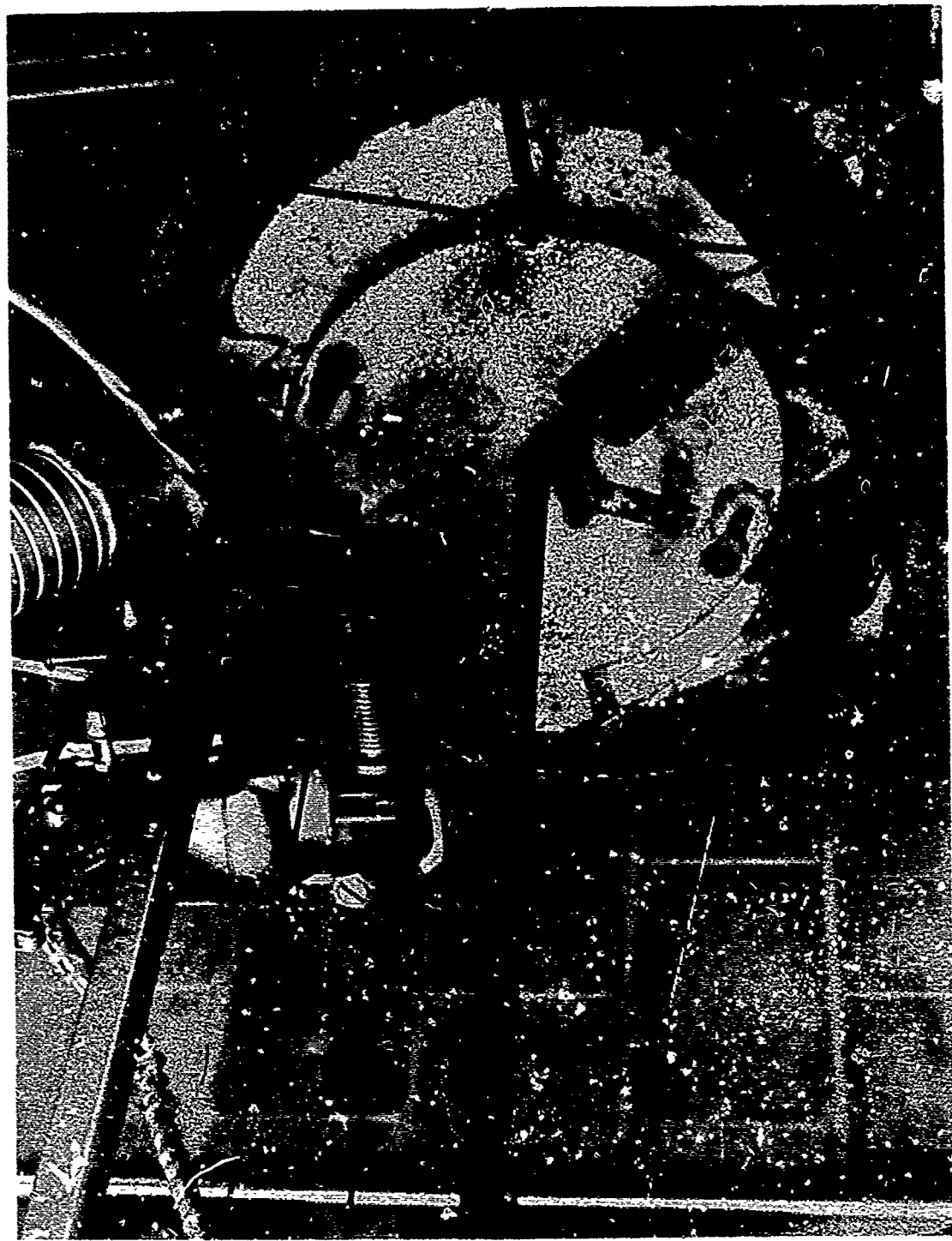


FIGURE 15



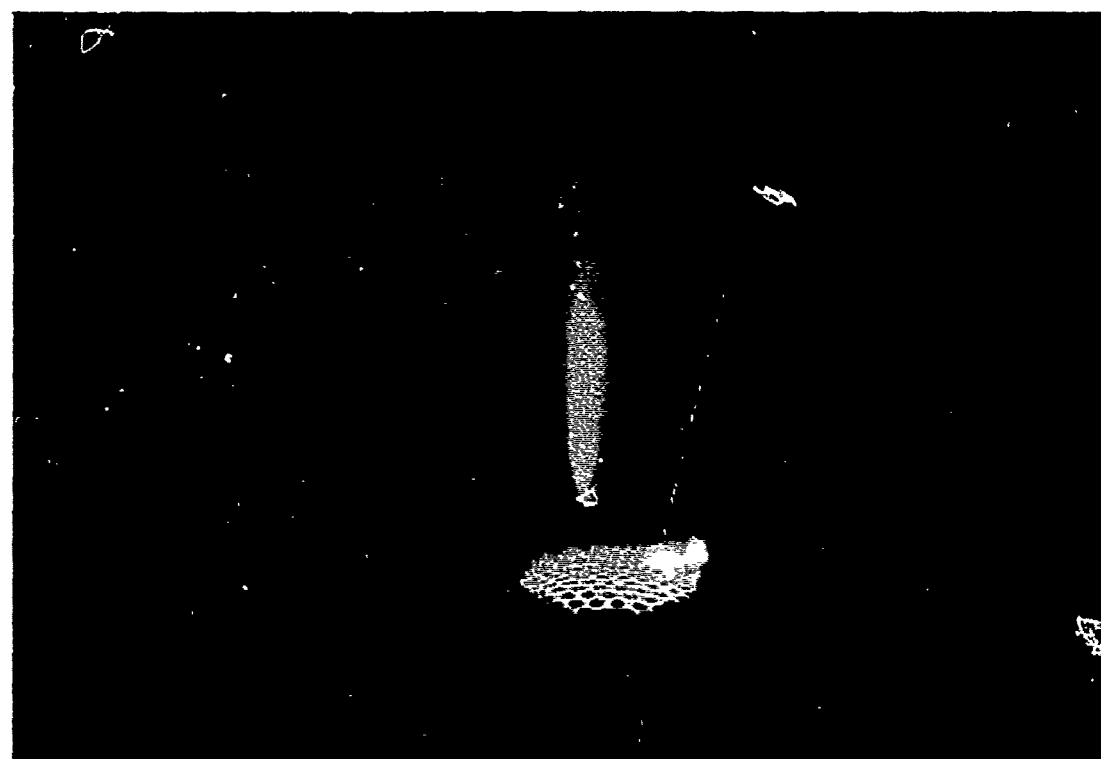
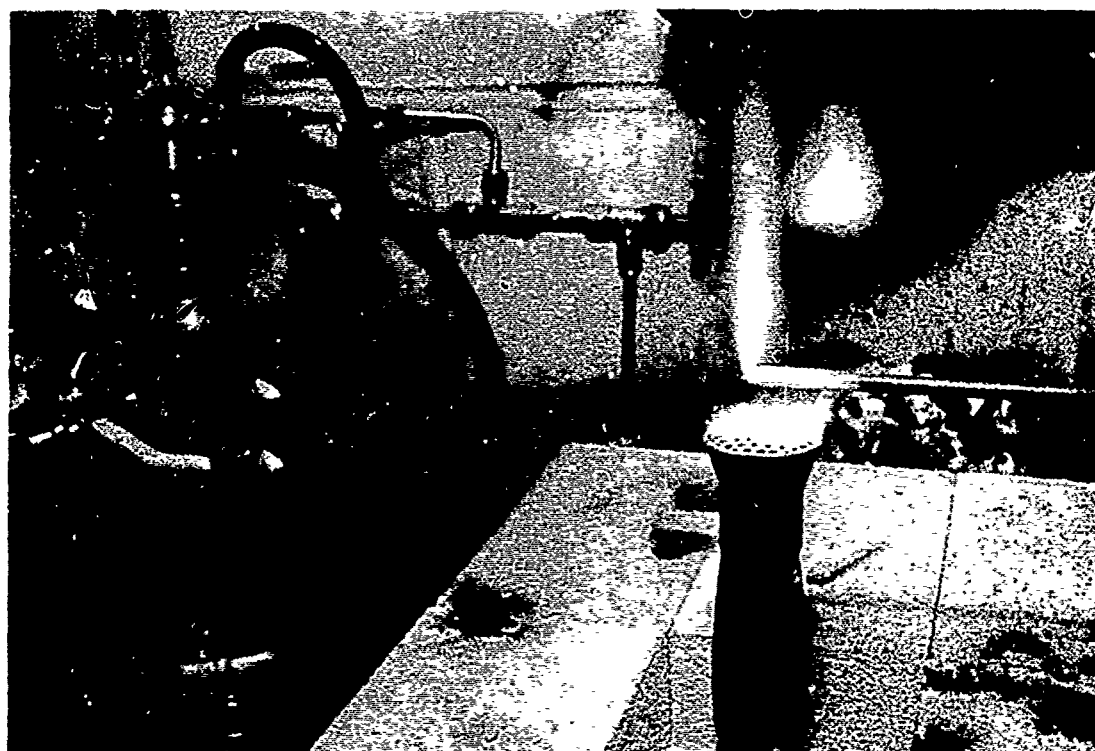
TEMPERATURE MEASURING AND RECORDING INSTRUMENTS

FIGURE 16



TEMPERATURE PROBE DRIVE ASSEMBLY

FIGURE 17



PROBE COATING APPARATUS

FIGURE 18

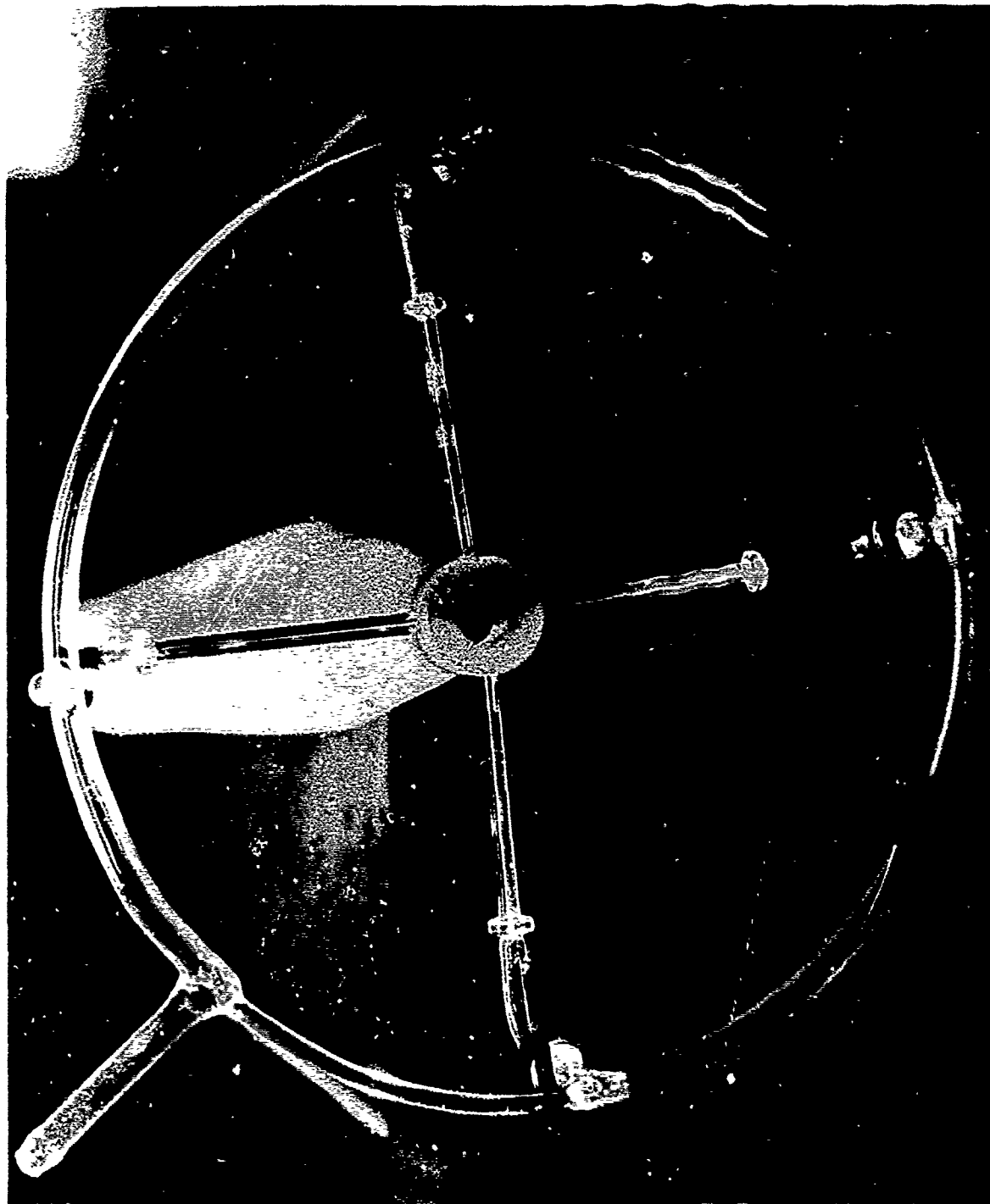


FIGURE 19

# SCHEMATIC OF FUEL VAPOR AND DILUENT NITROGEN SYSTEM

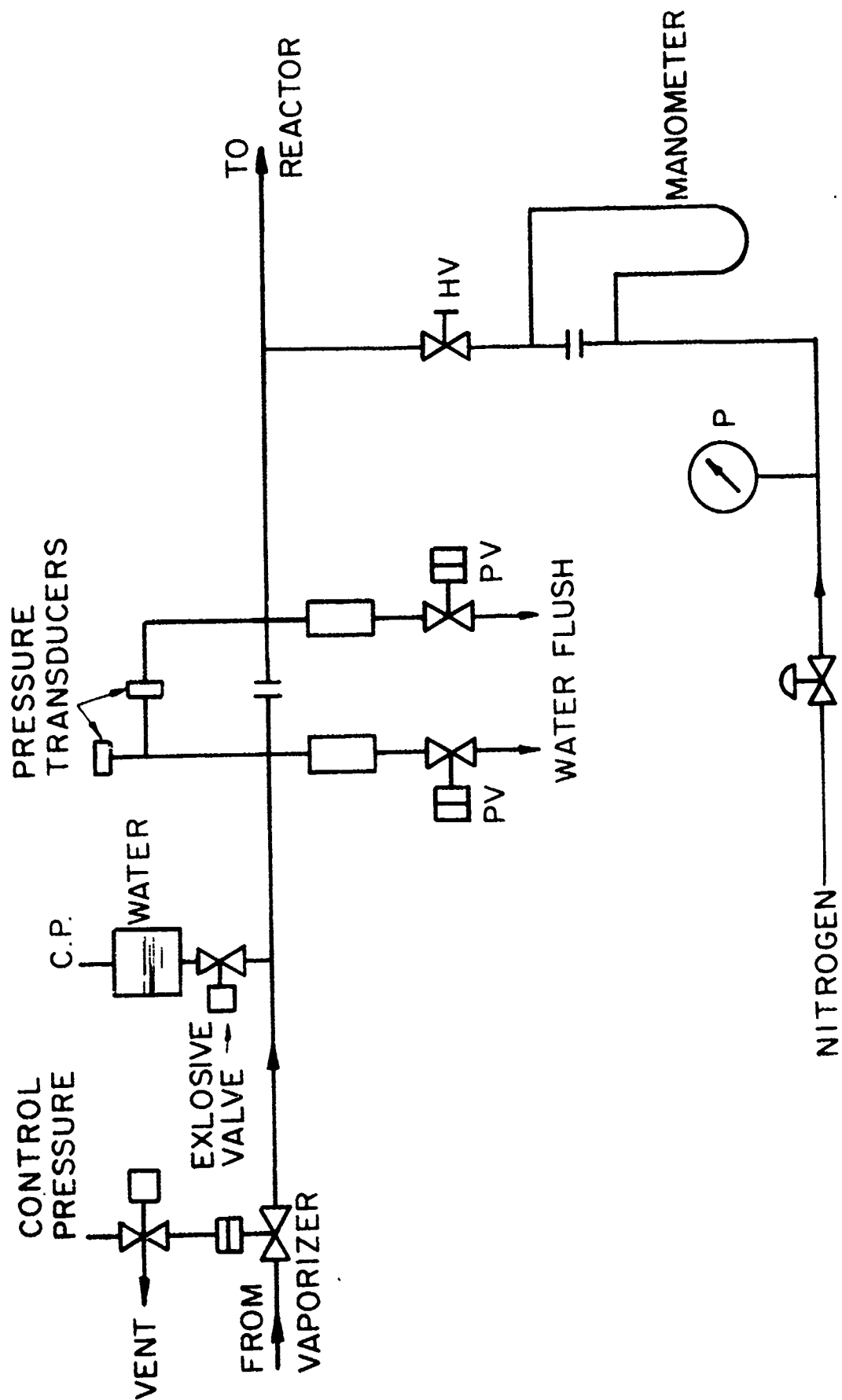


FIGURE 20

JPR 1807a

# SCHEMATIC OF REACTANT FEED SYSTEM

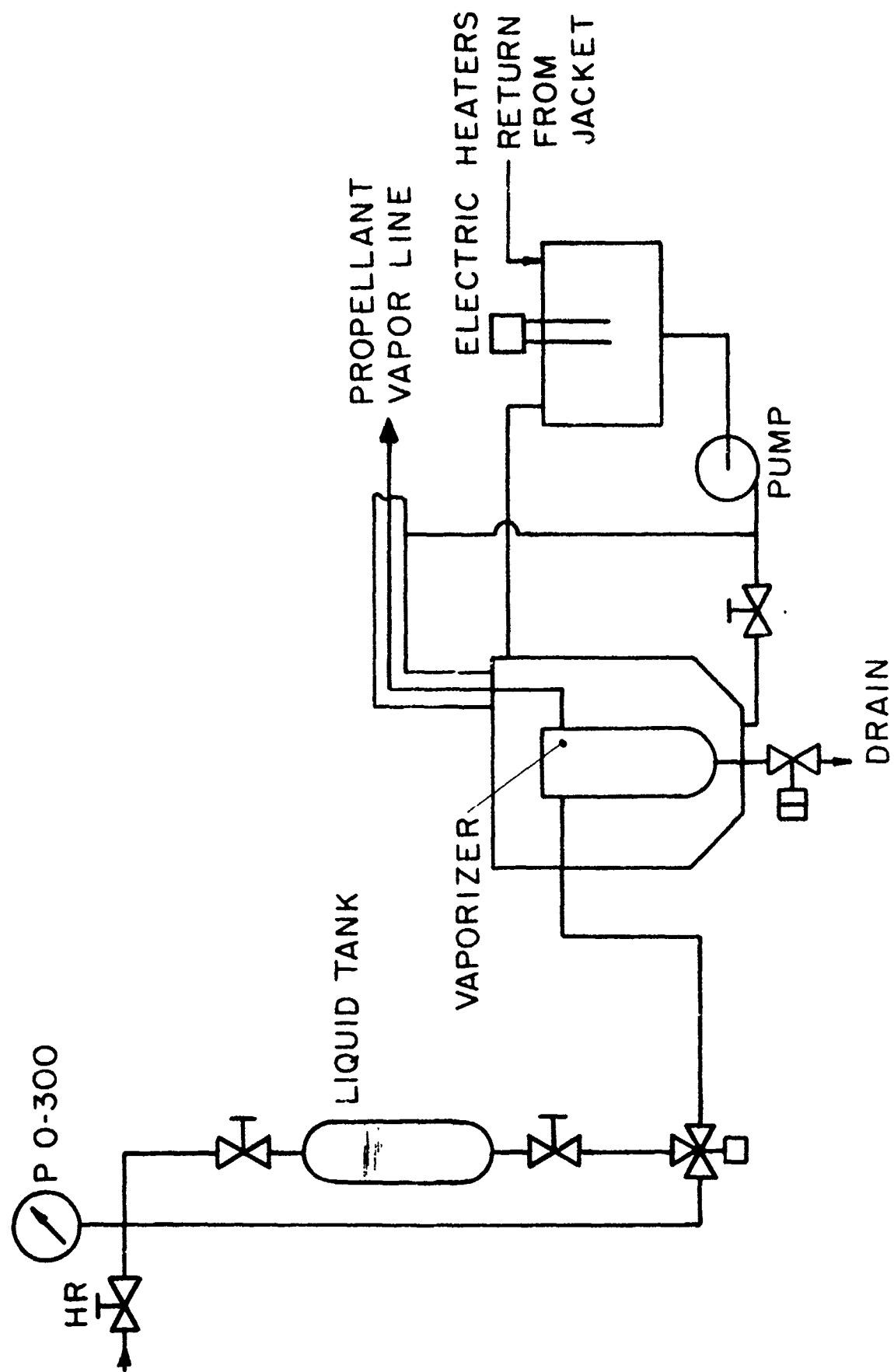
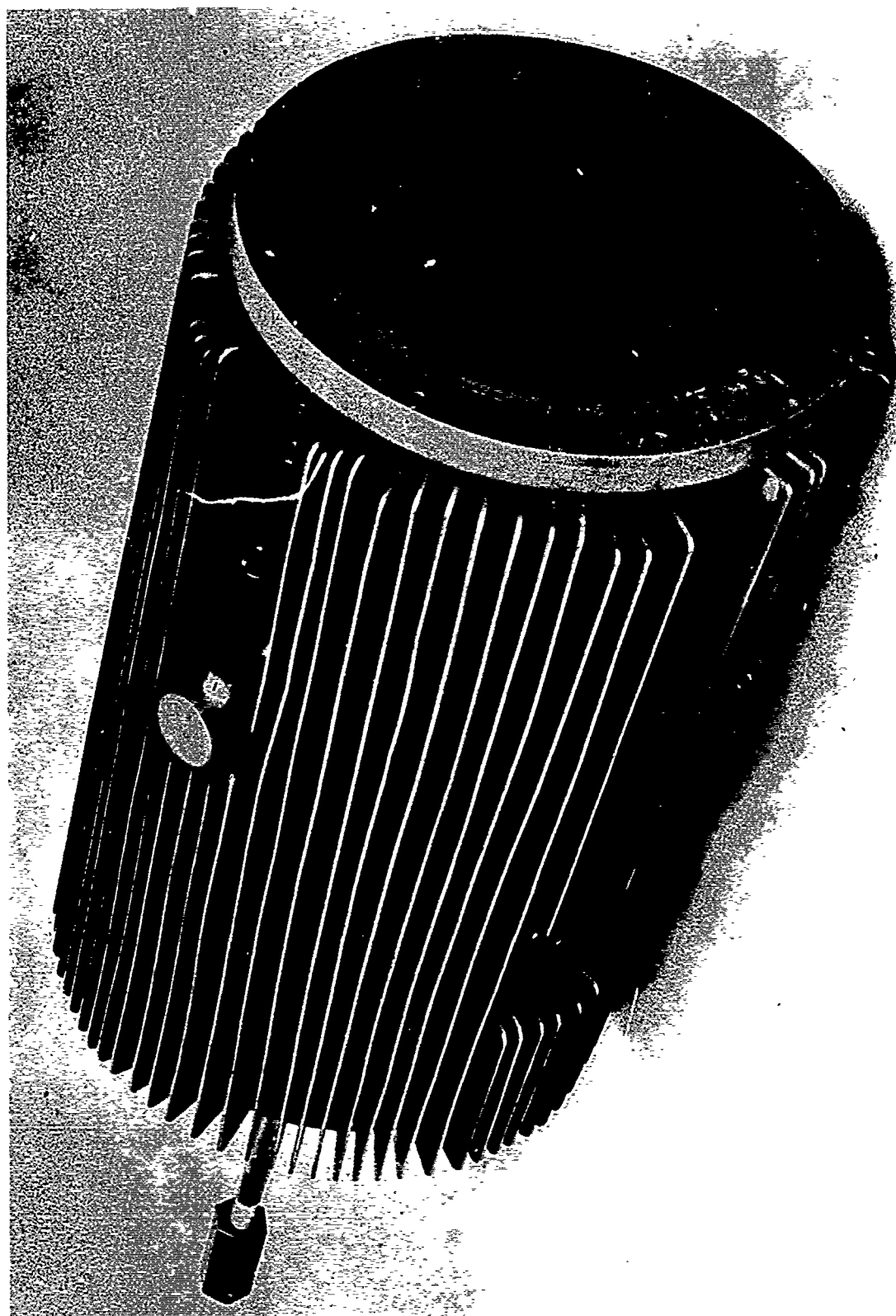
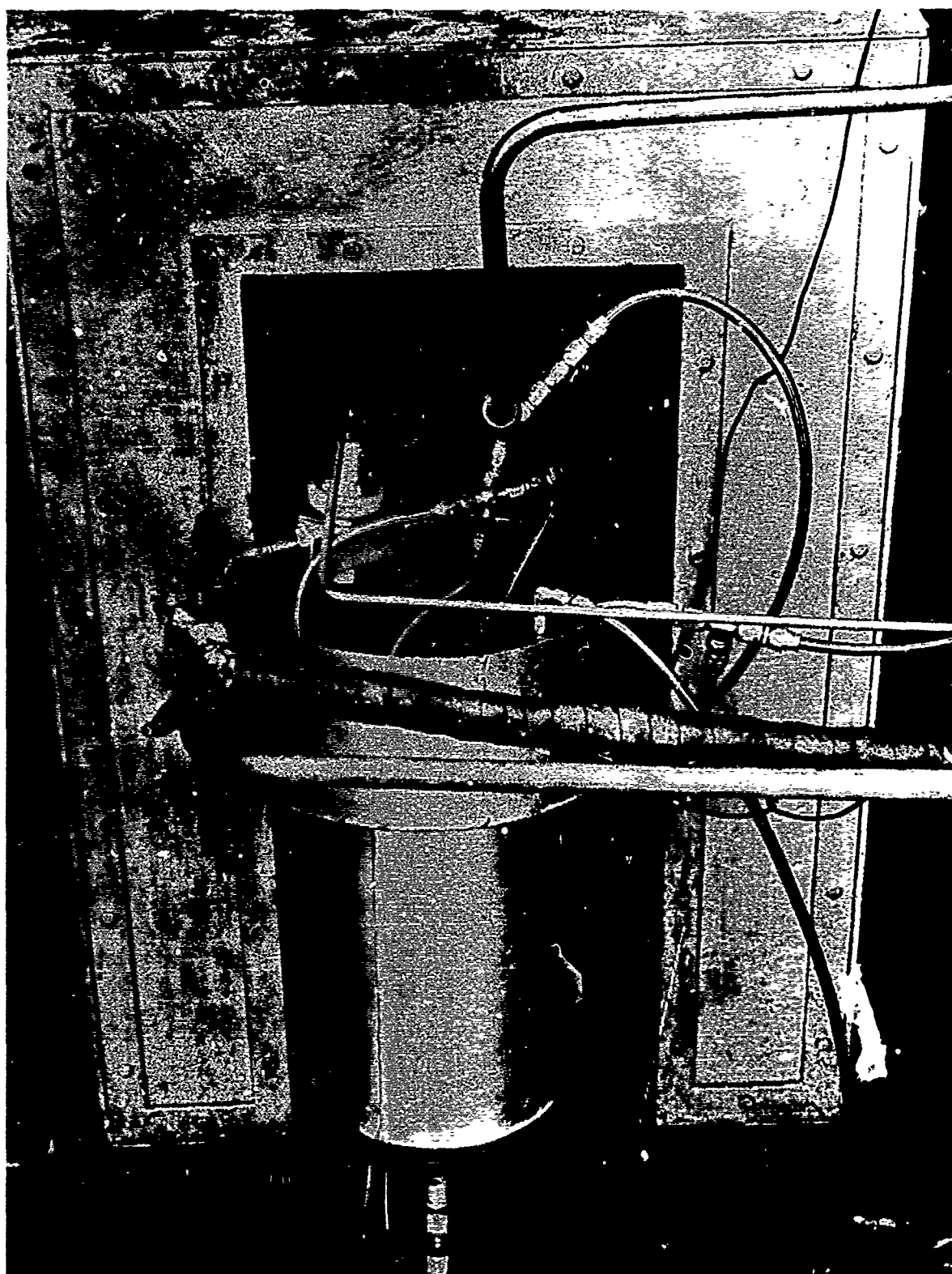


FIGURE 21



EVAPORATOR

FIGURE 22



EVAPORATOR ASSEMBLY

CHEMICAL SAMPLING PROBE

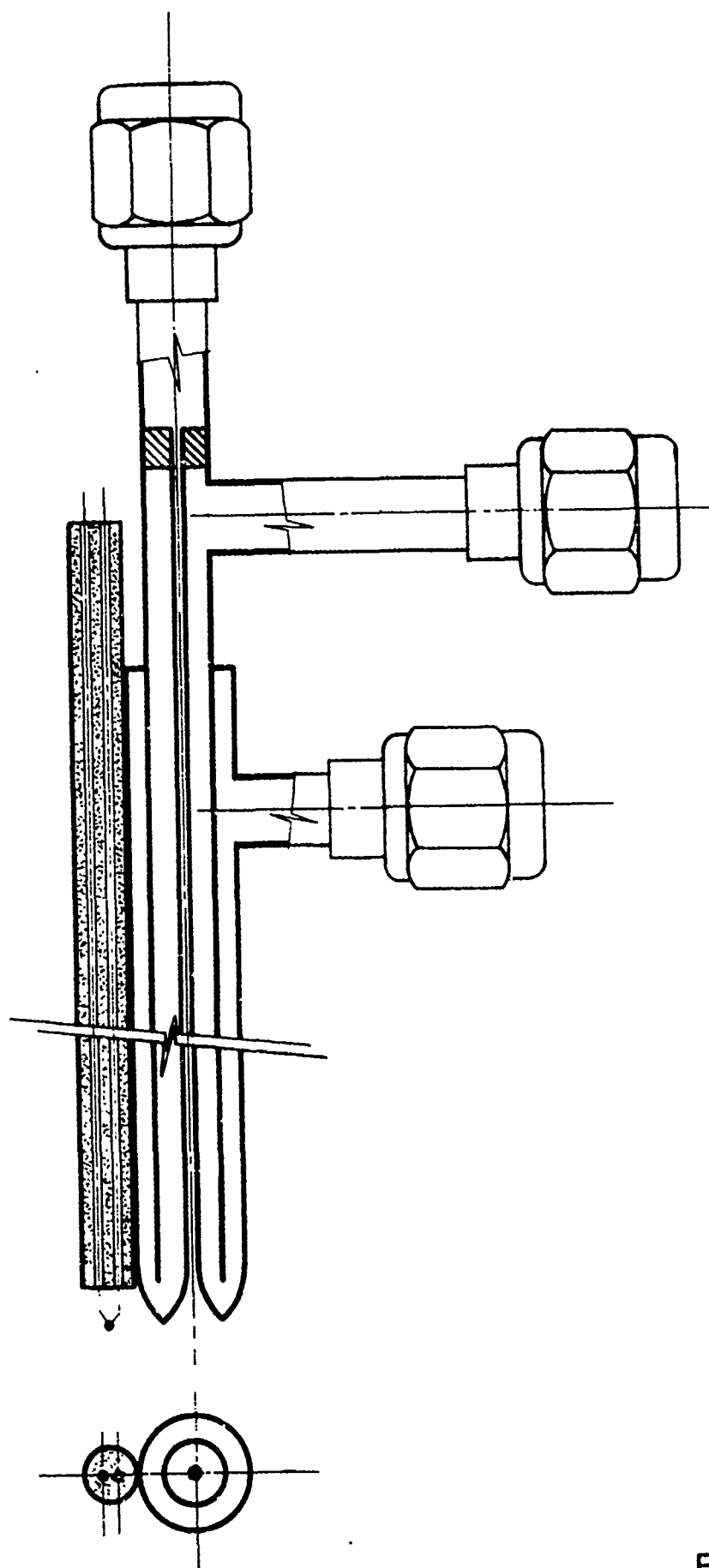
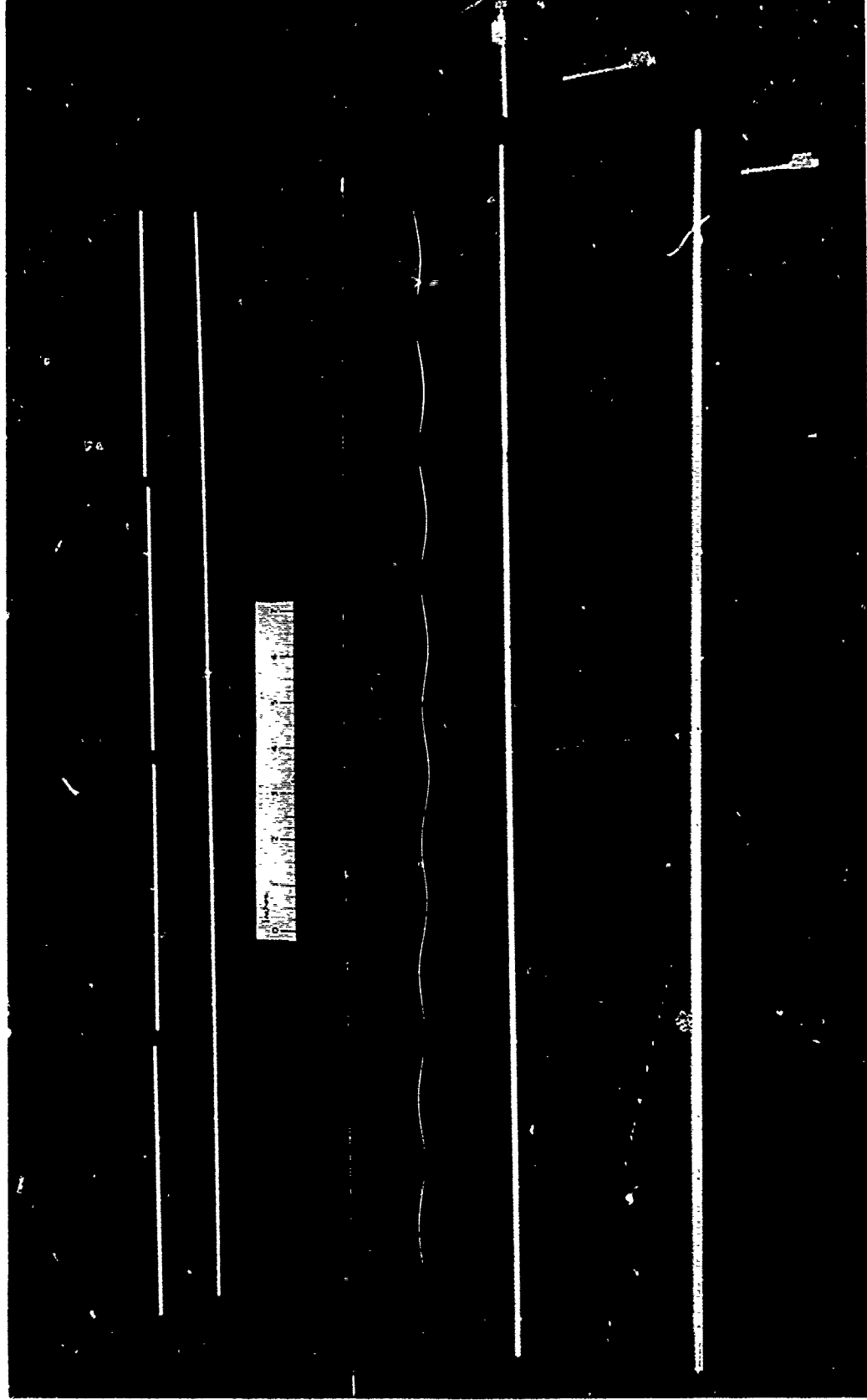
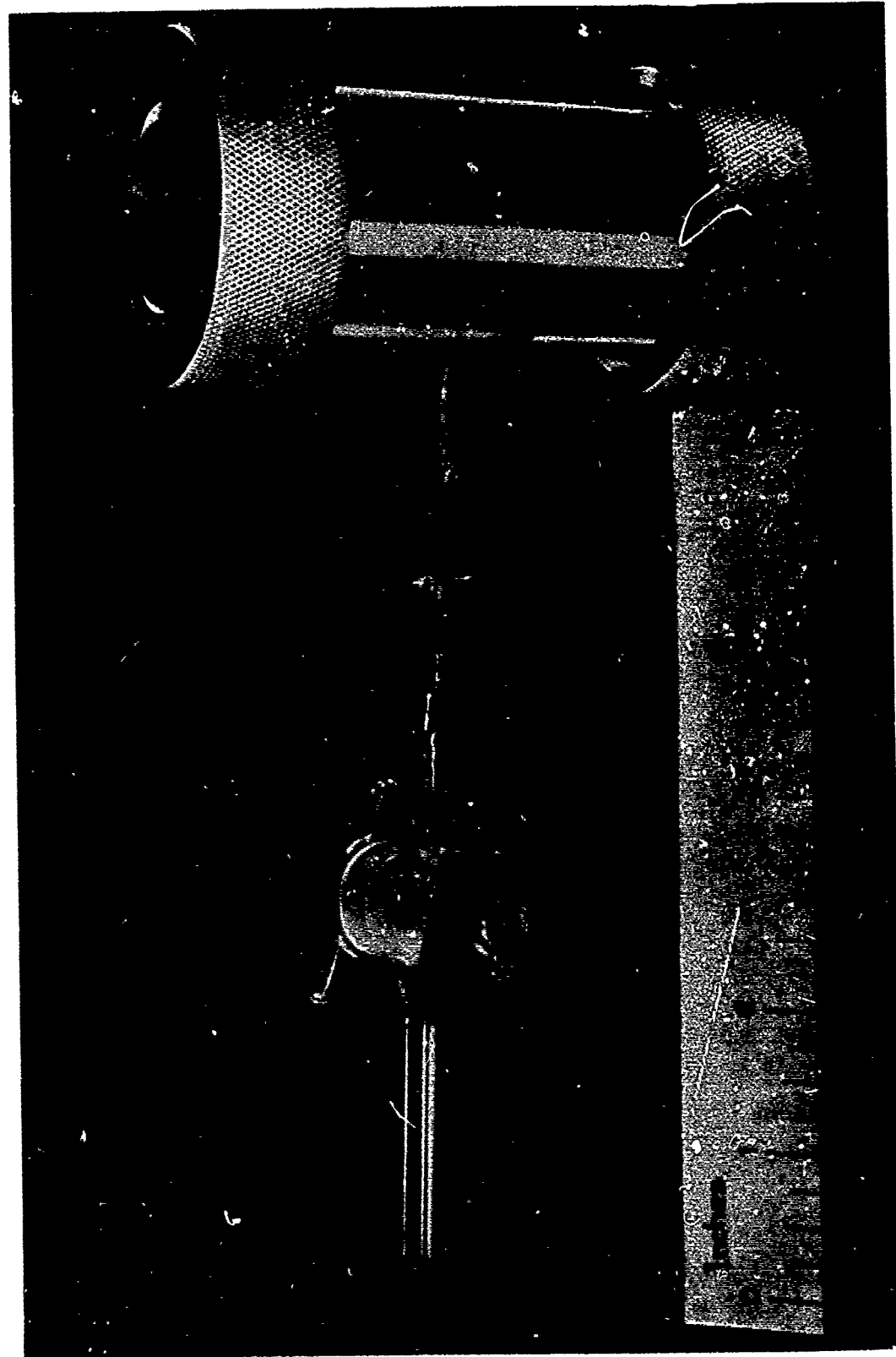


FIGURE 24



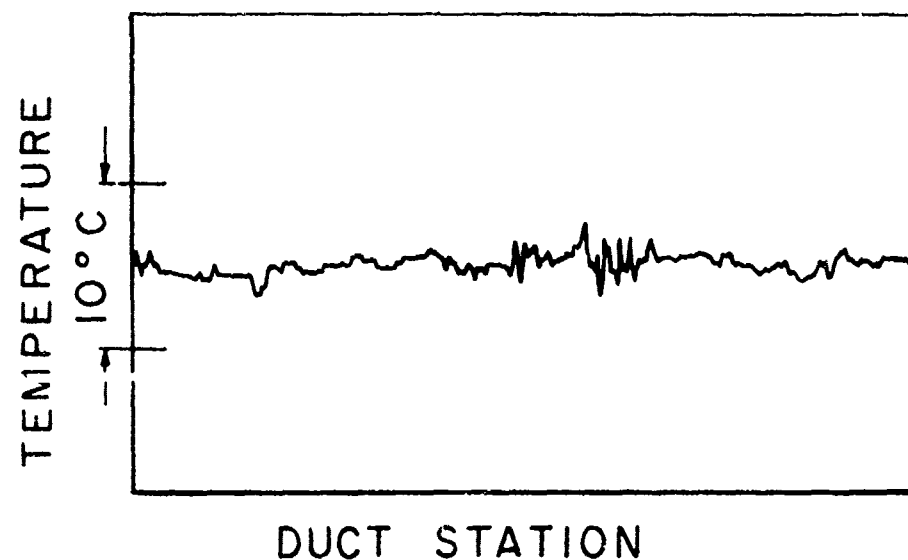
SAMPLING PROBE COMPONENTS

FIGURE 25



INFRARED ABSORPTION CELL

# RADIAL TEMPERATURE PROFILE



DUCT DIAMETER : 3 INCHES  
TEMPERATURE : 705° C  
FLOW VELOCITY : 650 INCHES/SEC

FIGURE 27

JPR 2119

# RADIAL VELOCITY PROFILE 2 INCH DUCT

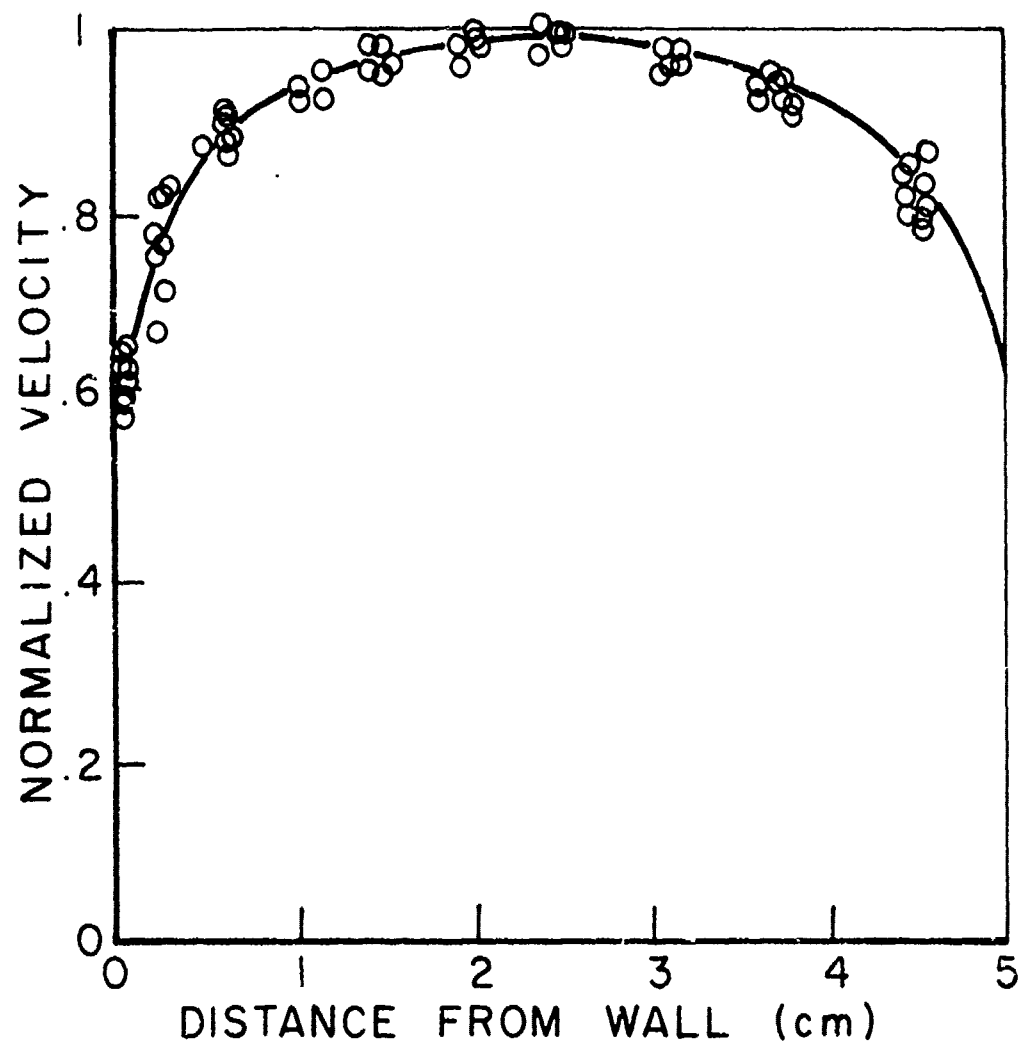
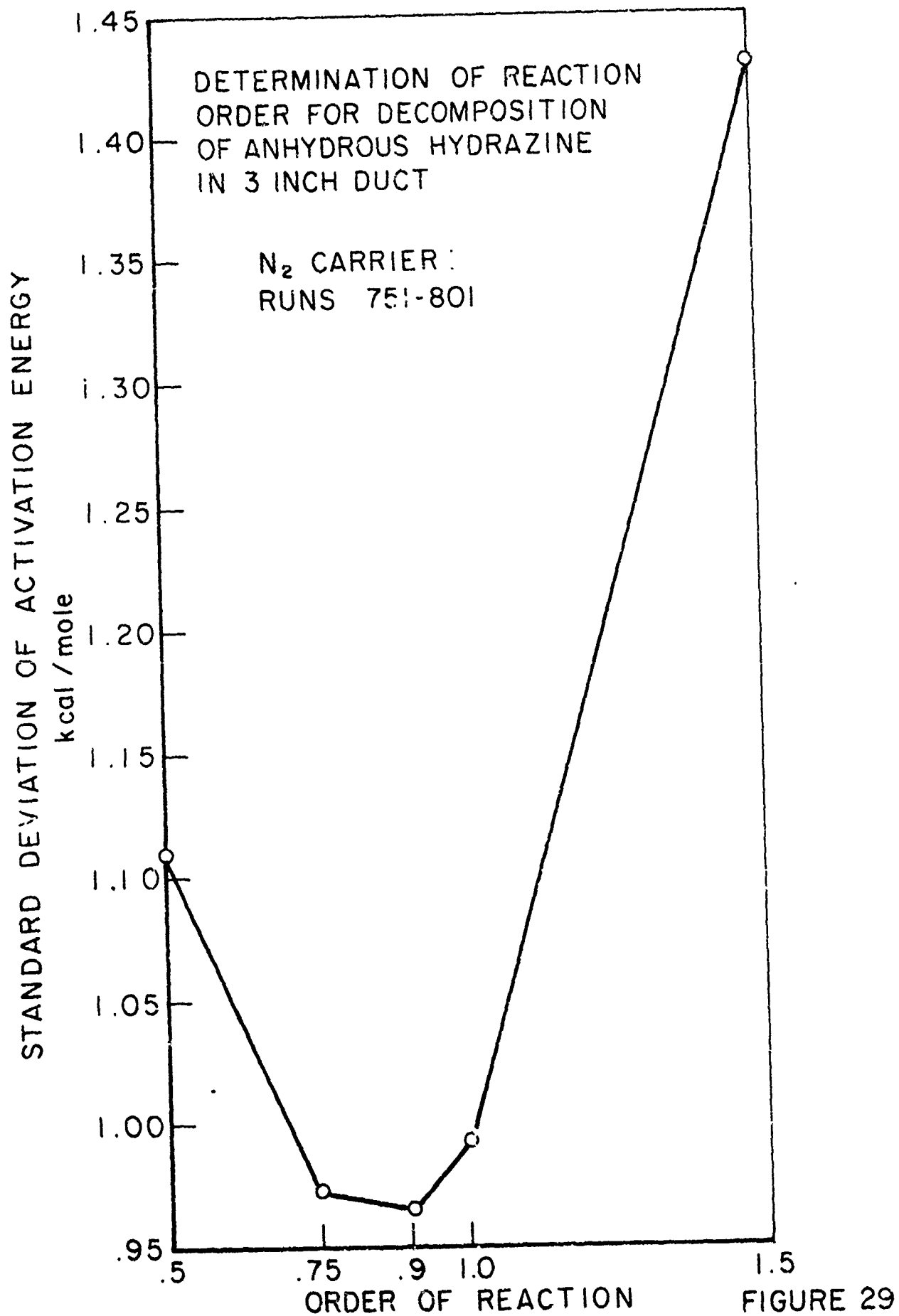


FIGURE 28



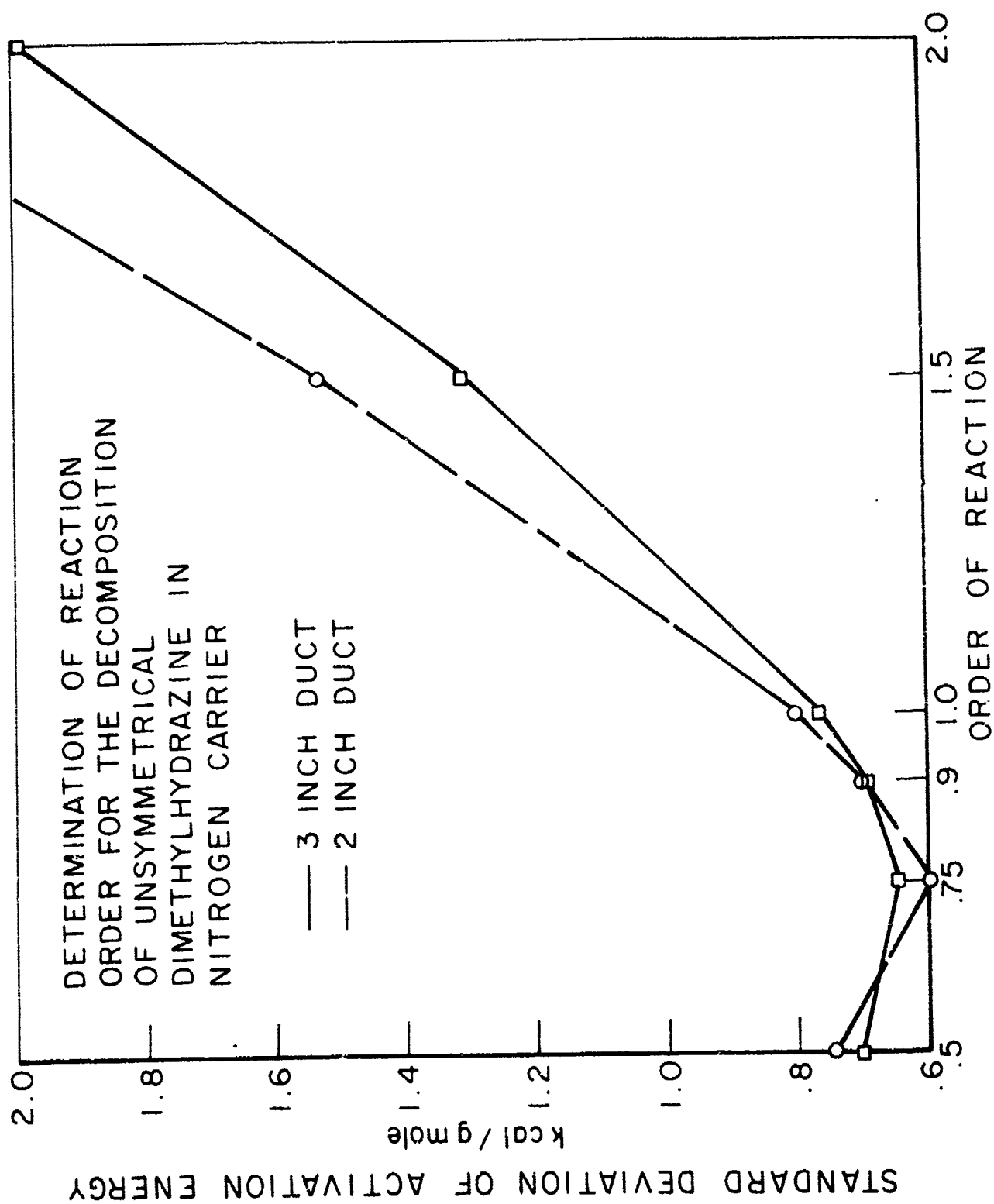


FIGURE 30

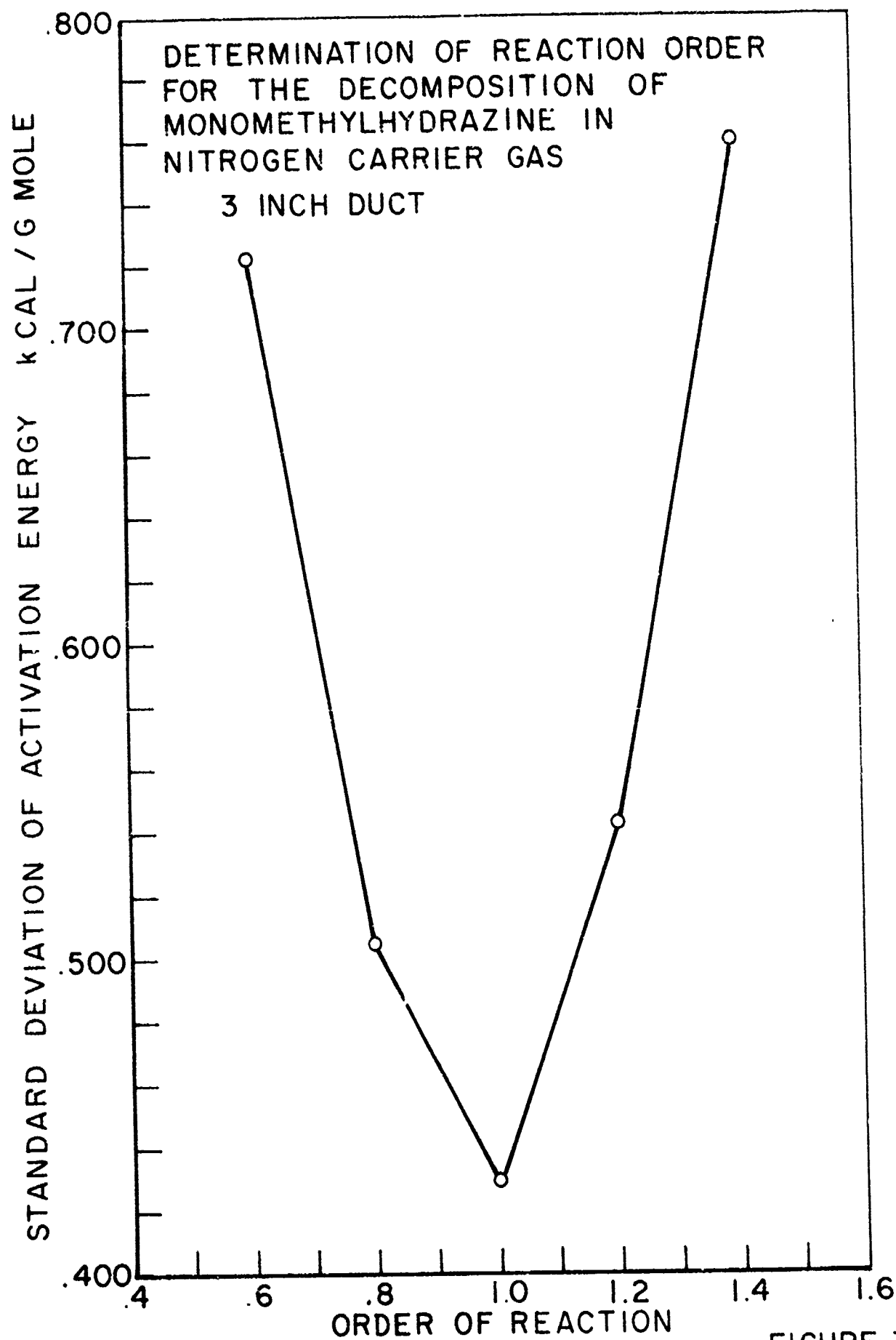


FIGURE 31

# REPRODUCIBILITY OF HYDRAZINE DATA

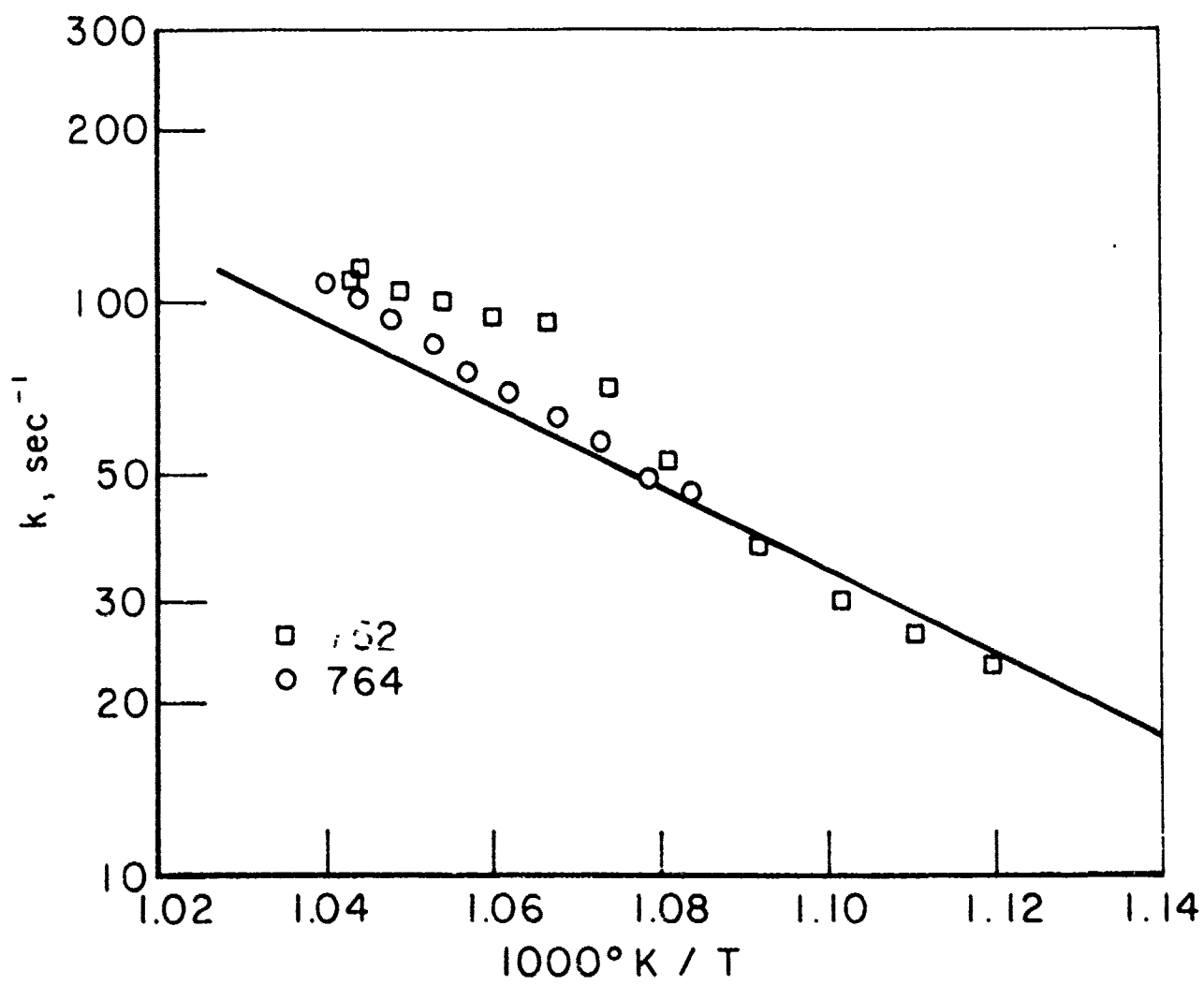


FIGURE 32

# REPRODUCIBILITY OF UDMH DATA

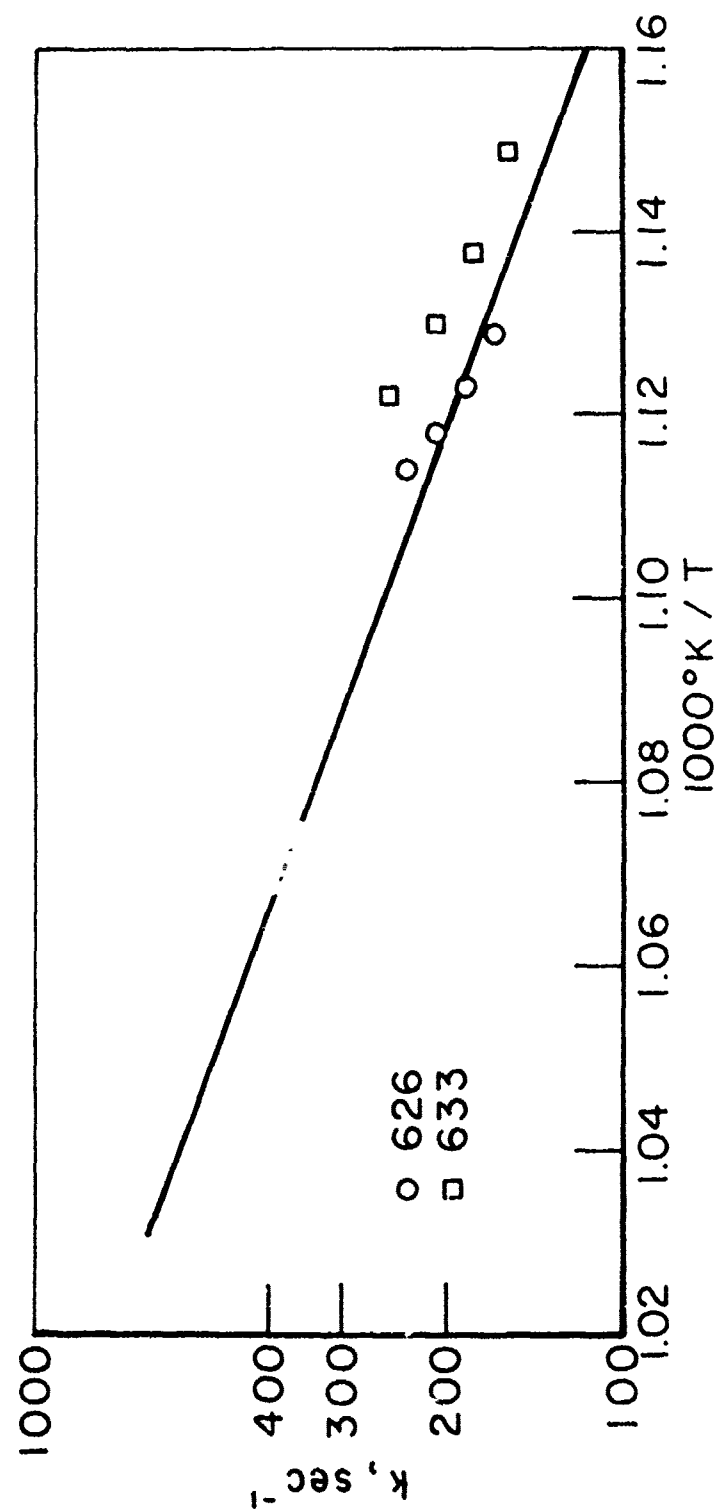


FIGURE 33

DECOMPOSITION OF MONOMETHYLHYDRAZINE  
REPRODUCIBILITY OF DATA

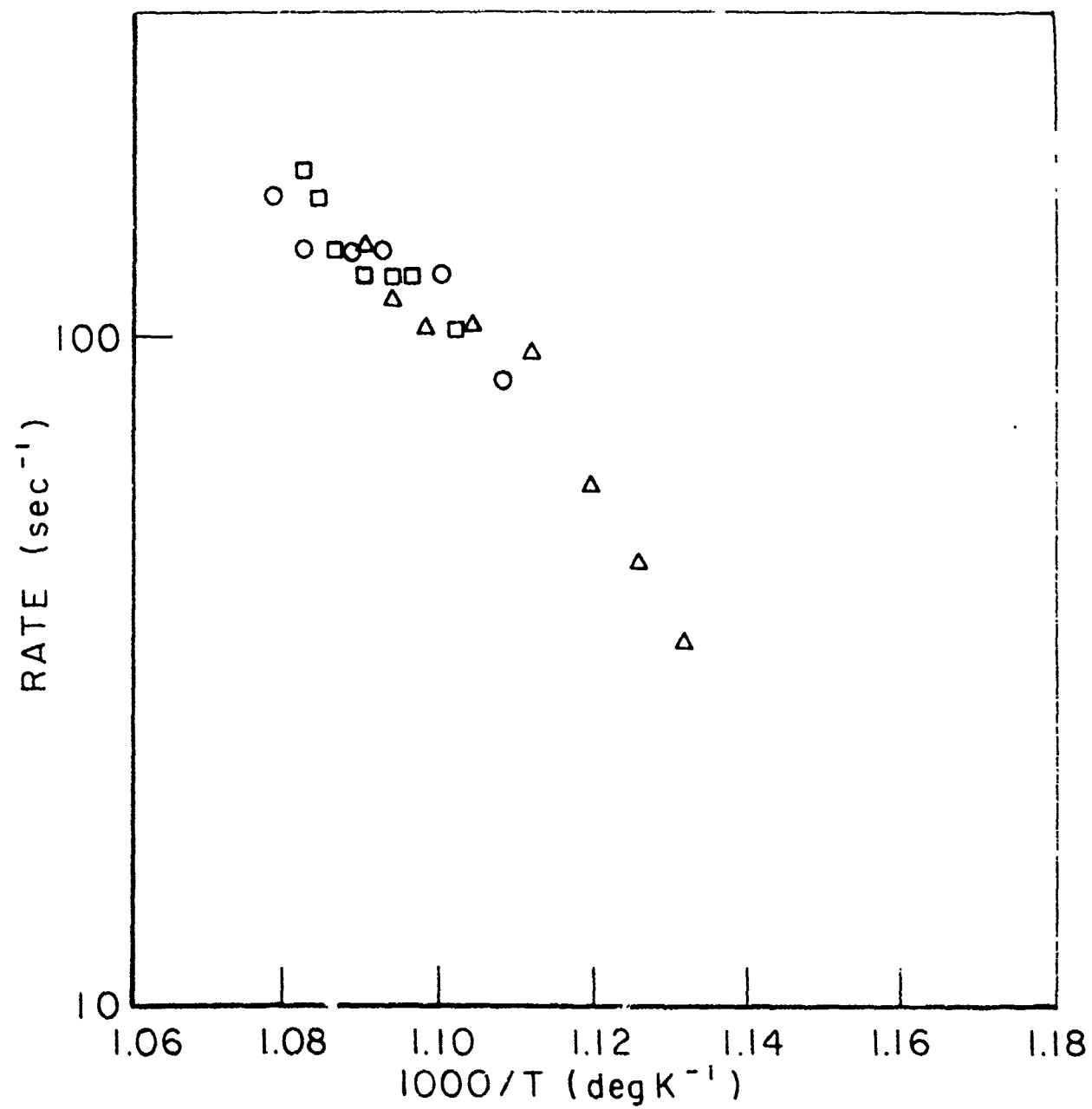


FIGURE 34

JPR 1374

# HYDRAZINE DECOMPOSITION

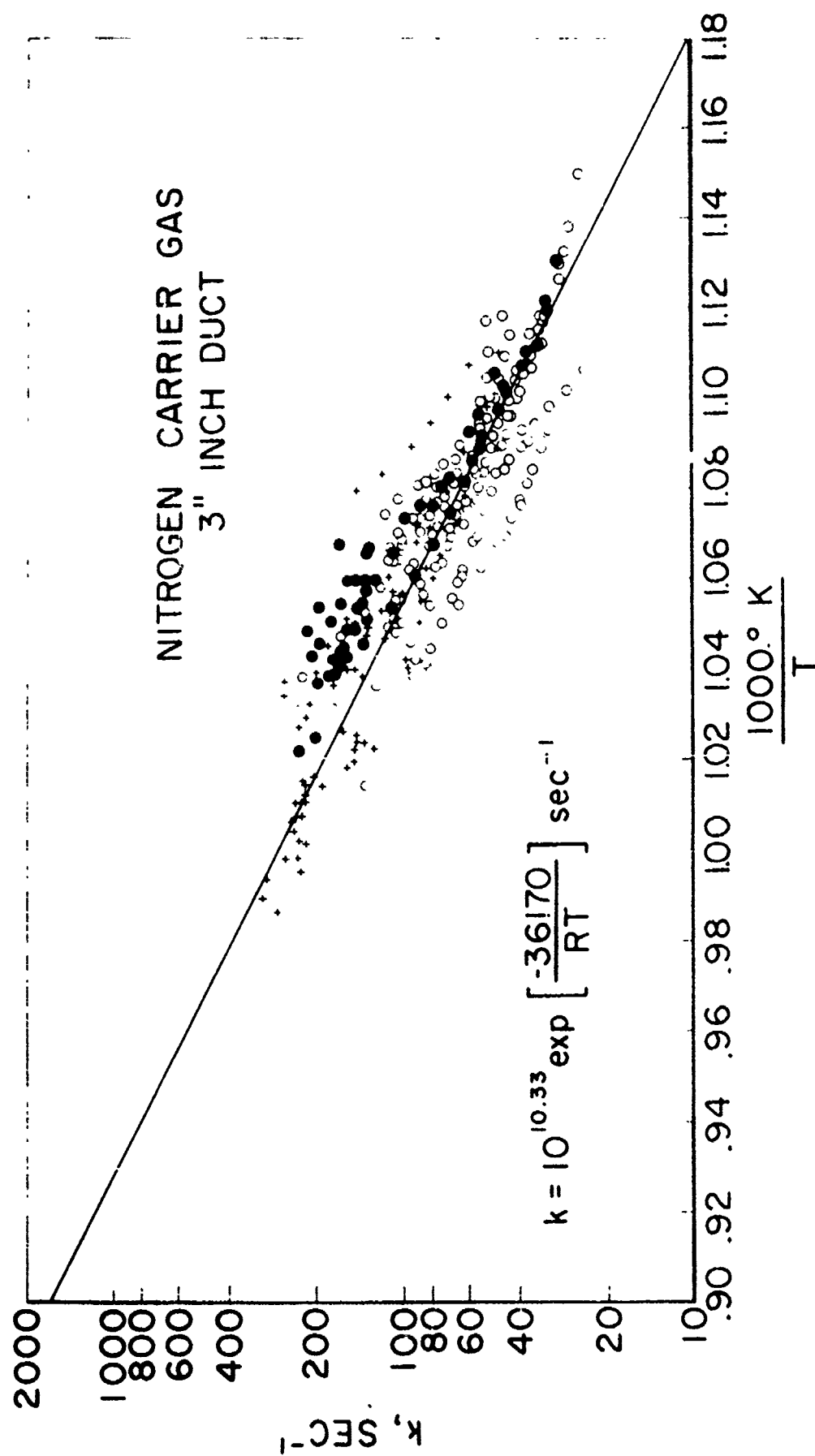


FIGURE 35

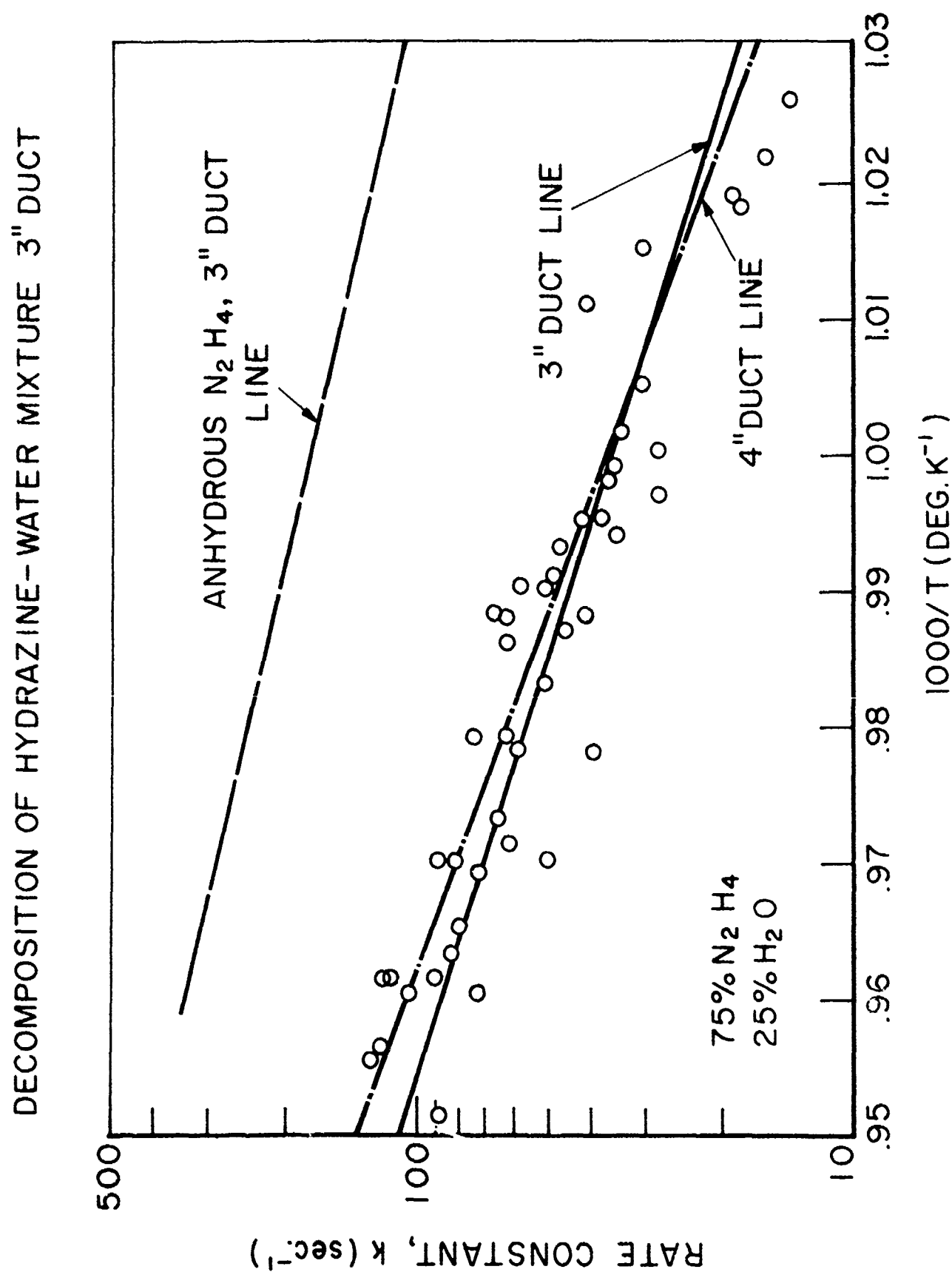


FIGURE 36

JPR 2125

DECOMPOSITION OF HYDRAZINE-WATER MIXTURE 4" DUCT

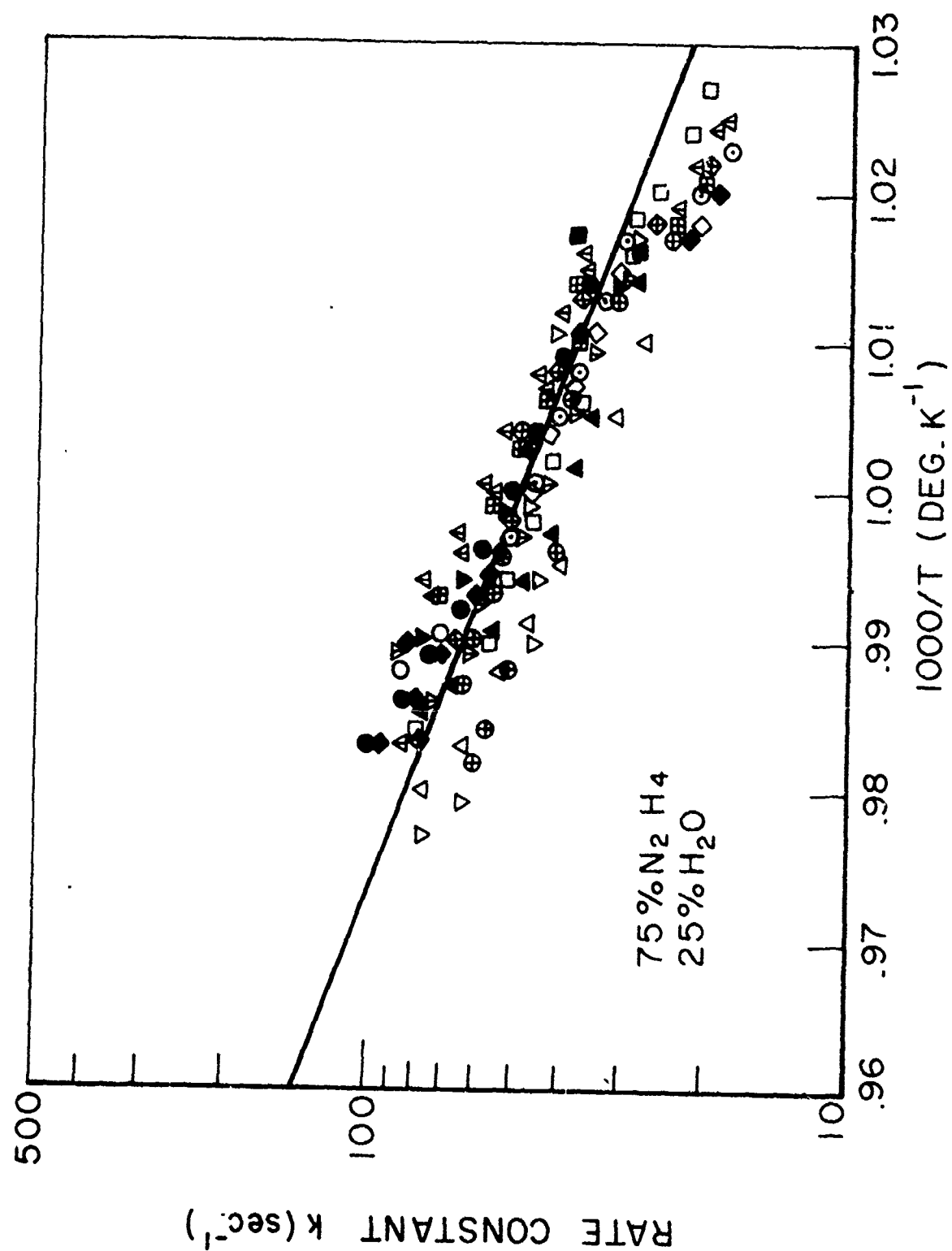


FIGURE 37

WET HYDRAZINE DECOMPOSITION 3" DUCT

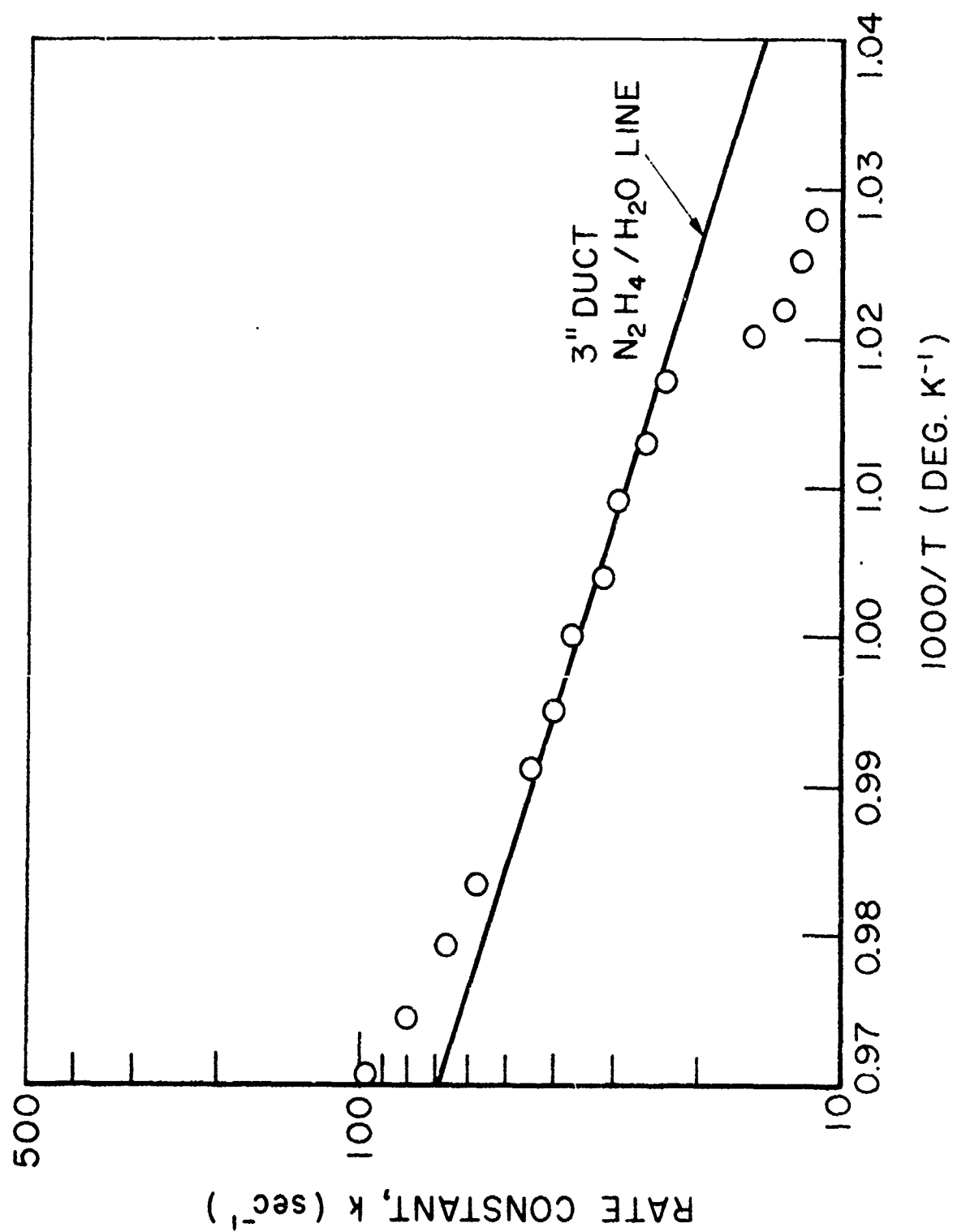


FIGURE 38

# WET HYDRAZINE DECOMPOSITION 4" DUCT

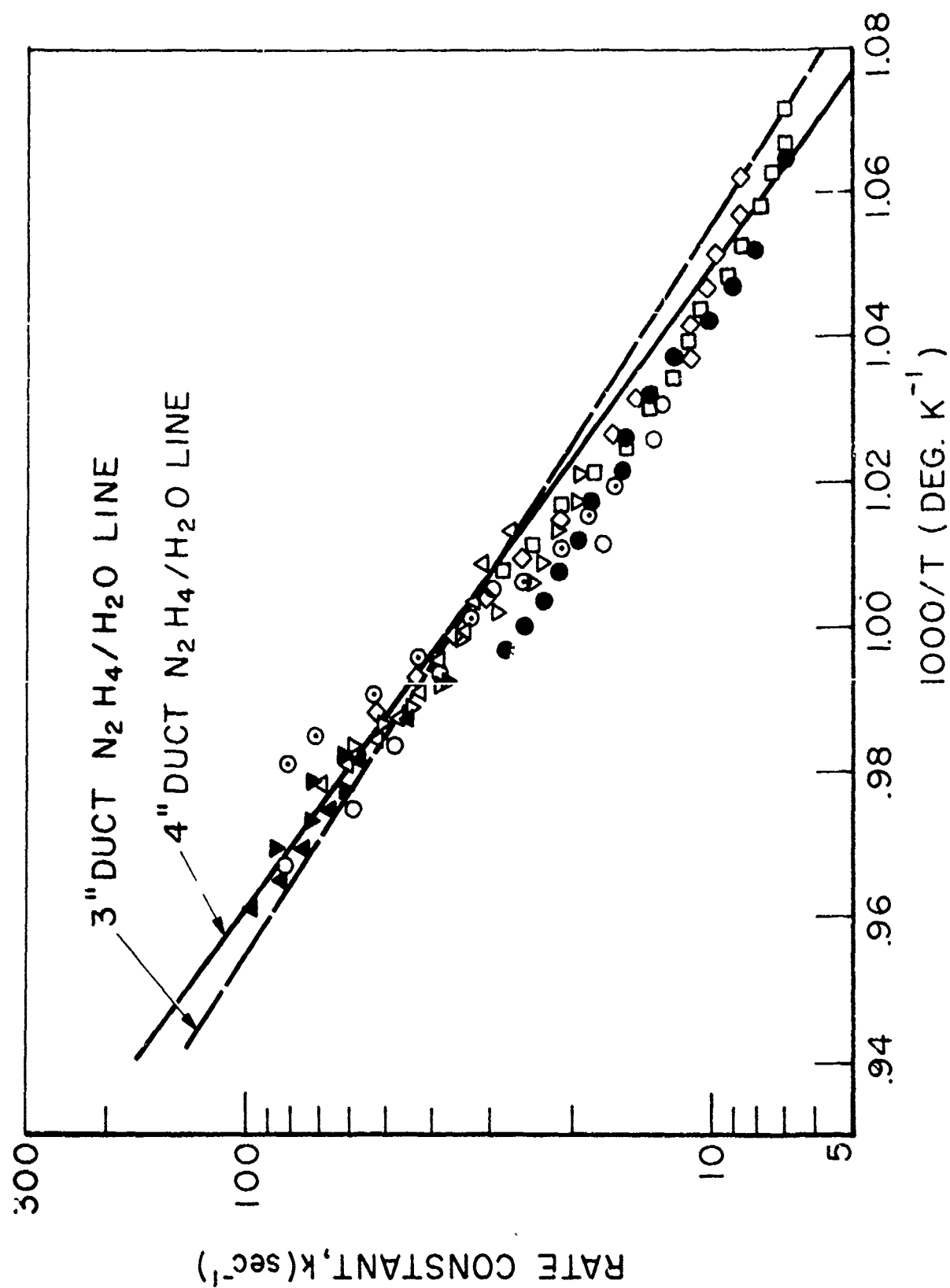


FIGURE 39

# UNSYMMETRICAL DIMETHYLHYDRAZINE DECOMPOSITION

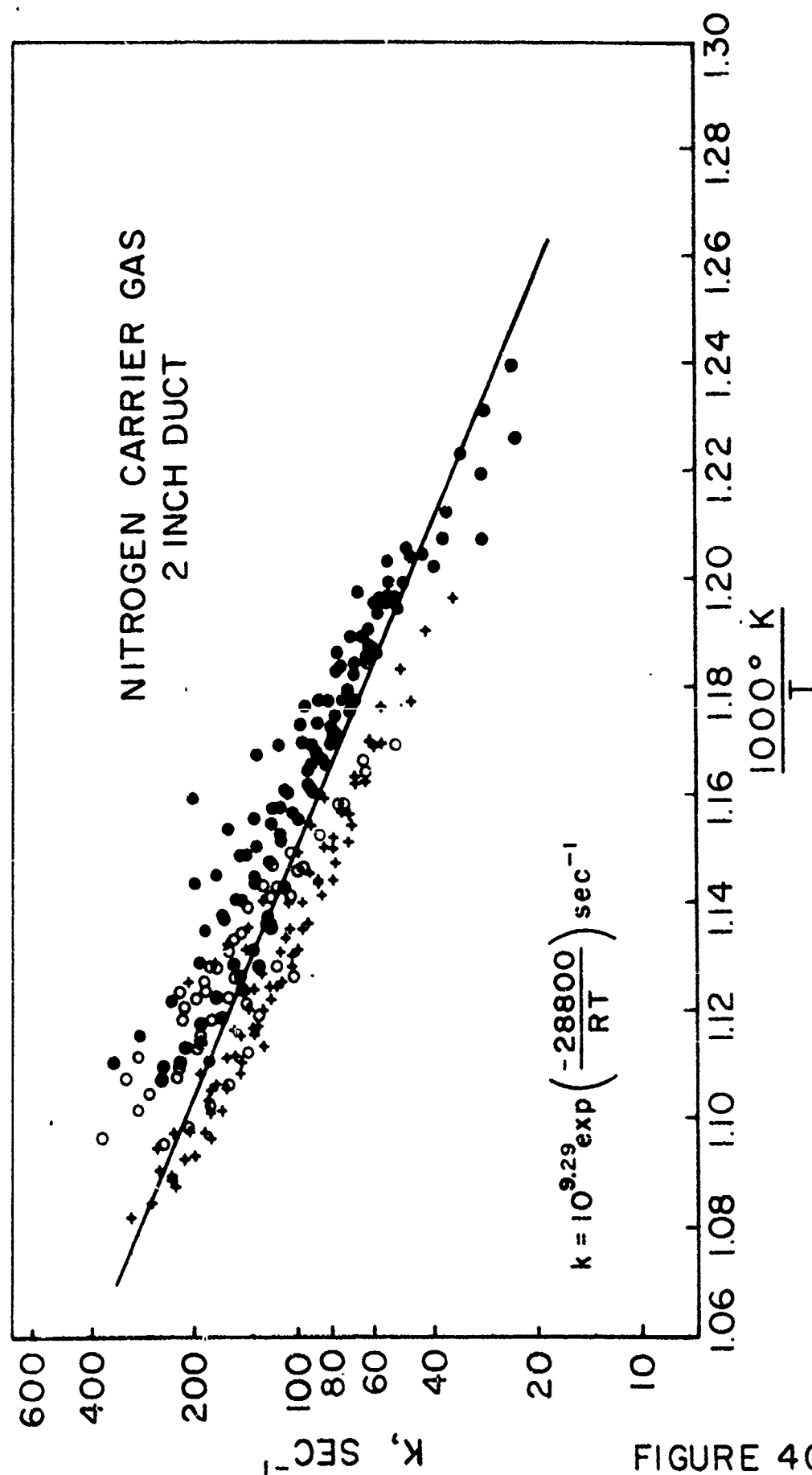


FIGURE 40

JPR 1253

# UNSYMMETRICAL DIMETHYLHYDRAZINE DECOMPOSITION

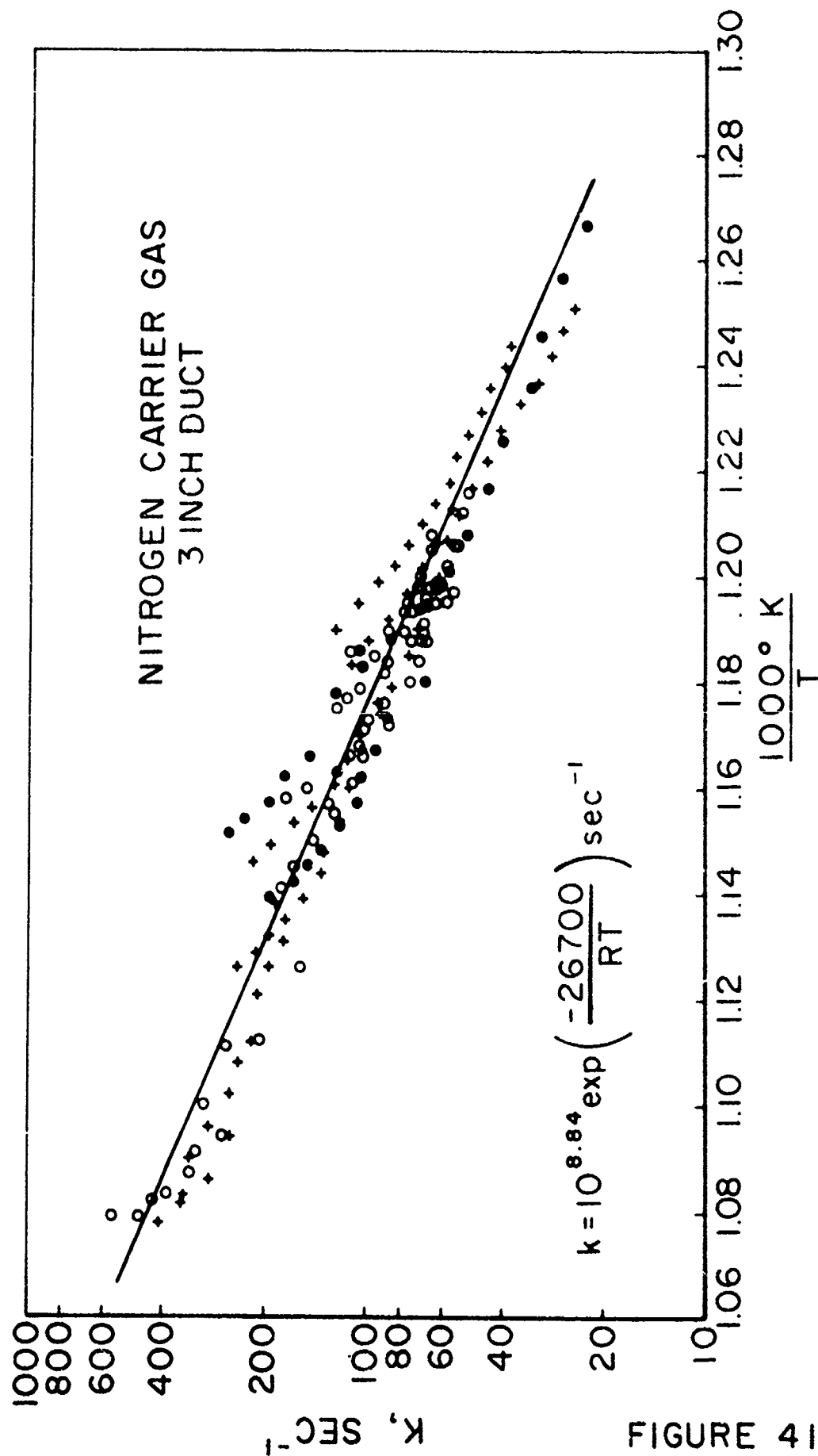


FIGURE 41

# UNSYMMETRICAL DIMETHYLHYDRAZINE DECOMPOSITION

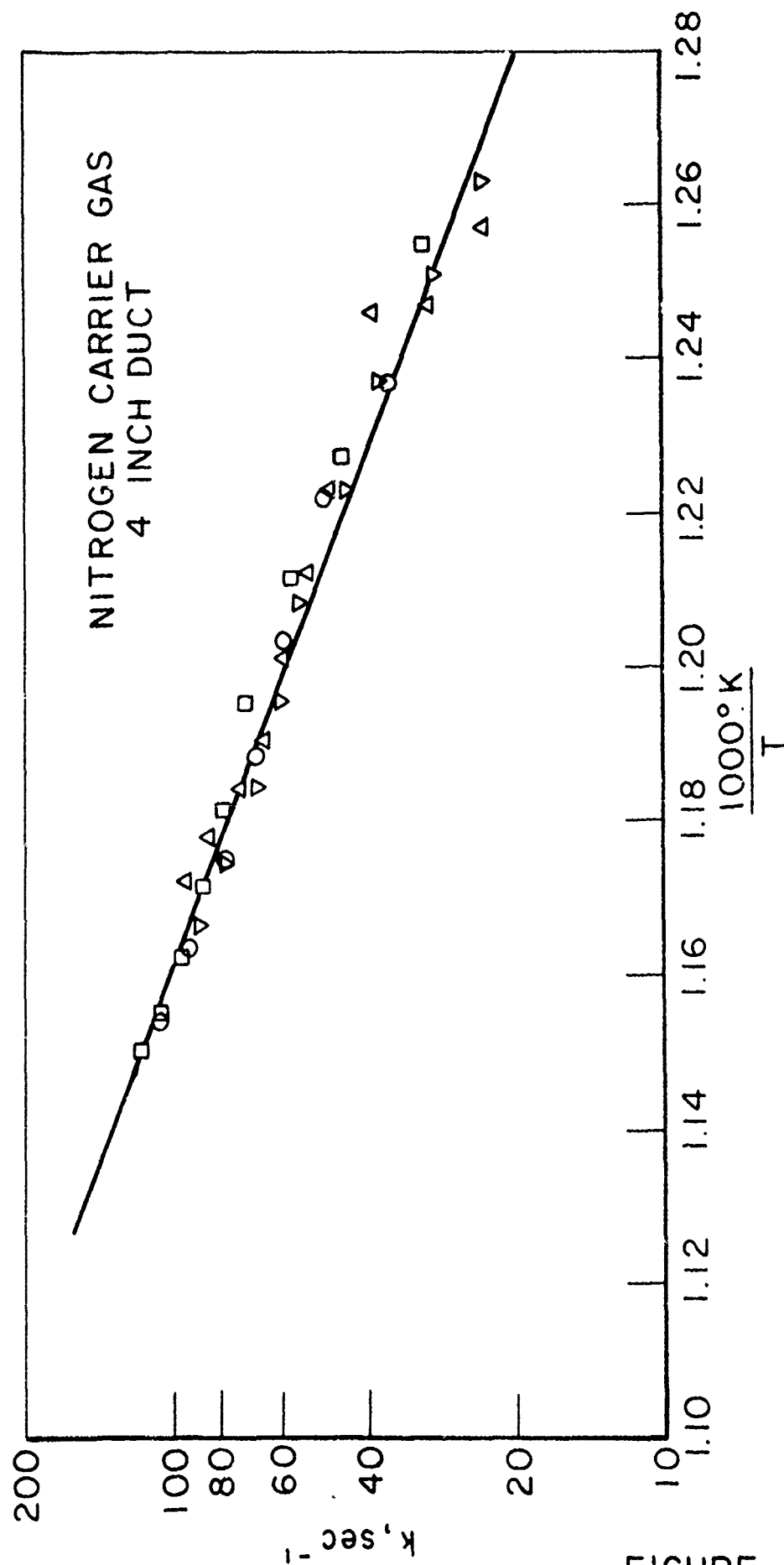


FIGURE 42

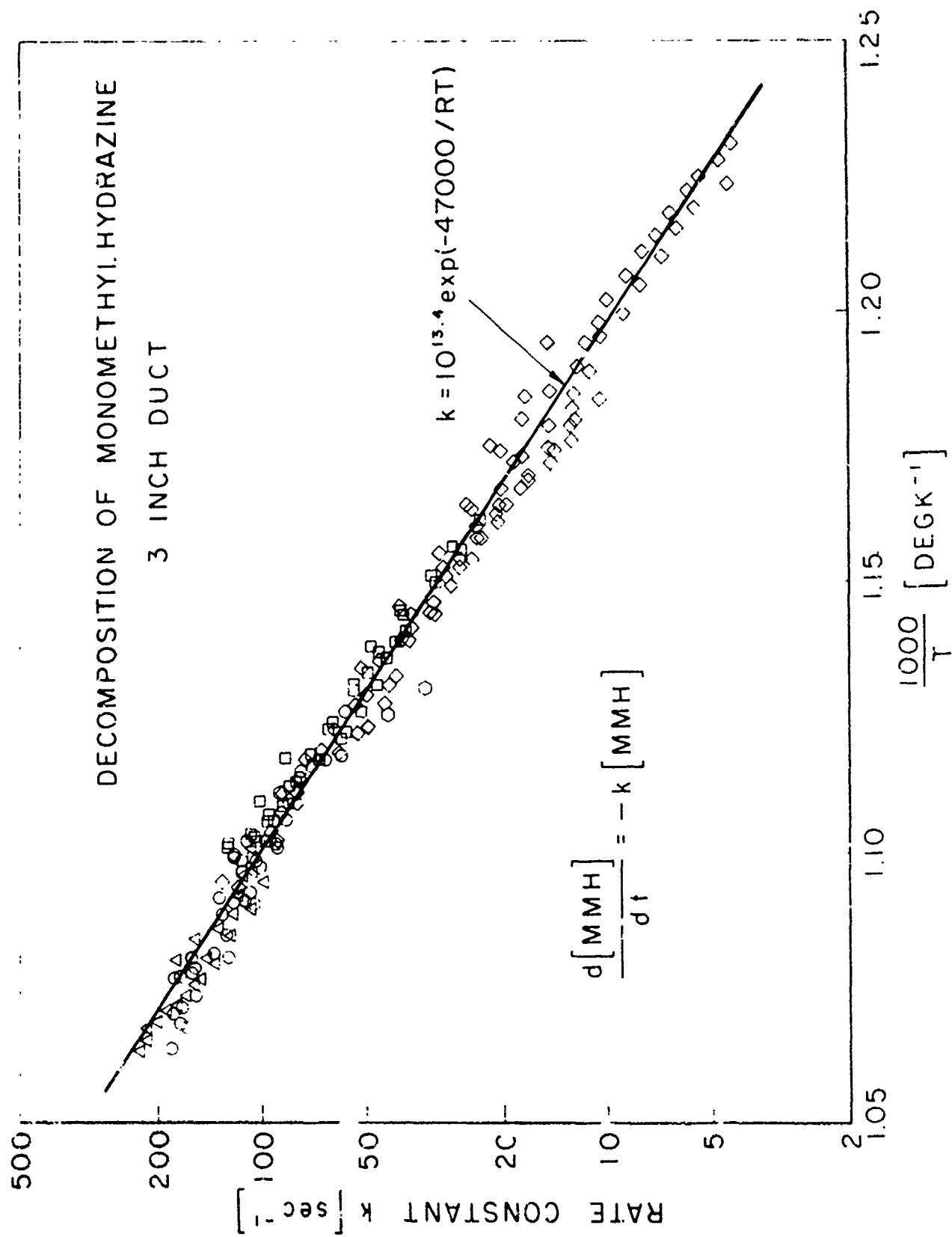


FIGURE 43

# DECOMPOSITION OF MONOMETHYLHYDRAZINE 4" DUCT

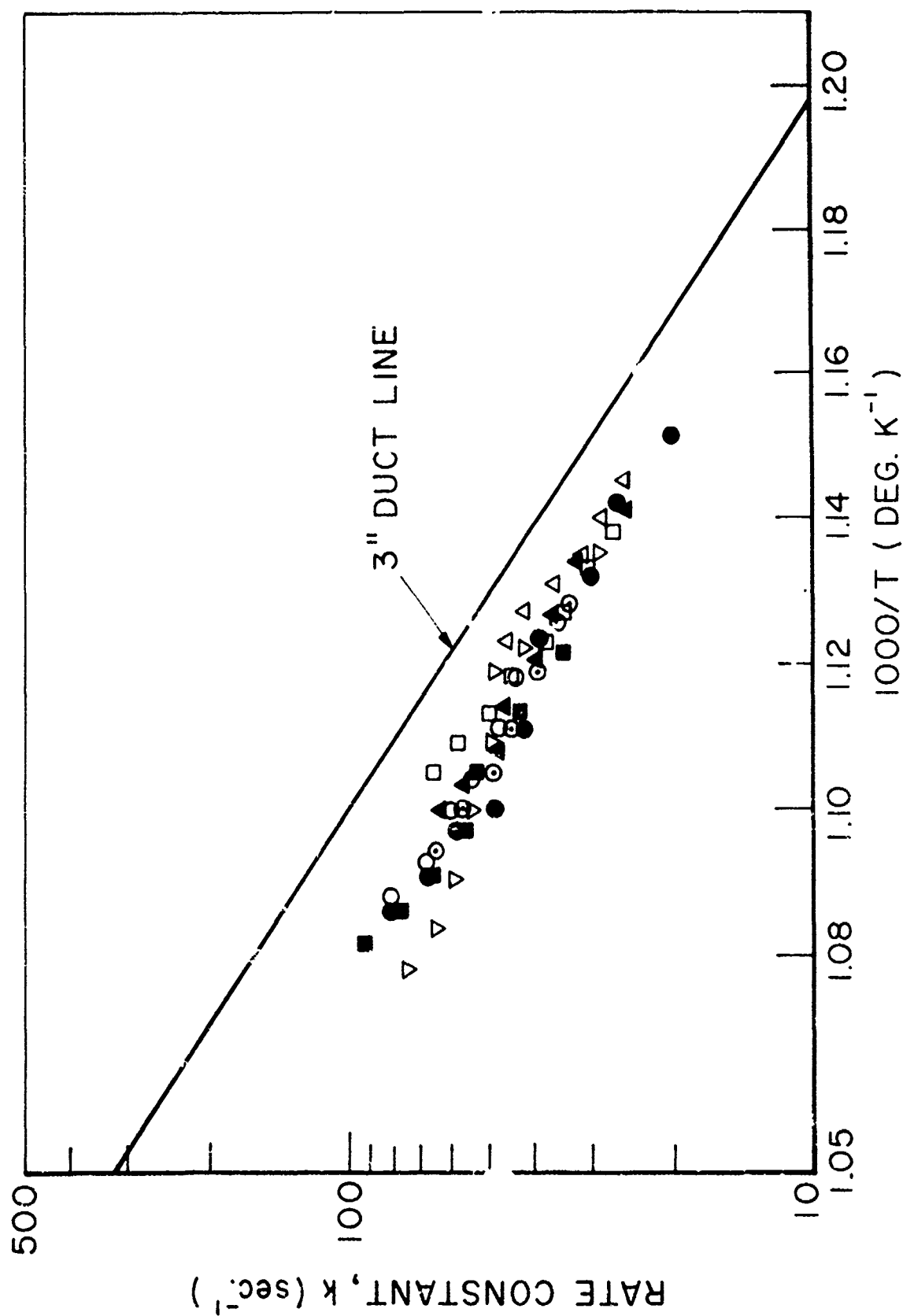


FIGURE 44

## INTEGRATION ANALYSIS OF HYDRAZINE DATA

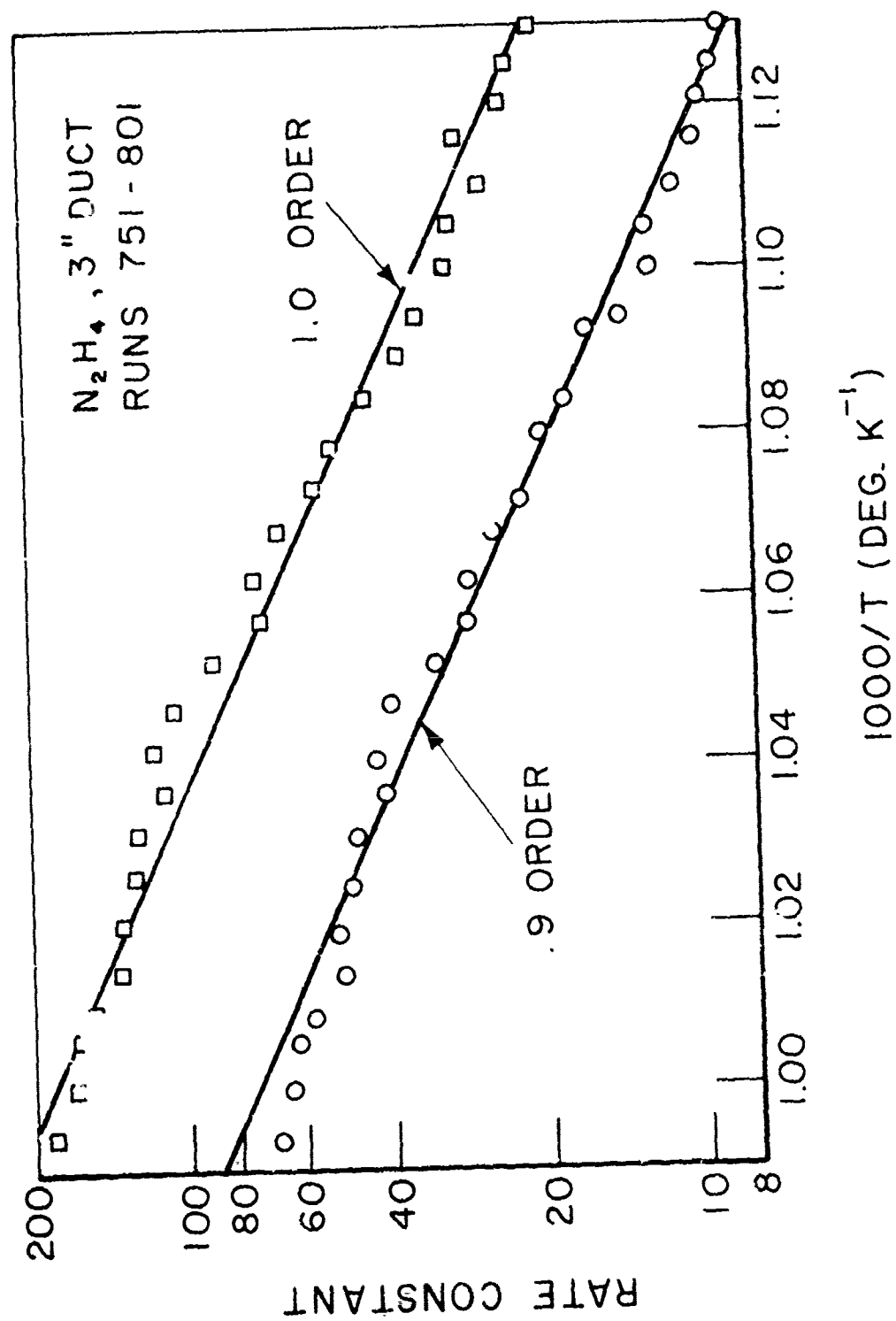


FIGURE 45

INTEGRATION ANALYSIS OF  
UNSYMMETRICAL DIMETHYLHYDRAZINE  
DATA

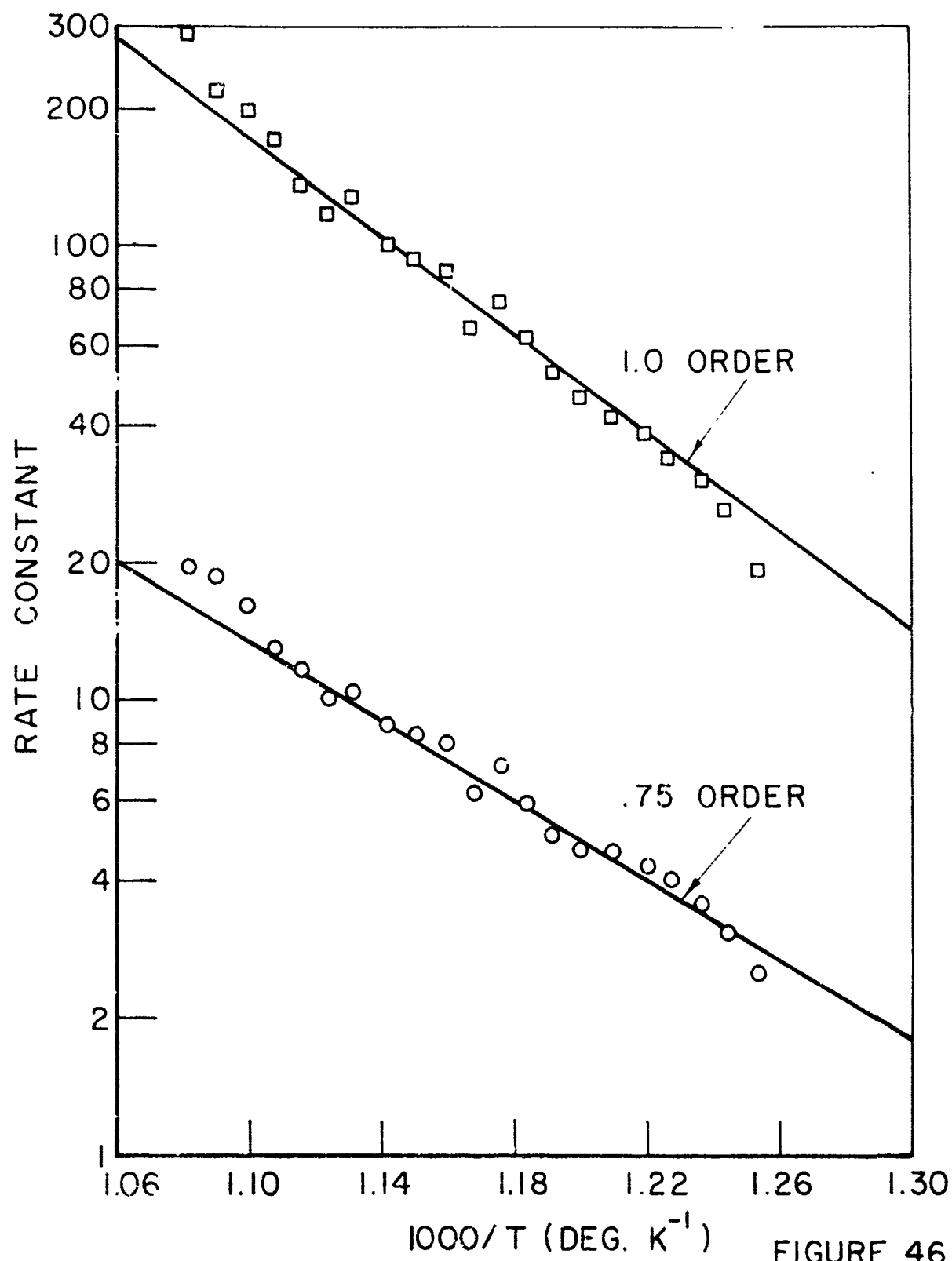


FIGURE 46

INTEGRATION ANALYSIS OF  
MONOMETHYLHYDRAZINE DECOMPOSITION

3 INCH DUCT, 1.0 ORDER

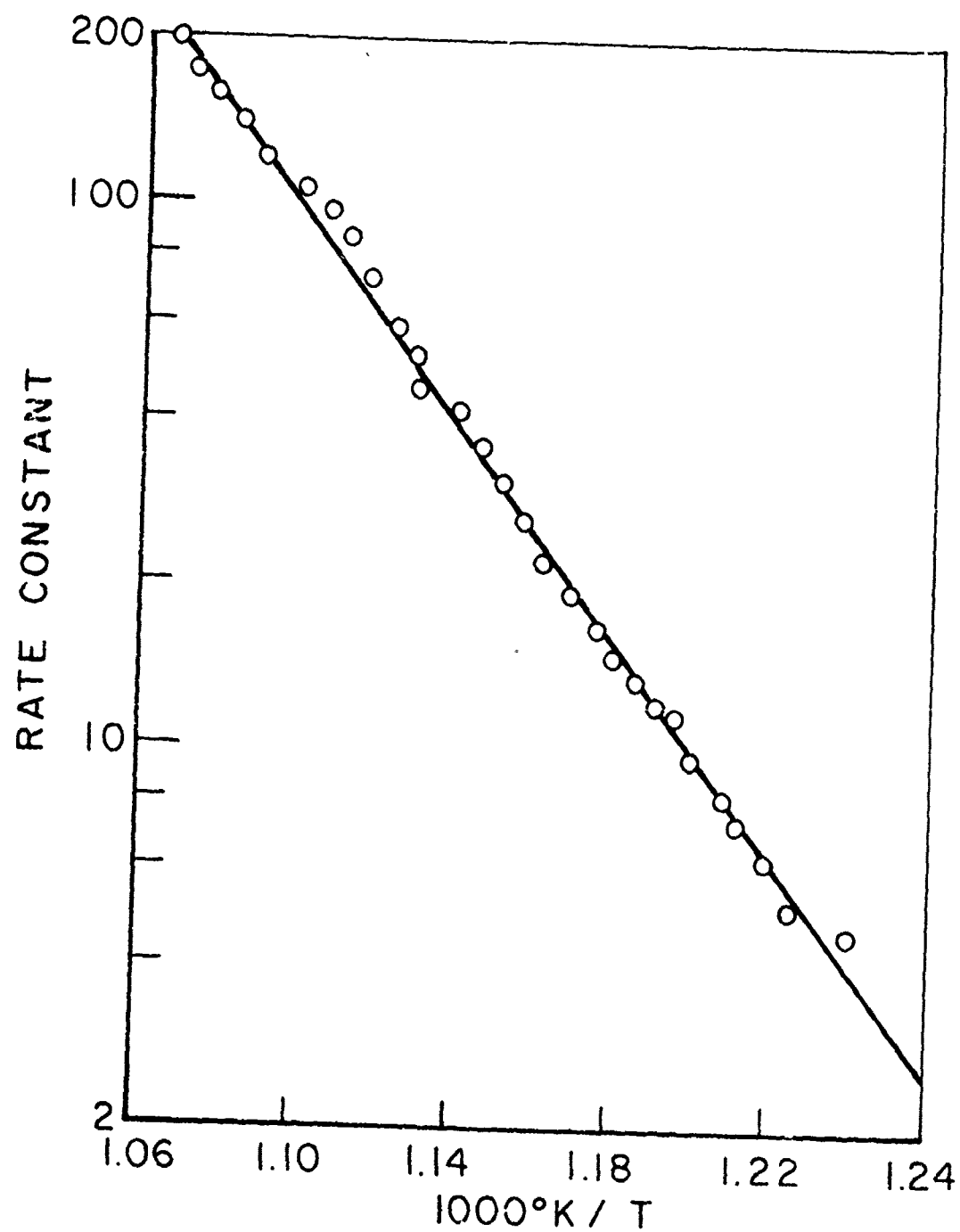


FIGURE 47

# SPECTRUM OF STANDARD AMMONIA SAMPLE

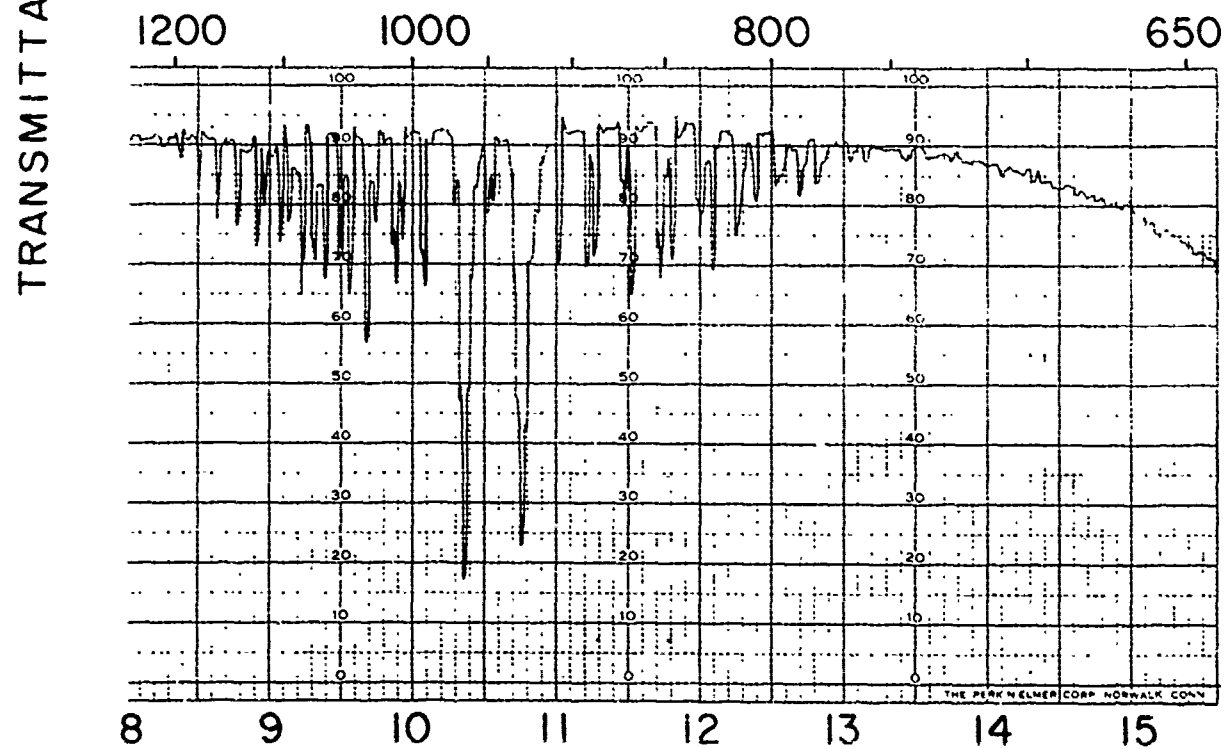
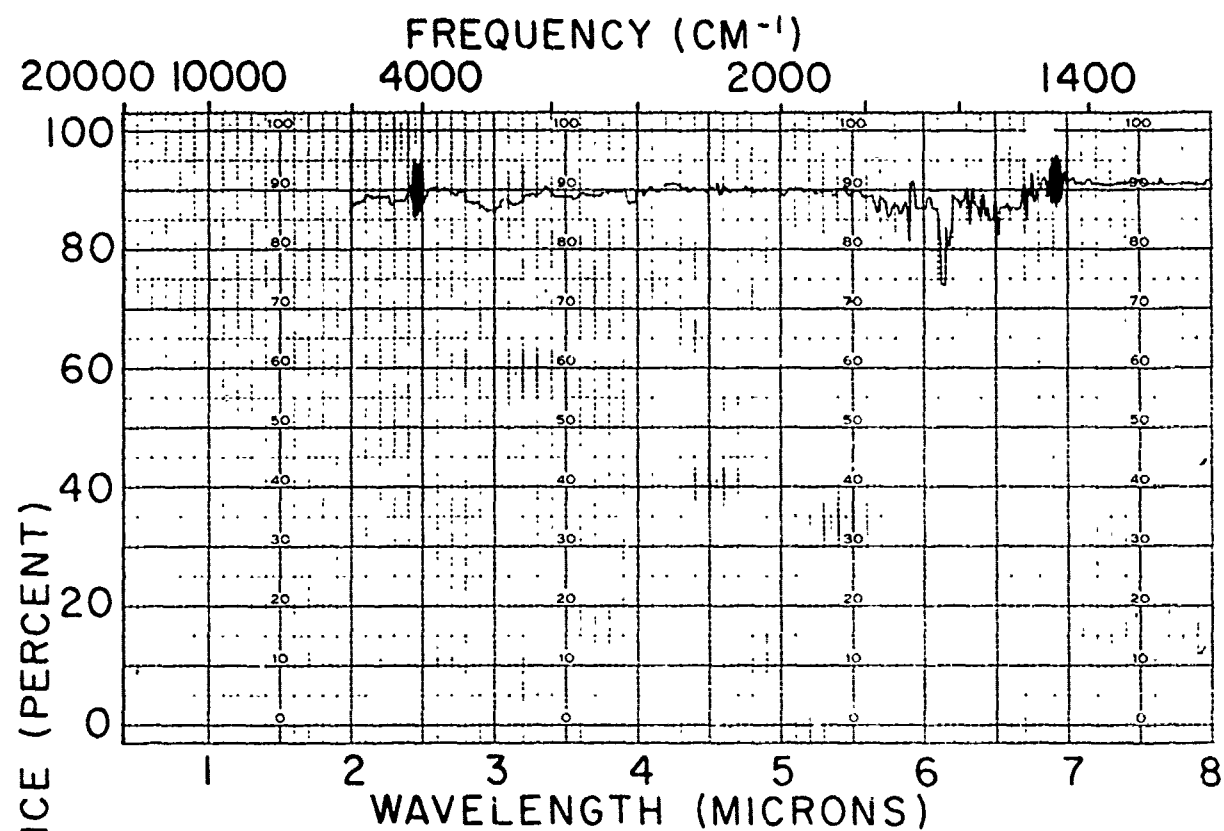


FIGURE 48

# SPECTRUM OF GASEOUS DECOMPOSITION PRODUCTS OF UDMH

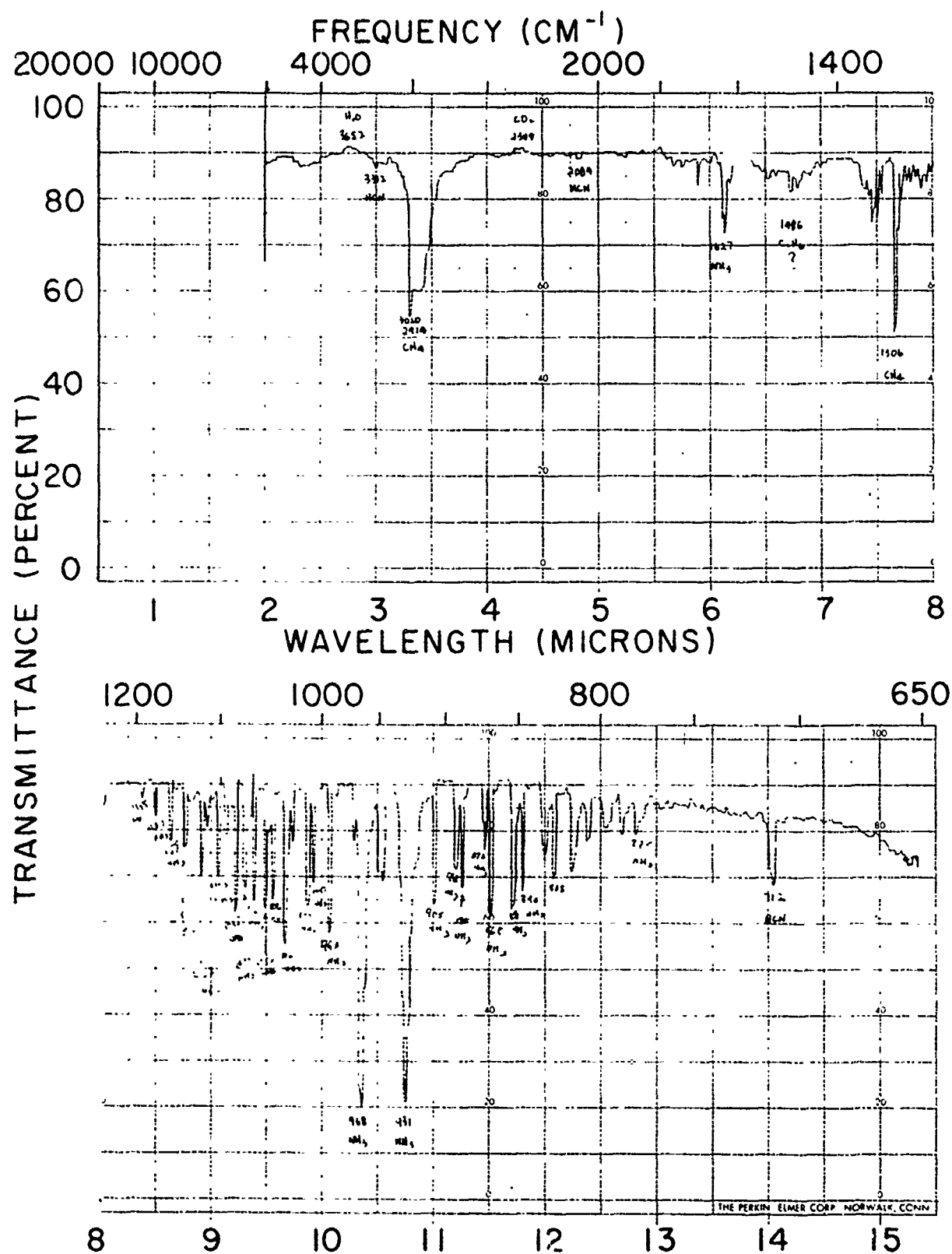


FIGURE 49

JPR 1957

# SPECTRUM OF GASEOUS DECOMPOSITION PRODUCTS OF MONOMETHYLHYDRAZINE

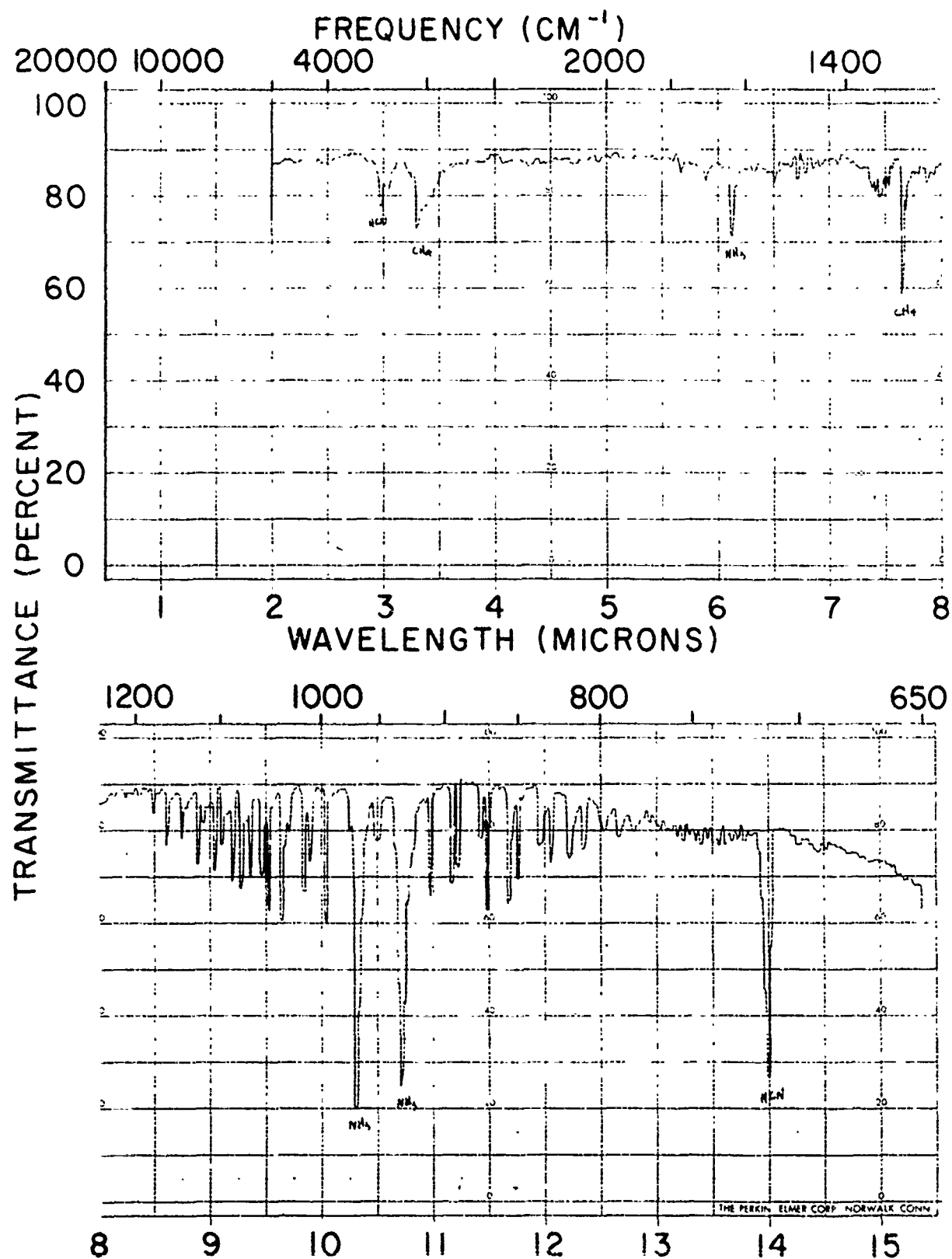


FIGURE 50

# SPECTRUM OF CONDENSATE IN ACETONE SOLUTION

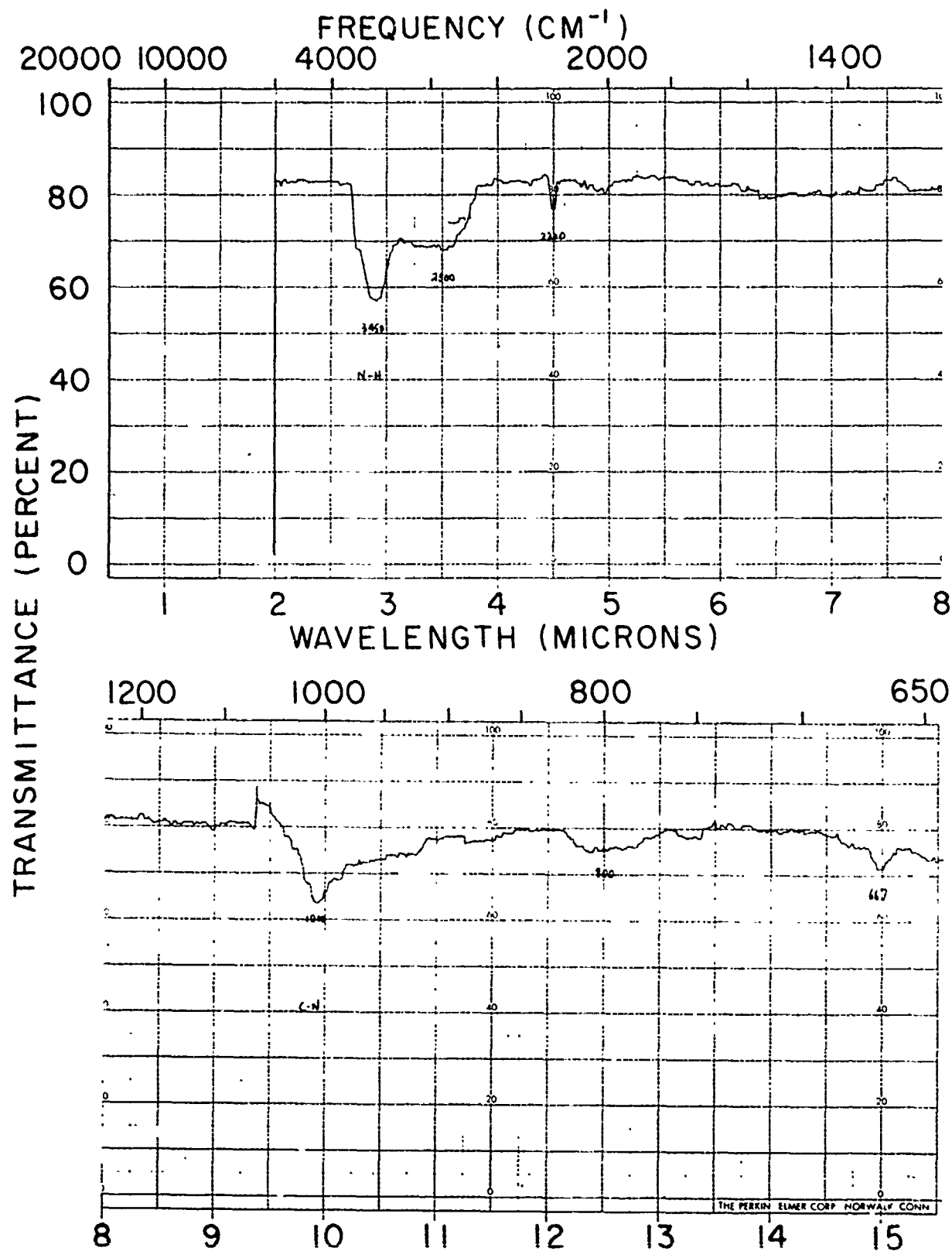


FIGURE 51

JPC 1957

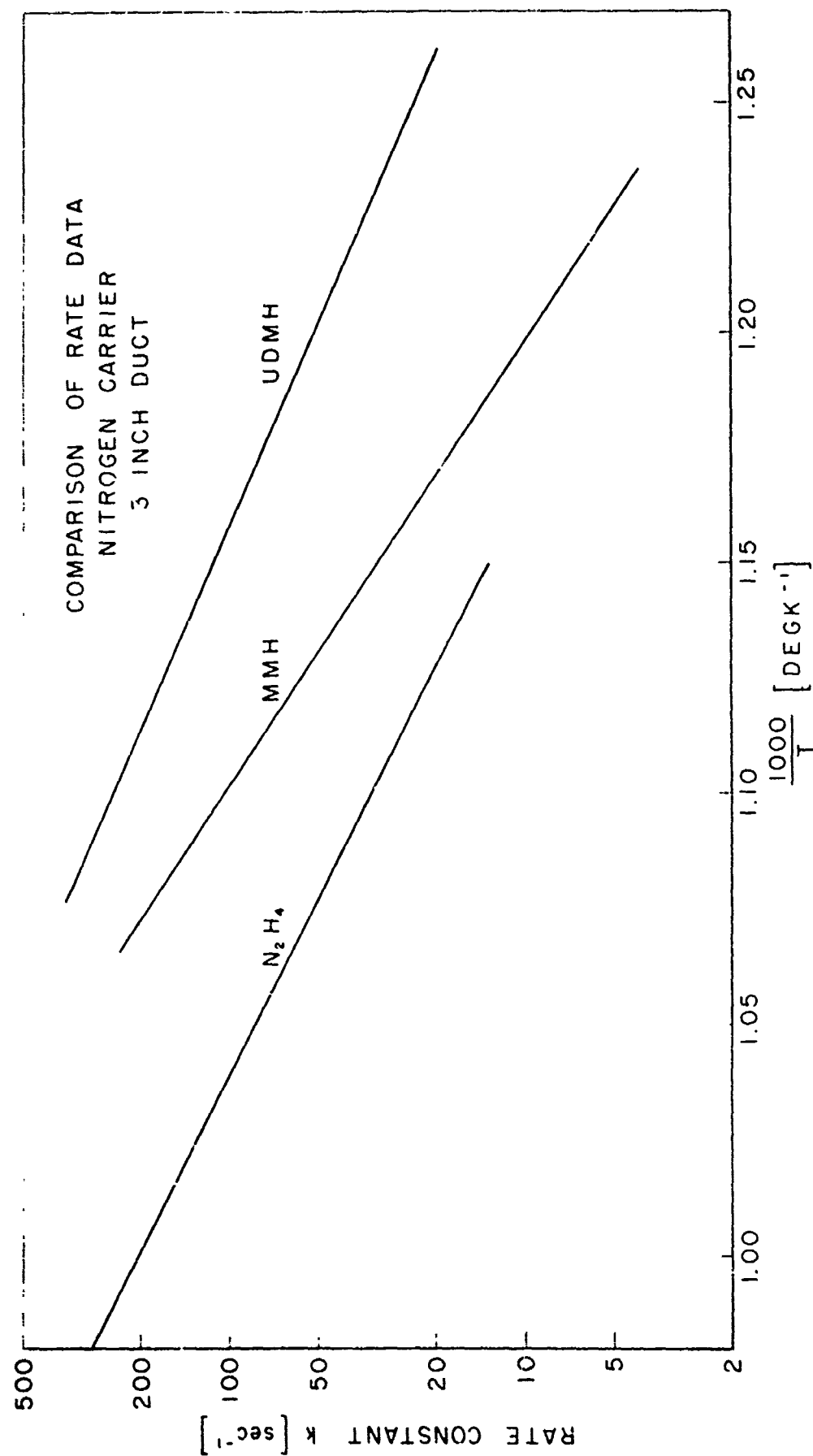


FIGURE 52

FIRST ORDER RATE CONSTANTS FOR  
HYDRAZINE DECOMPOSITION

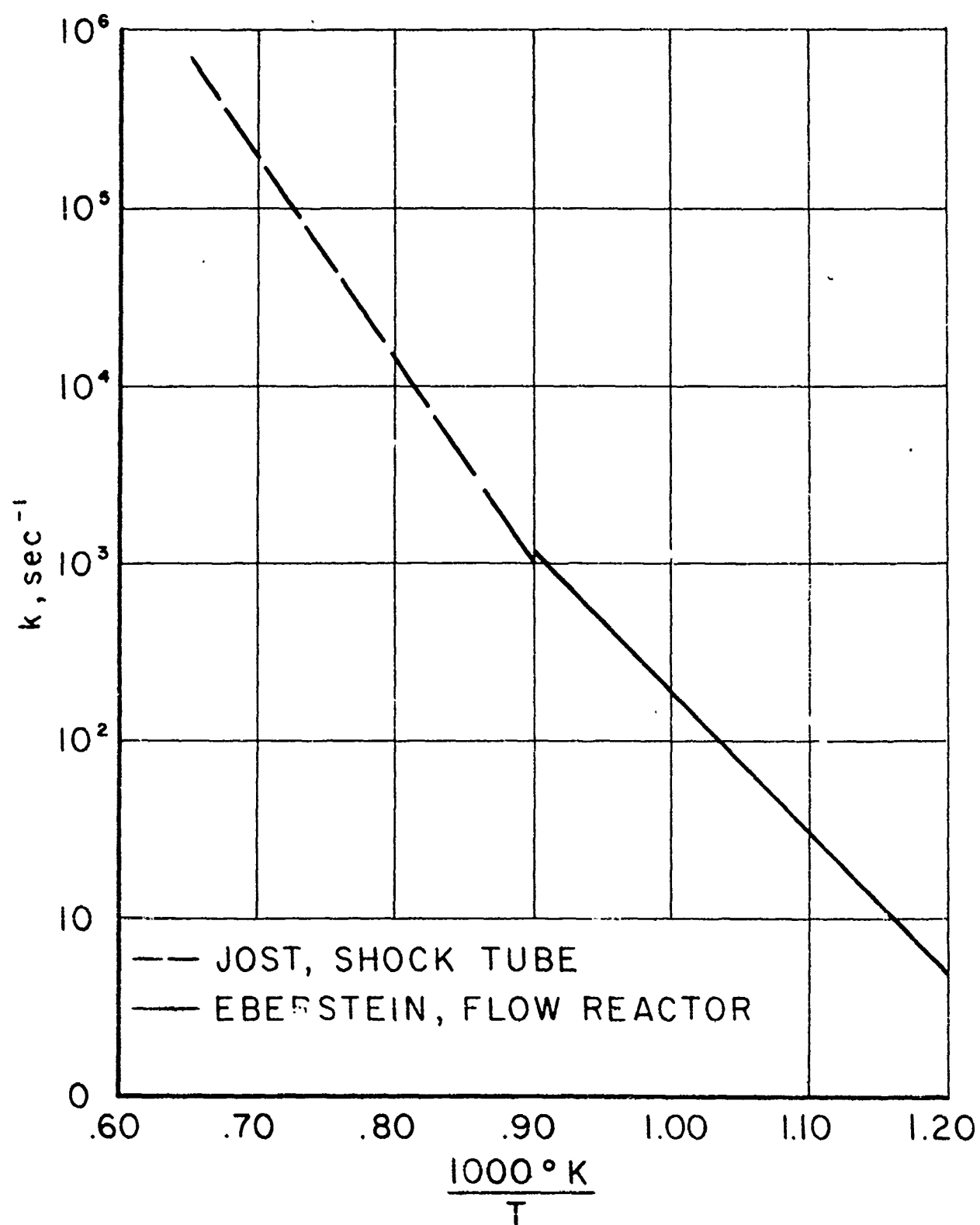


FIGURE 53

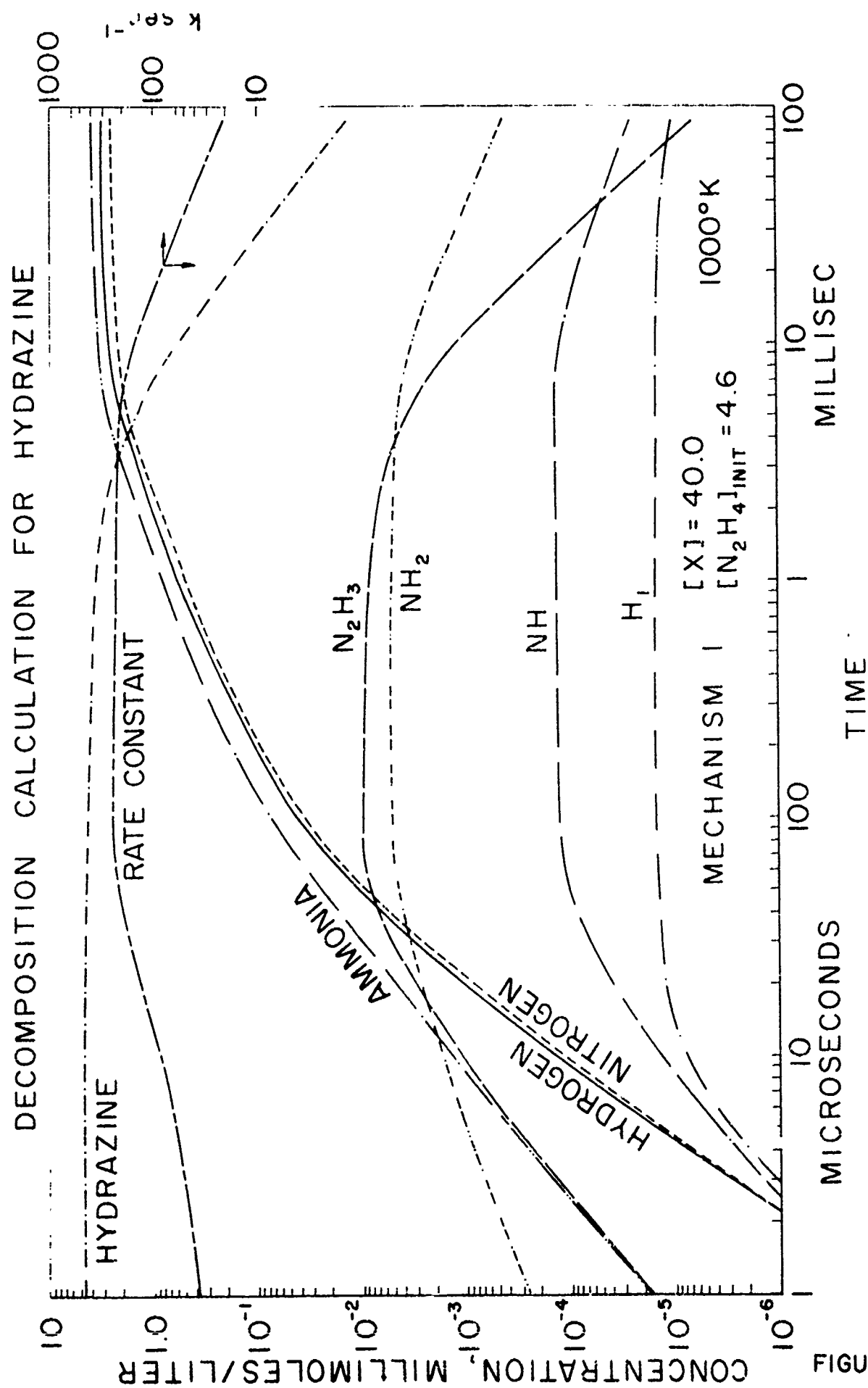


FIGURE 54

# DECOMPOSITION CALCULATIONS FOR HYDRAZINE

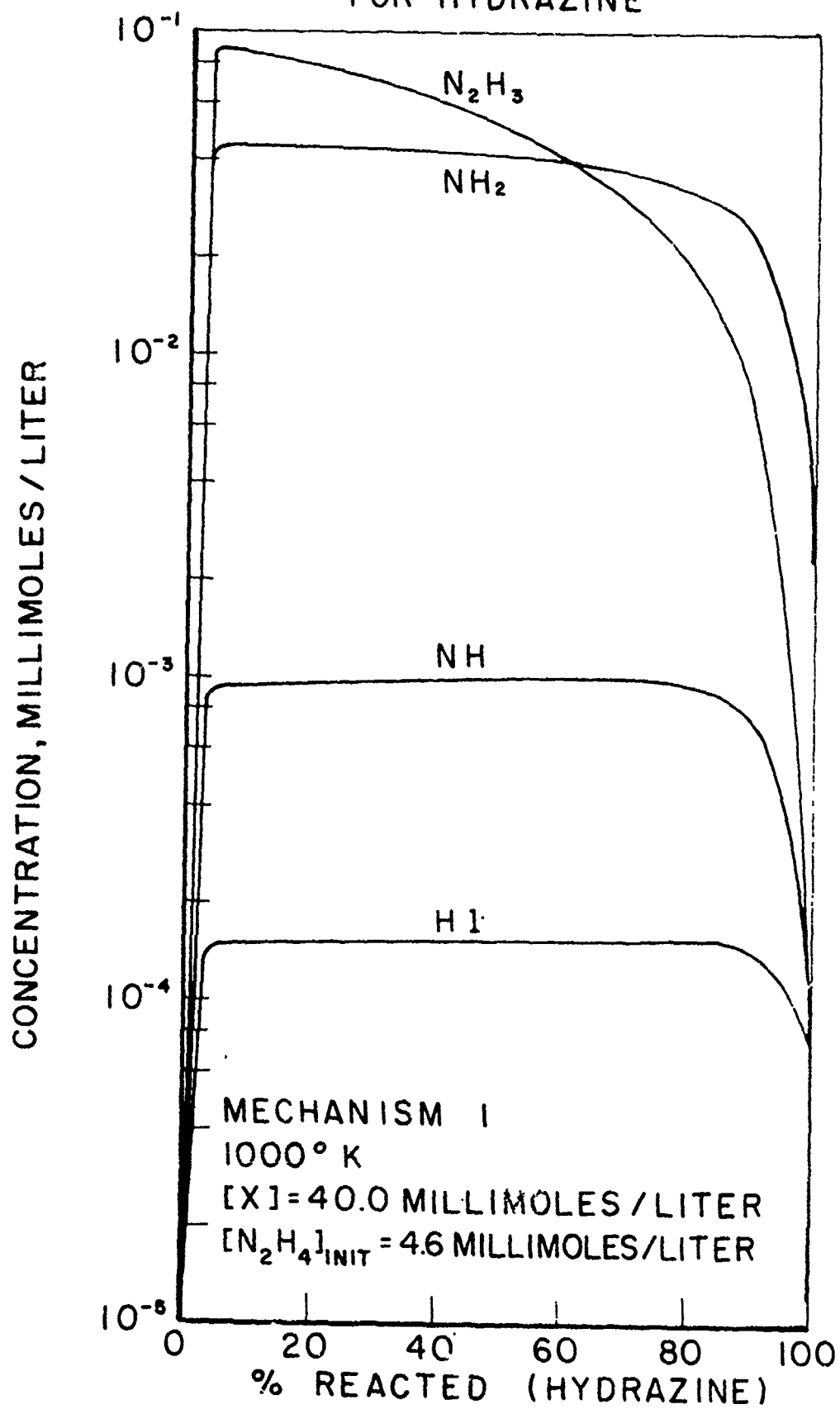


FIGURE 55

# DECOMPOSITION CALCULATIONS FOR HYDRAZINE

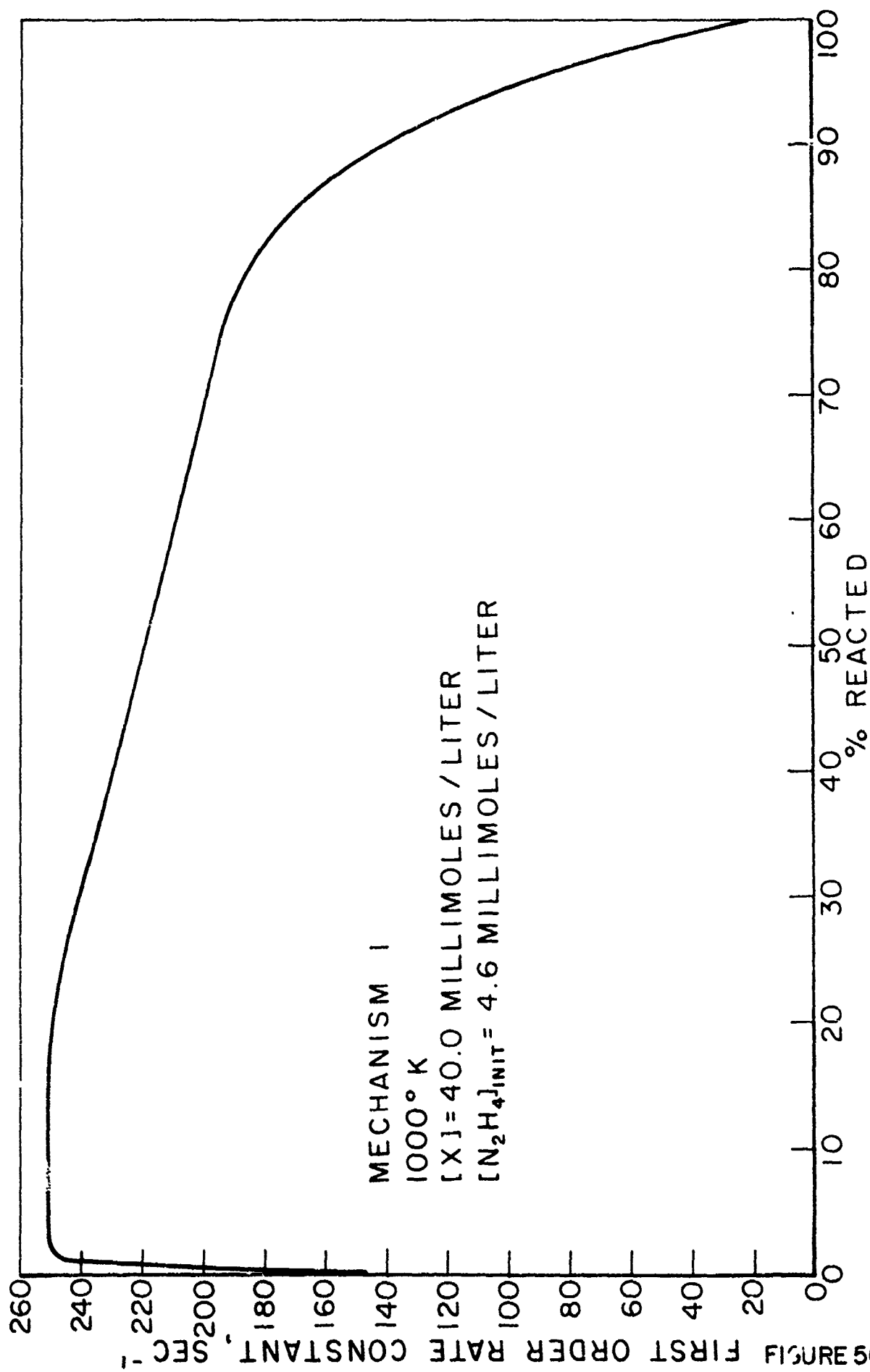


FIGURE 56

# DECOMPOSITION CALCULATIONS FOR HYDRAZINE

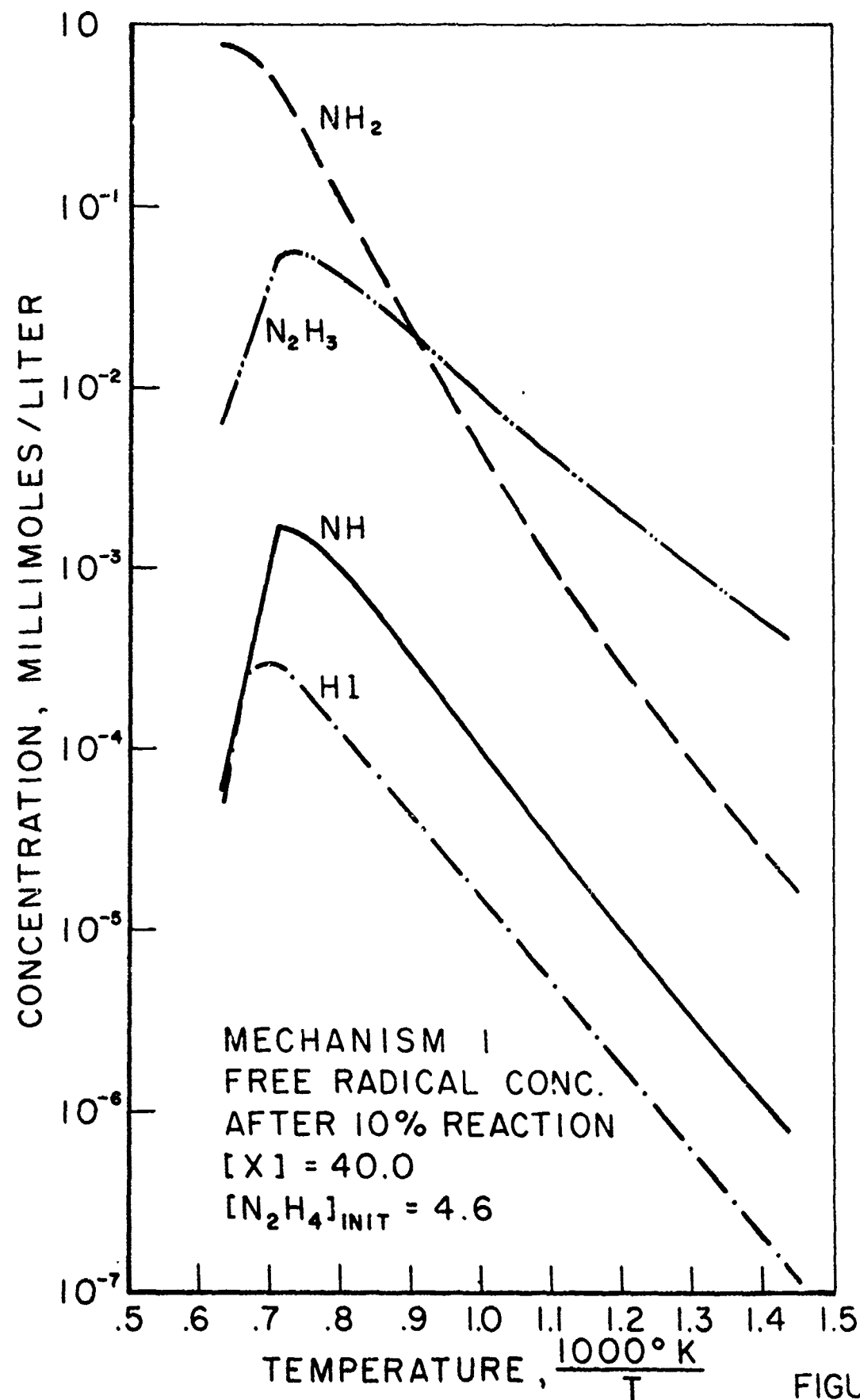


FIGURE 57

# DECOMPOSITION OF HYDRAZINE

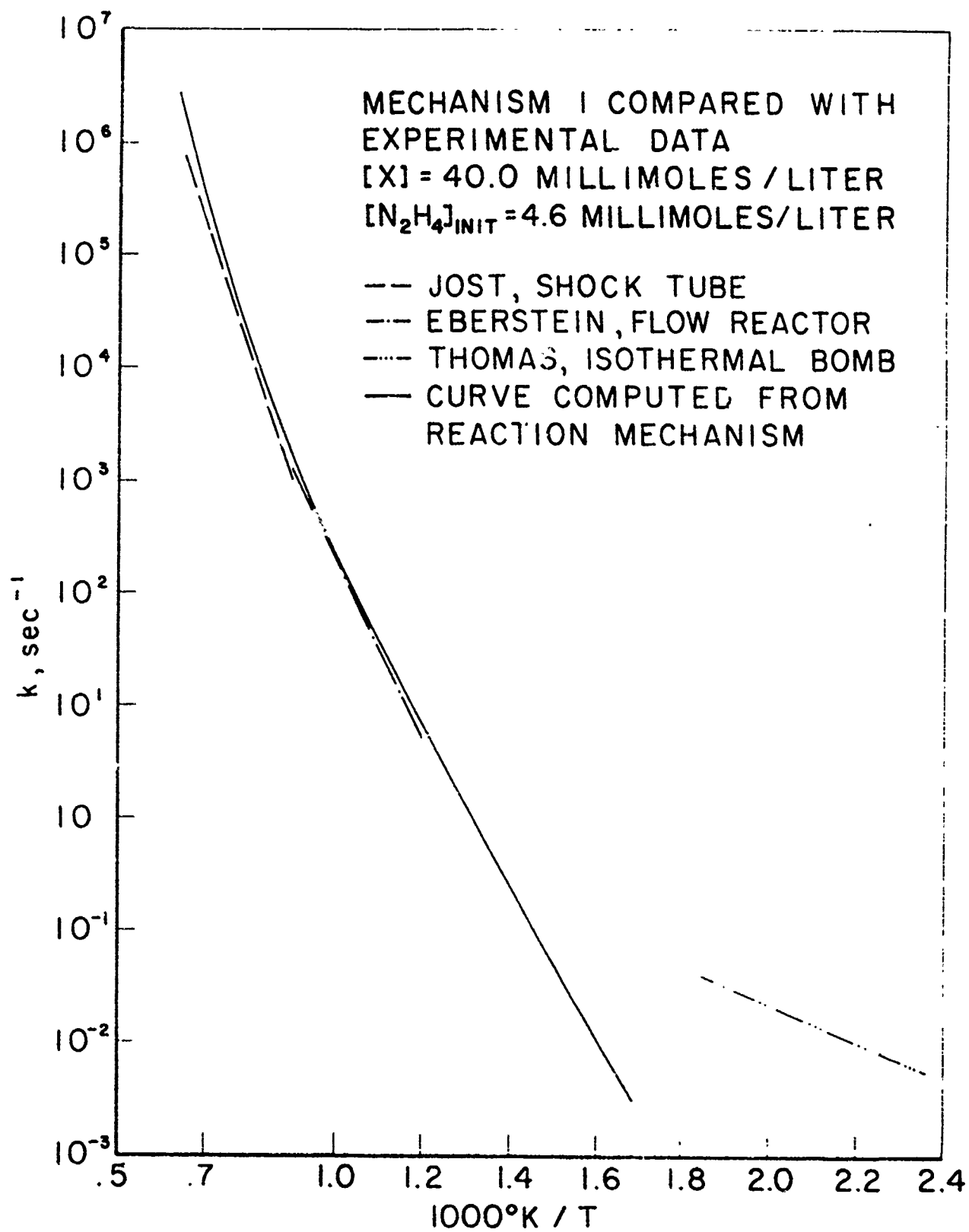


FIGURE 58

# DEPENDENCE OF OVERALL DECOMPOSITION RATE ON HYDRAZINE CONCENTRATION

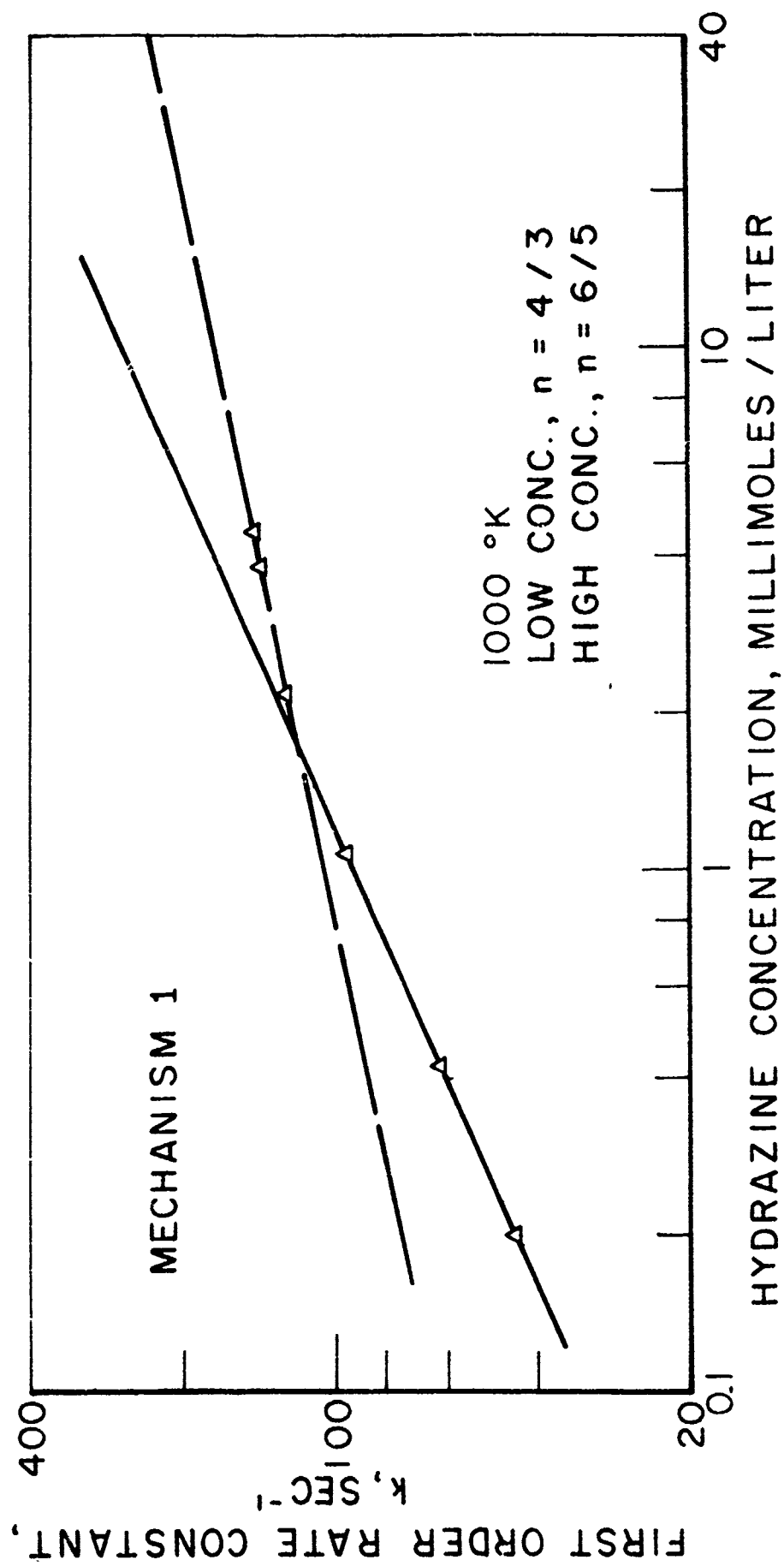


FIGURE 59

# DEPENDENCE OF HYDRAZINE DECOMPOSITION RATE ON THIRD BODY CONCENTRATION

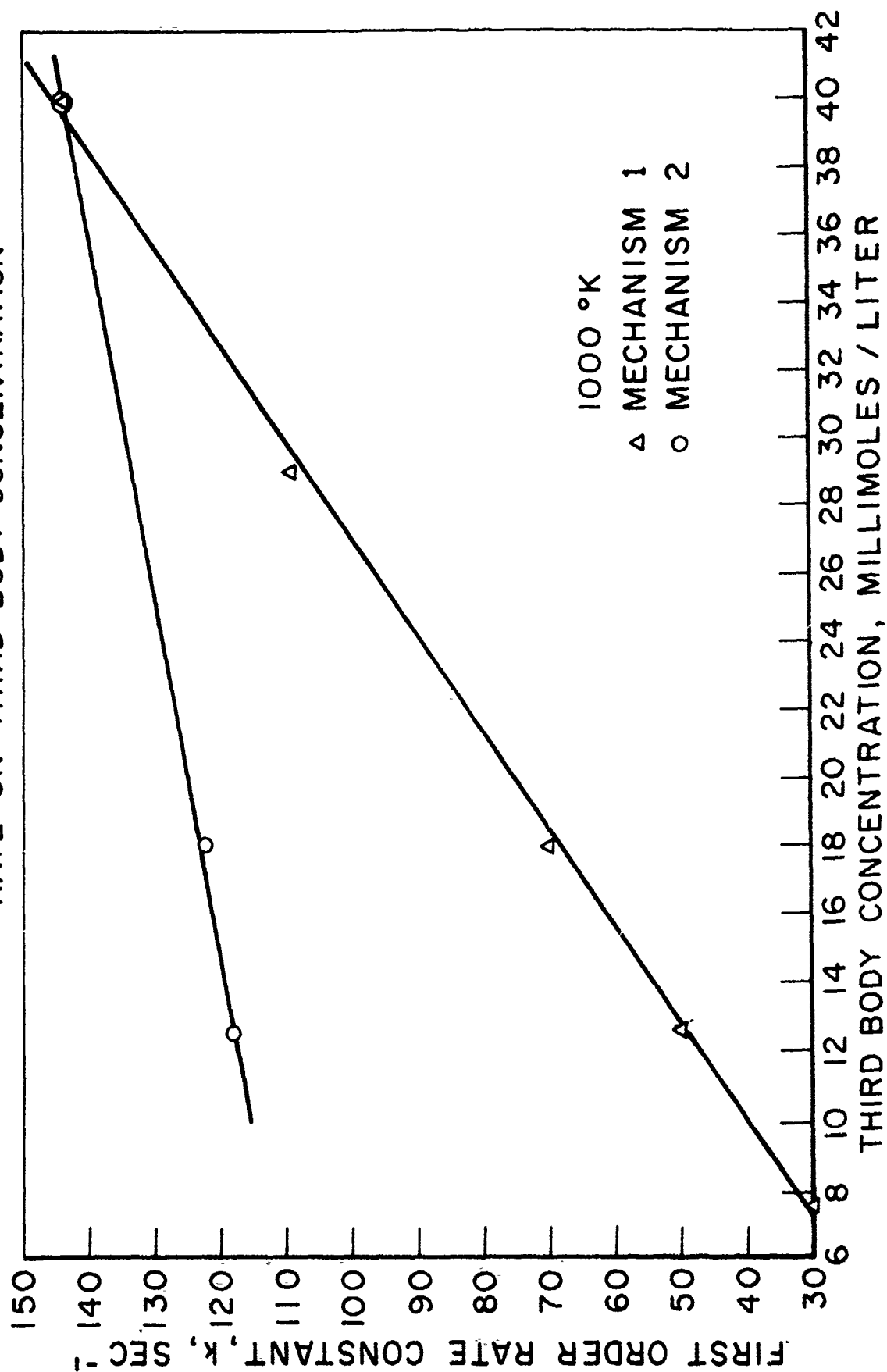


FIGURE 60

# EFFECT ON OVERALL RATE OF THE VARIATION OF INITIATION AND BRANCHING RATE CONSTANTS

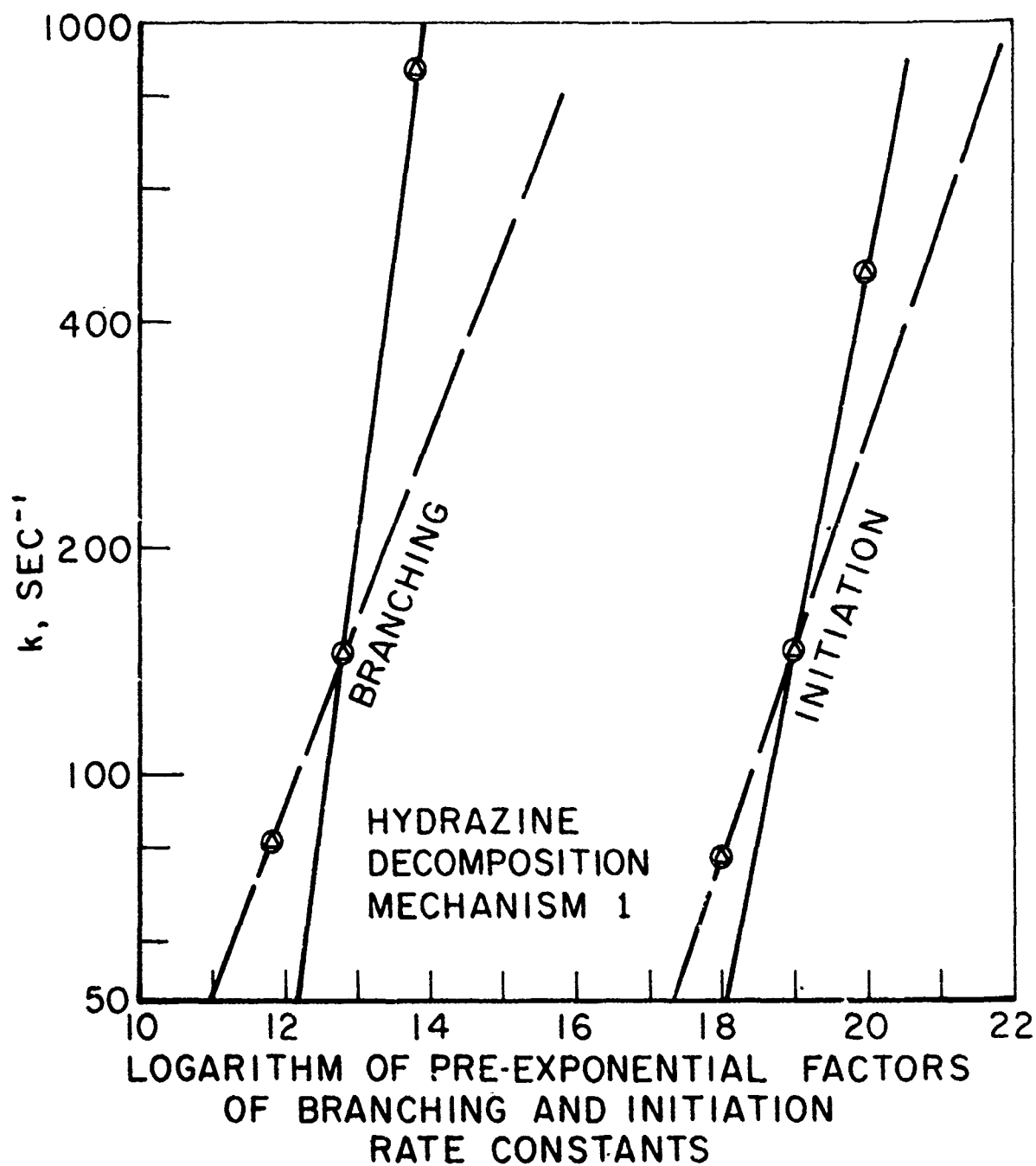


FIGURE 61

# UDMH DECOMPOSITION CALCULATIONS

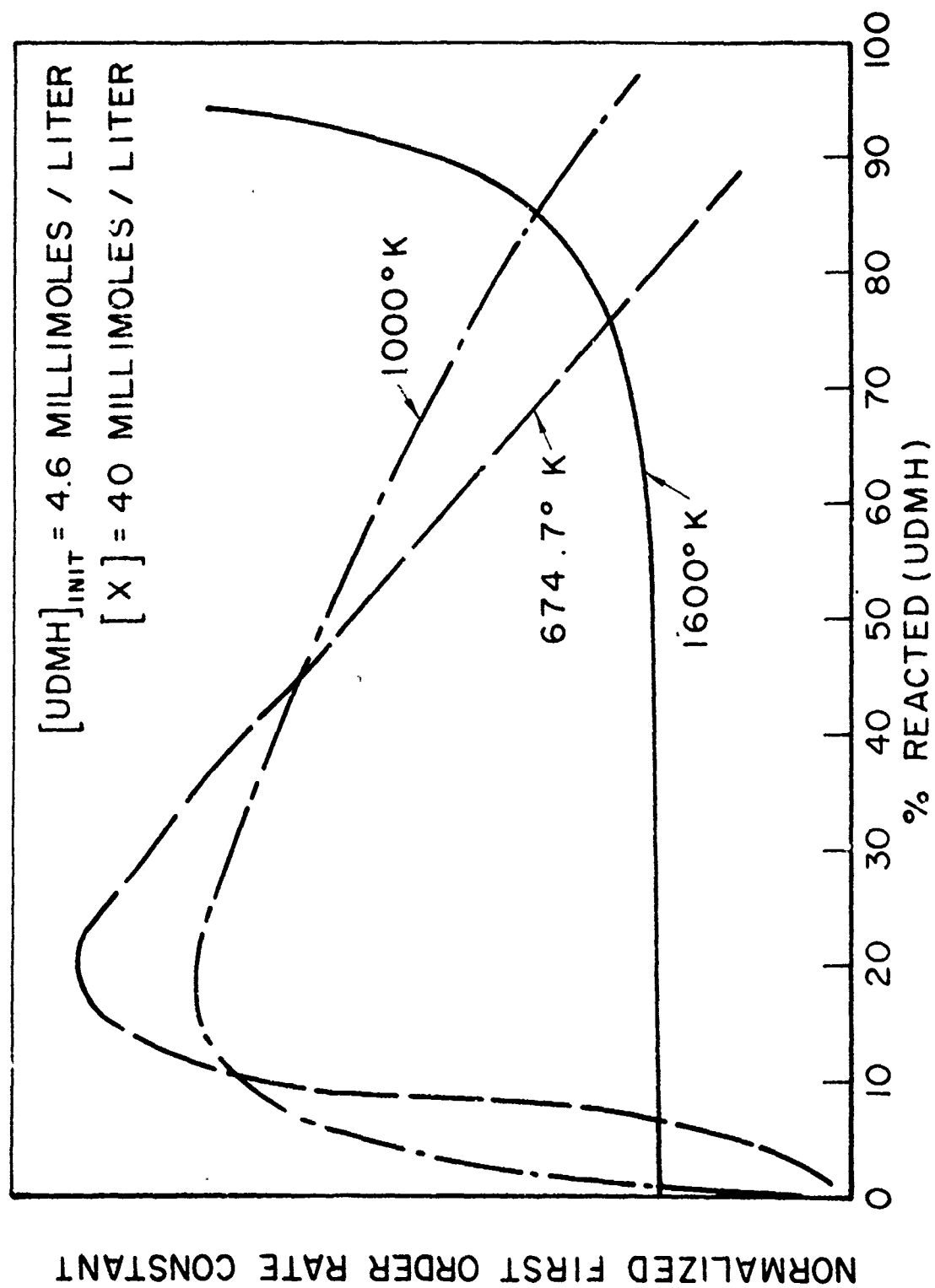


FIGURE 62

## Appendix A: Data Reduction

The data reduction was performed using an IBM 1620 electronic computer, with 8 digit accuracy.

The principle upon which the data reduction was based has been discussed in the body of the thesis and will not be repeated here.

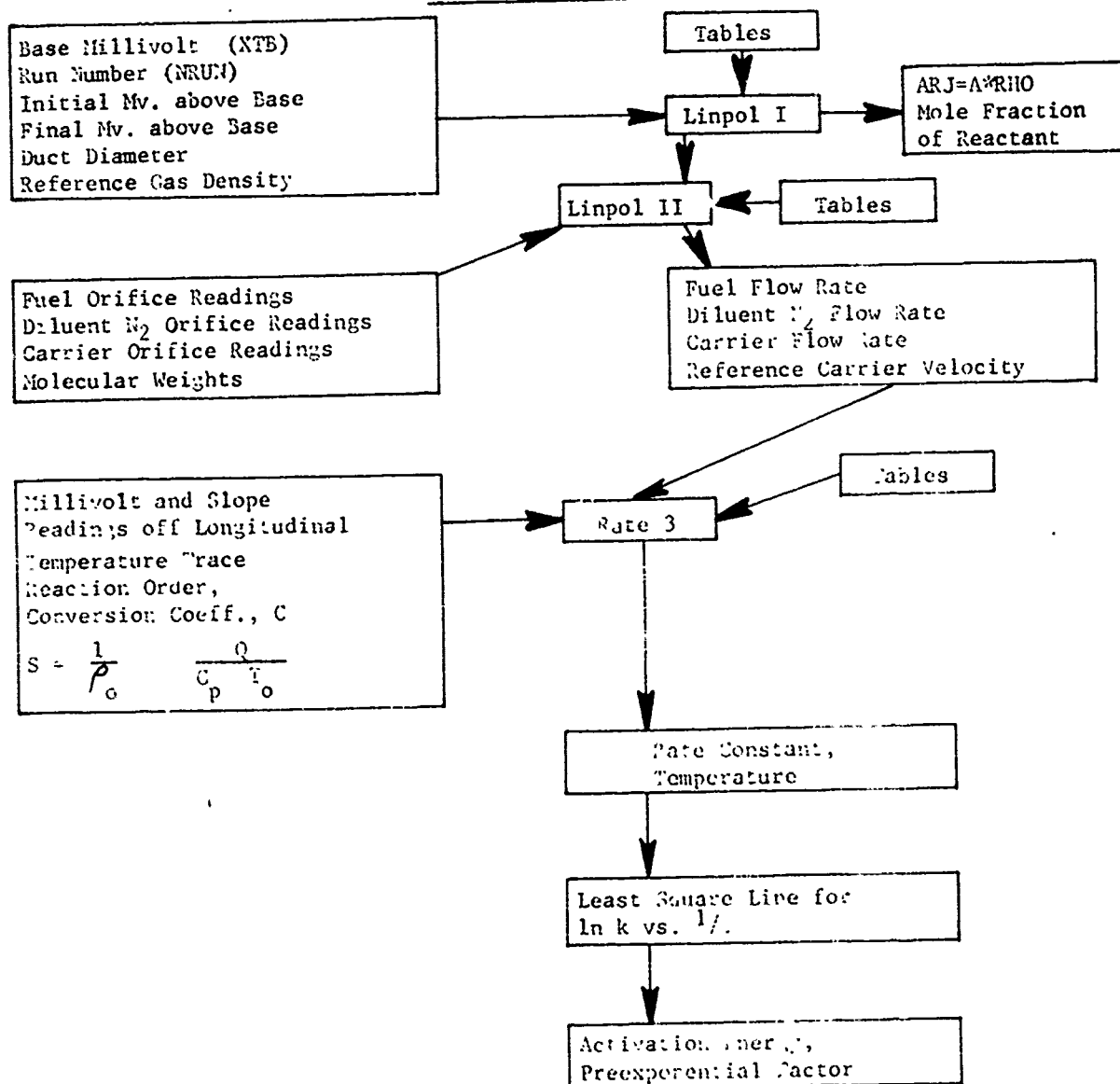
Rather, the data reduction programs actually used are outlined in chart form, and then shown as they appear in FORTRAN form.

The tables used were taken either from standard references, such as NBS or JANEF tables, or from experimentally obtained calibration curves. The calibrations will be discussed in appendix B.

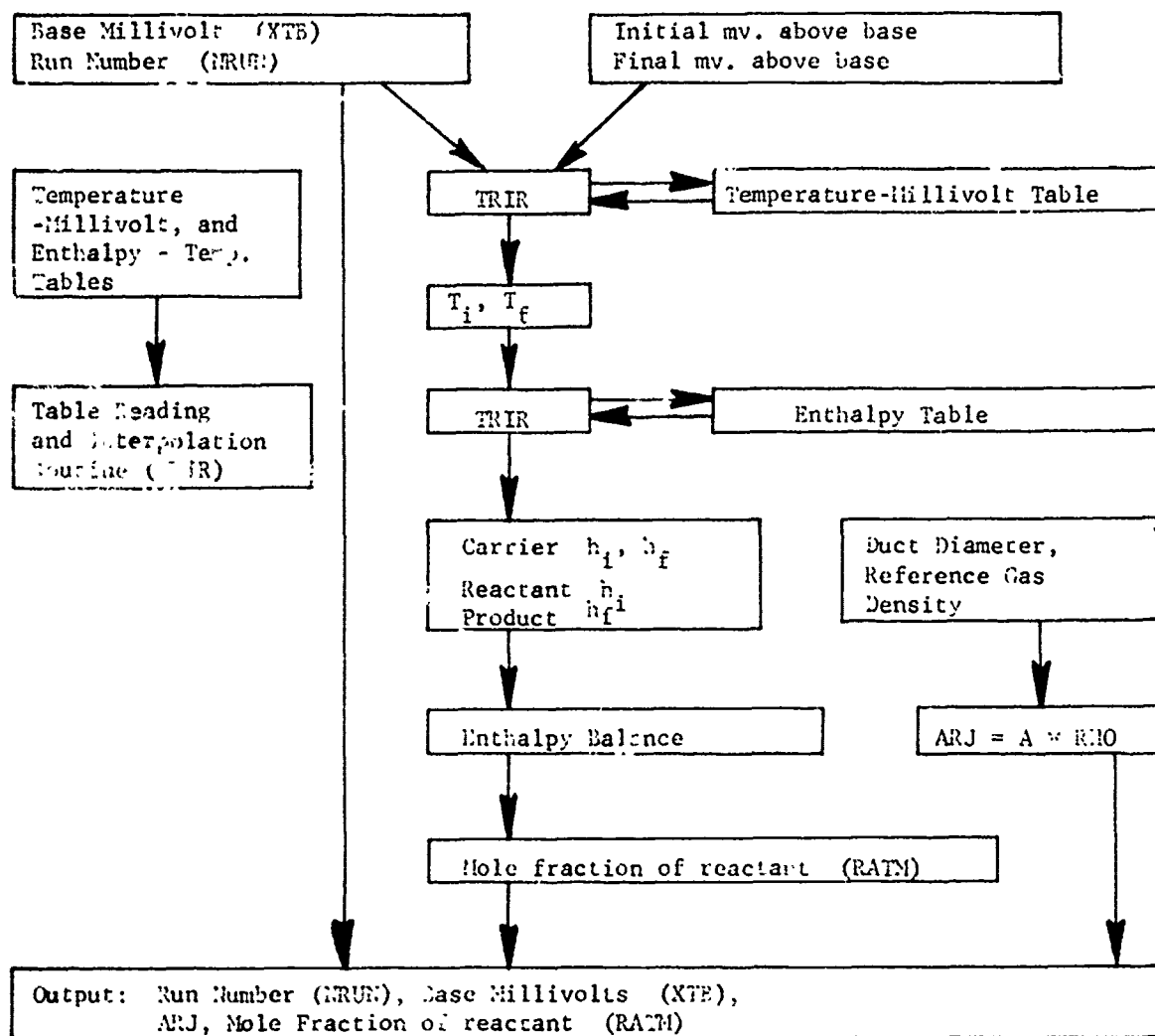
The table reading and interpolation routine (TRIR) worked as follows. The table was searched for values of the abscissa,  $X_1$ , such that  $X_1 < X < X_2$ , where  $X$  is the value of independent variable for which it was desired to find the corresponding value of dependent variable  $Y$ . A straight line was then drawn through the points  $(X_1, Y_1)$  and  $(X_2, Y_2)$ , and the equation of this line was used to determine  $Y$ .

The slope of the millivolt-distance trace for longitudinal temperature was read graphically from the Speedomax traces, using a Gerber derivimeter, then fed into the data reduction program RATE 3.

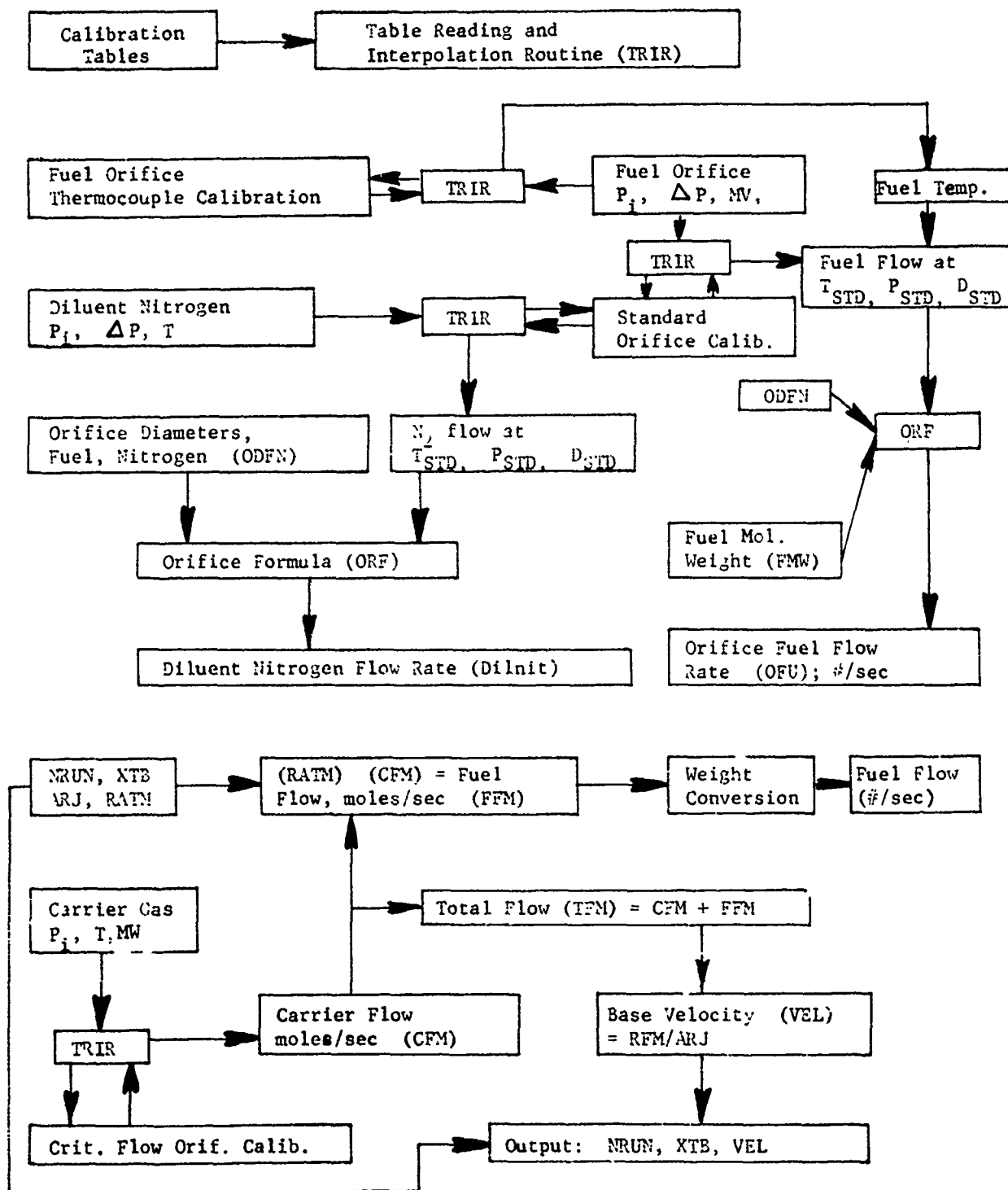
## DATA REDUCTION SEQUENCE



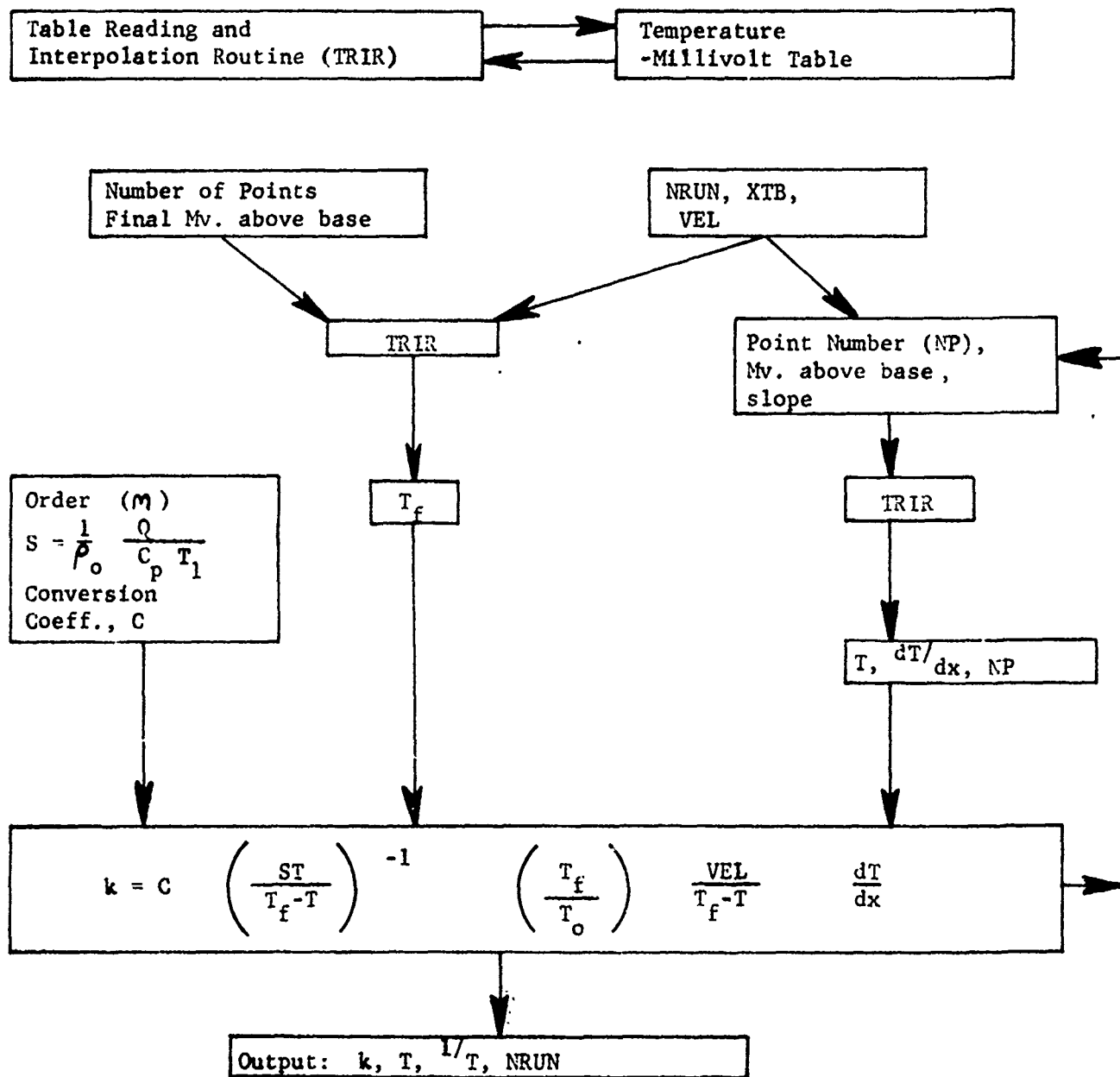
## PROGRAM LINPOL I



## PROGRAM LINPOL II



## PROGRAM RATE 3



```

C      IGOR J. EBERSTEIN
C      MODIFIED LINPOL
C      FIRST PART OF TWO PARTS
C      JUNE 1, 1962
C      DATA REDUCTION PROGRAM
C      CHEMICAL KINETICS FLOW REACTOR
      DIMENSION XT(75),YT(75)
      DIMENSION X(25),YHE(25),YHP(25),YHN(25)
      DIMENSION YPR(25),YIA(25),XIP(25),YOP(25),XTE(25),YTE(25)
      DIMENSION W(75),Z(75)
      READ,Q,ETTA
      READ,DIA,I,J
      ALPHABETIC PRINT
MODIFIED LINPOL,PART ONE, JUNE 1,1962
      ALPHABETIC PRINT
DATE OF EXPERIMENT
      ALPHABETIC PRINT
CARRIER GAS
      ALPHABETIC PRINT
FUEL
      ALPHABETIC PRINT
      DUCT DIAMETER, INCHES
      PRINT,DIA,I
      ARJ=DIA*PIAM*(3.1416/4.)
      ARJ=ARJ*RIJ
      ALPHABETIC PRINT
      Q      ARJ      ETTA
      PRINT,Q,ARJ,ETTA
      READ,HT
      ALPHABETIC PRINT
      TEMPERATURE, MILLIVOLT TABLE
      PRINT,HT
00701 DO 702 KT=1,HT
00702 READ,YT(KT),XT(KT)
00702 CONTINUE
      ALPHABETIC PRINT
ENTHALPY, TEMPERATURE TABLE
      READ,HI
      PRINT,HI
00201 DO 202 I=1,HI
00000 READ,X(I),YHE(I),YHP(I),YHN(I)
00202 CONTINUE
      PAUSE
00735 READ,XTB,HRUN
00000 PRINT,HRUN
00705 READ,JTT,XTT
00000 IF (JTT-7) 716,1001,1001
00716 XTT=XTT+XTB
00000 IKLAS=INT
00000 INT=1
00000 U=XTT
00000 DO 703 KT=1,NT
00000 IK=KT
00000 W(IK)=XT(KT)
00703 Z(IK)=YT(KT)

```

```

00000 GO TO 1709
00001 GO TO (709,710,711,712),JTT
00709 IKLAS=II
00000 INT=2
00000 U=V
00000 DO 203 I=1,II
00000 IK=I
00000 W(IK)=X(I)
00203 Z(IK)=YHE(I)
00000 GO TO 1709
00002 YHEE=V
00000 GO TO 705
00710 IKLAS=II
00000 INT=3
00000 U=V
00000 DO 303 I=1,II
00000 IK=I
00000 W(IK)=X(I)
00303 Z(IK)=YHP(I)
00000 GO TO 1709
00003 YHPP=V
00000 GO TO 705
00711 IKLAS=II
00000 INT=4
00000 U=V
00000 DO 403 I=1,II
00000 IK=I
00000 W(IK)=X(I)
00403 Z(IK)=YHN(I)
00000 GO TO 1709
00004 YHNI=V
00000 GO TO 705
00712 IKLAS=II
00000 INT=5
00000 U=V
00000 DO 404 I=1,II
00000 IK=I
00000 W(IK)=X(I)
00404 Z(IK)=YHN(I)
00000 GO TO 1709
00005 YHNL=V
YHPP=YHPP-ETTA
00000 RATIO=(YHNL-YHNI)/(C+YHEE-YHPP)
ALPHABETIC PRINT
FUEL/CARRIER RATIO
PUNCH,HRUN,LAT,ALT,PT.
PRINT,RATIO,HRUN
GO TO 735
01709 DO 1206 IK=1,IKLAS
IF(U-W(IK))1204,1207,1206
1206 CONTINUE
01204 IF (IK-1) 1210,1205,1210

```

```

1205 CONTINUE
      ALPHABETIC PRINT
TABLE READING ERROR
00000 GO TO 1001
01210 E=Z(IK)-Z(IK-1)
03000 S=W(IK)-W(IK-1)
00000 SLOPE=E/S
00000 V=SLOPE*(U-W(IK-1))+Z(IK-1)
00000 GO TO 1211
01207 V=Z(IK)
      IF(SENSE SWITCH 3)1211,1212
01211 PRINT,U,V,1 IT
1212 GO TO(1,2,3,4,5,6,7,1600),INT
1001 PAUSE
      END

```

```

C      IGOR J. EBERSTEIN
C      MODIFIED LINPOL
C      SECOND PART OF TWO PARTS
C      JUNE 1, 1962
C      DATA REDUCTION PROGRAM
C      CHEMICAL KINETICS FLAM REACTION
      DIMENSION XT(75), YT(75)
      DIMENSION X(25), YHE(25), YHF(25), YLA(25)
      DIMENSION YPR(25), YKA(25), XTP(25), YCP(25), XTE(25), YTE(25)
      DIMENSION V(75), Z(75)
      ALPHABETIC PRINT
MODIFIED LINPOL, PART TWO, JUNE 1, 1962
      READ, BETAF, BETAN
      ALPHABETIC PRINT
      BETAF      BETAN
      PRINT, BETAF, BETAN
      ALPHABETIC PRINT
      PRESSURE, FLOW RATE TABLE
      READ, RI
      PRINT, RI
00301  DO 302 I=1, RI
00000  READ, YPR(I), YKA(I)
00302  CONTINUE
      ALPHABETIC PRINT
      ORIFICE FLOW TABLE
      READ, NL
      PRINT, NL
00401  DO 402 L=1, NL
00000  READ, XTP(L), YCP(L)
00402  CONTINUE
      ALPHABETIC PRINT
      ORIFICE TEMPERATURE TABLE
      READ, RK
      PRINT, RK
      DO 502 K=1, RK
00501  READ, XTE(K), YTE(K)
00502  CONTINUE
      PAUSE
1735  READ, HRUN, RAT1, ARJ, YTL
736  READ, HRUN, XATP, XATF, XATF
      IF (HRUN-GRUP) 1301, 1302, 1301
1301  CONTINUE
      ALPHABETIC PRINT
      MISMATCHED DATA
      PAUSE
      PRINT, HRUN, HRUN
      GO TO 1735
1302  CONTINUE
      READ, KRUN, YPR, XPT, XLT, YOUNK
      IF (KRUN-HRUN) 1301, 310, 1301

```

```

310 IKLAS=NL
    INT=6
00000 U=YPRR
00000 DO 233 L=1,NL
00000 IK=L
00000 W(IK)=YPR(I)
00233 Z(IK)=YPA(I)
00000 GO TO 1709
00006 YHIF=V
00000 DM=510./ (XPT+460.)
00000 DM=(XHP/28.966)*DM
    YICA=YHIF*SQR(DM)
    ALPHABETIC PRINT
    CARRIER FLOW,LBS/SEC.
    PRINT,YICA
    INT=9
    IKLAS=NL
    DO 1243 L=1,NL
    IK=L
    W(IK)=XDP(L)
    Z(IK)=YDP(L)
1243 CONTINUE
    U=SQR(XHIF)
    GO TO 1709
1600 YHIF=V
    BU=530./ (460.+XHIF)
    DU=BU*(XHP+14.7)/24.7
    DUM=SQR(DU)
    YHIF=DUM*YHIF*BETA
    YHIF=YHIF*1.E-13
    ALPHABETIC PRINT
    NITROGEN FLOW,LBS./SEC.
    PRINT,YHIF
00000 YHIC=YICA*YHIF
    YICA=YICA+YHIF
    YIT=YICA+YHIF
    GO 310 VEL=(YICA+YHIF)/ANG
00000 PUNCH,IRUN,XTL,VEL
    ALPHABETIC PRINT
    IRUN, FUEL FLOW,LBS/SEC
00000 REAT,XPE,XXDP,YOM,YTE
    YEL=YHIF*(YOM/XAL)
    PRINT,IRUN,YHIF
    ALPHABETIC PRINT
    TOTAL GAS FLOW,LBS./SEC. REFERRED TO CARRIER FLOW
    PRINT,YIT
    ALPHABETIC PRINT
    VELOCITY,INCHES/SEC.
    PRINT,VEL
00000 INT=7
00000 IKLAS=NL
00000 DO 243 L=1,NL
00000 IK=L
00000 W(IK)=XDP(L)
00243 Z(IK)=YDP(L)

```

```

      U=SQR(XXCP)
00003 GO TO 1709
00007 YDPP=V
      INT=8
      IKLAS=NK
      DO 253 K=1,NK
      IK=K
      V(IK)=XTE(K)
      Z(IK)=YTE(K)
253 CONTINUE
00000 U=XTEE
00000 GO TO 1709
      8 TEF=V
      ALPHABETIC PRINT
      FUEL TEMPERATURE, DEG. CENT.
      PRINT, TEF
      VOT=304.4/(V+273.1)
00000 VOP=(XPE+14.7)/24.7
00000 VMW=YDW/28.5
00000 VOOU=VOT*VOP*VMW
00000 YOGH=SQR(VOOU)
00000 YDEP=YDPP*YOGH
      YDEP=YDEP*BETAF
      YDEP=YDEP*1.0E-03
      ALPHABETIC PRINT
      ORIFICE FUEL FLOW, LBS/SEC
      PRINT, YDEP
      PRINT, NRUN
      ALPHABETIC PRINT
      ANALYSIS OF RUN COMPLETED
      GO TO 1735
01709 DO 1206 IK=1,IKLAS
      IF(U-W(IK))1204,1207,1206
1206 CONTINUE
01204 IF (IK-1) 1210,1205,1210
1205 CONTINUE
      ALPHABETIC PRINT
      TABLE READING ERROR
00000 GO TO 1001
01210 E=Z(IK)-Z(IK-1)
00000 S=W(IK)-W(IK-1)
00000 SLOPE=E/S
00000 V=SLOPE*(U-W(IK-1))+Z(IK-1)
00000 GO TO 1211
01207 V=Z(IK)
      IF(SENSE SWITCH 3)1211,1212
01211 PRINT,U,V,INT
1212 GO TO(1,2,3,4,5,6,7,8,1600),INT
1001 PAUSE
      END

```

```

C   PROGRAM RATE3
C   IGOR J. EDERSTEIN
C   OCTOBER 24, 1962
C   RATE CONSTANTS OF ORDER N
      DIMENSION ZOO(25), S2(25)
      DIMENSION XTT(25), YTT(25), YT(75), XT(75)
      DIMENSION IX(20), YIX(20), YIV(20)
      DIMENSION ZIP(20), ZAK(20), ZT(20), TOT(20)
      DIMENSION T(21), SLO(20), YIEL(20)
      ALPHABETIC PRINT
IGOR EDERSTEIN, PROGRAM RATE3
      READ, ORDER, S3
      OR=ORDER-1.
      ALPHABETIC PRINT
ORDER, S3
      PRINT, ORDER, S3.
      READ, COEF1
      ALPHABETIC PRINT
COEF1
      DO 102 KT=1, NT
102   READ, YT(KT), XT(KT)
600   READ, NRUN, XTD, VEL
      READ, NRUN, Y, YIF
      IF (NRUN-NRUN) 313, 310, 313
313   CONTINUE
      ALPHABETIC PRINT
      MISMATCHED DATA
      PAUSE
      GO TO 600
310   JTT=1
      XTT(1Y)=Y IF+XTL+1. + 1
      = Y
      GO TO 106
1   TF=YTT(1)+273.1
      PRINT, TF, NRUN
      JTT=2
      DO 302 I=1, NY
      READ, YIV(I), IX(I), SLO(I)
      YIX(I)=IX(I)
      XTT(I)=YIV(I)+XTD
106 DO 126 KT=1, NT

```

```

      IF(XTT(I)-XT(KT))124,127,126
126 CONTINUE
124 IF(KT-1)121,125,121
125 CONTINUE
      ALPHABETIC PRINT
TABLE READING ERROR
      PAUSE
      GO TO 600
121 E=YT(KT)-YT(KT-1)
      S=XT(KT)-XT(KT-1)
      SLOPE=E/S
      YTT(M)=SLOPE*(XTT(I)-XT(KT-1))+YT(KT-1)
      GO TO(1,2),JTT
2 GO TO 301
127 YTT(I)=YT(KT)
      T(I)=YTT(I)+273.1
      ALPHABETIC PRINT
EXACT MV.-TEMP. CORRESPONDENCE
      PRINT,Y X(I),T(I)
      GO TO 303
301 T(I)=YTT(I)+273.1
      YDEL(I)=SLOPE
      XAPPA=COEF1*VEL*(TF/1000.,I)
      ZIP(M)=XAPPA*YDEL(I)*SLO(I)*(1./(TF-T(I)))
      OT(I)=1./T(I)
      ZOO(M)=S3*T(I)/(TF-T(I))
      S2(I)=(ZOO(I))**OR
      ZIP(M)=S2(I)*ZIP(I)
      IF(SENSE SWITCH 1)610,620
610 PRINT,OT(I),ZIP(I),S2(I)
620 PUNCH,NRUN,T(I),ZIP(I)
303 CONTINUE
302 CONTINUE
      GO TO 600
1111 END
      PRINT,COEF1
      READ,NT

```

```

C      IGOR J. EBERSTEIN
C      JUNE 11, 1962
C      LEAST SQUARE LINE FOR
C      CHEMICAL KINETICS DATA
C      PART ONE OF TWO PARTS
      DIMENSION X(450), Y(450)
      READ, XK1, XK2, XK3
      READ, NRUN, TI, ZIPI
      N=1
      T=TI
      ZIP=ZIPI
      GO TO 11
10     READ, NRUN
      IF (NRUN) 12, 12, 14
14     READ, T, ZIP
11     X(N)=1./T
      Y(N)=XK1*LOGF(ZIP)
      N=N+1
      GO TO 10
12     NRUNL=-NRUN
      NFIN=N-1
      XN=NFIN
      SUMXY=0.0
      SUMX=0.0
      SUMY=0.0
      SUMX2=0.0
      SUMY2=0.0
      DO 21 N=1, NFIN
      SUMXY=SUMXY+X(N)*Y(N)
      SUMX=SUMX+Y(N)
      SUMY=SUMY+Y(N)
      SUMX2=SUMX2+X(N)*X(N)
      SUMY2=SUMY2+Y(N)*Y(N)
21     CONTINUE
      PUNCH, XK1, XK2, XK3
      PUNCH, NRUN, NRUNL, XN
      PUNCH, SUMXY, SUMX, SUMY
      PUNCH, SUMX2, SUMY2
      ALPHABETIC PRINT
      PROCEED TO LEESQ, PART TWO
      CONTINUE
      STOP
      END

```

```

C      IGOR EBERSTEIN
C      LEAST SQUARE LINE FOR CHEM.KINET. PART TWO
      READ,XK1,XK2,XK3
      READ,NRUN1,NRUNL,XN
      READ,SUMXY,SUMX,SUMY
      READ,SUMX2,SUMY2
      ALPHABETIC PRINT
CHEMICAL KINETICS DATA LEAST SQUARE LINE
      ALPHABETIC PRINT
DUCT DIAMETER, INCHES
      ALPHABETIC PRINT
CARRIER GAS
      ALPHABETIC PRINT
FUEL
      ALPHABETIC PRINT
ADDITIVE
      ALPHABETIC PRINT
RUN SERIES
      PRINT,NRUN1,NRUNL
      SUM1=XN*SUMXY-SUMX*SUMY
      SUM2=XN*SUMX2-SUMX*SUMX
      SLOPE=SUM1/SUM2
      ACTE=1.99*SLOPE
      ALPHABETIC PRINT
ACTIVATION ENERGY, CALORIES PER GRAM-MOLE
      PRINT,ACTE
      SUM3=SUMXY-(SUMX*SUMY)/XN
      SUM4=SUMX2-(SUMX*SUMX)/XN
      SUM5=SUM3*SUM3/SUM4
      SUM6=SUMY2-(SUMY*SUMY)/XN-SUM5
      S2=SUM6/(XN-2.0)
      XAV=SUMX/XN
      YAV=SUMY/XN
      SUM7=SUMX2-XN*XAV*XAV
      VASLO=S2/SUM7
      SDSLO=SQR(VASLO)
      SDEN=1.99*SDSLO
      ALPHABETIC PRINT
STANDARD DEVIATION OF ACTIVATION ENERGY
      ALPHABETIC PRINT
CALORIES PER GRAM-MOLE
      PRINT,SDEN
      A=YAV-SLOPE*XAV
      SUM18=XN*SUMX2-SUMX*SUMX
      SUM19=SUMX2/SUM18
      SA2=S2*SUM19
      SA=SQR(SA2)

```

```

      PREEX=EXP(A)
      ALPHABETIC PRINT
PRE EXPONENTIAL FACTOR
      PRINT,PREEX
      SAA=SA/XK2
      ALPHABETIC PRINT
STANDARD DEVIATION OF EXPONENT
      ALPHABETIC PRINT
OF PREEXPONENTIAL FACTOR
      PRINT,SAA
      ALPHABETIC PRINT
MAIN ANALYSIS COMPLETE
      ALPHABETIC PRINT
AUXILIARY INFORMATION FOLLOWS
      ALPHABETIC PRINT
SUMX          SUMY          SUMXY
      PRINT,SUMX,SUMY,SUMXY
      ALPHABETIC PRINT
SUMX2          SUMY2          XAV          YAV
      PRINT,SUMX2,SUMY2,XAV,YAV
      ALPHABETIC PRINT
ANALYSIS COMPLETE
      CONTINUE
      STOP
      END

```

```

C      PROGRAM SEAV, IGOR J. EBERSTEIN
      ALPHABETIC PRINT
IGOR J. EBERSTEIN, PROGRAM SEAV
      DIMENSION X(450),Y(450),Z(50),W(50)
100 J=1
8 READ,NDIV,OR
10 READ,NRUN
  IF(NRUN)12,12,14
14 READ,T,RATE
  X(J)=1./T
  Y(J)=LOGF(RATE)
  J=J+1
  GO TO 10
12 N=J-1
  XN=N
  XMAX=X(1)
  XMIN=X(1)
  DO 20 J=1,N
    IF(XMAX-X(J))212,213,213
212 XMAX=X(J)
213 IF(X(J)-XMIN)214,215,215
214 XMIN=X(J)
215 CONTINUE
20 CONTINUE
  DEX=XMAX-XMIN
  ADIV=NDIV
  DX=DEX/ADIV
  XAX=XMIN
  DO 301 K=1,NDIV
    XII=XAX
    XAX=XAX+DX
    IF(SENSE SWITCH 1)601,602
601 PRINT,XAX,XII
602 I=1
    SUMZ=0.0
    SUMW=0.0
    DO 302 J=1,N
      IF(XAX-X(J))303,304,304
304 IF(X(J)-XMIN)303,305,305
305 Z(I)=X(J)
      W(I)=Y(J)
      SUMZ=SUMZ+Z(I)
      SUMW=SUMW+W(I)
      I=I+1
303 CONTINUE
302 CONTINUE
    IF(I-1)701,701,702
701 I=2
702 XI=I-1
    XI=I-1
    NI=I-1
    ZAV=SUMZ/XI
    WAV=SUMW/XI
    VAR=0.0
    DO 402 I=1,NI
402 VAR=VAR+(W(I)-WAV)*(W(I)-WAV)
    VAR=VAR/XI
    STD=SQRF(VAR)
    TAV=1./ZAV
    RAV=EXPF(WAV)

```

A-18

301 PRINT,ZAV,RAV,WAV,STD  
PUNCH,K,TAV,RAV  
PAUSE  
GO TO 100  
END

## Appendix B: Calibrations

All essential pressure gauges, thermocouples, and orifices were calibrated.

### Pressure Gauges

The pressure gauges were calibrated using a dead weight tester, and were found to be accurate to  $\pm 1$  psi.

### Orifice Thermocouples

The orifice thermocouples were calibrated against a standard mercury thermometer. All these thermocouples were calibrated in the system. The thermocouple temperatures for the critical flow, and diluent nitrogen orifices were read in degrees Fahrenheit from a direct reading (West) meter. In the temperature range of interest, i.e. 20 deg. F to 100 deg. F, the error was generally found to be less than 5 deg. F.

The output from the fuel flow orifice thermocouple was fed to a millivoltmeter. A calibration curve of temperature vs. millivolts was obtained, and was used directly in the data reduction program.

### Probe Thermocouples

The Pt/Pt-Rh probe thermocouples were calibrated against a secondary standard Pt/Pt-Rh thermocouple supplied by the Leeds and Northrup Company. The error of this secondary standard is guaranteed by Leeds and Northrup to be less than 0.75 deg. C. The temperature range of the calibration was 600 degrees Kelvin to 1200 deg. K. Below 1000 deg. K. the error was found to be generally less than 2 deg. K. At temperatures above 1100 deg. K errors as high as 5 deg. K were observed.

These calibrations were carried out in an electric furnace. The thermocouple to be calibrated was placed in contact with the standard in the furnace, and the open space around the thermocouples was packed with

quartz wool to prevent the readings from being disturbed by stray air currents. Care was taken to establish a steady state before any readings were made. A Leeds and Northrup standard potentiometer was used to measure the thermocouple potentials.

### Orifices

The critical flow orifice was calibrated using a calibration set up designed by Pelmas\* specifically for the calibration of critical flow orifices. Essentially, a class 1-A cylinder was connected to a heat exchanger and pressure regulator, which in turn was connected to the orifice to be calibrated. The change of weight of the gas cylinder, as it was emptied, was measured. The scale was calibrated using standard weights. Air was used in the calibration, and it was necessary to correct for the molecular weight difference when the orifice was used to meter nitrogen rather than air.

The fuel flow orifice was calibrated as follows. Water was vaporized in the fuel vaporizer, then passed through the jacketed line and the orifice. Downstream of the orifice the water was passed through a cooling coil and condensed.

The diluent nitrogen orifice was not calibrated directly. The flow through this orifice (0.097 inch diam.) was calculated by using a calibration curve for a smaller orifice. A 0.033 inch diameter orifice had been calibrated with nitrogen and ethylene using a wet test meter. Both calibrations showed good conformity with behavior predicted by standard orifice formulas for an ideal gas. A similar calculation for the fuel flow orifice (0.075 inch diameter) showed good agreement with flow rates obtained using the water calibration described above.

---

\* Pelmas, R., Glassman, I., and Webb, M., An Experimental Investigation of Longitudinal Combustion Instability in a Rocket Motor using Premixed Gaseous Propellants. Aero. Eng'g. Lab. Report No. 589. Princeton University, Princeton, New Jersey, December 1961, p. 10.

APPENDIX C - Error Analyses

The first order rate constant,  $k$ , is given by the formula

$$k = \frac{T_f}{T_0} \frac{cV_0}{T_f - T} \frac{dT}{dX}$$

Let  $\delta y$  signify the fractional change in  $y$ , i.e.  $\delta y = \frac{\Delta y}{y}$

Then

$$k(1 + \delta k) = \left(1 + \delta\left(\frac{T_f}{T_0}\right)\right) \frac{T_f}{T_0} \frac{cV_0(1 + \delta V_0)}{(T_f - T)(1 + \delta(T_f - T))} (1 + \delta m) \frac{dT}{dX}$$

where

$$\delta m = \delta\left(\frac{dT}{dX}\right)$$

To estimate the fractional error in the rate constant, it is necessary to estimate the fractional errors in  $V_0$ ,  $\frac{T_f}{T_0}$ ,  $T_f - T$ ,  $\frac{dT}{dX}$

$$V_0 = \frac{\dot{n}}{\rho_n A}$$

where  $\dot{n}$  is the molar flow rate,  $\rho_n$  is the molar concentration, and  $A$  is the cross-sectional area of the duct.

$$\dot{n} = \dot{n}(\text{carrier}) + \dot{n}(\text{diluent nitrogen}) + \dot{n}(\text{fuel})$$

or

$$\dot{n} = \dot{n}_c + \dot{n}_N + \dot{n}_F$$

$$\frac{\dot{n}_F}{\dot{n}_c} \approx 0.02 ; \quad \frac{\dot{n}_N}{\dot{n}_c} \approx 0.02$$

Thus, it is seen that even large errors in the flow rates of fuel and diluent nitrogen will have very little effect on the flow velocity of gas in the reactor. This is why no attempt was made to calculate the effect on the gas velocity of the change in the number of moles of reactant as it becomes product.

Such effect is clearly of little significance under the above experimental conditions.

The flow rate through a critical orifice is given by:

$$\dot{m} = \frac{f(\gamma) P^0}{\sqrt{\gamma R T^0}}$$

$$\dot{m} (1 + \delta \dot{m}) = \frac{f(\gamma) P^0 (1 + \delta P^0)}{\sqrt{\gamma R T^0} \sqrt{1 + \delta T^0}}$$

The pressure gauge is accurate to  $\pm 1$  psi. Furthermore, fluctuations of  $\pm 2$  psi in the carrier pressure do occur. Normal carrier pressure is 200 psi. Thus,  $\delta P^0 \sim 1.5\%$ :  $1.015 \geq 1 + \delta P^0 \geq 0.985$ . The temperature error is less than  $50^\circ \text{F}$ . Normal operating temperature is  $40^\circ \text{F} = 500^\circ \text{K}$ . Thus  $\delta T^0 = 1\%$  and  $1.01 \geq 1 + \delta T^0 \geq 0.99$ . It follows that:

$$\frac{1.015}{0.99} \geq 1 + \delta \dot{m} \geq \frac{0.985}{1.01}$$

$$1.02 \geq 1 + \delta \dot{m} \geq 0.98$$

Thus the expected error in  $\dot{m}$  is approximately 2%, making the error in  $V_0$  approximately 2%.

It appears from the above that if major experimental error exists, then such error must be sought in the temperatures.

The following errors are estimated:

- (1) Thermocouple calibration error ( $2^\circ \text{K}$ )
- (2) Error due to difference between stagnation and static temperatures of the gas ( $0.5^\circ \text{K}$ ).
- (3) Thermocouple radiation error ( $5^\circ \text{K}$  at  $1000^\circ \text{K}$ ,  $0.5^\circ \text{K}$  at  $800^\circ \text{K}$ ).
- (4) Error in  $\frac{dT}{dX}$  due to heat transfer with reactor wall.

(5) Errors due to fuel fluctuations.

Consider the approximate formula  $\delta\left(\frac{T_f}{T}\right) \sim 0.5\%$  and may be neglected)

$$1 + \delta k \approx \frac{1 + \delta\left(\frac{dT}{dX}\right)}{1 + \delta(T_f - T)} = \left[1 + \delta\left(\frac{dT}{dX}\right)\right] \left[1 - \delta(T_f - T) + \delta^2(T_f - T)\right]$$

and

$$\delta k = \delta\left(\frac{dT}{dX}\right) - \delta(T_f - T) + \delta^2(T_f - T)$$

The thermocouple calibration errors and the radiation errors will not affect the above formula. The variation in thermocouple error with temperature is so slow that it will not affect  $\frac{dT}{dX}$  or  $(T_f - T)$ , since the error will be constant and will subtract out. Since the probe sees an integrated radiation from the whole duct, the radiation error will be approximately constant near the end of the reaction zone. Near the beginning of the reaction zone the radiation error will be less, and there will be an effect on  $T_f - T$ . However,  $T_f - T$  is large in this section, and  $\delta(T_f - T) = \frac{\Delta(T_f - T)}{T_f - T}$  will be small.

The highest temperature at which data points are taken is such that  $T_f - T$  is greater than  $10^\circ\text{K}$ . In this region the wall temperature is approximately  $50^\circ\text{K}$  lower than the gas temperature and the following error estimates are made

$$\frac{dT}{dX} \approx -0.15$$

$$(T_f - T) \approx -0.33$$

It follows that

$$\delta k = \delta\left(\frac{dT}{dX}\right) - \delta(T_f - T) + \delta^2(T_f - T) = 27\%$$

or, the error in the rate constant,  $k$  is 27%.

However, there is also an error in the temperature at which this rate constant is measured.

$$\delta T = \delta(\text{radiation}) + \delta(\text{calibration})$$

at  $T = 1000^\circ$

$$\delta T = -\frac{5}{1000} - \frac{2}{1000} = -0.7\%$$

$$d\left(\frac{1}{T}\right) = -\frac{1}{T^2} dT$$

$$\delta\left(\frac{1}{T}\right) = d\left(\frac{1}{T}\right)/\frac{1}{T} = -\frac{dT}{T}$$

$$\delta(T) = \frac{dT}{T} = -\delta\left(\frac{1}{T}\right)$$

The temperature error may be considered as an effective rate constant error, since the rate is assumed to be at a wrong temperature. Writing:

$$k = A e^{-E/RT}$$

$$\delta k = -\frac{E}{R} \left( \delta\left(\frac{1}{T}\right) \right) = -\frac{E}{RT} \delta\left(\frac{1}{T}\right)$$

taking  $E = 40$  cal/mole

$R = 2$  cal/mole

$T = 1000^\circ\text{K}$

$$\delta k = -20 \delta\left(\frac{1}{T}\right)$$

$$\delta\left(\frac{1}{T}\right) = -0.7\%$$

$$\delta k = 14\%$$

Thus the total percent error in the rate constant due to errors in temperature measurement is approximately 40%.

To this must be added a 5% error in reading slopes, and an error introduced by fuel flow fluctuations. The error due to fuel flow fluctuations

C-5

can be as high as 20%-30%, but may often be limited to much lower values.

The error actually observed was approximately 50%. It is seen that this error may be accounted for by experimental inaccuracies.

#### Appendix D: Computations

The numerical integrations of the systems of differential equations describing the suggested reaction mechanisms were integrated on an IBM 7090 electronic computer using the standard eight digit accuracy.

The method of integration used was a modification of Milne's Method adapted for computer use. This method is described by Hamming (1) and Peskin (2).

The error in this method is proportional to the fifth power of the integration interval times the fifth derivative of the dependent variable, making the method exact for the integration of functions whose sixth derivative is zero.

The relative value of the error is used as a control on the computation, and the size of the integration interval is adjusted to always have a pre-set error. Normally the desired accuracy was specified to be seven significant figures, though in a few cases a lower accuracy limit was used.

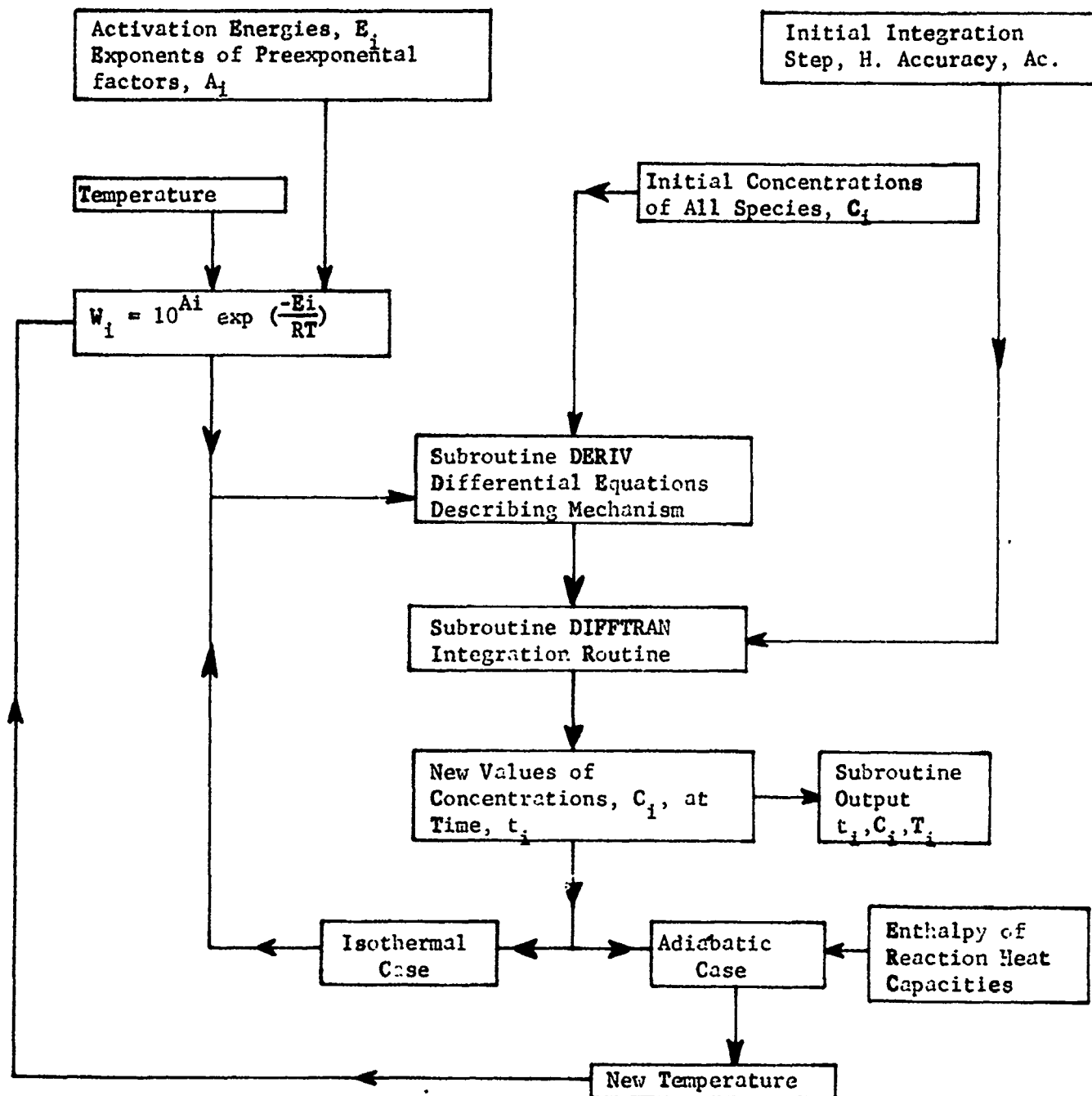
The main defect of the Milne method is a tendency toward instability (1), especially for negative values of the derivatives or for integration in the negative direction for the independent variable. However, the sets of equations treated did not appear to be unstable. The preset accuracy was maintained throughout the computation. Integration backward in time reproduced the forward integration as exactly as could be determined, and the predictions of the Milne integration compared very favorably with integrations of the same set of equations using the Runge-Kutta method.

Thus it seems reasonable to assume that the accuracy of the computations is sufficient to warrant their use in the discussion of the reaction mechanisms.

The same type program was used to study the different mechanisms. An outline of the program and a reproduction of the complete FORTRAN program are presented in what follows.

References

- (1) Hamming, R. W. Stable Predictor-Corrector Methods for Ordinary Differential Equations. Jour. ACM, Vol. 6, No. 1, Jan 1959, p. 37.
- (2) Peskin, J. R. and Rabinowitz, I. N. DIFTRAN I and II. 650 Package Subroutines for the Solution of Systems of First Order Ordinary Differential Equations. Tech. Memo. 154. Plasma Physics Lab. Princeton University, Princeton, New Jersey May 6, 1962.

MECHANISM INTEGRATION PROGRAM

```

C      PROGRAM HYZE1C
C      MODIFIED DECOMPOSITION MECHANISM, JUNE 8, 1963
      DIMENSION Y(5,15), YP(5,15), YOUT(15), YPOUT(15)
      DIMENSION DUMMY(12)
      COMMON DUMMY, W1, W2, W3, W4, W5, W6, W7, W8, W9, W10, W11
      DIMENSION C(50)
      DIMENSION E(25), A(25), W(25)
      COMMON E, A, W, KAPPA, K, H, TAU, K1, K2, K3, NJ, X, T, YYY, JTT, NCC, NNC
      COMMON C, Q, CP
      WRITE OUTPUT TAPE 6, 599
599    FORMAT (31H1IGOR EBERSTEIN, PROGRAM HYZE1C )
      WRITE OUTPUT TAPE 6, 598
598    FORMAT(40HDECOMPOSITION CALCULATIONS FOR HYDRAZINE)
      KAPPA=1
      K=0
      READ INPUT TAPE 5, 5100, K1, K2, K3
5100   FORMAT(315)
      CALL DATE(K1, K2, K3)
      12  READ INPUT TAPE 5, 501, NJ
      DO 14 JJ=1, NJ
      READ INPUT TAPE 5, 502, LJ, A(JJ), E(JJ)
      14  CONTINUE
      13  READ INPUT TAPE 5, 503, T, TAU, YYY, JTT
1995   DO 15 JJ=1, NJ
      W(JJ)=EXP(2.3*A(JJ)-E(JJ)/(1.99*T))
      15  CONTINUE
      22  WRITE OUTPUT TAPE 6, 597
597    FORMAT(64HREACTION NUMBER    ACTIVATION ENERGY  PREEX, A(JJ)  RATE
1CONSTANT)
      DO 16 JJ=1, NJ
      WRITE OUTPUT TAPE 6, 504, JJ, E(JJ), A(JJ), W(JJ)
      16  CONTINUE
      WRITE OUTPUT TAPE 6, 523
      WRITE OUTPUT TAPE 6, 596, T
      WRITE OUTPUT TAPE 6, 523
596    FORMAT(27HTEMPERATURE, DEGREES KELVIN=, F9.1)
      24  W1=W(1)
      W2=W(2)
      W3=W(3)
      W4=W(4)
      W5=W(5)
      W6=W(6)
      W7=W(7)
      W8=W(8)
      W9=W(9)
      W10=W(10)
      W11=W(11)
      21  READ INPUT TAPE 5, 501, NCC
      READ INPUT TAPE 5, 501, NNC
      READ INPUT TAPE 5, 516, INI, TIME
      TIME=(1.0E-06)*TIME
      DO 17 IC=1, NNC
      READ INPUT TAPE 5, 516, INI, C(IC)
      C(IC)=(1.0E-06)*C(IC)
      17  CONTINUE
      23  X=C(1)
      HYD=C(2)
      HYR=C(3)

```

```

AZOT=C(4)
AMM0=C(5)
AMIN=C(6)
AMID=C(7)
H1=C(8)
H2=C(9)
HYRA=1000.0
N=9
C SET UP Y ARRAY
Y(1,1)=TIME
Y(1,2)=HYD
Y(1,3)=HYR
Y(1,4)=AZOT
Y(1,5)=AMM0
Y(1,6)=AMIN
Y(1,7)=AMID
Y(1,8)=H1
Y(1,9)=H2
Y(1,10)=HYRA
H=TAU
READ INPUT TAPE 5,1,METHD,ACC,SIG,FINAL
READ INPUT TAPE 5,550,Q,CP
CALL INIT(Y,YP,YOUT,YPOUT)
IF(SENSE SWITCH 5)595,505
595 BACKSPACE 15
GO TO 1192
505 WRITE TAPE 15,T,K1,K2,K3,NJ,TIME,C(1),C(2)
WRITE TAPE 15,(A(I),I=1,NJ),(E(I),I=1,NJ),(W(I),I=1,NJ)
1192 CONTINUE
CALL DIFTRN(N,METHD,H,ACC,SIG,Y,YP,YOUT,YPOUT,FINAL)
GO TO 1192
1 FORMAT(15,3E10.4)
501 FORMAT(15)
502 FORMAT(15,2F10.1)
503 FORMAT(F10.1,2E10.5,15)
504 FORMAT(115,2F16.1,E10.4)
516 FORMAT(111,E15.5)
523 FORMAT(3H ///)
579 FORMAT(15H ADIABATIC CASE)
550 FORMAT(2E10.5)
END

```

```

SUBROUTINE OUTPUT (Y,YP,YOUT,YPOUT)
DIMENSION Y(5,15),YP(5,15),YOUT(15),YPOUT(15)
DIMENSION DUMMY(12)
COMMON DUMMY,W1,W2,W3,W4,W5,W6,W7,W8,W9,W10,W11
DIMENSION C(50)
DIMENSION E(25),A(25),W(25)
DIMENSION Z(25,55),DZ(25,55)
DIMENSION R(100),R2(100)
COMMON E,A,W,KAPPA,K,H,TAU,K1,K2,K3,NJ,X,T,YYY,JTT,NCC,NNC
COMMON C
DIMENSION T1(50),R314(10),PR(10),R312(10)
MINIM=10
997 KAPPA=KAPPA+1
1338 IF (SENSE SWITCH 2) 4002,2338
2338 IF(YOUT(7))605,606,606
606 IF(YPOUT(2))607,607,605
607 IF(SENSE SWITCH 4)383,608
608 IF(KAPPA-101)992,383,383
383 KAPPA=1
K=K+1
T1(K)=T
DO 337 J=1,MINIM
Z(J,K)=YOUT(J)*1.E+6
DZ(J,K)=YPOUT(J)
IF(YOUT(J))605,1701,1701
1701 CONTINUE
337 CONTINUE
401 IF(K-24)411,408,11
411 IF (SENSE SWITCH 3) 1339,992
1339 PRINT 508,Z(1,K),Z(2,K),K
GO TO 992
408 WRITE OUTPUT TAPE 6,523
WRITE OUTPUT TAPE 6,522
410 WRITE OUTPUT TAPE 6,506
506 FORMAT(120H      TIME      HYDRAZINE      NITROGEN      AMMONIA
1 HYDROGEN      NH2      NH      N2H3      H1      /)
417 DO 403 K=1,9,4
813 WRITE OUTPUT TAPE 6,507,Z(1,K),Z(2,K),Z(4,K),Z(5,K),Z(9,K),Z(6,K),
8131 Z(7,K),Z(3,K),Z(8,K)
WRITE TAPE 15,Z(1,K),Z(2,K),Z(4,K),Z(5,K),Z(9,K),Z(6,K),Z(7,K),Z(3
1,K),Z(8,K)
403 CONTINUE
WRITE OUTPUT TAPE 6,523
416 WRITE OUTPUT TAPE 6,509
509 FORMAT(120H      TIME      RATE CONSTANT      HYRA CONC.      HYRA DER.
1 RATE2      RATE 3/2      RATE 3/4      PERC. REACT.      TEMPERATURE /)
413 DO 404 K=1,9,4
R(K)=-(DZ(2,K)*1.0E+06)/Z(2,K)
R2(K)=R(K)/(Z(2,K)*1.3E-06)
R314(K)=R(K)*((Z(2,K)*1.0E-06)**0.25)
R312(K)=R(K)/((Z(2,K)*1.0E-06)**0.5)
PR(K)=100.0*(C(2)-Z(2,K)*1.0E-06)/C(2)
1,R314(K),PR(K),T1(K)

```

```

WRITE TAPE 15,Z(1,K),R(K),Z(10,K),R2(K),R312(K),R314(K),PR(K),T1(K
1)
404 CONTINUE
WRITE OUTPUT TAPE 6,523
WRITE OUTPUT TAPE 6,521
406 WRITE OUTPUT TAPE 6,506
702 DO 704 K=1,9,4
WRITE OUTPUT TAPE 6,507,Z(1,K),DZ(2,K),DZ(4,K),DZ(5,K),DZ(9,K),
1DZ(6,K),DZ(7,K),DZ(3,K),DZ(8,K)
704 CONTINUE
WRITE OUTPUT TAPE 6,523
DO 4338 K=1,15
T1(K)=T1(K+9)
DO 4338 J=1,MMIIIM
Z(J,K)=Z(J,K+9)
DZ(J,K)=DZ(J,K+9)
4338 CONTINUE
K=15
GO TO 992
605 PRINT 580
WRITE OUTPUT TAPE 6,523
WRITE OUTPUT TAPE 6,580
WRITE OUTPUT TAPE 6,523
580 FORMAT(15H RESET INTERVAL)
IF(K-4)4002,4002,7838
7838 LK=K-3
DO 6838 J=1,MMMM
YOUT(J)=Z(J,LK)*1.E-6
4703 K=LK
6838 CONTINUE
K=LK
GO TO 992
4002 PRINT 4003
WRITE OUTPUT TAPE 6,1588
1588 FORMAT(1H1)
WRITE OUTPUT TAPE 6,523
WRITE OUTPUT TAPE 6,4003
WRITE OUTPUT TAPE 6,523
U40=0.0
WRITE TAPE 15,U40,U40,U40,U40,U40,U40,U40,U40,U40
ENDFILE 15
BACKSPACE 15
4003 FORMAT(15H CASE INTERRUPT )
WRITE OUTPUT TAPE 6,599
WRITE OUTPUT TAPE 6,1599
1599 FORMAT(14H TO BE PUNCHED)
WRITE OUTPUT TAPE 6,5100,K1,K2,K3
PUNCH 5100,K1,K2,K3
PUNCH 501,NJ

```

```

SUBROUTINE TERM (IBACK, FINAL, YOUT)
DIMENSION Y(5,15), YP(5,15), YOUT(15), YPOUT(15)
DIMENSION DUMMY(12)
COMMON DUMMY, W1, W2, W3, W4, W5, W6, W7, W8, W9, W10, W11
DIMENSION C(50)
DIMENSION E(25), A(25), W(25)
COMMON E, A, W, KAPPA, K, H, TAU, K1, K2, K3, NJ, X, T, YYY, JTT, NCC, NNC
COMMON C, Q, CP
C
THIS SUBROUTINE WILL NOT TERMINATE IN THIS FORM.
IF(SENSE SWITCH 6)102,301
301 TIN=T
GO TO 101
102 AMRE=C(2)-YOUT(2)
CTOT=C(1)+C(2)
DELT=(Q/CP)*(AMRE/CTOT)
T=TIN+DELT
11 SENSE LIGHT 1
IF(SENSE SWITCH 4)201,1995
201 PRINT 500,DELT,T
500 FORMAT(2E15.8)
1995 DO 15 J=1,NJ
W(JJ)=EXP(2.3*A(JJ)-E(JJ)/(1.99*T))
15 CONTINUE
24 W1=W(1)
W2=W(2)
W3=W(3)
W4=W(4)
W5=W(5)
W6=W(6)
W7=W(7)
W8=W(8)
W9=W(9)
W10=W(10)
W11=W(11)
101 IBACK=1
RETURN
END

```

```

WRITE OUTPUT TAPE 6,501,NJ
DO 1662 JJ=1,NJ
WRITE OUTPUT TAPE 6,502,JJ,A(JJ),E(JJ)
PUNCH 502,JJ,A(JJ),E(JJ)
1662 CONTINUE
LANNY=21
LOLA=1
BIGX=1.E6*X
WRITE OUTPUT TAPE 6,503,T,TAU,YYY,JTT
PUNCH 503,T,TAU,YYY,JTT
WRITE OUTPUT TAPE 6,501,NCC
PUNCH 501,NCC
WRITE OUTPUT TAPE 6,501,NNC
PUNCH 501,NNC
WRITE OUTPUT TAPE 6,516,LANNY,Z(1,1)
PUNCH 516,LANNY,Z(1,1)
WRITE OUTPUT TAPE 6,516,LOLA,BIGX
PUNCH 516,LOLA,BIGX
DO 1661 J=2,NNC
WRITE OUTPUT TAPE 6,516,J,Z(J,1)
PUNCH 516,J,Z(J,1)
1661 CONTINUE
11 CALL EXIT
992 RETURN
501 FORMAT(15)
502 FORMAT(15,2F10.1)
503 FORMAT(F10.1,2E10.5,15)
504 FORMAT(115,2F16.1,E10.4)
523 FORMAT(3H ///)
516 FORMAT(111,E15.5)
521 FORMAT(13H DERIVATIVES /)
522 FORMAT(16H CONCENTRATIONS /)
547 FORMAT(5E13.5)
526 FORMAT(2E15.6,13)
507 FORMAT(9E13.5)
508 FORMAT(2E13.4,13)
599 FORMAT(31H11G0R EBERSTEIN,PROGRAM HYZE1C )
5100 FORMAT(315)
END

```

```
SUBROUTINE INIT(Y,YP,YOUT,YPOUT)
DIMENSION Y(5,14),YP(5,14)
DIMENSION YOUT(14),YPOUT(14)
DIMENSION AAAAA(4),BBBBB(4),CCCCC(4)
COMMON AAAAA,BBBBB,CCCCC
AAAAA(1)=.5
AAAAA(2)=.2928932188134524755991556380
AAAAA(3)=1.7071067811865475244008443620
AAAAA(4)=.16666666666666666666666666667
BBBBB(1)=1.0
BBBBB(2)=.2928932188134524755991556380
BBBBB(3)=1.7071067811865475244008443620
BBBBB(4)=.33333333333333333333333333333
CCCCC(1)=.5
CCCCC(2)=.2928932188134524755991556380
CCCCC(3)=1.7071067811865475244008443620
CCCCC(4)=.5
DO 900 KKKKK=1,5
900 YP(KKKKK,1)=1.0
RETURN
END
```

[illegible]

[illegible]

```
SUBROUTINE DATE(K1,K2,K3)
  IF(K2-31) 2702,2702,2701
2701 K2=K2-31
     K1=K1+1
2702 CONTINUE
     GO TO (201,202,204),K3
     201 NYEAR=1961
         GO TO 203
     202 NYEAR=1962
         GO TO 203
     204 NYEAR=1963
     203 CONTINUE
         GO TO (101,102,103,104,105,106,107,108,109,110,111,112),K1
     101 WRITE OUTPUT TAPE 6,5101,K2,NYEAR
5101 FORMAT(125,7HJANUARY,15)
     GO TO 120
     102 WRITE OUTPUT TAPE 6,5102,K2,NYEAR
5102 FORMAT(125,8HFEBRUARY,15)
     GO TO 120
     103 WRITE OUTPUT TAPE 6,5103,K2,NYEAR
5103 FORMAT(125,5HMARCH,15)
     GO TO 120
     104 WRITE OUTPUT TAPE 6,5104,K2,NYEAR
5104 FORMAT(125,5HAPRIL,15)
     GO TO 120
     105 WRITE OUTPUT TAPE 6,5105,K2,NYEAR
5105 FORMAT(125,3HMay,15)
     GO TO 120
     106 WRITE OUTPUT TAPE 6,5106,K2,NYEAR
5106 FORMAT(125,4HJUNE,15)
     GO TO 120
     107 WRITE OUTPUT TAPE 6,5107,K2,NYEAR
5107 FORMAT(125,4HJULY,15)
     GO TO 120
     108 WRITE OUTPUT TAPE 6,5108,K2,NYEAR
5108 FORMAT(125,6HAUGUST,15)
     GO TO 120
     109 WRITE OUTPUT TAPE 6,5109,K2,NYEAR
5109 FORMAT(125,9HSEPTEMBER,15)
     GO TO 120
     110 WRITE OUTPUT TAPE 6,5110,K2,NYEAR
5110 FORMAT(125,7HOCTOBER,15)
     GO TO 120
     111 WRITE OUTPUT TAPE 6,5111,K2,NYEAR
5111 FORMAT(125,8HNOVEMBER,15)
     GO TO 120
     112 WRITE OUTPUT TAPE 6,5112,K2,NYEAR
5112 FORMAT(125,8HDECEMBER,15)
     120 RETURN
       END
```

```

SUBROUTINE DERIV(Y,YP,K)
DIMENSION Y(5,15),YP(5,15),YOUT(15),YPOUT(15)
DIMENSION DUMMY(12)
COMMON DUMMY,W1,W2,W3,W4,W5,W6,W7,W8,W9,W10,W11
DIMENSION E(25),A(25),W(25)
COMMON E,A,W,KAPPA,L,H,TAU,K1,K2,K3,NJ,X,T,YYY,JIT,HCC,NNC
TIME=Y(K,1)
HYD=Y(K,2)
HYR=Y(K,3)
AZOT=Y(K,4)
AMMO=Y(K,5)
AMIN=Y(K,6)
AMID=Y(K,7)
H1=Y(K,8)
H2=Y(K,9)
HYRA=Y(K,10)
VOW1=W1*X
VOW2=(W3+W5)*X
VOW3=2.0*W1*X
VOW4=W5*X
VOW5=W5*X
VOW6=W3*X
W001=W2*AMIN
W002=W7*AMIN
W003=W4*H1
W004=H1*W9
W005=W6*AMIN
W006=HYR*W8
W007=W001+W003
W008=W002+W004
W009=VOW6+W008
W0010=W10*AMIN*AMIN
DHYD=-HYD*(VOW1+W007+W6*AMID)
DHYP=DHYD+W0010
DH1=HYD*(W001+W005)-HYR*(VOW2+W008+W006)
DH2=HYR-HYR*W006
DAMIN=HYD*(VOW3-W001+W003+W005)+HYF*(VOW4-W002)
DAMID=AMIN-W0010*2.0
DAMIF=VOW5*HYD-W005*HYD
DH1=HYR*(VOW6-W004)-HYF*W003
DAMMO=HYD*W007+HYF*(W002+W8*HYR*2.0)
DH2=HYR*(W009+W004)
DAZOT=HYR*(W009+W006)
YP(K,2)=DHYD
YP(K,3)=DHYP
YP(K,4)=DAZOT
YP(K,5)=DAMMO
YP(K,6)=DAMIN
YP(K,7)=DAMID
YP(K,8)=DH1
YP(K,9)=DH2
YP(K,10)=-0.1*HYRA
RETURN
END

```

```

SUBROUTINE DERIV(Y,YP,K)
DIMENSION Y(5,15),YP(5,15),YOUT(15),YPOUT(15)
DIMENSION DUMMY(12)
COMMON DUMMY,W1,W2,W3,W4,W5,W6,W7,W8,W9,W10,W11
DIMENSION E(25),A(25),W(25)
COMMON E,A,W,KAPPA,L,H,TAU,K1,K2,K3,NJ,X,T,YYY,JTT,NCC,NHC
TIME=Y(K,1)
HYD=Y(K,2)
HYR=Y(K,3)
AZOT=Y(K,4)
AMMO=Y(K,5)
AMIN=Y(K,6)
AMID=Y(K,7)
H1=Y(K,8)
H2=Y(K,9)
HYRA=Y(K,10)
DHYRA=W2*HYD*AMIN+W6*HYD*AMID-HYRA*X*(W3+W11)-2.0*W8*HYRA*HYRA
1-W5*HYRA
DHYR=W11*HYRA*X-HYR*(W7*AMIN+W9*H1)
DHYD=-HYD*(W2*AMIN+W4*H1+W1*X+W6*AMID)+W10*AMIN*AMIN
DAMIN=HYD*(2.0*W1*X+W4*H1+W6*AMID)+W5*HYRA-AMIN*(W2*HYD+W7*HYR+W
110*AMIN*2.0)
DAMID=W5*HYRA-W6*HYD*AMID
DH1=W3*HYRA*Y-H1*(W4*HYD+W9*HYR)
DAMMO=HYD*(W2*AMIN+W4*H1)+HYR*(W7*AMIN)+W8*HYRA*HYRA*2.0
LAHJZ=HYD*W3*X+HYR*(W7*AMIN+W9*H1)
LAZOT=LAHJZ+W8*HYRA*HYRA
DH2=LAHJZ+HYR*H1*W9
YP(K,2)=HYD
YP(K,3)=HYR
YP(K,4)=LAZOT
YP(K,5)=AMID
YP(K,6)=DAMIN
YP(K,7)=DAMID
YP(K,8)=H1
YP(K,9)=H2
YP(K,10)=DHYRA
RETURN
END

```

```

SUBROUTINE DERIV(Y,YP,K)
  DIMENSION Y(5,15),YP(5,15),YOUT(15),YPOUT(15)
  DIMENSION DUMMY(12)
  COMMON DUMMY,W1,W2,W3,W4,W5,W6,W7,W8,W9,W10,W11,W12
  DIMENSION C(50)
  DIMENSION E(25),A(25),W(25)
  COMMON E,A,W,KAPPA,K,H,TAU,K1,K2,K3,NJ,X,T,YYY,JTT,NCC,NNC
  TIME=Y(K,1)
  UDMH=Y(K,2)
  AMMO=Y(K,3)
  AMIN=Y(K,4)
  HYR=Y(K,5)
  ETANE=Y(K,6)
  THANE=Y(K,7)
  ZINE=Y(K,8)
  XMET=Y(K,9)
  HCN=Y(K,10)
  H2=Y(K,11)
  AZOT=Y(K,12)
  AMID=(W9*HYR)/(W5*UDMH)
  UN=UDMH*(W3*XMET+W5*AMID)/W6
  R1=UDMH*(W1*X+W4*AMIN)/W2
  DUDMH=-UDMH*(W1*X+W3*XMET+W4*AMIN+W5*AMID)
  DAMIN=UDMH*(W1*X+W5*AMID-W4*AMIN)+W9*HYR-AMIN*(W8*ZINE+2.0*W11*AMIN)
  DHYR=ZINE*(W7*XMET+W8*AMIN)-HYR*(W9+2.0*W10*HYR)
  DZINE=AMIN*(W4*UDMH+W11*AMIN)-ZINE*(W7*XMET+W8*AMIN)
  DXMET=W2*R1+W6*UN-XMET*(W3*UDMH+W7*ZINE+2.0*W12*XMET)
  DHCN=W2*R1
  DH2=W2*R1
  DAZOT=W6*UN+W10*HYR*HYR
  DAMMO=W8*ZINE*AMIN+2.0*W10*HYR*HYR
  DETANE=W12*XMET*XMET
  DTHANE=XMET*(W3*UDMH+W7*ZINE)+W6*UN
  YP(K,2)=DUDMH
  YP(K,3)=DAMMO
  YP(K,4)=DAMIN
  YP(K,5)=DHYR
  YP(K,6)=DETANE
  YP(K,7)=DTHANE
  YP(K,8)=DZINE
  YP(K,9)=DXMET
  YP(K,10)=DHCN
  YP(K,11)=DH2
  YP(K,12)=DAZOT
  Y(K,13)=R1
  Y(K,14)=AMID
  Y(K,15)=UN
  RETURN
END

```

The following abbreviations were used:

AMID	is NH
AMIN	is $\text{NH}_2$
AMMO	is ammonia
AZOT	is nitrogen
H1	is atomic hydrogen
H2	is molecular hydrogen
HYD	is hydrazine
HYR	is $\text{N}_2\text{H}_3^*$
HYRA	is $\text{N}_2\text{H}_3$
ETANE	is ethane
R1	is $\text{CH}_3\text{NCH}_3$
UN	is $\text{CH}_3\text{NNHCH}_3$
THANE	is methane
W(I)	is the rate constant of the $I^{\text{th}}$ elementary reaction.
XMET	is $\text{CH}_3$
ZINE	is hydrazine

For input and output the concentrations were in millimoles/liter, and time was in microseconds. For computation, concentrations were in moles/cc, and time was in seconds.

Second order rate constants were in cc./mole-sec. First order rate constants were in  $\text{sec}^{-1}$